Synthesis, Structure and Reactivity of the Later Transition Metal Complexes Containing a Multidentate Phosphorus-Nitrogen Hybrid Ligand

A dissertation presented in partial fulfilment of the requirements for the degree of Doctor of Philosophy in Chemistry at Massey University

Steven Michael Fornara Kennedy

2000

For Tracey

Acknowledgements

To: First and foremost, Associate Professor Eric Ainscough and Professor Andrew Brodie for their expertise, supervision and many entertaining discussions. Dr Pat Edwards for assistance with the NMR experiments. Professor Tony Burrell for solving the crystal structures. Associate Professor Paul Buckley for guidance with the kinetic studies. Mr Terry Canton for supplying everything I needed. Dr Allen Oliver of the University of Auckland for X-ray data collection. Mr John Allen of AgResearch for Mass Spectral data. Mrs Marianne Dick of Otago University for elemental analysis. Dr Sue Boyd, Manager Griffith University NMR Facility, for CP/MAS spectral data. Dr Peter Healy of Griffith University for helpful discussion concerning the CP/MAS spectral data. Associate Professor Dave Harding, MURF , GRF, RSNZ, Deans Fund and IFS-Chemistry for the much needed funding. Lastly and definitely not least: to my parents Michael and Gigliola; to my sisters Tracey and Angela; to my friends Andrew Steedman, Gavin Collis, Craig Depree, Giovanna Moretto, Rekha Parshot, Wayne Campbell, Rachel Williamson, Jo-Anna Hislop, Clem Powell, Justin Nairn, Warwick Belcher and everyone else in IFS-Chemistry. A big thank you to all.

Steven Kennedy
13th June 2000

Errata

Piii, line 5; pxiii, line 17 and -6; diphenylphosphino not diphenylphoshino
P4, line 3, metal's not metals
P6, line -5, nucleophilic not nucleophile
P10, Figure 1.8, complex should have a 1+ charge
P13, line 9, 'PN_2' ligand not ligand 'P_2N'
ref 28, Wiley not Wily
P14, delete ref 29 (it is on the previous page)
P25, line -6, carried out not carried
P29, line -6, dependent not dependant
P31, line -6, has not as
P33, line 2, en route not on route
line 11, the molybdenum not molybdenum
P34, line 9, the π not the a π
line 14, from heating not from the heating
line -8 and elsewhere, methyl iodide or iodomethane not methyliodide
line -4, dication not diction
P36, line -3, delete "and"
P38, line -10, arbitrarily not arbitrary
P43, line 1, 2.2.3.2 not 2.2.2.2
P45/73/119/124/129/134/169, Table 2.4/3.1/4.1/4.3/4.5/4.7/4.8/5.1, delete "Completeness to theta = 0.50° ... 0.0%"
P47, first para, line 9, section 2.2.2 not 2.2.9
ref 14 and elsewhere, Thornton-Pett not Thorton-Pett
P48, line -10; p173, line -6: from not form
line -2, 2.4.5 not 2.2.8
P51, line 1; p126, line 10: ligand's not ligands
P55, line 9; p57, line 11; p87, last line: latter not later
P55, references: titles of books should be italicised
P56, Table 2.9, fourth entry under ν(P-C) should be 1090 not 1890 cm^{-1}
P57, line -3, cuvette not curvette
P62, line 2, trifluoroacetic not uifuroacctic
P68, line 12; p164, line -11: delete "the"
line -5, previously not previuosly
P69, line 13, "A least squares difference map..." not "A least difference map..."
P70, delete lines 6 through 10 and "found in the title complex." of line 11
P73, Table 3.1, *mer*-[W(CO)$_3${PN(H)CHP-κ^2*P,P*-η^2(*N*=*C*)}]BF_4•$2CH_2Cl_2$ not , *mer*-[W(CO)$_3${PN(H)CHP-κ^2*P,P*-η^2(*N*=*C*)}]BF_4
Table 3.1, "Reflections collected...21461" not "Reflections collected...9391,"
Table 3.1, R(int) = 0.0192 not R(int) = 0.0000
P79, line -1, delete "in"
P81, heading; p89, line 14: ...CHP... not ...CP...
P81, line 4, quaternised not quarternarised
P86, and elsewhere: *ca* not c.a.
P89, and elsewhere δ 66 not δ66
P93, line -6, replace "band splitting in the solid state" with "a ν(^{13}C-O) stretch"
P98, Table 3.10; p148, Table 4.12 "-" (minus) not "•"
P99, line 1, "...D_2,[33] that is..." not "...D_2.[33] That is ..."
P99, line 7; p105, line -10: CF_3SO_3H not CF_3SO_2H
P101, line 8, > 90% not < 90%
line -8, itself not its self
P104/105, Tables 3.9/3.10/3.11 are incorrectly referred to --should be 3.8/3.9/3.10 respectively
P107, ref 1, Inorganic not Inorganic
line -3, readily not readly
P113, line 3, BF_4^- not $BF4^-$
P115, line -4, being unable not unable
P121, line -8, triphenylphosphane not triphenylphosphino
line -4, ligand not ligands
P126, line 4, complex's not complexes
P132, line 14, basal plane not basal
line -8, previous not previuos
line -2, mirror plane not two-fold axis
P144, Table 4.10, all coupling constants are accurate only to the first decimal point
P149, line 5, phenanthroline not phenantrolinc
P150, line 11, 0.401 mmol not 401 mmol
P155, line 5, 0.164 g not 164 g
P158, line 8, than not then
P160, ref 116, C. Hahn not Hahn
P162, The complexes/ligands F.5.2-* refer to Figure 5.2 on the same page only
P163 The complexes/liugands F.5.2-* refer to Figure 5.2 on the same page only
P166, line -1, nucleophilicity not nucleophilcity
P168, line 4, two-fold axis not mirror plane
P174, Table legend, to be assigned not to assigned
P177, Table legend, delete legend
line -6 to -5, chloride ligand not chloride atom
P179, line -5, Schlenk not Schlenck
P181, ref 11 should be ref 1, 1982-1994
P185, line 4, replace "asymmetric unit" with "unit cell"
P187, line -2, Peak not Peck
P205 line 4, mixtures not solutions
P207, line 12, Merck not Merk

References for Chapter 1 containing a full list of authors

[1] M. D. Fryzuk, *Can. J. Chem.*, 1992, **70**, 2839.
[2] R. G. Pearson, *Chemical Hardness*, 1997, Wiley-VCH, Weinhiem.
[3] B. T. Heaton, J. A. Iggo, C. Jacob, J. Nadarajah, M. A. Fontaine, R. Messere and A. F. Noels, *J. Chem. Soc. Dalton Trans.*, 1994, 2875.
[4] Z.-Z. Zhang, H.-P. Xi, W.-J. Zhao, K.-Y. Jiang, R.-J. Wang, H.-G. Wang and Y. Wu, *J. Organomet. Chem.*, 1993, **454**, 221.
[5] M. B. Hossain, L. W. Houk, P. K. Gupta and D. Van der Helm, *Acta Cryst.*, 1982, **B38**, 91.
[6] M. D. Fryzuk, G. Giebrecht, S. J. Rettig, *Organometallics*, 1996, **15**, 3329.
[7] P. J. Shapiro, E. Bunel, W. P. Schaefer and J. E. Bercaw, *Organometallics*, 1990, **9**, 867.
[8] P. J. Shapiro, W. P. Schaefer, J. A. Labinger, J. E. Bercaw and D. W. Cotter, *J. Am. Chem. Soc.*, 1994, **116**, 4623.
[9] P. G. Edwards, S. J. Coles, M. B. Hursthouse and P. W. Read, *J. Chem. Soc., Chem. Commun.*, 1994, 1967.
[10] K. J. Cavell, *Coordination Chemistry Reviews*, 1996, **155**, 209.
[11] L. Crociani, F. Tisato, F. Refosco, G. Bandoli and B. Corain, *Eur. J. Inorg. Chem.*, 1998, 1689, and refs within.
[12] F. Refosco, F. Tisato, G. Bandoli, C. Bolzati, A. Dolmella, A. Moresco and M. Nicolini, *J. Chem. Soc., Dalton Trans.*, 1993, 605.
[13] A. Togni *J. Am. Chem. Soc.*, 1996, **118**, 1031.
[14] P. S. Pregosin, *Organometallics*, 1996, **15**, 3496, and refs therein.
[15] J. Pfeiffer, G. Kickelbick and U. Schubert, *Organometallics*, 2000, **19**, 62, and refs with in.
[16] J. Boersma, W. de Graaf, S. Harder and G. van Koten, *J. Organomet. Chem.*, 1988, **358**, 545, and refs within.
[17] U. Burckhardt, V. Gramlich, P. Hofmann, R. Nesper, P. S. Pregosin, R. Salzmann and A. Togni, *Organometallics*, 1996, **15**, 3496.
[18] A. Togni, C. Breutel, A. Schnyder, F. Spindler, H. Landert and A. Tijani, *J. Am. Chem. Soc.*, 1994, **116**, 4062.
[19] P. Barbaro, P. S. Pregosin, R. Salzmann, A. Albinati and R. W. Kunz, *Organometallics*, 1994, **14**, 5160.
[20] F. Tisato, F. Refosco, A. Moresco, G. Bandoli, A. Dolmella and C. Bolzati, *Inorg. Chem.*, 1995, **34**, 1779.
[21] B. Milani, L. Vicentini, A. Sommazzi, F. Garbassi, E. Chairparin, E. Zangrando and G. Mestroni, *J. Chem. Soc., Dalton Trans.*, 1996, 3139.
[22] A. L. Balch and E. Y. Fung, *Inorg. Chem.*, 1990, **29**, 4764.
[23] N. Margiotta, A. Habtemariam and P. J. Sadler, *Angew. Chem. Int. Ed. Engl.*, 1997, **36**, 1185.
[24] E. Drent, P. Arnoldy and P. H. M. Budzelaar, *J. Organomet. Chem.*, 1994, **475**, 57.
[25] M. Kumada, T. Hayashi, M. Konishi, M. Fukushima, T. Mise, M. Kagotani and M. Tajika, *J. Am. Chem. Soc.*, 1982, **104**, 180.
[26] R. Noyori, J-X. Gao and T. Ikariya, *Organometallics*, 1996, **15**, 1087.
[27] C. Bianchini, E. Farnetti, L. Glendenning, M. Graziani, G. Nardin, M. Peruzzini, E. Rocchini and F. Zanobini, *Organometallics*, 1995, **14**, 1489.
[28] F. A. Cotton and H. Bo, *Progress in Inorganic Chemistry*, 1992, vol. 40, John Wily & Sons., p180.
[29] K. Vrieze, Organometallics, 1996, **15**, 3022.
[30] C. Bianchini, L. Glendenning, M. Peruzzini, A. Romerosa and F. Zanobini, *J. Chem. Soc., Chem. Commun.*, 1994, 2219.
[31] C. Bianchini, A. Meli, M. Peruzzini, F. Vizza, V. Herrera and R. A. Sanchez-Delgado, *Inorg. Chem.*, 1994, **33**, 1622.
[32] R. S. Brown, N. J. Curtis and J. Hugnet, *J. Am. Chem. Soc.*, 1981, **103**, 6953.
[33] J. P. Fackler, Jr., N. M. Khan, R. J. Staples, C. King and R. E. P. Winpenny, *Inorg. Chem.*, 1993, **32**, 5800.
[34] E. Deutsch, J. L. Vanderheyden, A. R. Ketring, K. Libson, M. J. Heeg, L. Roecker, D. Motz, R. Whittle and R. C. Elder, *Inorg. Chem.*, 1984, **23**, 3184.
[35] M. E. Kastner, M. J. Lindsay and M. J. Clarke, *Inorg. Chem.*, 1982, **21**, 2037, and refs therein.
[36] P. Guillaume and M. Postel, *Inorg. Chim. Acta*, 1995, **223**, 109.
[37] S. T. Howard, J. P. Foreman and P. G. Edwards, *Inorg. Chem.*, 1996, **35**, 5805.
[38] C. Bianchini, E. Farnetti, M. Graziani, G. Nardin, A. Vacca and F. Zanobini, *J. Am. Chem. Soc.*, 1990, **112**, 9190.
[39] The description of the catalytic cycle is taken from ref 51
[40] A. Schnyder, L. Hintermann and A. Togni, *Angew. Chem., Int. Ed. Engl.*, 1995, **34**, 931.
[41] B. M. Trost, M. G. Organ and G. A. O'Doherty, *J. Am. Chem. Soc.*, 1995, **117**, 9662.
[42] B. M. Trost, C. B. Lee and J. M. Weiss, *J. Am. Chem. Soc.*, 1995, **117**, 7247.
[43] G.C. Lloyd-Jones and A. Pfaltz, Angew. *Chem., Int. Ed. Engl.*, 1995, **34**, 462.
[44] H. Kuboto and K. Koga, *Tetrahedron Lett.*, 1994, **35**, 6689.
[45] Y. Cheng and D. J. Schiffin, *Inorg. Chem.*, 1994, **33**, 765.
[46] D.G. Evans, J. S. Bone, J. J. Perriam and R. C. T. Slade, *Angew. Chem., Int. Ed. Engl.*, 1996, **35**, 1850.
[47] E. Deutsch, B. Mohr, J. Schmidt, E. E. Brooks, M. J. Heeg and D. M. Ho, *Inorg. Chem.*, 1993, **32**, 3236.
[48] S. O. Grim, R. C. Barth, J. D. Mitchell and J. Del Gaudio, *Inorg. Chem.*, 1977, **16**, 1776.
[49] P. A. Duckworth, *Polydentate Phosphorus-Nitrogen Hybrid Ligands Containing the 2-Aminophenyl Group*, 1984, Ph.D. Thesis, University of Sydney.
[50] M. J. R Halstead, *Iminophosphine Complexes of Ni(II)*, B.Sc(Hons) report, 1991, Massey University.
[51] X. Fan, *Structural Studies on the Interactions of a P_2N Tridentate ligand with Copper(I), Silver(I) and Sulfur*, 1995, MSc Thesis, Massey University.
[52] P. S. Braterman, *Metal Carbonyl Spectra*, Academic Press, 1975.
[53] See for example: G. Franciò, R. Scopelliti, C. G. Arena, G. Bruno, D. Drommi and F. Faraone, *Organometallics*, 1998, **17**, 338; R. Noyori and S. Hashiguchi, *Acc. Chem. Res.* 1997, **30**, 97; F. Ungváry, *Coord. Chem. Rev.*, 1997, **167**, 233; A. Carmona, A. Corma, M. Iglesias, A. San José and F. Sánchez, *J. Organomet. Chem.*, 1995, **492**, 11.

Abstract

Chapter 1 - This first part of the chapter aims to give the reader a flavour of the chemistry concerning phosphorus-nitrogen hybrid ligands containing both phosphorus and nitrogen donor atoms. This will be achieved by highlighting selected relevant examples from the literature. The second part will introduce the ligand 2-(diphenylphosphino)-N-[2-(diphenylphoshino)benzylidene]benzeneamine, (PNCHP), which is the subject of Chapters 2 through 6.

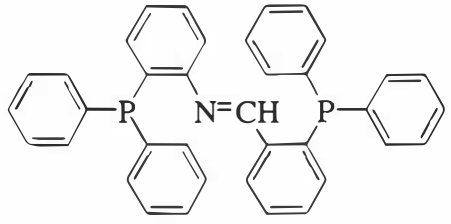

PNCHP

Chapter 2 - The ligand PNCHP reacts with [$Mo(CO)_3$(1,3,5-cycloheptatriene)] to give the complex *fac*-[$Mo(CO)_3$(PNCHP-κ^3*P,N,P*)] which readily isomerises to *mer*-[$Mo(CO)_3$(PNCHP-κ^3*P,N,P*)]. Kinetic studies on the isomerisation in acetone yielded the first-order forward rate constants (k_1) 1.22×10^{-5}, 4.18×10^{-5}, 1.72×10^{-4} and 4.89×10^{-4} s^{-1} at 19.5, 29.7, 40.0 and 49.5 °C respectively, with thermodynamic activation parameters $\Delta H_1^{\ddagger}$ and $\Delta S_1^{\ddagger}$ of 95 kJ mol^{-1} and –14.1 J mol^{-1} K^{-1} respectively. The related complex *fac*-[$Mo(CO)_3$($PNHCH_2P$-κ^3*P,N,P*)] ($PNHCH_2P$ = 2-(diphenylphosphino)-N-[(2-diphenylphosphino)benzyl]benzeneamine does not undergo isomerisation. The complex *cis*-[$Cr(CO)_4$(PNCHP-κ^2*N,P*)] reacts with sulfur to give *cis*-[$Cr(CO)_4$(SPNCHP-κ^2*N,P*)] and reacts with methyliodide under an atmosphere of carbon monoxide to yield the anion $[Cr(CO)_5I]^-$.

Chapter 3 - The complexes [$M(CO)_3$(PNCHP-κ^3*P,N,P*)] (M = Cr, Mo or W), containing a terdentate PNCHP ligand, react with H^+ to give the protonated products $[M(CO)_3\{PN(H)CHP\text{-}\kappa^2P,P\text{-}\eta^2(C{=}N)\}]^+$, where the imino group has 'slipped' from a κ^1N to a $\eta^2(C{=}N)$ coordination mode as a result of the protonation of the nitrogen atom. When

the acid is HCl the above cation $[M(CO)_3\{PN(H)CHP\text{-}\kappa^2P,P\text{-}\eta^2(C{=}N)\}]^+$ (M = Mo or W) converts to *cis*-$[M(CO)_2Cl_2(PNHCH_2P\text{-}\kappa^3P,N,P)]$. In this unusual reaction the imine group of the PNCHP ligand has been reduced to an amine concurrently with the two electron oxidation of the metal. In contrast, on reaction of *cis*-$[Cr(CO)_4(PNCHP\text{-}\kappa^2N,P)]$ with H^+, the bidentate PNCHP ligand dissociates from the metal resulting in cyclisation of the ligand to give a phosphonium salt.

Chapter 4 - PNCHP favours terdentate coordination with Pd(II) and Pt(II). The complexes $[MCl(PNCHP\text{-}\kappa^3P,N,P)]Cl$ and $[Pd(CH_3)(PNCHP\text{-}\kappa^3P,N,P)]Cl$ are synthesised starting with $[MCl_2(1,5\text{-cyclooctadiene})]$ and $[M(CH_3)Cl(1,5\text{-cyclooctadiene})]$, respectively. The ionic chlorides can be exchanged with BF_4^- using $AgBF_4$. Abstraction of the covalent chloride with $AgBF_4$ in the presence of acetonitrile yields $[Pt(CH_3CN)(PNCHP\text{-}\kappa^3P,N,P)]^{2+}$. The acetonitrile ligand of this dication can be substituted with triphenylphosphane, 2-picoline, or 3-picoline. The reaction of $[Pt(CH_3CN)(PNCHP\text{-}\kappa^3P,N,P)]^{2+}$ with 1,10-phenanthroline, 2,2'-bipyridine, bis(diphenylphosphino)ethane or 2,2':6',2''-terpyridine (L-L) yields complexes of the type $[Pt(L\text{-}L)(PNCHP\text{-}\kappa^3P,N,P)]^{2+}$ - the first five-coordinate platinum(II) dications.

Chapter 5 - The complex $[RhCl(PNCHP\text{-}\kappa^3P,N,P)]$ is synthesised by reacting the PNCHP ligand with 0.5 equivalents of $[\{RhCl(1,5\text{-cyclooctadiene})\}_2]$. This extremely reactive compound undergoes oxidative addition of dichloromethane and chloroform to yield complexes of the type $[RhCl_2(R)(PNCHP\text{-}\kappa^3P,N,P)]$ (R = CH_2Cl or $CDCl_2$). Addition of carbon monoxide to $[RhCl(PNCHP\text{-}\kappa^3P,N,P)]$ results in the adduct $[RhCl(CO)(PNCHP\text{-}\kappa^3P,N,P)]$ which is in equilibrium with square planar complex $[Rh(CO)(PNCHP\text{-}\kappa^3P,N,P)]Cl$. The coordinated chloride ligand of $[RhCl(PNCHP\text{-}\kappa^3P,N,P)]$ can be substituted with tetrahydrofuran, acetonitrile or triphenylphosphane.

Chapter 6 - The triosmium clusters $[Os_3(CO)_{11}(CH_3CN)]$ and $[Os_3(CO)_{10}(CH_3CN)_2]$ react with PNCHP to give $[\{Os_3(CO)_{11}\}_2(PNCHP\text{-}\kappa^2P,P)]$ (containing PNCHP bridging equatorially two osmium triangles), two coordination isomers of $[Os_3(CO)_{11}(PNCHP\text{-}\kappa^1P)]$ and 1,1-$[Os_3(CO)_{10}(PNCHP\text{-}\kappa^2P,P)]$, respectively. When 1,1-$[Os_3(CO)_{10}(PNCHP\text{-}\kappa^2P,P)]$ is reacted with one equivalent of trimethylamineoxide the major product is $[Os_3(\mu\text{-}$

H)$(CO)_7(\mu_3$-PNCP)], in which the imine hydrogen of PNCHP has migrated to the osmium cluster and PNCP is left to act as a triply bridging nine-electron donor. Two geometrical isomers of [$Os_3(\mu$-H)$(CO)_8(\mu_2$-PNCP)] are found as minor products, with PNCP acting as a doubly bridging seven-electron donor ligand.

Table of Contents

Abbreviations

Ar	aryl
CHT	1,3,7-cycloheptatriene
COD	1,5-cyclooctadiene
CP/MAS	cross polarisation/magic angle spinning
dec	decomposition
diphos	1,2-bis(diphenylphosphino)ethane
Et	ethyl
Hz	hertz
IR	Infrared
^{x}J	coupling constant over X bonds (Hz)
M^{+}	molecular ion
Me	methyl
MeCN	acetonitrile
M.p.	melting point
m/z	mass to charge ratio
NMR	nuclear magnetic resonance
PNCHP	2-(diphenylphosphino)-N-[2-(diphenylphoshino)benzylidene]-benzeneamine
$PNHCH_2P$	2-(diphenylphosphino)-N-[(2-diphenylphosphino)benzyl]-benzeneamine
2-pico	2-picoline
3-pico	3-picoline
Ph	phenyl
phen	1,10-phenanthroline
ppm	parts per million
SPNCHP	2-(diphenylphosphinothioyl)-N-[2-(diphenylphoshino)-benzylidene]-benzeneamine
terpy	2,2':6',2''-terpyridine
THF	tetrahydrofuran
tlc	thin layer chromatography
UV-vis	ultraviolet-visible

δ	chemical shift in ppm
ν(XY)	stretching frequency of X-Y bond (cm^{-1})]

1 Introduction

1.0 Chapter overview

This chapter will be divided into two parts. **PART 1** will aim to give the reader a flavour of the chemistry concerning phosphorus-nitrogen hybrid ligands containing both phosphorus and nitrogen donor atoms. This will be achieved by highlighting selected examples from the literature. **PART 2** will introduce the ligand 2-(diphenylphosphino)-N-[2-(diphenylphoshino)benzylidene]benzeneamine, (**PNCHP**), which is the subject of Chapters 2 through 6.

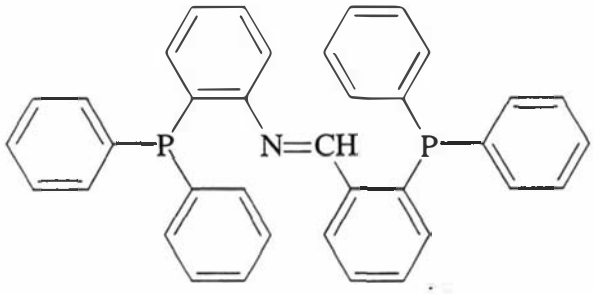

PNCHP

PART 1 A SELECTED REVIEW OF THE LITERATURE ON PHOSPHORUS-NITROGEN HYBRID LIGANDS AND THEIR COMPLEXES

"If the reactivity patterns of a metal complex can be considered a function of the metal's coordination environment then new ligand systems should result in the observation of new chemistry".

The above statement (abridged) by Fryzuk[1] is very true for the phosphorus-nitrogen hybrid ligand systems. These ligands have made possible the advent of many unique transition metal complexes with rare metal oxidation states, unusual coordination modes or novel reactivity patterns and new applications.

This chapter aims to illustrate the above with a survey of selected literature as it pertains to phosphorus-nitrogen hybrid ligands or, for short, 'P_nN_m' ligands (where n and m are the number of respective potential donor atoms in the ligand). The survey will be divided into five sections. The first section (*1.1*) will deal with the effects of having a 'hard' or 'borderline' nitrogen(s) in combination with a 'soft' phosphorus donor atom(s) within the same ligand. Section two (*1.2*) will look in more detail at the electronic effects imposed by 'P_nN_m' ligands on their metal complexes. Section three (*1.3*) will examine the reactivity of transition metal-'P_nM_m' ligand complexes, while section (*1.4*) will compare 'P_nN_m' ligands with analogous 'P_{n+m}' or 'N_{n+m}' systems with respect to coordination chemistry and reactivity. Finally, section (*1.5*) will highlight some application areas of phosphorus-nitrogen hybrid ligands.

1.1 The HSAB principle in relation to 'P_nN_m' ligands

In general, nitrogen donor atoms prefer to coordinate to metal centres of mid to high oxidation states whilst phosphorus bonding interactions are favoured with the low, zero and negative oxidation states. This observation is a reflection of the Hard Soft Acid Base (HSAB) principle. The HSAB principle can be used to great advantage when designing 'P_nN_m' ligand complexes for specific tasks, as will be discussed below. These advantages do not necessarily arise from situations where the HSAB principle is adhered to.

Phosphorus is considered a 'soft' atom in contrast to the nitrogen atom which ranges from 'borderline' to 'hard' in class.[2] Therefore, the affinity of 'soft' transition metals towards N-donors is generally considered to be lower than that towards phosphorus. It follows then, that the strength of the M-N bond is affected much more by steric effects

[1] M. D. Fryzuk, *Can. J. Chem.*, 1992, **70**, 2839.
[2] R. G. Pearson, *Chemical Hardness*, 1997, Wiley-VCH, Weinhiem.

than the corresponding M-P bond.[3] This situation can be advantageous when a vacant coordination site at the metal needs to be easily and reversibly opened up, as discussed below and in section *1.4*.

It is not surprising that the 'soft'/'hard' combination 'P_nN_m' ligands have found use in producing heterobinuclear complexes containing metals of different classes. The complex **F.1.1-1**, shown in **Figure 1.1**, is one such example; here the 'soft' phosphorus atoms are bound to a 'soft' iron(0) centre whilst the 'borderline' nitrogen atoms are bound to the 'borderline' nickel(II) centre. A wider range of heterobinuclear complexes should be accessible with 'P_nN_m' ligands, far greater than their 'P_{n+m}' and 'N_{n+m}' ligand analogues.[4]

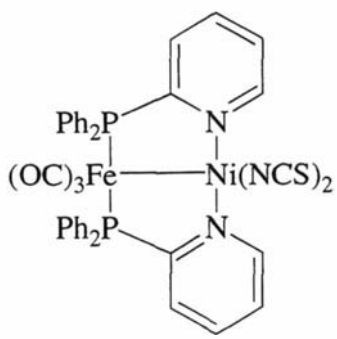

F.1.1-1

Figure 1.1 A heterobinuclear complex containing 'soft' Fe(0)-P and 'borderline/hard' N-Ni(II) interactions

Comparing the cadmium complex **F.1.2-1**, depicted in **Figure 1.2**, with its mercury analogue, one finds the Cd-N bond length to be 0.14Å shorter than the corresponding Hg-N distance and the Cd-P bond length to be 0.15Å longer than the Hg-P bond distance. Although certain specific steric and electronic factors may be operative, these changes in bond lengths are consistent with the 'harder' Lewis acid (Cd) being more tightly bound to the 'harder' base (N) and more weakly bound to the 'softer' base (P).[5]

[3] B. T. Heaton, J. A. Iggo, C. Jacob, J. Nadarajah, M. A. Fontaine, R. Messere and A. F. Noels, *J. Chem. Soc. Dalton Trans.*, 1994, 2875.
[4] Z. Zheng-Zhi et al., *J. Organomet. Chem.*, 1993, **454**, 221.
[5] M. B. Hossain et al., *Acta Cryst.*, 1982, B**38**, 91.

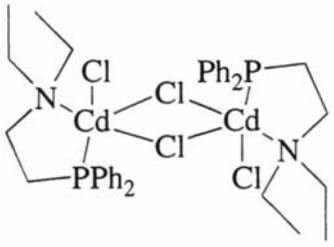

F.1.2-1

Figure 1.2 The 'harder' cadmium dimer binds more strongly to the 'harder' nitrogen donor, and vice versa for the 'softer' phosphorus donor, than its 'softer' mercury analogue

Metal oxidation state cycles and loss of a donor atom to accommodate incoming substrate(s) are common themes in homogeneous catalysis. The process can be facilitated when using 'P_nN_m' ligands, since changes in the metals oxidation state, due to oxidative addition or reductive elimination steps for example, translates to changes in the 'hardness'/'softness' properties of the metal, hence, one of the metal-donor bonds should weaken allowing an incoming substrate to more easily displace the weaker bound donor atom.

The above illustrates how the HSAB principle is obeyed, however, apparent coordination 'mismatches' have also been overcome with 'P_nN_m' ligands. This has been achieved by anchoring the ligand to the metal with a favourable interaction, e.g. a 'soft'-'soft' interaction, and by way of the chelate effect, a 'mismatched' bond, such as a 'hard'-'soft' pairing, is stabilised. For example, the 'P_2N' ligand **F.1.3-1** makes possible the stabilisation of the Sc-P bond found in the complex **F.1.3-2**. Here, the 'hard' amido anchors the ligand to the 'hard' Sc(III) centre and by way of close proximity the 'soft' phosphane is forced to bind.[6] The Sc-P bond lengths are of the order 2.8Å, which implies weak bonding, but still stronger than monodentate phosphanes at 3.00Å where dissociation is rapid.[7,8] This approach has made possible the synthesis of complexes containing bonds that are rare, like the Sc(III)-phosphane above, and others such as the first authenticated U(V)-phosphane complex.[9]

[6] M. D. Fryzuk et al., *Organometallics*, 1996, **15**, 3329.
[7] P. J. Shapiro et al., *Organometallics*, 1990, **9**, 867.
[8] P. J. Shapiro et al., *J. Am. Chem. Soc.*, 1994, **116**, 4623.
[9] P. G. Edwards et al., *J. Chem. Soc., Chem. Commun.*, 1994, 1967.

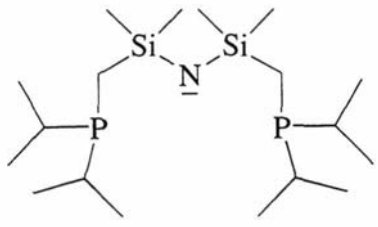

F.1.3-1

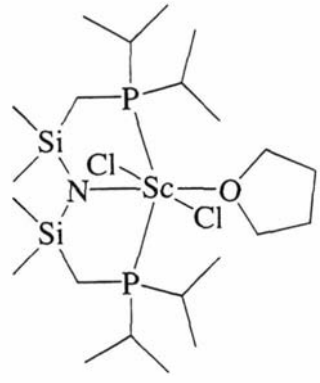

F.1.3-2

Figure 1.3 The stabilisation of a weak 'hard'-'soft' Sc(III)-P pairing by use of a strong 'hard'-'hard' Sc(III)-N 'anchor'

It has been established that this 'mismatched' bonding interaction is generally weak. However, this offers an advantage of possible high reactivity of the complex due to facile cleavage of the weak bond. This hemilability of the chelate ligand has been considered important in reactions involving migratory insertion into metal carbon bonds.[10]

'P_2N_2' ligands such as *N,N'*-bis[2-diphenylphosphanyl)phenyl]ethane-1,2-diamine and *N,N'*-bis[2-diphenylphosphanyl)phenyl]propane-1,3-diamine have been employed as efficient ligands for preparing unprecedented and previously elusive copper(II) phosphane complexes. The finely balanced 'soft'/'hard' character of the 'P_2N_2' ligating set has been proposed to play a major role in their stability.[11]

1.2 Electronic aspects of 'P_nN_m' ligands

The ready availability of antibonding sigma orbitals in phosphorus accounts for many of the differences in chemistry compared to those of nitrogen. Having these two electronically different atoms tethered together in one ligand, one might expect 'P_nN_m' ligands to behave somewhere between that of a polydentate phosphane ligand and a polydentate nitrogen donor ligand. In some situations this has been the case,[12] but other

[10] K. J. Cavell, *Coordination Chemistry Reviews*, 1996, **155**, 209.
[11] L. Crociani, F. Tisato, F. Refosco, G. Bandoli and B. Corain, *Eur. J. Inorg. Chem.*, 1998, 1689, and refs within.
[12] F. Refosco et al., *J. Chem. Soc.*, Dalton Trans., 1993, 605.

work on 'P_nN_m' ligands has seen these systems give rise to their own unique chemistry which has been peculiar to the polydentate phosphane and nitrogen analogues; this will be dealt with in section *1.4*.

The *trans* influence difference, set up by the P and N donors of the 'P_nN_m' ligand, can be used to great advantage over 'P_{n+m}' and N_{n+m}' analogues. Studies of palladium-catalysed substitution reactions of allylic substrates, such as that illustrated in **Scheme 1.1**, have produced some valuable results.[13]

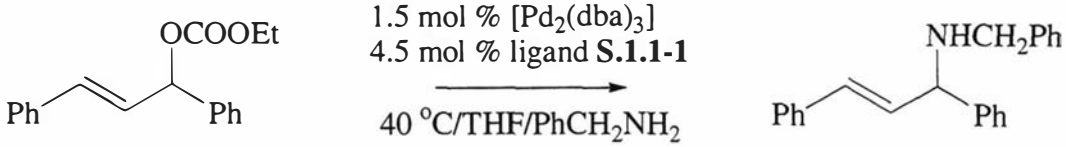

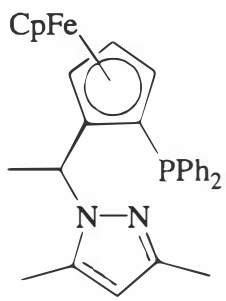

S.1.1-1

Scheme 1.1 An allylic amination reaction (above) catalysed by a palladium complex containing the 'PN' ligand **S.1.1-1** (below)

In this type of reaction the incoming nucleophile has a choice of attack sites on the allyl intermediate, as shown by **F.1.4-1** of **Figure 1.4**. When L^1-L^2 is a P-N chelating ligand with a P and N coordinated as L^1 and L^2, the nucleophile attack takes place preferentially at the allyl terminus *trans* to the phosphorus. One approach to explain this is to evoke the different electronic natures of the donor atoms of the P-N chelating ligand which set up a *trans* influence difference where the P-donor exerts a greater *trans* influence than the N-donor. Crystallographic and nuclear magnetic resonance (NMR) spectroscopy

studies supports the rendering of the *trans*-phosphorus carbon more electrophilic than its companion *trans* to the nitrogen.[14] Hence nucleophilic attack proceeds preferentially as indicated by **F.1.4-2**. In other words the 'P_nN_m' ligand makes use of the *trans* influence to steer the nucleophile toward one side of the allyl ligand.

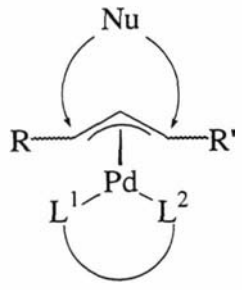

F.1.4-1

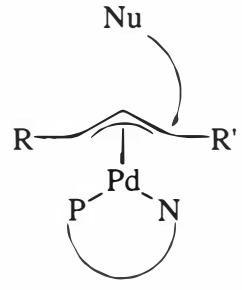

F.1.4-2

Figure 1.4 The choice of attack sites for an incoming nucleophile on a coordinated allyl intermediate

Square planar complexes of late transition metals bearing 'PN'-chelating ligands [MX_2(P-N)] (M = Pd, Pt; X: e.g., halide, alkyl) are known to allow highly stereoselective substitution reactions of the ligands X.[15] The stereochemical outcome of the ligand substitution reaction can be explained by the different electronic properties of the nitrogen and phosphorus donor atoms. For example, in the reaction of MeLi with [$PdBr_2$(PN)] (**F.1.5-1**) (PN = *o*-diphenylphosphino-*N,N*-dimethylbenzylamine), as depicted in **Figure 1.5**, the *trans*-labilising effect, which is larger for phosphorus than for nitrogen, should result in the incoming methyl group entering *trans* to the phosphorus to give the palladium-methyl complex **F.1.5-2**. However, it is the opposite, thermodynamically controlled, palladium methyl complex **F.1.5-3** where phosphorus and carbon avoid mutual *trans* positioning, that is found. The configuration between the phosphorus and the carbon, which is in accord with the strong *trans* influence of these atoms, ensures that competition for the same, *s,d*-hybrid orbital is prevented.[16]

---

[13] A. Togni *J. Am. Chem. Soc.*, 1996, **118**, 1031.
[14] P. S. Pregosin, *Organometallics*, 1996, **15**, 3496, and refs therein.
[15] J. Pfeiffer, G. Kickelbick and U. Schubert, *Organometallics*, 2000, **19**, 62, and refs with in.
[16] J. Boersma, W. de Graaf, S. Harder and G. van Koten, *J. Organomet. Chem.*, 1988, **358**, 545, and refs within.

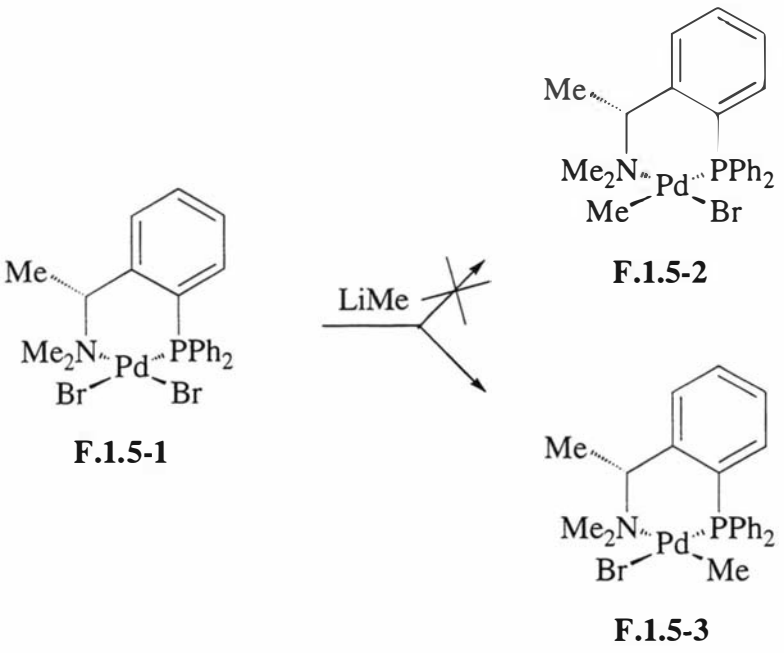

Figure 1.5 The different electronic properties of the phosphorus and nitrogen donor atom controls the stereochemical outcome of the ligand substitution reaction

The palladium-allyl complex **F.1.6-1**, depicted in **Figure 1.6**, shows unexpected electronic properties. Its ^{13}C NMR spectrum displays both new low and high frequency extremes for the CH_2 and CH chemical shifts of the ß-pinene (allyl) ligand in a cationic palladium(II) compound when compared to several analogous 'P_{n+m}' and 'N_{n+m}'/ß-pinene palladium complexes.[17] Complex **F.1.6-1** also shows greater differentiation of the CH_2 and CH carbons when compared to analogous complexes containing 'P_{n+m}' and 'N_{n+m}' ligands, such as the 'P_{n+m}' ligand **F.1.6-2**,[18] suggesting the observed chemical shifts have more to do with a P/N combination rather than the ferrocene moiety. Further support for this are the NMR results for an analogue of **F.1.6-1**, containing the ligand **F.1.6-3**,[19] whose CH_2 and CH carbons have chemical shifts on par with that of **F.1.6-1**. These NMR results are interesting as they reflect useful ground state properties of 'P_nN_m' ligands in that they significantly differentiate between the two allyl termini.

[17] U. Burckhardt, V. Gramlich, P. Hofmann, R. Nesper, P. S. Pregosin, R. Salzmann and A. Togni, *Organometallics*, 1996, **15**, 3496.
[18] A. Togni et al., *J. Am. Chem. Soc.*, 1994, **116**, 4062.
[19] P. Barbaro et al., *Organometallics*, 1994, **14**, 5160.

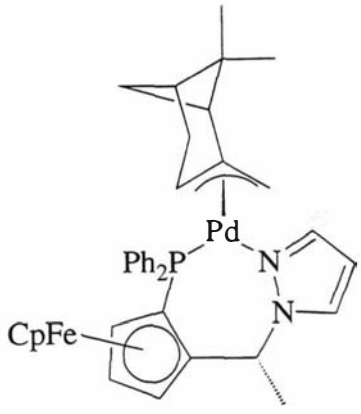

F.1.6-1

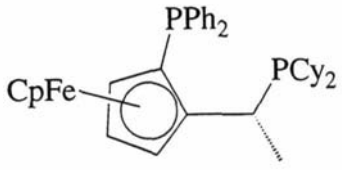

F.1.6-2

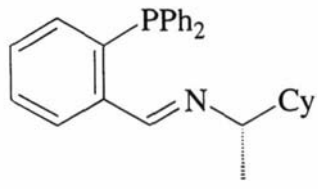

F.1.6-3

Figure 1.6 The palladium(II)-allyl complex (left) exhibits new high and low frequency extremes in the ^{13}C NMR spectrum of the allyl ligand. Similar extremes are found for the palladium(II)-allyl complex containing the 'PN' ligand shown far right. The palladium(II)-allyl complex containing the phosphorus analogue (middle) does not show any extraordinary characteristics

1.3 The reactivity of complexes containing 'P_nN_m' ligands

The unhooking of one of the 'P_nN_m' ligand donor atoms to create a vacant coordination site was touched on in section *1.1*. This chelate 'unzipping' plays a key role in the reactivity mechanisms of many 'P_nN_m' ligand complexes, for example, producing the active species in catalytic cycles.[20] Note however that 'P_{n+m}' and 'N_{n+m}' ligands have also shown this ring opening ability,[21] but, the added advantage with 'P_nN_m' ligands is that they may facilitate the formation of the active species by providing a weaker bond for cleavage, or at the very least offer selectivity towards which arm of the chelate would dissociate

With a view to further applications, facile 'P_nN_m' ligand ring opening could find possible advantages in cancer research. Gold(I) chelating phosphane complexes have been found to have significant antitumor properties. The chelate ring opening is expected to be a critical step in the mode of antitumor action.[22]

[20] F. Tisato et al., *Inorg. Chem.*, 1995, **34**, 1779.
[21] B. Milani et al., *J. Chem. Soc., Dalton Trans.*, 1996, 3139.
[22] A. L. Balch and E. Y. Fung, *Inorg. Chem.*, 1990, **29**, 4764.

The cytotoxic platinum complex (**F.1.7-1**), shown in **Figure 1.7**, has the unusual ability to bind strongly and rapidly to the N3 atom of thymine (**F.1.7-2**) (and uracil) under physiological conditions. There are few precedents for the rapid reaction of platinum complexes with thymine bases. The strong *trans* effect of the phosphorus atom in square-planar platinum(II) complexes is considered important. For **F.1.7-1**, the facile reaction with thymine is believed to be enhanced by the dangling arm amino group of the complex assisting the removal of the proton at the N3 position of the thymine substrate.[23]

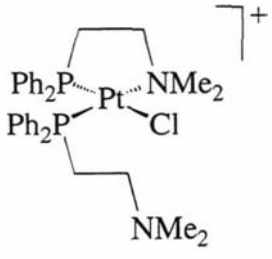

F.1.7-1

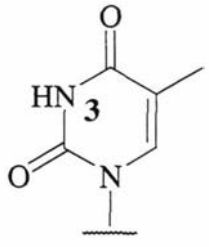

F.1.7-2

Figure 1.7 The complex (left) binds rapidly to the DNA base thymine (right) under physiological conditions

The complex **F.1.8-1**, in **Figure 1.8**, shows unprecedented activity and precision for the carbonylation of alkynes. These features are attributed to the unique ability of the 'PN' ligand to function as a chelate, playing a crucial role in the selectivity and rate-determining step of the catalytic cycle depicted by step **3** of **Scheme 1.2,** and at the same time as a mono-coordinating ligand, functioning as a 'proton messenger' to the active palladium centre in step **6**, the protonolysis step.[24]

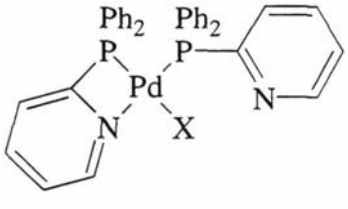

F.1.8-1

Figure 1.8 An exceptional alkyne carbonylation catalyst

[23] N. Margiotta, A. Habtemariam and P. J. Sadler, *Angew. Chem. Int. Ed. Engl.*, 1997, **36**, 1185.

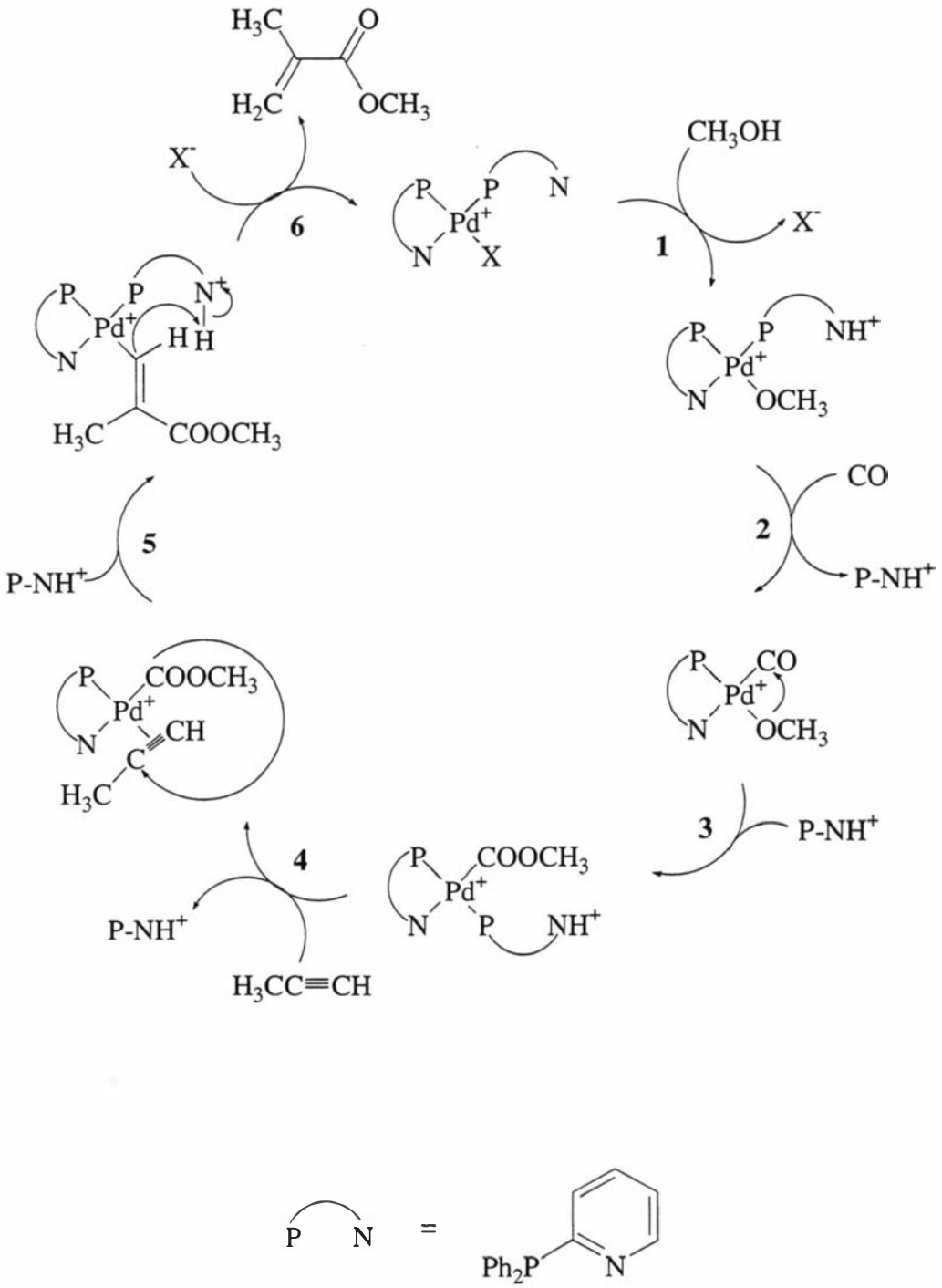

Scheme 1.2 A catalytic cycle for the carbonylation of an alkyne

[24] E. Drent et al., *J. Organomet. Chem.*, 1994, **475**, 57.

An additional bonus to the ligand unhooking in catalytic processes, is that a donor atom is now free to interact with the incoming substrate, which allows the potential for a preorganisation step before any association step with the metal. An interaction of this type is shown in **Scheme 1.3**. It shows the proposed mechanism for an asymmetric Grignard cross coupling reaction, involving the interaction of an unhooked nitrogen donor atom with the functional groups on the incoming substrate as shown by structure **S.1.3-2** in **Scheme 1.3**.[25]

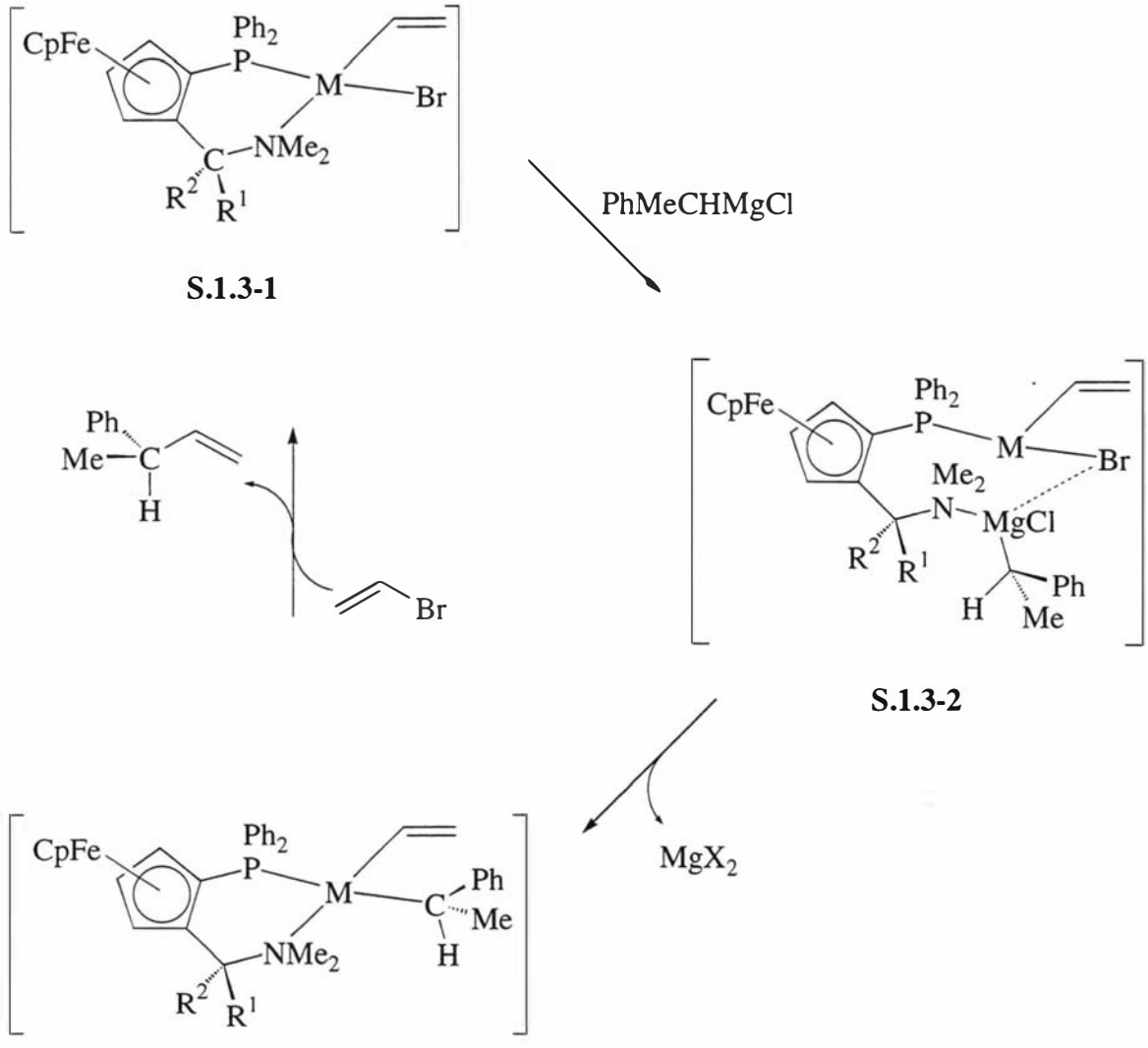

S.1.3-1

S.1.3-2

S.1.3-3

Scheme 1.3 The ring-opening reaction of a 'PN'-chelating ligand preceding a substrate preorganisation step in an asymmetric Grignard cross coupling reaction

[25] M. Kumada et al., *J. Am. Chem. Soc.*, 1982, **104**, 180.

This last point leads to an important aside; chirality can much more easily be appended to the nitrogen atom than the phosphorus atom. Arguments have been given in favour of better chirality transmission, within the catalyst, from optically active nitrogen ligands to prochiral substrates compared to optically active phosphanes. Having the chirality associated with,[26] or appended to,[27] the nitrogen centre of 'P_nN_m' ligands may offer 'better chirality transmission', in addition to stabilisation offered to the metal by the phosphane moiety and the benefit of multiple donor chelation.[28]

Novelty is becoming synonymous with the chemistry of 'P_nN_m' ligands. Another example is found in the palladium chemistry of the ligand 'P_2N' **F.1.9-1**, given in **Figure 1.9**. The stability of both the zerovalent (**F.1.9-2**) and divalent (**F.1.9-3**) palladium complexes of **F.1.9-1**, as well as the proven multifunctional behaviour of this 'PN_2' ligand, now opens a way to catalytic applications through a Pd(0)-Pd(II) cycle without additional stabilising ligands. Indeed, preliminary studies of allylic alkylation reactions have shown that palladium complexes of **F.1.9-1** are very active.[29]

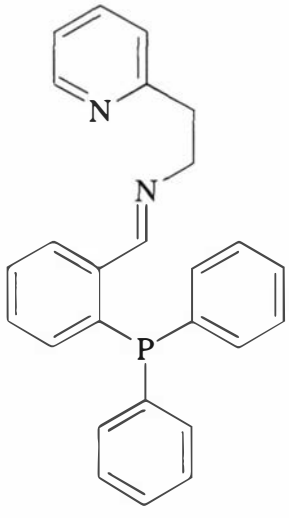

F.1.9-1

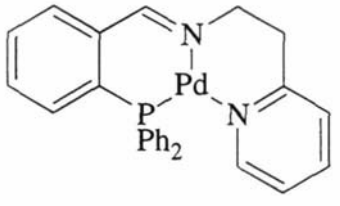

F.1.9-2

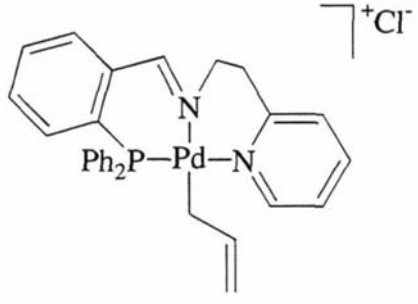

F.1.9-3

Figure 1.9 The 'PN_2' ligand (above) affords stable palladium(0) and palladium(II) complexes (below left and right respectively) and opens the way for a Pd(0)-Pd(II) catalytic cycle

[26] R. Noyori et al., *Organometallics*, 1996, **15**, 1087.
[27] C. Bianchini et al., *Organometallics*, 1995, **14**, 1489.
[28] F. A. Cotton and H. Bo, *Progress in Inorganic Chemistry*, 1992, vol. 40, John Wily & Sons., p180.
[29] K. Vrieze, Organometallics, 1996, **15**, 3022.

An intriguing reactivity pattern involving the 'P_2N' ligand **S.1.4-1** is shown in **Scheme 1.4**. Here, the ruthenium(II) fragment [(**S.1.4-1**)$RuCl_2$] assists the coupling of phenylacetylene with H_2S to give 2-phenylethanethial. This complex can then be reacted with cyclopentadiene in a stereoselective Diels-Alder reaction to give endo-6-benzyl-1-thiabicyclo[2.2.1]hept-3-ene.[30]

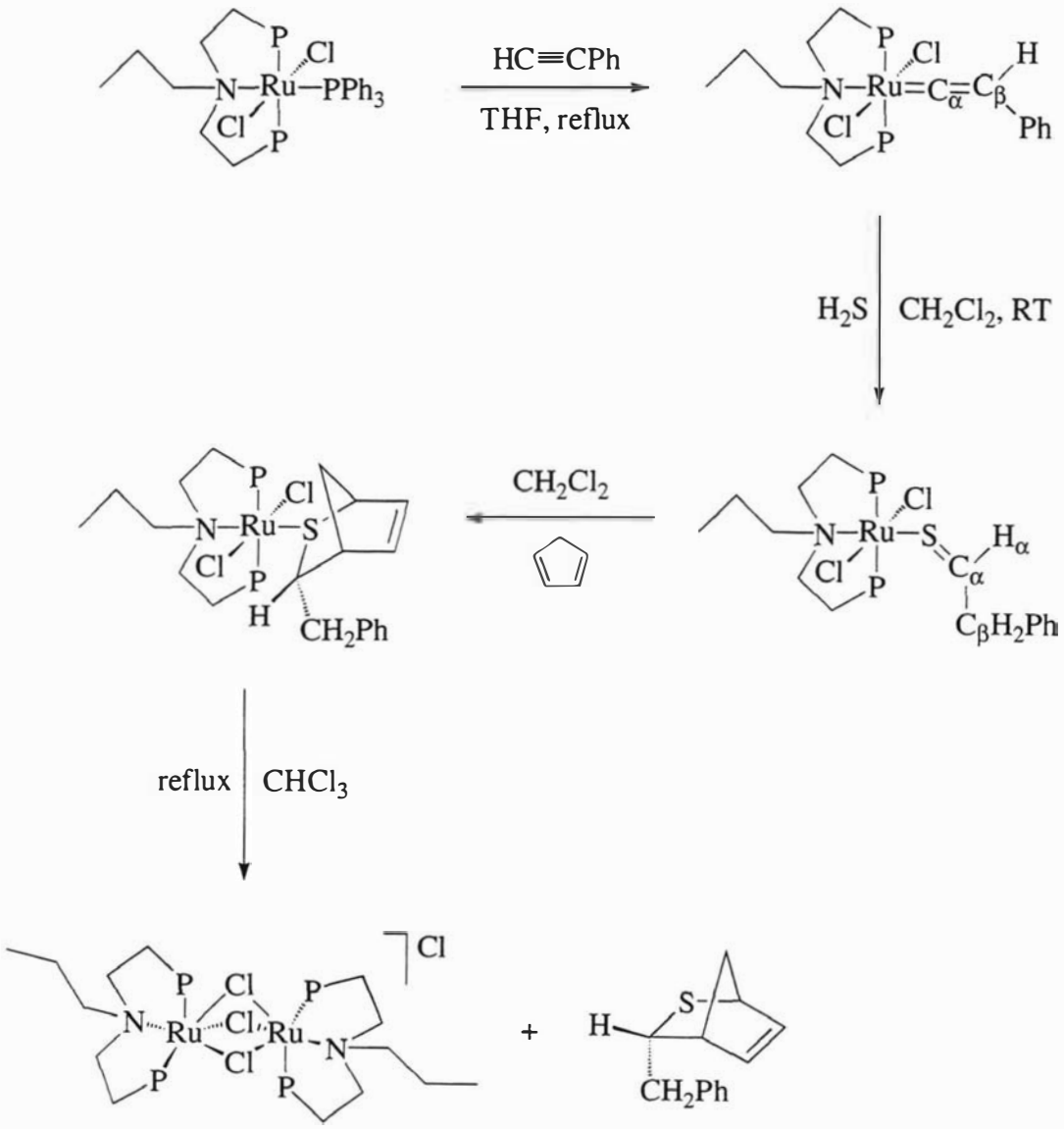

Scheme 1.4 A stereoselective Diels-Alder reaction involving the ancillary 'P_2N' ligand **S.1.4-1** shown below

[29] K. Vrieze, Organometallics, 1996, **15**, 3022.
[30] C. Bianchini, L. Glendenning, M. Peruzzini, A. Romerosa and F. Zanobini, *J. Chem. Soc., Chem. Commun.*, 1994, 2219.

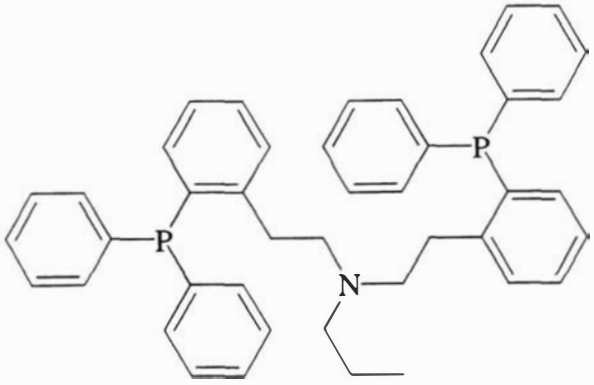

S.1.4-1

Other areas of reactivity studies have seen the 'PN' ligand **F.1.10-1**, shown in **Figure 1.10**, stabilising rhodium and iridium complexes which reversibly bind the small molecules O_2 and CO[31] and the 'P_nN_m' ligand **F.1.10-2** investigated in the modelling of carbonic anhydrase enzymes.[32]

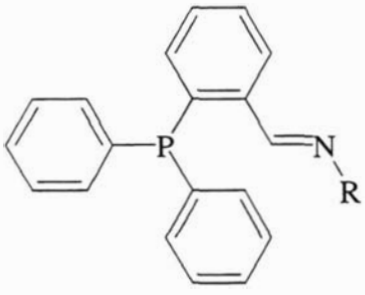

F.1.10-1

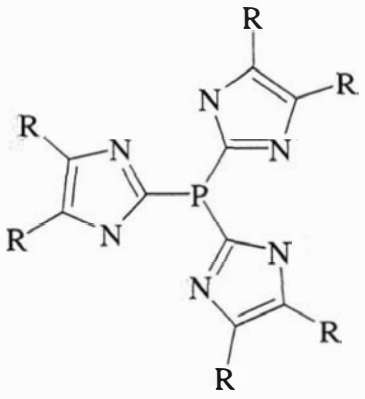

F.1.10-2

Figure 1.10 Some other 'P_nN_m' ligands

[31] C. Bianchini et al., *Inorg. Chem.*, 1994, **33**, 1622.
[32] R. S. Brown et al., *J. Am. Chem. Soc.*, 1981, **103**, 6953.

1.4 A comparison of the 'P_nN_m' ligands with their 'P_{n+m}' and 'N_{n+m}' ligand analogues

This section aims to throw light on the question; do mixed 'P_nN_m' ligands offer any advantages or, for that matter, disadvantages over polyphosphane ('P_{n+m}') or polynitrogen ('N_{n+m}') donor ligands? It appears certain that for the majority of work reported, 'P_nN_m' ligands always behave quite differently and sometimes unexpectedly from their 'P_{n+m}' or 'N_{n+m}' ligand counterparts.

For instance, the platinum dimethyl complex [$Pt(Me)_2(Ph_2PCH_2CH_2NMe_2\text{-}\kappa^2P,N)$] readily undergoes oxidative addition of trimethoxysilane, while the corresponding bis(phosphane) complex [$Pt(Me)_2(dppe\text{-}\kappa^2P,P)$] (dppe = $Ph_2PCH_2CH_2PPh_2$) is unreactive. The higher reactivity was attributed to the reversible decoordination of the weakly bonded nitrogen atom that reversibly opens a coordination site at the metal.[15]

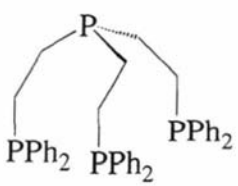

F.1.11-1

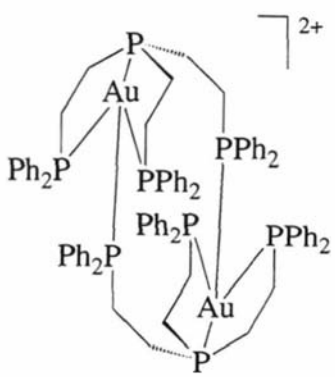

F.1.11-2

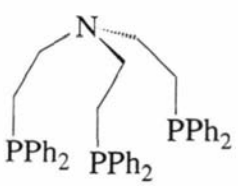

F.1.11-3

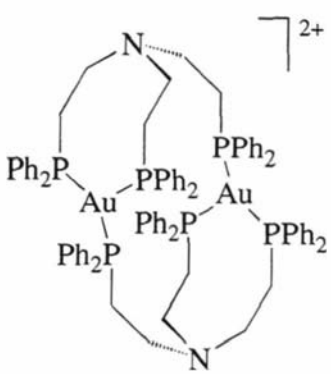

F.1.11-4

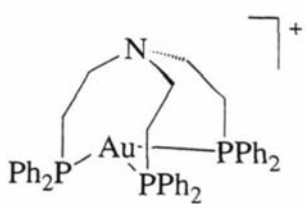

F.1.11-5

Figure 1.11 A comparison between the gold(I) chemistry of a 'P_3N' ligand (above) and its 'P_4' analogue (below)

Balch and Fung[22] demonstrated that Au(I) complexes of the ligand **F.1.11-1** are four-coordinate at the metal centre and exist as dimers, as in **F.1.11-2**. In contrast, Fackler et al.[33] showed the nitrogen analogue **F.1.11-3** forms three-coordinate dimers of type **F.1.11-4** with the pivotal nitrogen not bound and, in addition, three-coordinate monomer cations such as **F.1.11-5** can also be isolated.

Another example of comparative differences, between 'P_nN_m' ligands and their 'P_{n+m}' and 'N_{n+m}' analogues, occurs in the chemistry of the rare technetium(V)-phosphane species. Consider the reaction of $[NBu_4][TcO_4]$ with a ligand L under appropriate conditions. When L is a diphosphane ('P_2') or diamino ('N_2'), dioxotechnetium(V) complexes are always obtained.[34,35] However, when L is the 'PN' ligand **F.1.12-1**, shown in **Figure 1.12**, the dioxo species can not be obtained despite exhaustive efforts. In this case the mono oxo species **F.1.12-2** is the product of the reaction [11]. A mono oxo complex is also produced when L is the 'P_2N_2' ligand **F.1.12-3**, giving the complex **F.1.12-4**.[20]

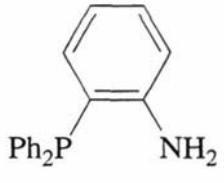

F.1.12-1

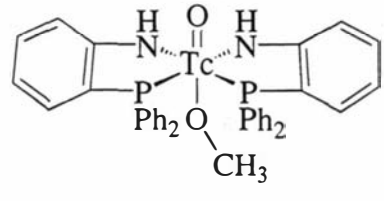

F.1.12-2

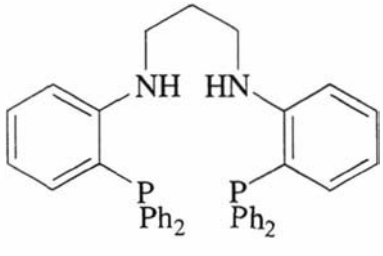

F.1.12-3

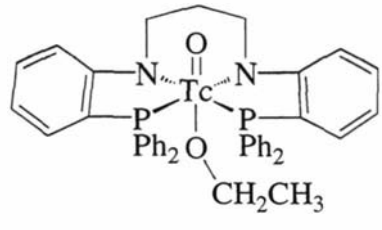

F.1.12-4

Figure 1.12 Mono oxo complexes (right) containing 'P_nN_m' ligands (left)

[33] J. P. Fackler, Jr. et al., *Inorg. Chem.*, 1993, **32**, 5800.
[34] E. Deutsch et al., *Inorg. Chem.*, 1984, **23**, 3184.
[35] M. E. Kastner, M. J. Lindsay and M. J. Clarke, *Inorg. Chem.*, 1982, **21**, 2037, and refs therein.

The complex $[Fe(NO)_2Cl(L)]$ when L is 2-(diphenylphosphino)pyridine and bound through the phosphorus donor atom, is unstable in solution and readily forms the species **F.1.13-1**, depicted by **Figure 1.13**, where an O has been extracted from an NO ligand. When L is triphenylphosphane the $[Fe(NO)_2Cl(L)]$ complex is stable. Guillane and Postel concluded from these observations that the σ/π bonding character of L plays a key role in the stabilisation of the Fe-NO bond.[36] In contrast to this conclusion, theoretical studies on 2-(diphenylphosphino)pyridine have shown no evidence of significant perturbation of the phosphorus atom's electronic structure by the presence of a nitrogen heteroatom in the aromatic ring. Therefore the reason, why pyridylphosphanes behave differently to the analogous phenylphosphanes as ligands, was concluded to lie in the nitrogen heteroatom being able to provide extra electron donation or basic centres, rather than any through bond electronic influence.[37]

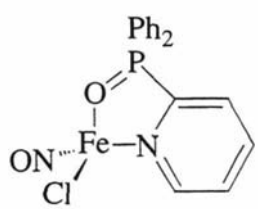

F.1.13-1

Figure 1.13 The breakdown product of the unstable complex $[Fe(NO)_2Cl(2\text{-}(diphenylphosphino)pyridine)]$

As touched on in section *1.3*, there are advantages in catalysis with 'P_nN_m' ligands over their 'P_{n+m}' and 'N_{n+m}' ligand analogues. In enantioselective allylic amination reactions, for example see **Scheme 1.1**, 'P_nN_m' ligands perform routinely better than their 'P_{n+m}' counter parts,.[17]

Chemoselective reduction of α,β-unsaturated ketones to allylic alcohols, as demonstrated by **Scheme 1.5**, is shown by a restricted number of transition metal complexes. Only two examples are known for the enantioselective version of this reduction; both of these involve 'P_nN_m' ligands.[27] The ligands are the 'P_2N' ligand **F.1.14-1** and the 'P_2N_2' ligand **F.1.14-2**, shown in **Figure 1.14**, the nitrogen donor was postulated to

[36] P. Guillaume and M. Postel, *Inorg. Chim. Acta*, 1995, **223**, 109.

play a key role. A key step in the proposed mechanism was the unhooking of the nitrogen donor, as shown in **Scheme 1.5**. This was supported by the fact that when the 'P_3' ligand **F.1.14-3**, the phosphorus analogue of **F.1.14-1** and **F.1.14-2**, was used in place of the 'P_nN_m' ligands **F.1.14-1** and **F.1.14-2**, the result was inactivation of the catalytic process;[38] probably due to the reluctant cleavage of the stronger metal-phosphorus bond formed by **F.1.14-3** when compared to the analogous metal-nitrogen bond formed by **F.1.14-1** and **F.1.14-2**.

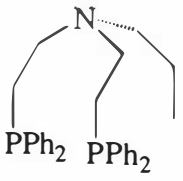

F.1.14-1

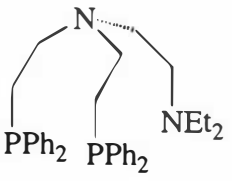

F.1.14-2

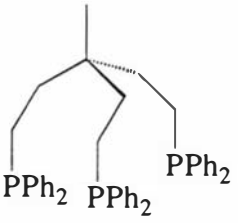

F.1.14-3

Figure 1.14 The two ligands on the left have been successfully employed in the chemoselective reduction of α,β-unsaturated ketones to allylic alcohols, as shown in **Scheme 1.5**, whilst the phosphorus analogue on the right inactivates the catalyst

[37] S. T. Howard et al., *Inorg. Chem.*, 1996, **35**, 5805.
[38] C. Bianchini et al., *J. Am. Chem. Soc.*, 1990, **112**, 9190.

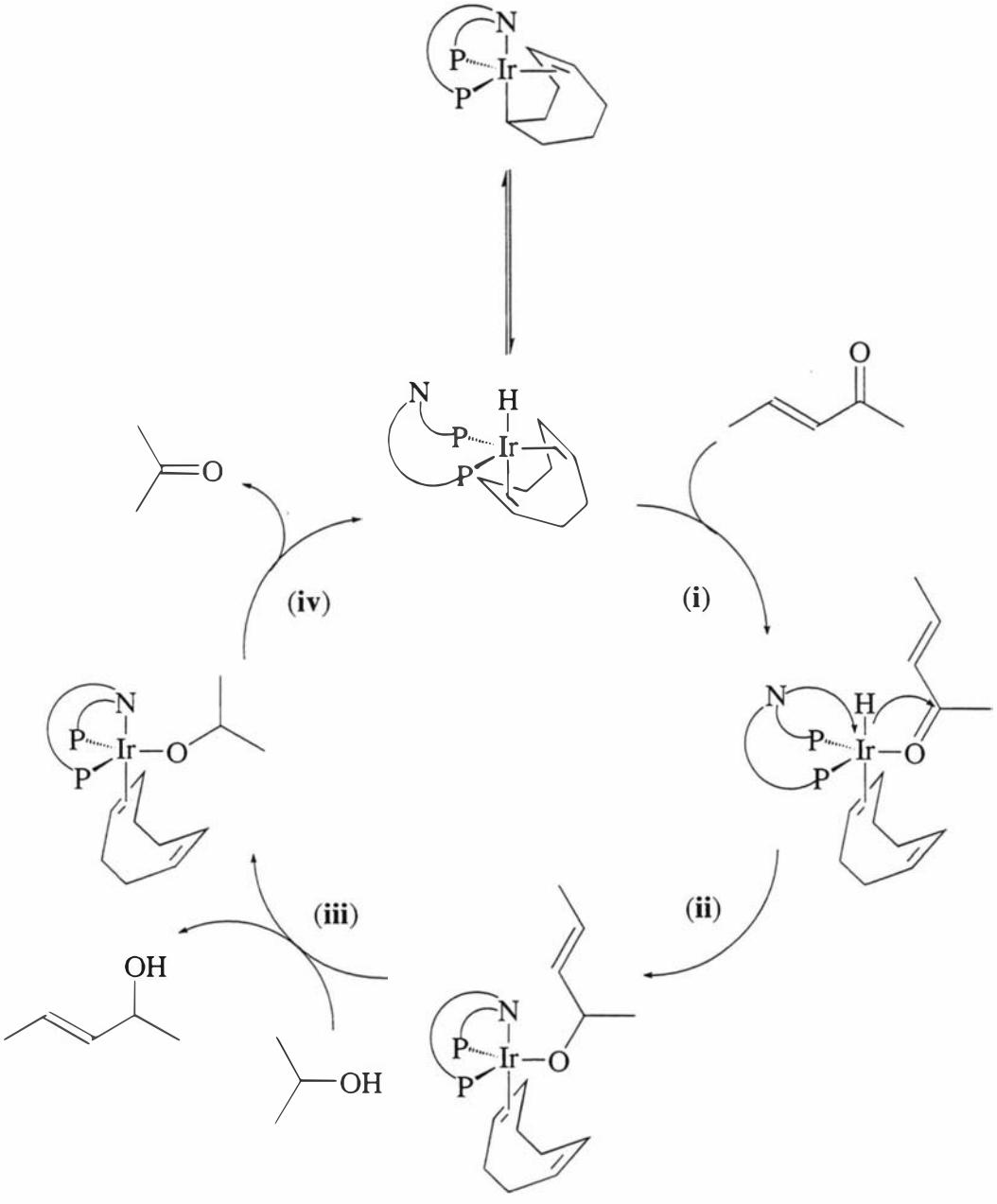

Scheme 1.5 A proposed mechanism for the chemoselective catalysis in the hydrogen-transfer reduction of α,β-unsaturated ketones involving a 'P_2N' ligand. (**i**) The ketone approaches the metal and displaces one olefinic end of the 1,5-cyclooctadiene. (**ii**) The selective transfer of a hydride to the carbonyl group occurs to give an alkoxy complex, a path that may be promoted by intramolecular coordination of the nitrogen donor to the metal. (**iii**) A new alkoxy complex and allylic alcohol is formed with the secondary alcohol in excess. (**iv**) Finally, the hydrido catalyst is restored via a β-H elimination process.[39]

[39] The description of the catalytic cycle is taken from ref 51

1.5 Applications of 'P_nN_m' ligands

The area of applied chemistry concerning 'P_nN_m' ligands is relatively small at present. The reason being simply the relative newness of the ligand type with respect to what is understood about its fundamental coordination, organometallic and catalytic chemistry. Despite this, there is still a remarkably diverse range of applications.

The major applied area of chemistry covering 'P_nN_m' ligands, is without doubt, catalysis. The reason for this seems to be that many 'P_nN_m' ligands are viewed as derivatives of the ubiquitous ancillary ligand in catalysis - the aryl/alkylphosphane. Catalytic uses of 'P_nN_m' ligands span from areas of industrial chemistry[24] to laboratory reagents in synthetic organic chemistry..[40,41,42,43,44]

The 'P_2N_2' ligand **F.1.12-3**, shown in **Figure 1.12** has been found to suit metal extraction processes and is extremely selective for copper.[45] 'P_nN_m' ligands have also seen excursions into materials science,[46] as found for the ligand **F.1.15-1**, depicted in **Figure 1.15**. The ligand **F.1.15-2** has shown potential in radiopharmacology.[47]

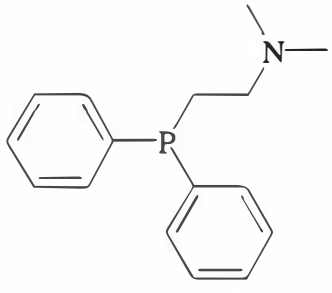

F.1.15-1

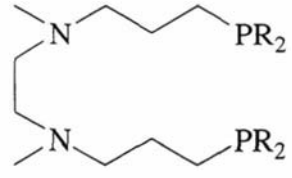

F.1.15-2

Figure 1.15 Ligands which have shown promise in areas of application

[40] A. Schnyder et al., *Angew. Chem., Int. Ed. Engl.*, 1995, **34**, 931.
[41] B. M. Trost et al., *J. Am. Chem. Soc.*, 1995, **117**, 9662.
[42] B. M. Trost et al., *J. Am. Chem. Soc.*, 1995, **117**, 7247.
[43] G.C. Lloyd-Jones and A. Pfaltz, Angew. *Chem., Int. Ed. Engl.*, 1995, **34**, 462.
[44] H. Kuboto and K. Koga, *Tetrahedron Lett.*, 1994, **35**, 6689.
[45] Y. Cheng and D. J. Schiffin, *Inorg. Chem.*, 1994, **33**, 765.
[46] D.G. Evans et al., *Angew. Chem., Int. Ed. Engl.*, 1996, **35**, 1850.
[47] E. Deutsch et al., *Inorg. Chem.*, 1993, **32**, 3236.

The platinum(II) compound **F.1.6-1** is cytotoxic to several cancer cell lines including *cis*-platin-resistant cells. In water it exists as a mixture of ring-closed (**F.1.6-2**) and ring-opened forms, as shown in **Figure 1.16**.[23]

F.1.6-1 **F.1.6-2**

Figure 1.16 A 'PN' ligand complex with anticancer properties

In the future, many more examples in the above areas are destined to emerge alongside new areas altogether, as research carried out on new 'P_nN_m' ligands is continually producing much new and sometimes unusual chemistry, as demonstrated by sections *1.1* through *1.5*.

PART 2 THE PRESENT STUDY

1.6 Introduction for Part 2

From Part 1, one may feel that the majority of 'P_nN_m' ligands investigated are of either PN or P_2N_2 type ligands. This is indeed the case. Relatively few systems have been studied where the ligand has only three potential donor P/N atoms in the ligand, such as 'P_2N' or 'PN_2' systems, the ligand 2-(diphenylphosphino)-N-[2-(diphenylphosphino)benzylidene]benzeneamine (**PNCHP**) is one such 'P_2N' ligand and is the focus for the research in this thesis.

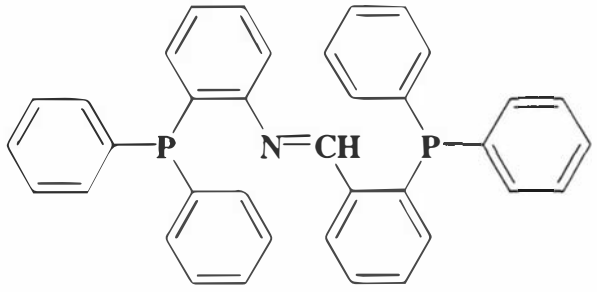

PNCHP

1.7 The 'P_2N' ligand PNCHP

The 'P_2N' Schiff base ligand PNCHP can be visualised as two triphenylphosphane moieties tethered together in the *ortho* positions by an imine linker. Since the imine bond has no plane of symmetry perpendicular to the C=N axis, the two phosphorus atoms are inequivalent. This feature alone is unusual to diphosphane systems[48] and provides an excellent handle for characterising the metal complexes solution structure by ^{31}P NMR.
The ligand PNCHP was first synthesised by Duckworth.[49] However, the compound was only used as an intermediate in synthesis of the 'P_2N' 2-(diphenylphosphino)-N-[(2-diphenylphosphino)benzyl]benzeneamine (**PNHCH$_2$P**). Consequently, only the coordination chemistry of the PNHCH$_2$P ligand was explored by Duckworth.

[48] S. O. Grim, R. C. Barth, J. D. Mitchell and J. Del Gaudio, *Inorg. Chem.*, 1977, **16**, 1776.

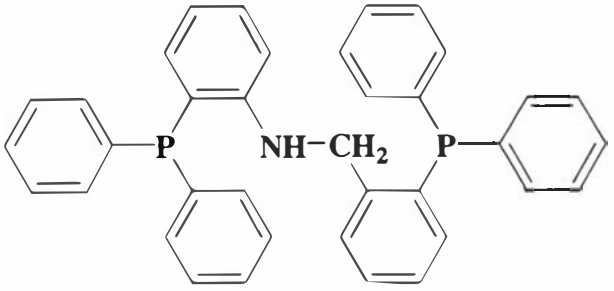

PNHCH$_2$P

1.8 Previous coordination chemistry of the ligand PNCHP

The first coordination chemistry studies on the PNCHP ligand were carried out by Halstead.[50] In the work, the coordination chemistry of the ligand with nickel(II) was investigated, resulting in the characterisation of the square-planar compounds [Ni(PNCHP-κ^3*P,N,*P)X]ClO_4, where X^- is Cl^-, Br^- or I^- and the octahedral compound [Ni(PNCHP)$(NO_3)_2$]. The perchlorate salts were synthesised in a straight forward manner by reaction of the PNCHP ligand with Ni$X(ClO_4)$ and the nitrate compound formed by reacting one equivalent of PNCHP with $Ni(NO_3)_2 \bullet 6H_2O$. However, when two equivalents of the PNCHP ligand were reacted with $Ni(ClO_4)_2 \bullet 6H_2O$, in an attempt to obtain [Ni(PNCHP-κ^3*P,N,P*)$_2$]$(ClO_4)_2$, an analogue of the known compound [Ni(hyzPNN-κ^3*P,N,N*)$_2$]ClO_4 (**F.1.7-1**),[50] two unusual products resulted. The products were [Ni(PNCHP-κ^3*P,N,*P)Cl]ClO_4 and the cyclic phosphonium salt [PN(H)CHP]ClO_4 (**F.1.7-2**).

[49] P. A. Duckworth, *Polydentate Phosphorus-Nitrogen Hybrid Ligands Containing the 2-Aminophenyl Group*, 1984, Ph.D. Thesis, University of Sydney.
[50] M. J. R Halstead, *Iminophosphine Complexes of Ni(II)*, B.Sc(Hons) report, 1991, Massey University.

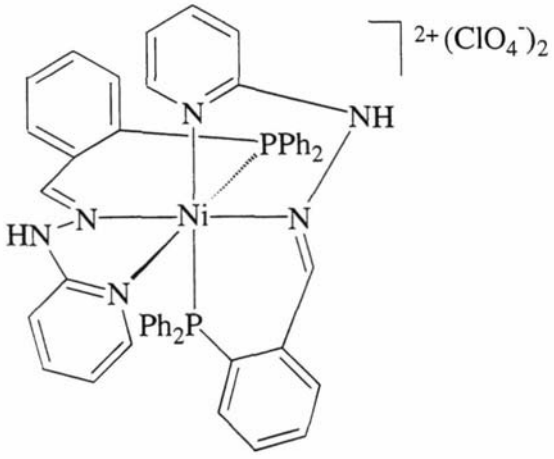

F.1.7-1

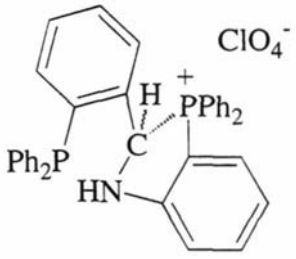

F.1.7-2

Figure 1.17 A bis-'PN_2' Ni(II) complex (left) and the cyclic phosphonium salt $[PN(H)CHP]ClO_4$ (right)

It was proposed that the coordinated Cl^- in $[Ni(PNCHP\text{-}\kappa^3P,N,P)Cl]ClO_4$ had resulted from the reduction of ClO_4^- by ethanol, in the presence of nickel and PNCHP, and that the acetic acid generated provided the proton source for formation of $[PN(H)CHP]ClO_4$, as shown by **Equation 1.1**.

$$Ni(ClO_4)_2 \bullet 6H_2O + 2CH_3CH_2OH + 2PNCHP \rightarrow [Ni(PNCHP)Cl]ClO_4 + 8H_2O + CH_3COOH + [PN(H)CHP]^+ + CH_3COO^-$$

Equation 1.1

The cyclic phosphonium salt $[PN(H)CHP]ClO_4$ can be synthesised by direct reaction of PNCHP with $HClO_4$.

Further coordination studies on the PNCHP ligand were carried with the metals copper(I) and silver(I) by Fan.[51] The copper(I) complexes $[Cu(PNCHP)ClO_4]$ and [Cu(PNCHP)L] (L = ligands containing S or N donor atoms) were prepared along with the silver(I) complex $[Ag(PNCHP)ClO_4]$ and the dinuclear complex $[\{Ag(PNCHP)(SCN)\}_2$. Single-crystal X-ray diffraction studies on the $[M(PNCHP)ClO_4]$ (M = Cu or Ag) complexes revealed that the PNCHP ligand behaved differently for each complex. For the

[51] X. Fan, *Structural Studies on the Interactions of a P_2N Tridentate ligand with Copper(I), Silver(I) and Sulfur*, 1995, MSc Thesis, Massey University.

copper(I) complex, the PNCHP ligand was terdentate with two short Cu-P bonds (2.2032(12) and 2.208(13) Å) and a Cu-N bond (2.159(5) Å). In contrast for the silver(I) complex, the PNCHP ligand was bordering on bidentate with two Ag-P bonds (2.447(3) and 2.438(3) Å) and a long and weak Ag-N bond (2.926(10) Å). Both the copper and silver complexes showed a distorted tetrahedral coordination geometry around the metal. Fan also demonstrated the quite different nature of the two inequivalent phosphorus atoms in the ligand. The phosphorus atom closest to the nitrogen atom appeared to have a greater nucleophilicity than the phosphorus atom furthest away. This was concluded from monitoring the reaction of the ligand with sulfur (S_8), where the product S=PNCHP predominated over the product PNCHP=S.

In summary, the work of Halstead has shown that the PNCHP ligand has introduced some unpredictable and unusual chemistry for square-planar nickel(II) complexes, whilst in Fan's studies, the PNCHP ligand showed how the effect of having mixed donor atoms within the same ligand can subtly influence a complexes molecular structure and coordination preferences within a tetrahedral coordination environment.

In a previous study, the author set out to establish the coordination preferences of PNCHP in a octahedral coordination environment. The group 6 metal carbonyls were chosen due to the structural information available from C-O stretching frequencies.[52] In addition, they offered a entry point into the realms of organometallic chemistry, where such ligand types have shown promise in catalysis.[53] The results of these fundamental coordination studies on PNCHP are summarised in the introduction of Chapter 2, suffice to say that six new coordination modes, in addition to those in the complexes above, were fully characterised. The coordination modes of PNCHP, characterised thus far, are given in **Figure 1.8**.

---

[52] P. S. Braterman, *Metal Carbonyl Spectra*, Academic Press, 1975.

[53] See for example; G. Franciò, R. Scopelliti, C. G. Arena, G. Bruno, D. Drommi and F. Faraone, *Organometallics*, 1998, **17**, 338; R. Noyori and S. Hashiguchi, *Acc. Chem. Res.* 1997, **30**, 97; F. Ungváry, *Coord. Chem. Rev.*, 1997, **167**, 233; A. Carmona, A. Corma, M. Iglesias, A. San José and F. Sánchez, *J. Organomet. Chem.*, 1995, **492**, 11.

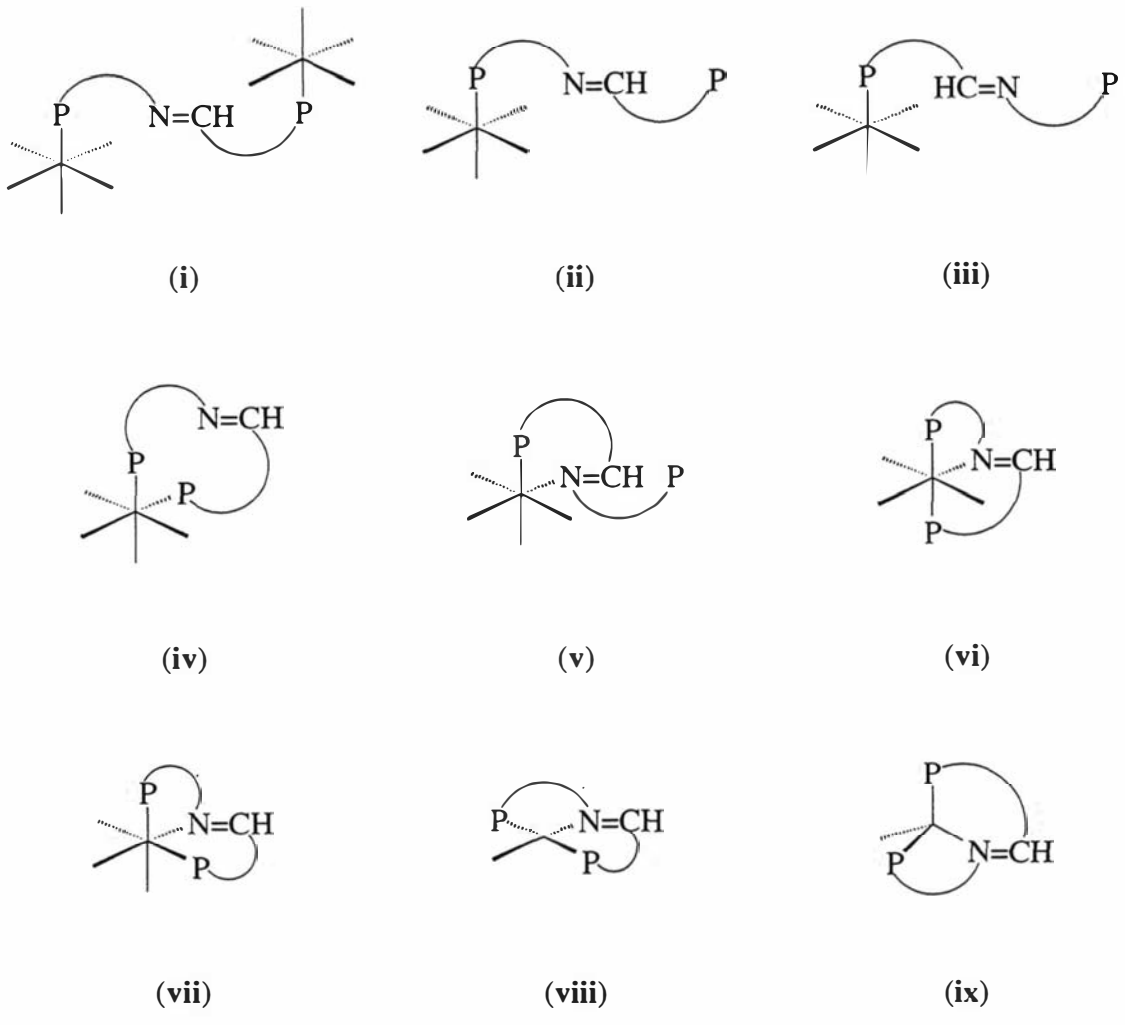

Figure 1.8 Observed coordination modes of the PNCHP ligand (PNCHP = P-N=CH-P)

1.9 The Present Study

In this thesis, extension to some of the work above will be presented, along with the coordination chemistry and reactivity of new complexes containing the PNCHP ligand, This includes the further exploration of the coordination chemistry of the ligand in square-planar and octahedral complexes, as well as investigating the coordinated ligands reaction to both nucleophiles and electrophiles. Studies on the interaction of the PNCHP ligand with trinuclear clusters will also be undertaken. The work is divided as follows:

• **Chapter 2** will extend the previous investigations on the PNCHP ligand with the group 6 metal-carbonyls, including a *fac* to *mer* isomerisation kinetic study and a comparison of the complexes of the PNCHP and $PNCH_2P$ ligands.

• **Chapter 3** will look at the reactivity of the PNCHP-group 6 metal-carbonyl complexes with protic acids.

• **Chapter 4** will discuss the palladium(II) and platinum(II) chemistry of PNCHP, which focuses on the competition of PNCHP with strong bidentate and terdentate ligands in an attempt to obtain unusual five and six coordinate M(II) species.

• **Chapter 5** is a study of the rhodium(I) chemistry, with particular emphasis on complex reactivity.

• **Chapter 6** investigates the coordination chemistry of PNCHP in a trinuclear osmium cluster environment so as to encourage new coordination modes of the ligand.

2 The Group 6 Metal Carbonyl Complexes

2.1 Introduction

The 'P_2N' mixed donor ligand 2-(diphenylphosphino)-N-[2-(diphenylphosphino)benzylidene]benzeneamine **PNCHP** produces some unexpected and interesting coordination chemistry with the group 6 metal carbonyls, as previously investigated by the author[1] and summarised here.

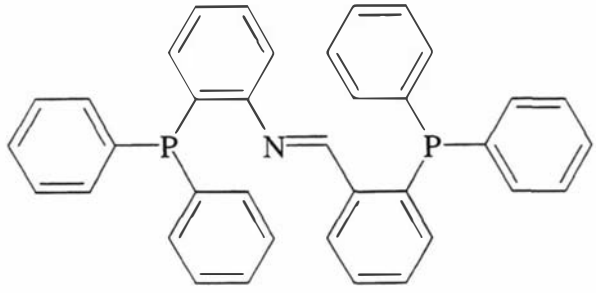

PNCHP

The PNCHP ligand reacts with $[Cr(CO)_4(NBD)]$ or $[M(CO)_4(C_5H_{11}N)_2]$ (M = Mo or W; NBD = norbornadiene; $C_5H_{11}N$ = piperidine), to yield complexes of the type *cis*-$[M(CO)_4(PNCHP)]$, where PNCHP is coordinated as a κ^2 bidentate ligand. In these complexes, however, it was found that the bidentate donor set of PNCHP is dependant on the metal. When the metal is chromium (**F.2.1-1**) , PNCHP behaves as a 'P,N' bidentate ligand, but when the metal is molybdenum (**F.2.1-2**) or tungsten (**F.2.1-3**), a 'P,P' bidentate PNCHP ligand is favoured, as shown in **Figure 2.1**. This difference can be rationalised by using the hard/soft acid/base (HSAB) principle, that is, the relative hardness or softness of the metal and donor atom concerned.[2] Both the chromium atom and the imine nitrogen

[1] S. M. F. Kennedy, *Structural Studies on a P_2N Triligate with Group 6 Metal Carbonyls*, B.Sc(Hons) report,1995, Massey University.
[2] R. G. Pearson, *Chemical Hardness*, 1997, Wiley-VCH, Weinheim

donor atom can be considered chemically harder than the softer molybdenum/tungsten-phosphorus atom pairing.

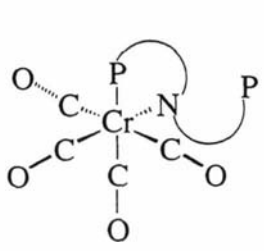

(P-N-P = PNCHP)
F.2.1-1

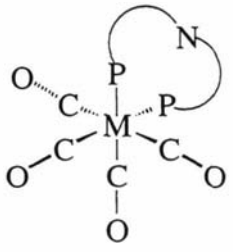

(M = Mo) **F.2.1-2**

(M = W) **F.2.1-3**

Figure 2.1 The bidentate coordination modes of the PNCHP ligand (P-N-P) with group 6 metal tetracarbonyl complexes.

Note that the **PNCHP** ligand is unsymmetrical, giving rise to inequivalent phosphorus atoms. This raises the question of which phosphorus atom is coordinated in the chromium tetracarbonyl complex, *cis*-[$CrCO)_4$(PNCHP-κ^2*N,P*)] (**F.2.1-1**)? The answer was not resolved in the previous study, but, is one of the findings that will be reported in this chapter. With one phosphorus atom and the nitrogen atom coordinated in the *cis*-[$CrCO)_4$(PNCHP-κ^2*N,P*)] (**F.2.1-1**) complex, a phosphorus atom is left 'dangling'. It was decided to investigate its reactivity, by making use of reagents such as sulfur or methyliodide, to see if the 'dangling' phosphorus atom was open to electrophilic attack. These findings will also be reported here.

Heating the tetracarbonyl complexes, *cis*-[$Cr(CO)_4$(PNCHP-κ^2*N,P*)] (**F.2.1-1**) or *cis*-[$M(CO)_4$(PNCHP-κ^2*P,P*)] (M = Mo (**F.2.1-2**) or W (**F.2.1-3**)), in toluene, results in coordination of both phosphorus atoms and the nitrogen atom of the PNCHP ligand, at the expense of one CO ligand from the starting material, to afford the tricarbonyl complexes *mer*-[$M(CO)_3$(PNCHP-κ^3*P,N,P*)] (M = Cr (**F.2.2-1**), Mo (**F.2.2-2**) or W (**F.2.2-3**)).

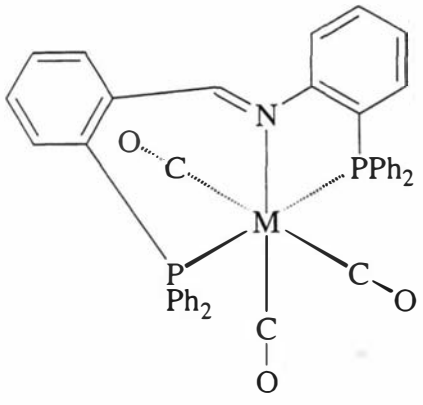

F.2.2-1 (M = Cr)
F.2.2-2 (M = Mo)
F.2.2-3 (M = W)

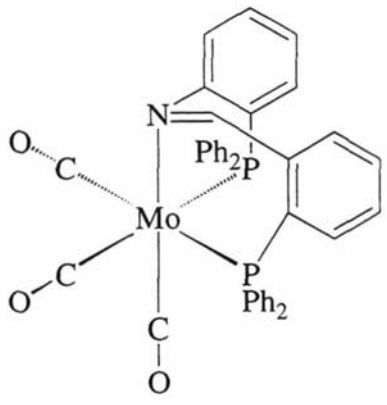

F.2.2-4

Figure 2.2 The terdentate coordination modes of the PNCHP ligand with group 6 metal tricarbonyl complexes.

At least in the cases when the metal is molybdenum or tungsten, the complex must also undergo a ligand rearrangement, as the *cis* phosphorus atoms of *cis*-[M(CO)$_4$(PNCHP-κ^2*P,P*)] (M = Mo (**F.2.1-2**) or W (**F.2.1-3**)), become *trans* in *cis*-[M(CO)$_3$(PNCHP-κ^3*P,N,P*)] (Mo (**F.2.2-2**) or W (**F.2.2-3**)). This is indeed the case, as when monitoring the conversion of *cis*-[Mo(CO)$_4$(PNCHP-κ^2*P,P*)] (**F.2.1-2**) to *mer*-[Mo(CO)$_3$(PNCHP-κ^3*P,N,P*)] (**F.2.2-2**), an intermediate species is observed, which was identified *in situ* as *fac*-[Mo(CO)$_3$(PNCHP-κ^3*P,N,P*)] (**F.2.2-4**). It is in the *fac* to *mer* isomerism step, that the rearrangement of the phosphorus atoms occur. In this chapter the kinetics and thermodynamics of the isomerisation step are reported, along with the full characterisation of the *fac* compound, which as been, up to now, nonisolatable due to its transient nature.

Recently, as an aside, *fac-mer* isomerisation involving a tridentate P_2N mixed donor ligand has been implicated in the C-C bond cleavage of terminal alkynes by water.[3] Kleverlaan et al. give a concise background to the area of *fac-mer* isomerisations.[4] In general, the unassisted *fac-mer* isomerisation in six-coordinate octahedral complexes can occur, essentially, in two ways. In one of these, dissociation of a ligand can be followed by

[3] C. Bianchini, J. A. Casares, M. Peruzzini, A. Romerosa and F. Zanobini, *J. Am. Chem. Soc.*, 1998, **118**, 4585.
[4] C. J. Kleverlaan, F. Hartl and D. J. Stufkens, *J. Organomet. Chem.*, 1998, **561**, 57.

rearrangement of the resultant five-coordinate coordinatively unsaturated intermediate.[10] Or alternatively, rearrangement may occur via a nondissociative intramolecular mechanism.[5] The majority of kinetic studies put forward to support either of the above isomerisation mechanisms have involved ligands of the mono- and/or bidentate variety, see for example.[4,6,7] To the authors knowledge, only one kinetic study, that of the photoisomerisation of *fac*- to *mer*-[$Mo(CO)_3\{(Ph_2PCH_2CH_2)_2PPh$-$\kappa^3P,P,P\}$], has been reported involving a tridentate ligand.[8]

Finally, monodentate PNCHP complexes have been previously obtained by reacting the ligand with UV-irradiated tetrahydrofuran solutions of [$M(CO)_6$] (M = Cr or W) to yield P bound coordination isomers of [$M(CO)_5$(PNCHP-κ^1P)] (**F.2.3-1a** and **F.2.3-1b**). However, the ratio of the two isomers is not a statistical 1:1 mixture, but, 2:1 in favour of **F.2.3-1a**. The same reaction when carried out with one half equivalent of PNCHP yielded the PNCHP bridged dinuclear species [$\{M(CO)_5\}_2$(PNCHP-κ^2P,P)] (**F.2.3-2**).

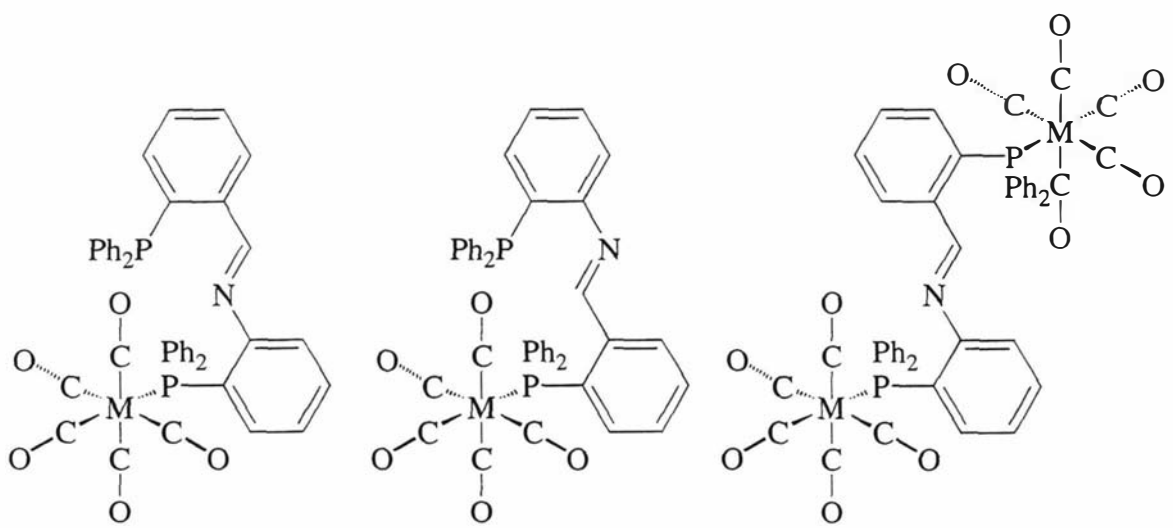

F.2.3-1a **F.2.3-1b** **F.2.3-2**

Figure 2.3 The monodentate and bridging coordination modes of the PNCHP ligand with group 6 metal pentacarbonyl complexes.

[5] A. Rodger and B. F. G. Johnson, *Inorg. Chem.*, 1998, **27**, 3062.
[6] J. A. S. Howell, P. C. Yates, N. F. Ashford, D. T. Dixon and R. Warren, *J. Chem. Soc., Dalton Trans.*, 1996, 3959.
[7] R. G. Wilkins, *Kinetics and Mechanism of Reactions of Transition Metal Complexes*, 2nd Ed., VCH, 1991.

2.2 Results and discussion

2.2.1 Synthesis

Previously,[1] the *facial* isomer *fac*-[Mo(CO)$_3$(PNCHP-κ^3*P,N,P*)] (**F2.2-4**) had been identified only as a transient species on route to the final product *mer*-[Mo(CO)$_3$(PNCHP-κ^3*P,N,P*)] (**F.2.2-2**). The facial isomer has now been isolated and fully characterised, as discussed in the sections to follow. The key to its isolation is its low solubility in ice-cold toluene. Hence, the reaction of PNCHP with [Mo(CO)$_3$(CHT)], in minimal volumes of ice-cold toluene, results in the precipitation of the kinetic product *fac*-[Mo(CO)$_3$(PNCHP-κ^3*P,N,P*)], as a crimson powder, before it can convert to the thermodynamically favoured *mer* isomer. On dissolving, the *facial* isomer readily converts to the *meridional* isomer. The isomerisation is characterised by the kinetic study reported in section *2.2.9*. Unfortunately, the corresponding *fac* chromium and tungsten analogues could not be prepared, hence the *fac* to *mer* isomerisation kinetics was only carried out for molybdenum complex.

In an interesting contrast, the reaction of reduced PNCHP, that is **PNHCH$_2$P**, shown below, with [Mo(CO)$_3$(CHT)], gives rise to only the *facial* isomer *fac*-[Mo(CO)$_3$(PNHCH$_2$P-κ^3*P,N,P*)], which will not convert to the *mer* isomer, even in boiling toluene. In addition, unlike *fac*-[Mo(CO)$_3$(PNCHP-κ^3*P,N,P*)], *fac*-[Mo(CO)$_3$(PNHCH$_2$P-κ^3*P,N,P*)] is unstable and slowly decomposes in air, even in the solid state. The compound was spectroscopically characterised and is discussed in the sections below.

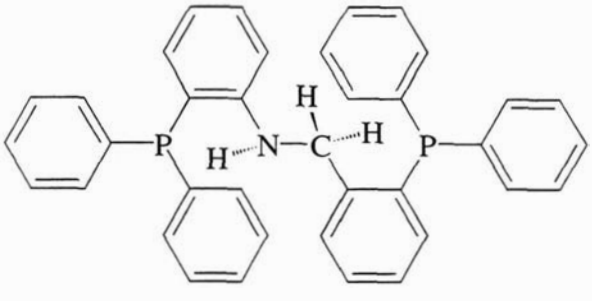

PNHCH$_2$P

[8] R. G. Compton, J. C. Eklund, A. Hallik, S. Kumbhat, A. M. Bond and R. Colton, *J. Chem. Soc. Perkin Trans.*, 2, 1995, 1327.

The major difference between the above two *fac* compounds is in the nature of the nitrogen donor atom. The nitrogen donor atom is an imine nitrogen in *fac*-[$Mo(CO)_3$(PNCHP-κ^3*P,N,P*)] and a secondary amine in *fac*-[$Mo(CO)_3$($PNHCH_2P$-κ^3*P,N,P*)]. This difference not only alters the electronic characteristics of the two complexes (for example, the imine bound nitrogen atom is capable of back bonding due to the π^*_{imine} orbital, whilst the amine nitrogen atom is an exclusively σ-donor), but changes the flexibility characteristics of the ligand as well. Therefore, the increased stability of *fac*-[$Mo(CO)_3$(PNCHP-κ^3*P,N,P*)], with respect to decomposition, is likely electronic in origin with the a π component of the molybdenum-nitrogen bond affording additional stability by strengthening the Mo-N bond. On the other hand, the stability of the *fac* isomer *fac*-[$Mo(CO)_3$($PNHCH_2P$-κ^3*P,N,P*)], with respect to isomerisation, most likely arises from the greater flexibility of $PNHCH_2P$ to more easily adopt the required *fac* geometry when compared to the more rigid PNCHP ligand. The complex *fac*-[$Mo(CO)_3$($PNHCH_2P$-κ^3*P,N,P*)] can also be made from the heating *cis*-[$Mo(CO)_4$($PNHCH_2P$-κ^2*P,P*)].[9]

The dark-red compound *cis*-[$Cr(CO)_4$(PNCHP-κ^2*N,P*)] (**S.2.1-1**), shown in **Scheme 2.1**, is made by reacting PNCHP with [$Cr(CO)_4$(NBD)] under mild conditions, as previously reported by the author.[1] The reactivity of the coordinated PNCHP was of interest primarily due to the presence of a non-coordinated or 'dangling' phosphorus atom. It was possible to oxidise the phosphorus atom with S_8 to give the dark-red complex *cis*-[$Cr(CO)_4$(SPNCHP-κ^2*N,P*)] (**S.2.1-2**). When carbon monoxide or methyliodide is introduced into a solution of *cis*-[$Cr(CO)_4$(PNCHP-κ^2*N,P*)], no observed reaction takes place. However, when carbon monoxide and methyliodide are present together with *cis*-[$Cr(CO)_4$(PNCHP-κ^2*N,P*)], the anion $[Cr(CO)_5I]^-$ (**S.2.1-3**) is formed, along with what has been tentatively assigned as the diction $[MePNCHPMe]^{2+}$, where the two phosphorus atoms of the PNCHP ligand have been quaternarised by the methyliodide. The reactions were characterised spectroscopically and are discussed in detail in sections *2.2.3.2*, *2.2.3.3* and *2.2.5.2*.

[9] B. M. Jones, *Investigations of Interactions of a P_2N Tridentate Ligand*, Undergraduate project, 1995, Massey University.

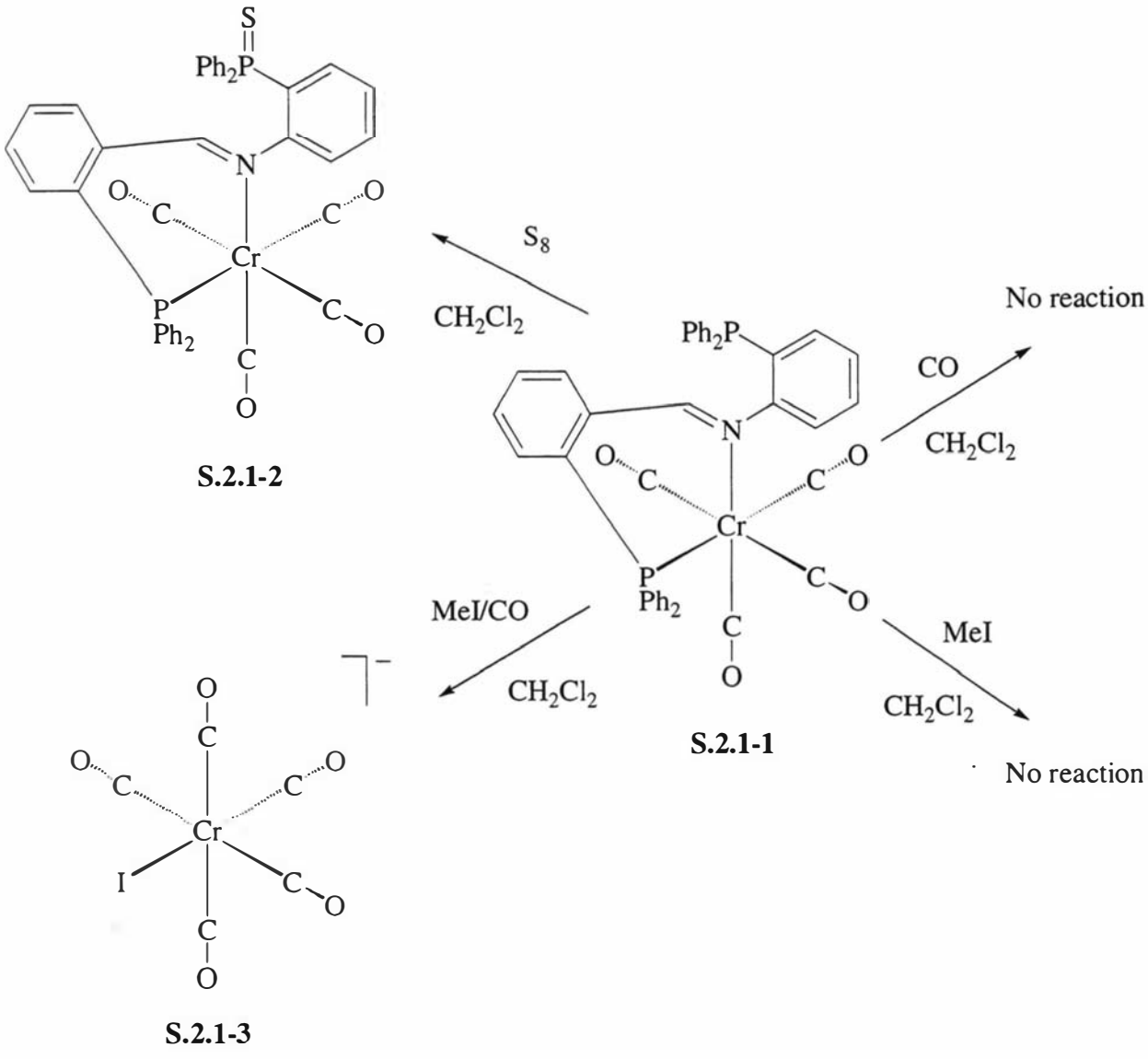

S.2.1-2

S.2.1-1

S.2.1-3

Scheme 2.1 The reactions of *cis*-[Cr(CO)$_4$(PNCHP-κ^2*N,P*)] with sulfur, methyliodide and carbon monoxide, under various conditions

2.2.2 Kinetic and equilibrium studies

Kinetic and thermodynamic data for the isomerisation of *fac*-[Mo(CO)$_3$(PNCHP-κ^3P,N,P)](**F.2.2-4**) to *mer*-[Mo(CO)$_3$(PNCHP-κ^3P,N,P))](**F.2.2-2**) is given in **Table 2.1**. The geometrical isomerisation of *fac*-[Mo(CO)$_3$(PNCHP-κ^3P,N,P)](**F.2.2-4**) was studied in acetone, acetonitrile, chloroform and dichloromethane by UV-vis spectroscopy using the appearance of the purple product *mer*-[Mo(CO)$_3$(PNCHP-κ^3P,N,P))](**F.2.2-2**) at 700 nm. The *fac-mer* isomerisation proceeds with considerable decomposition in chloroform and to

a lesser but still significant extent in dichloromethane while solubility problems were encounted with acetonitrile as solvent at the lower temperatures. In acetone solubility was not a problem and the isomerisation took place without decomposition. Hence comprehensive kinetic and thermodynamic parameters could only be obtained for the isomerisation in acetone. The absorbance at 700 nm increases with time as the result of the isomerisation given by **Equation 2.1**, where k_1 and k_{-1} denote the forward and reverse rate constants respectively. Measurements were carried out in the temperature range 19.5-49.5 °C. There is no spectroscopic evidence for detectable concentrations of any intermediates. In each kinetic run, the plot of $\ln(A-A_\infty)$ versus time gave a straight line for at least three half-lives, (A and A_∞ denote the absorbance at 700 nm at time t and at infinite time respectively. At infinite time, *fac-mer* mixture at thermodynamic equilibrium are obtained). The slope gave the first-order rate constant k_{obsd}. The observed rate constant was determined at four different temperatures (19.5, 29.7, 40.0 and 49.5 °C). The rate constants for isomerisation were calculated from the equilibrium constant K_{eq}, obtained from the integrated ^{1}H NMR signals of the imine proton in equilibrated solutions (**Equation 2.2**), and the observed rate constant (**Equation 2.3**).

$$fac \underset{k_{-1}}{\overset{k_1}{\rightleftharpoons}} mer \qquad \textbf{Equation 2.1}$$

$$K_{eq} = k_1 / k_{-1} = \int \delta C\underline{H}{=}N_{mer} / \int \delta C\underline{H}{=}N_{fac} \qquad \textbf{Equation 2.2}$$

$$k_{obsd} = k_1 + k_{-1} \qquad \textbf{Equation 2.3}$$

The K_{eq} value was found to be 7.3 and independent of temperature in acetone. The k_{obsd} values along with the forward (k_1) and and reverse (k_{-1}) rate constants are collected in **Table 2.1**. The activation enthalpies for the forward ($\Delta H_1^{\ddagger}$)and reverse ($\Delta H_{-1}^{\ddagger}$) reactions were (95 ± 3) kJ mol^{-1} and (94 ± 2) kJ mol^{-1} respectively. The activation entropies for the

forward ($\Delta S_1^{\ddagger}$) and reverse ($\Delta S_{-1}^{\ddagger}$) reactions were (-14.1 ± 0.7) J mol^{-1} K^{-1} and (-36 ± 2) J mol^{-1} K^{-1} respectively.

Driving forces for *fac-mer* isomerisation can be attributed to electronic advantages and/or steric pressure exerted by the ligands around the metal.[10,11] In this case the PNCHP ligand prefers to be coplanar as it is in *the mer* isomer.

In general, a large positive activation enthalpy, of bond breaking magnitude (e.g ~ 100 $kJmol^{-1}$ for metal-phosphanes), coupled with a positive activation entropy is supportive of a dissociative mechanism whilst a small activation enthalpy, less than bond breaking magnitude, coupled with a large negative entropy (~ -200 J $mol^{-1}K^{-1}$) is supportive of a twist mechanism.[12] For our system, $\Delta H_1^{\ddagger}$ and $\Delta H_{-1}^{\ddagger}$ values of 95 kJ mol^{-1} and 94 kJ mol^{-1} coupled respectively with $\Delta S_1^{\ddagger}$ and $\Delta S_{-1}^{\ddagger}$ values of -14.1 J mol^{-1} K^{-1} and -36 J mol^{-1} K^{-1} are inconclusive with respect to which mechanism the isomerisation might follow. Note that if solvent restriction occurs $\Delta S^{\ddagger}$ could be negative for a dissociative mechanism. Rate constants did decrease slightly with the increasing coordinating powers of the solvent. For example for the coordinating solvent acetonitrile the rate constant halves whilst moving to the poor coordinating solvent dichloromethane the rate constant doubles. One might equate this observation with a dissociative mechanism. However, whilst following the isomerisation by ^{31}P NMR in the presence of a ten-fold excess of triphenylphosphite no intermediates on the NMR timescale were detected where triphenylphosphite may have been expected to bind if a dissociative mechanism was in effect. However, without thermodynamic activation parameters for the isomerisation in acetonitrile and dichloromethane a more substantial conclusion with respect to the solvent effect can not be drawn.

[10] S. C. N. Hsu and W-Y. Yeh, *J. Chem. Soc., Dalton Trans.*, 1998, 125, and refs. therein.
[11] M. Cano, J. A. Campo, V. Pérez-García, E. Gutiérrez-Puebla and C. Alvarez-Ibarra, *J. Organomet. Chem.*, 1990, **382**, 397.
[12] A. A. Ismail, F. Sauriol and S. Butler, *Inorg. Chem.* 1989, **28**, 1007.

Table 2.1 First-order rate constants and activation energies[a] for geometrical isomerisation of *fac*-to-*mer*-[Mo(CO)$_3$(PNCHP-κ*P,N,P*)]: $k_{obsd} = k_1 + k_{-1}$, $K_{eq} = k_1/k_{-1} = 7.3$

Solvent	T/ °C	$10^{-5}k_{obsd}$/ (s^{-1})	$10^{-5}k_1$/ (s^{-1})	$10^{-5}k_{-1}$/ (s^{-1})
Acetone	19.5	1.39	1.22	0.170
	29.7	4.75	4.18	0.574
	40.0	19.6	17.2	2.08
	49.5	55.6	48.9	6.71
CH_2Cl_2	19.4	3.46	[b]	
MeCN	40.0	11.6	[b]	

[a] $\Delta H_1^{\ddagger} = (95 \pm 3)$ kJ mol^{-1}, $\Delta H_{-1}^{\ddagger} = (94 \pm 2)$ kJ mol^{-1}, $\Delta S_1^{\ddagger} = (-14.1 \pm 0.7)$ J mol^{-1} K^{-1}, $\Delta S_{-1}^{\ddagger} = (-36 \pm 2)$ J mol^{-1} K^{-1}. [b] K_{eq} not recorded.

2.2.3 Description of the crystal structures

2.2.3.1 Crystal structure of cis-[Cr(CO)$_4$(PNCHP-κ^{2}N,P)]•0.5CHCl$_3$

The structure of the complex *cis*-[Cr(CO)$_4$(PNCHP-κ^2*N,P*)] is shown in **Figure 2.5**, with crystal data and structure refinement details given in **Table 2.2** and selected bond lengths and angles given in **Table 2.3**. Two independent molecules are contained in the asymmetric unit showing no significant differences from one another. One of the independent molecules has been arbitrary selected for the purpose of this discussion. The coordination geometry is that of a slightly distorted octahedron, with the largest distortion from the 90° of an ideal octahedron being found in the angle N(1A)-Cr(1)-P(2A) (82.06(13)°), which is part of a six-membered ring. The nitrogen atom and one of the phosphorus atoms occupy *cis* coordination sites forming the six-membered ring. It is interesting that the metal-bound phosphorus atom is not the same phosphorus atom that has been proposed to be coordinated in the major isomer of the reaction of PNCHP with [Cr(CO)$_5$(THF)],[1] that is **F.2.3-1a** shown in **Figure 2.3** above. As expected the carbonyl *trans* to the N atom (Cr-C(107)) has the shorter distance of 1.795(7) Å than the carbonyl group *trans* to the P atom (Cr-C(106), 1.857(8) Å), which is consistent with the greater

trans influence of the phosphorus atom over the nitrogen atom.[13] The bond distances observed for N(1A)-C(12A), N-C(1A) and C(1A)-C(42A) (1.405(6), 1.257(6) and 1.451(6) Å respectively) suggest that there is little if any electron delocalisation throughout the imine system. Bond lengths and angles are identical to the very similar system *cis*-[{$Cr(CO)_4$}$_2$(P_2N_2-κ^4P,N,N,P)] (**F.2.4-1**), where P_2N_2 is N,N'-bis[*o*-(diphenylphosphino)-benzylidine]ethylenediamine) (**F.2.4-2**), shown in **Figure 2.4**.

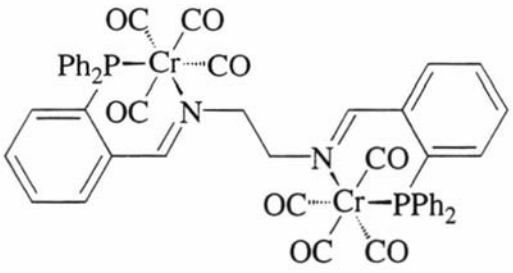

F.2.4-1

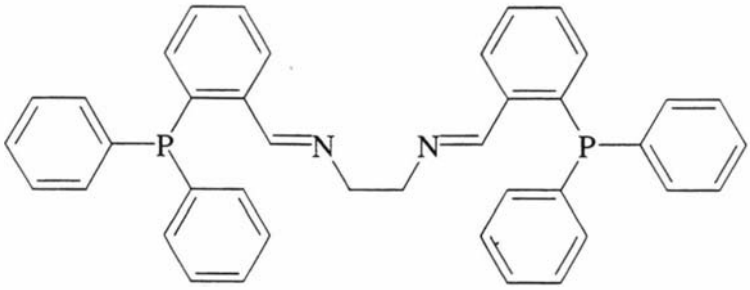

F.2.4-2

Figure 2.4 The ligand N,N'-bis[*o*-(diphenylphosphino)-benzylidine]ethylenediamine) and its chromium tetracarbonyl complex

[13] D. Dowerah, L. J. Radonovich and N. F. Woolsey, *Organometallics*, 1990, **9**, 614.

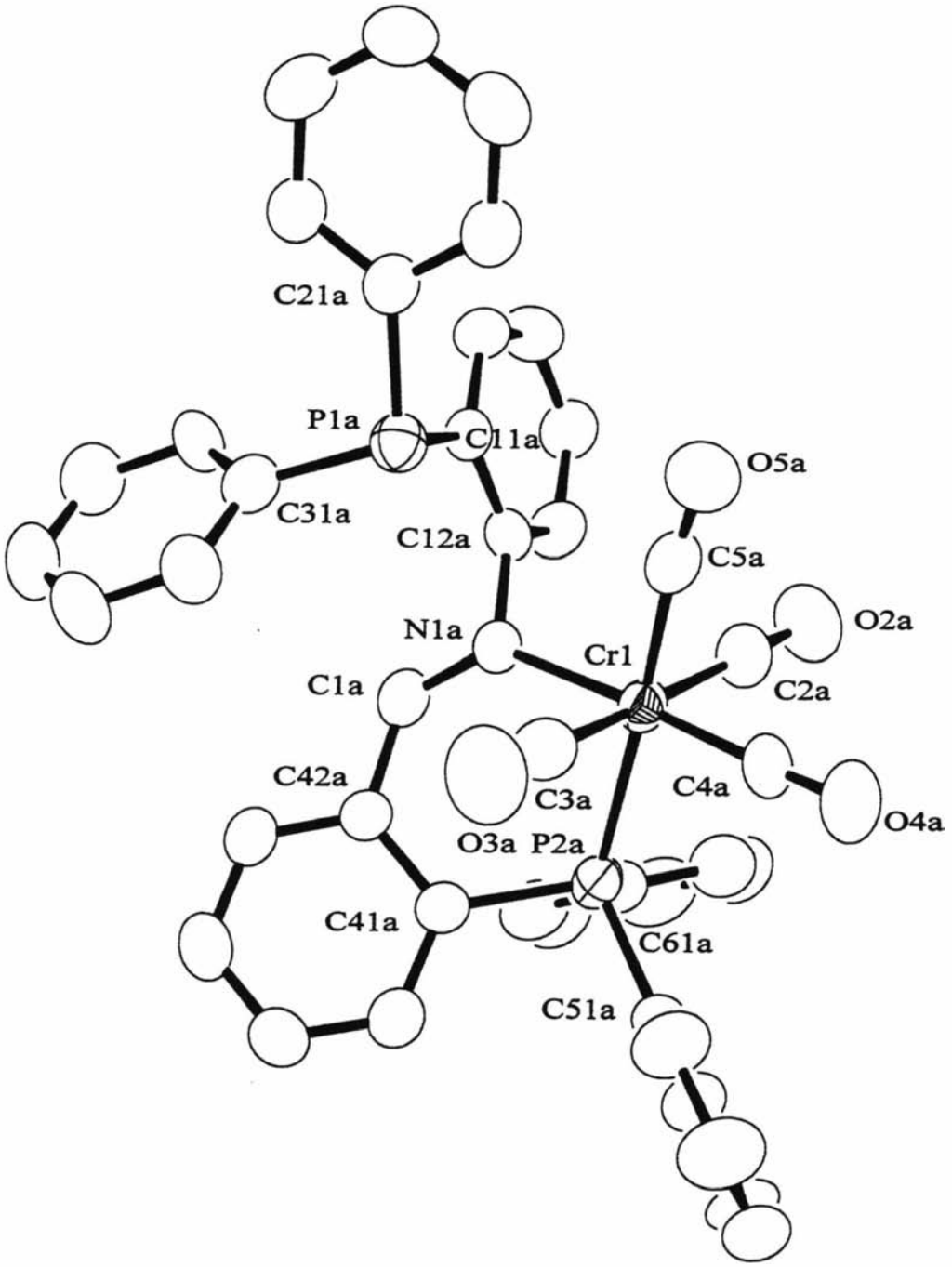

Figure 2.5 ORTEP diagram for the complex *cis*-[Cr(CO)$_4$(PNCHP-κ^2*N*,*P*)]•0.5CHCl$_3$ (Molecule A) showing the numbering system used. Thermal ellipsoids are at the 50% probability level. Hydrogen atoms and solvent molecules have been omitted for clarity

Table 2.2

Crystal data and structure refinement for *cis*-[$Cr(CO)_4$(PNCHP-κ^2*N,P*)]•0.5$CHCl_3$

Identification code	amb2	
Empirical formula	C41 H29 Cr N O4 P2	
Formula weight	713.59	
Temperature	293(2) K	
Wavelength	0.71073 Å	
Crystal system	Monoclinic	
Space group	P 2(1)/c	
Unit cell dimensions	a = 14.429(3) Å	α = 90°.
	b = 29.433(6) Å	β = 108.40(3)°.
	c = 17.389(3) Å	γ = 90°.
Volume	7007(2) $Å^3$	
Z	8	
Density (calculated)	1.353 Mg/m^3	
Absorption coefficient	0.461 mm^{-1}	
F(000)	2944	
Crystal size	0.23 x 0.18 x 0.10 mm^3	
Theta range for data collection	1.38 to 20.02°.	
Index ranges	0<=h<=13, 0<=k<=28, -16<=l<=15	
Reflections collected	6871	
Independent reflections	6533 [R(int) = 0.0359]	
Absorption correction	Empirical via scans (North, Phillips & Mat	
Max. and min. transmission	0.9553 and 0.9014	
Refinement method	Full-matrix least-squares on F^2	
Data / restraints / parameters	6533 / 0 / 883	
Goodness-of-fit on F^2	1.019	
Final R indices [I>2sigma(I)]	R1 = 0.0363, wR2 = 0.1030	
R indices (all data)	R1 = 0.1028, wR2 = 0.1329	
Largest diff. peak and hole	0.775 and -0.248 e.$Å^{-3}$	

Table 2.3

Selected bond lengths (Å) and angles (°) for *cis*-[Cr(CO)$_4$(PNCHP-κ^2*N*,*P*)]•0.5CHCl$_3$ (Molecule A) with estimated standard deviations in parentheses

Bond lengths:			
Cr(1)-P(2A)	2.3570(18)	P(2A)-C(51A)	1.825(6)
Cr(1)-N(1A)	2.141(5)	P(2A)-C(61A)	1.818(6)
Cr(1)-C(2A)	1.895(8)	O(2A)-C(2A)	1.141(7)
Cr(1)-C(3A)	1.879(8)	O(3A)-C(3A)	1.157(7)
Cr(1)-C(4A)	1.794(7)	O(4A)-C(4A)	1.162(6)
Cr(1)-C(5A)	1.854(7)	O(5A)-C(5A)	1.150(7)
P(1A)-C(11A)	1.830(6)	N(1A)-C(1A)	1.279(6)
P(1A)-C(21A)	1.828(6)	N(1A)-C(12A)	1.449(7)
P(1A)-C(31A)	1.825(6)	C(1A)-C(42A)	1.464(8)
P(2A)-C(41A)	1.817(6)		
Bond angles:			
N(1A)-Cr(1)-P(2A)	82.06(13)	C(21A)-P(1A)-C(31A)	105.6(3)
P(2A)-Cr(1)-C(2A)	95.0(2)	C(41A)-P(2A)-C(51A)	102.8(3)
P(2A)-Cr(1)-C(3A)	89.1(2)	C(41A)-P(2A)-C(61A)	102.1(3)
P(2A)-Cr(1)-C(4A)	94.3(2)	C(51A)-P(2A)-C(61A)	102.7(3)
P(2A)-Cr(1)-C(5A)	177.2(2)	C(41A)-P(2A)-Cr(1)	108.89(19)
C(2A)-Cr(1)-C(3A)	175.5(3)	C(51A)-P(2A)-Cr(1)	120.1(2)
C(2A)-Cr(1)-C(4A)	89.2(3)	C(61A)-P(2A)-Cr(1)	117.8(2)
C(2A)-Cr(1)-C(5A)	87.5(3)	O(2A)-C(2A)-Cr(1)	174.8(6)
C(3A)-Cr(1)-C(4A)	88.8(3)	O(3A)-C(3A)-Cr(1)	175.6(6)
C(3A)-Cr(1)-C(5A)	88.4(3)	O(4A)-C(4A)-Cr(1)	177.3(6)
C(4A)-Cr(1)-C(5A)	86.9(3)	O(5A)-C(5A)-Cr(1)	173.1(6)
C(2A)-Cr(1)-N(1A)	91.4(2)	C(1A)-N(1A)-Cr(1)	130.5(4)
C(3A)-Cr(1)-N(1A)	90.9(2)	C(12A)-N(1A)-Cr(1)	115.9(3)
C(4A)-Cr(1)-N(1A)	176.4(2)	C(1A)-N(1A)-C(12A)	113.6(5)
C(5A)-Cr(1)-N(1A)	96.7(2)	N(1A)-C(1A)-C(42A)	129.4(5)
C(11A)-P(1A)-C(21A)	100.3(3)	C(11A)-C(12A)-N(1A)	121.4(5)
C(11A)-P(1A)-C(31A)	100.2(3)	C(13A)-C(12A)-N(1A)	117.7(5)

2.2.2.2 Crystal structure of cis-[Cr(CO)$_4$(SPNCHP-κ^2N,P)]•3CH$_2$Cl$_2$

The structure of the complex *cis*-[Cr(CO)$_4$(SPNCHP-κ^2*N,P*)] is shown in **Figure 2.6** with crystal data and structure refinement details given in **Table 2.4** and selected bond lengths and angles given in **Table 2.5**. Due to an incomplete and poor data set, only the atom connectivity will be discussed. The complex is similar, apart from the additional sulfur atom S(1), to that of the parent complex *cis*-[Cr(CO)$_4$(PNCHP-κ^2*N,P*)] discussed in section *2.2.2.1* above. The complex has an octahedral coordination geometry. The PNCHP ligand is bound to the chromium atom through the same donor atoms, P(2) and N(1), as found for the complex *cis*-[Cr(CO)$_4$(PNCHP-κ^2*N,P*)]. The remaining four coordination sites are occupied by CO ligands (C(2)-O(2), C(3)-O(3), C(4)-O(4) and C(5)-O(5)).

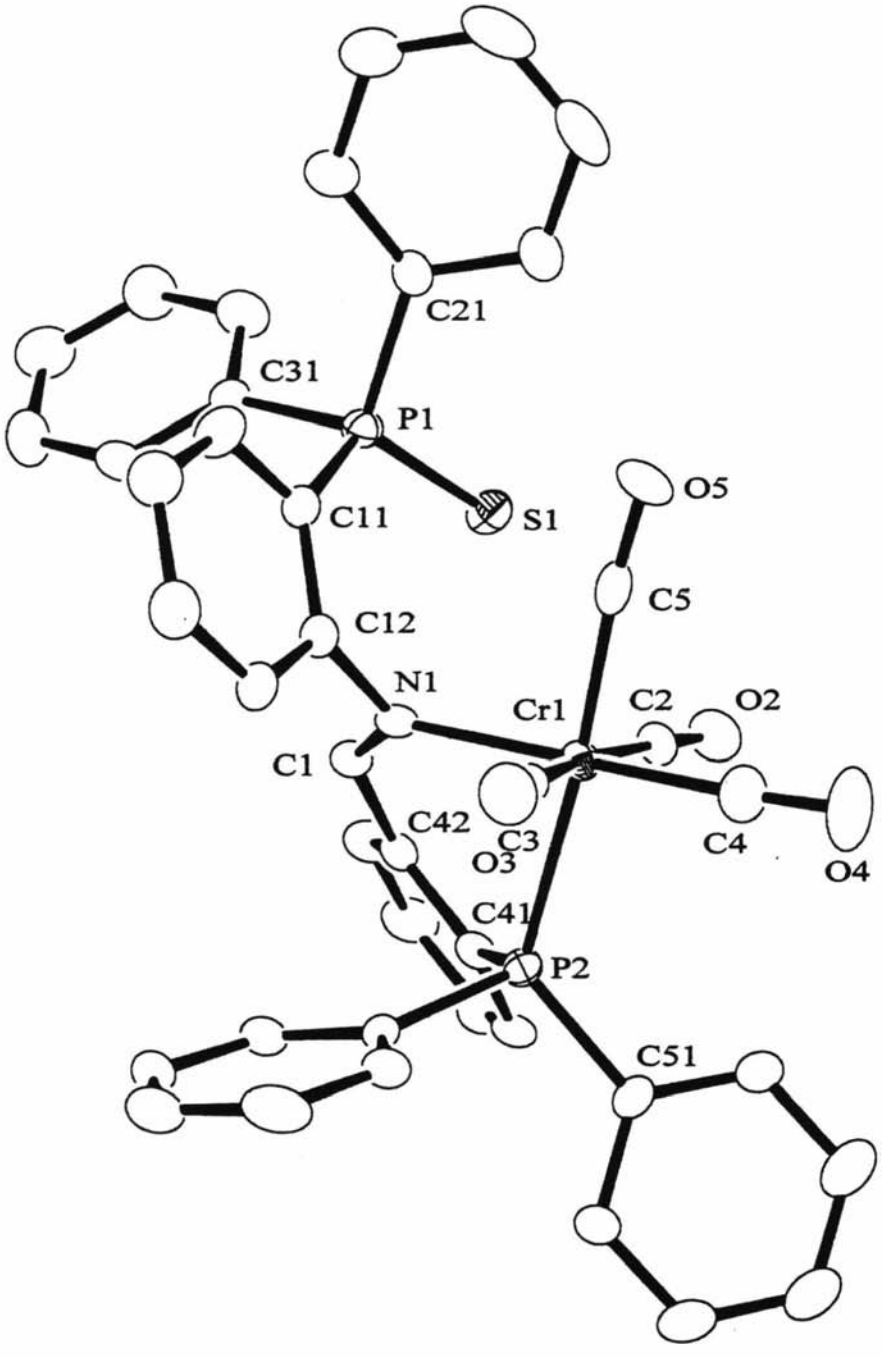

Figure 2.5 ORTEP diagram for the complex *cis*-[$Cr(CO)_4$(SPNCHP-κ^2*N*,*P*)]•3CH_2Cl_2 showing the numbering system used. Thermal ellipsoids are at the 50% probability level. Hydrogen atoms and solvent molecules have been omitted for clarity

Table 2.4

Crystal data and structure refinement for *cis*-[$Cr(CO)_4$(SPNCHP-κ^2*N*,*P*)]•$3CH_2Cl_2$

Identification code	amb7	
Empirical formula	C44 H35 Cl6 Cr N O4 P2 S	
Formula weight	1000.43	
Temperature	203(2) K	
Wavelength	0.71073 Å	
Crystal system	Triclinic	
Space group	P-1	
Unit cell dimensions	a = 10.401(2) Å	α = 89.48(3)°.
	b = 12.593(3) Å	β = 74.32(3)°.
	c = 17.817(4) Å	γ = 84.07(3)°.
Volume	2234.4(8) $Å^3$	
Z	2	
Density (calculated)	1.487 Mg/m^3	
Absorption coefficient	0.777 mm^{-1}	
F(000)	1020	
Crystal size	0.31 x 0.25 x 0.16 mm^3	
Theta range for data collection	1.19 to 26.07°.	
Index ranges	0<=h<=12, -15<=k<=15, -21<=l<=9	
Reflections collected	6930	
Independent reflections	6425 [R(int) = 0.2450]	
Completeness to theta = 0.50°	0.0 %	
Absorption correction	Empirical via scans	
Max. and min. transmission	0.8858 and 0.7948	
Refinement method	Full-matrix least-squares on F^2	
Data / restraints / parameters	6425 / 0 / 527	
Goodness-of-fit on F^2	1.033	
Final R indices [I>2sigma(I)]	R1 = 0.0798, wR2 = 0.2093	
R indices (all data)	R1 = 0.1167, wR2 = 0.2519	
Largest diff. peak and hole	0.811 and -1.531 $e.Å^{-3}$	

Table 2.5

Selected bond lengths (Å) and angles (°) *cis*-[$Cr(CO)_4$(SPNCHP-κ^2*N*,*P*)]•3CH_2Cl_2 with estimated standard deviations in parentheses

Bond lengths:			
Cr(1)-P(2)	2.3499(17)	P(2)-C(51)	1.807(6)
Cr(1)-N(1)	2.132(5)	P(2)-C(61)	1.813(6)
Cr(1)-C(2)	1.868(8)	O(2)-C(2)	1.159(8)
Cr(1)-C(3)	1.877(7)	O(3)-C(3)	1.156(8)
Cr(1)-C(4)	1.815(6)	O(4)-C(4)	1.156(8)
Cr(1)-C(5)	1.857(6)	O(5)-C(5)	1.153(7)
P(1)-C(11)	1.824(7)	N(1)-C(1)	1.303(7)
P(1)-C(21)	1.831(6)	N(1)-C(12)	1.422(8)
P(1)-C(31)	1.803(6)	C(1)-C(42)	1.434(9)
P(2)-C(41)	1.828(6)	P(1)-S(1)	1.945(3)
Bond angles:			
N(1)-Cr(1)-P(2)	80.72(12)	C(41)-P(2)-C(51)	104.5(3)
P(2)-Cr(1)-C(2)	87.46(17)	C(41)-P(2)-C(61)	104.6(3)
P(2)-Cr(1)-C(3)	94.36(17)	C(51)-P(2)-C(61)	104.3(3)
P(2)-Cr(1)-C(4)	99.4(2)	C(41)-P(2)-Cr(1)	106.26(17)
P(2)-Cr(1)-C(5)	172.86(17)	C(51)-P(2)-Cr(1)	121.73(19)
C(2)-Cr(1)-C(3)	169.9(3)	C(61)-P(2)-Cr(1)	113.9(2)
C(2)-Cr(1)-C(4)	85.5(3)	O(2)-C(2)-Cr(1)	173.1(5)
C(2)-Cr(1)-C(5)	89.5(3)	O(3)-C(3)-Cr(1)	172.6(5)
C(3)-Cr(1)-C(4)	84.4(3)	O(4)-C(4)-Cr(1)	176.9(6)
C(3)-Cr(1)-C(5)	89.7(3)	O(5)-C(5)-Cr(1)	174.1(5)
C(4)-Cr(1)-C(5)	86.8(3)	C(1)-N(1)-Cr(1)	129.1(5)
C(2)-Cr(1)-N(1)	93.4(2)	C(12)-N(1)-Cr(1)	115.6(3)
C(3)-Cr(1)-N(1)	96.7(2)	C(1)-N(1)-C(12)	115.2(5)
C(4)-Cr(1)-N(1)	178.9(3)	N(1)-C(1)-C(42)	127.4(6)
C(5)-Cr(1)-N(1)	93.0(2)	C(11)-C(12)-N(1)	124.7(6)
C(11)-P(1)-C(21)	104.6(3)	C(13)-C(12)-N(1)	115.0(5)
C(11)-P(1)-C(31)	105.1(3)	C(11)-P(1)-S(1)	117.7(2)
C(21)-P(1)-C(31)	104.1(3)	C(21)-P(1)-S(1)	111.8(2)
		C(31)-P(1)-S(1)	112.4(2)

2.2.3 ^{31}P NMR spectroscopic studies

2.2.3.1 The compounds *fac*-[Mo(CO)$_3$(PNCHP-κ^3*P,N,P*)], *fac*-[Mo(CO)$_3$(PNHCH$_2$P-κ^3*P,N,P*)] and *cis*-[Mo(CO)$_4$(PNHCH$_2$P-κ^2*P,P*)]

The isomer *fac*-[Mo(CO)$_3$(PNCHP-κ^3*P,N,P*)](**F.2.2-4**) displays a ^2J(P,P) coupling constant of 26 Hz typical of *cis* phosphorus atoms, see **Table 2.6**, which supports the *fac* isomer assignment.[14] Since isolation of a *fac/mer* isomer pair is rare, it is worthwhile to compare the spectroscopic characteristics of the two. Both isomers display AB type spectra. The ^2J(P,P) coupling constant of the *mer* isomer is considerably larger at 93 Hz, which is consistent with *trans* phosphorus atoms.[15] The signals of the *fac* isomer at δ39.4 and δ36.3 are at lower frequency than the *mer* isomer at δ59.0 and δ53.7. With time the *fac* isomers signals recede, giving rise to the signals of the *mer* isomer. Kinetic and thermodynamic details of the *fac* to *mer* isomerisation are given in section *2.2.9*.

A similar spectrum to *fac*-[Mo(CO)$_3$(PNCHP-κ^3*P,N,P*)], is obtained for the related tricarbonyl compound *fac*-[Mo(CO)$_3$(PNHCH$_2$P-κ^3*P,N,P*)]. Unlike *fac*-[Mo(CO)$_3$(PNCHP-κ^3*P,N,P*)], the ^2J(P,P) coupling in *fac*-[Mo(CO)$_3$(PNHCH$_2$P-κ^3*P,N,P*)] is surprisingly not observed. The two phosphorus atoms of *fac*-[Mo(CO)$_3$(PNHCH$_2$P-κ^3*P,N,P*)] have quite different chemical shifts, at δ41.1 and 31.1. Both chemical shifts are typical of metal-coordinated arylphosphanes. Similar to *fac*-[Mo(CO)$_3$(PNCHP-κ^3*P,N,P*)], the chemical shift at higher frequency is most likely caused by the phosphorus atom involved in the five-membered ring, due to the 'ring contribution or ΔR effect'.[16]

The tetracarbonyl compound *cis*-[Mo(CO)$_4$(PNHCH$_2$P-κ^2*P,P*)] displays signals at δ37.7 and 19.7, again, the shifts are typical of both phosphorus atoms being coordinated. The ^2J(P,P) coupling of 25 Hz, and the magnitude is consistent with the phosphorus atoms being in a *cis* arrangement around the molybdenum atom. The ^{31}P NMR spectral features are virtually identical to the related compound *cis*-[Mo(CO)$_4$(PNCHP-κ^2*P,P*)] (δ36.9 and 19.8, ^2J(P,P) = 26 Hz).[1]

---

[14] a) U. U. Ike, S. D. Perera, B. L. Shaw and M. Thorton-Pett, *J. Chem. Soc. Dalton Trans.*, 1995, 2057; b) S. D. Perera, B. L. Shaw and M. Thorton-Pett, *J. Chem. Soc. Dalton Trans.*, 1992, 1469; c) J. Mason, (ed.) *Multinuclear NMR*, 1987, Plenium Press, New York, p394.

[15] See ref 14c

2.2.3.2 The reactivity of cis-[Cr(CO)$_4$(PNCHP-κ^2N,P)] towards sulfur and methyliodide

The ^{31}P NMR data for the products of the reactions of *cis*-[Cr(CO)$_4$(PNCHP-κ^2*N,P*)] with sulfur and methyliodide are given in **Table 2.6**. The spectrum of the parent compound *cis*-[Cr(CO)$_4$(PNCHP-κ^2*N,P*)] has been discussed elsewhere,[1] suffice to say that its signals at δ53.4(s) and -18.9(s) are consistent with the solid state structure discussed in section *2.2.2.1*.

Monitoring of the reaction between *cis*-[Cr(CO)$_4$(PNCHP-κ^2*N,P*)] (**S.2.1-1**) and one equivalent of sulfur, by ^{31}P NMR spectroscopy, revealed the formation of at least five new species. One of these has been confirmed as the complex *cis*-[Cr(CO)$_4$(SPNCHP-κ^2*N,P*)] (**S.2.1-2**) in a concentration of 19 % (by integration of the peak area). The spectrum of this product consists of singlet signals at δ54.1 and 39.3. Essentially, the only change to occur, when comparing the starting material *cis*-[Cr(CO)$_4$(PNCHP-κ^2*N,P*)] (**S.2.1-1**) with the product *cis*-[Cr(CO)$_4$(SPNCHP-κ^2*N,P*)] (**S.2.1-2**), is a shift of the signal at δ-18.9 moving to 39.3 which is consistent with a change in oxidation state form P(III) to P(V),[17] that is, the 'dangling' phosphorus atom has been oxidised with sulfur.

The reaction between *cis*-[Cr(CO)$_4$(PNCHP-κ^2*N,P*)] (**S.2.2-1**, shown in **Scheme 2.2**) and excess methyliodide under an atmosphere of carbon monoxide, results in a product which displays signals at δ21.8 and 20.7 tentatively assigned to the dication [MePNCHPMe]$^{2+}$ (**S.2.2-4**). Additional support of the product assignment is obtained from the reaction of 'free' PNCHP with methyliodide, which gives an identical ^{31}P NMR spectrum. Assignment of one of the counter ions as [Cr(CO)$_5$I]$^-$ is discussed in sections *2.2.5* and *2.2.8*. **Scheme 2.2** shows a plausible reaction sequence for the formation of the dication [MePNCHPMe]$^{2+}$ (**S.2.2-4**), although the mono cation **S.2.2-2** was not observed.

---

[16] a) S. Berger, S. Braun and H-O. Kalinowski, *NMR Spectroscopy of the Non-Metallic Elements*, 1997, John Wiley & Sons Ltd, Chichester, 837; b) G. Dyer and J. Roscoe, *Inorg. Chem.*, 1996, **35**, 4098, and refs. within.

[17] See ref 16a, p703.

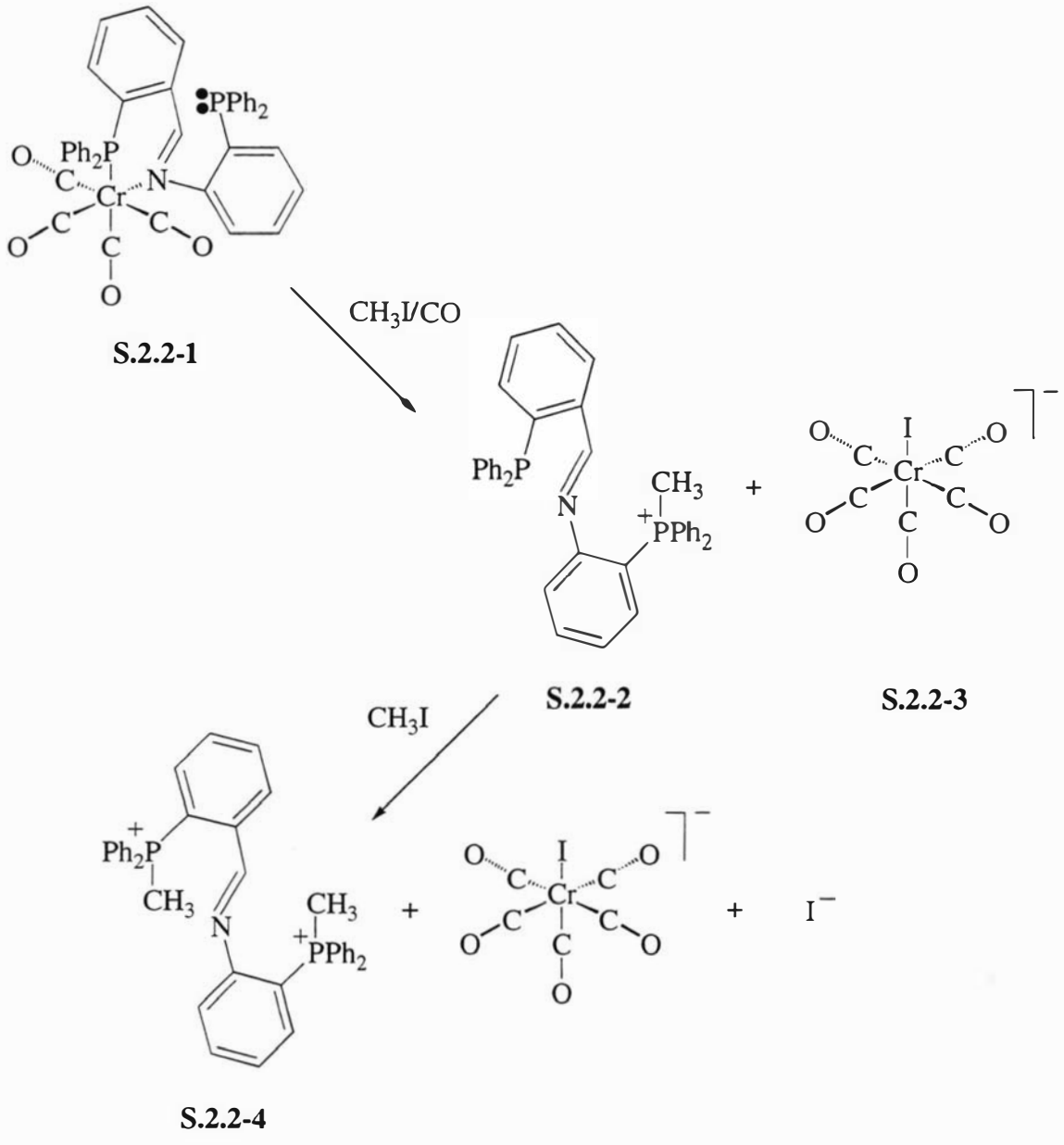

Scheme 2.2 A possible reaction sequence for the reaction of *cis*-[Cr(CO)$_4$(PNCHP-κ^2*N*,*P*)] with excess methyliodide under a carbon monoxide atmosphere

Table 2.6

^{31}P NMR data for the compounds [a]

Compound	δ		^{2}J(PMP)/Hz
PNCHP[18]	-14.2(s)	-14.8(s)	
SPNCHP[18]	42.2(s)	-15.3(s)	
Cis-[Cr(CO)$_4$(PNCHP-κ^2*N,P*)][1]	53.4(s)	-18.9(s)	
Cis-[Cr(CO)$_4$(SPNCHP-κ^2*N,P*)]	54.1(s)	39.3(s)	
[(Me)PNCHP(Me)][Cr(CO)$_5$I]I	21.8(s)	20.7(s)	
Fac-[Mo(CO)$_3$(PNCHP-κ^3*P,N,P*)]	39.4 (d)	36.3 (d)	26
Cis-[Mo(CO)$_4$(PNHCH$_2$P-κ^2*P,P*)][9]	37.7	19.7	25
Fac-[Mo(CO)$_3$(PNHCH$_2$P-κ^3*P,N,P*)]	41.4(s)	31.1(s)	[b]

[a] Recorded at 109 MHz, chemical shifts are in ppm relative to 85% H_3PO_4, solvent $CHCl_3$.
[b] Not resolved. s = singlet, d = doublet.

[18] X. Fan, *Structural Studies on the Interactions of a P_2N Tridentate ligand with Copper(I), Silver(I) and Sulfur*, 1995, MSc Thesis, Massey University.

2.2.4 ^{1}H NMR spectroscopic studies of selected compounds and the ^{13}C NMR of the 'free' PNCHP ligand

2.2.4.1 Introduction

The PNCHP ligands most easily recognised characteristic, in the ^{1}H NMR spectrum, is that of the imino proton (-C<u>H</u>=N-). It is found at δ8.92, for the 'free' ligand, as a doublet with a ^{4}J(H,P) coupling constant of 5.5 Hz.[19] It has been found that the coupling is destroyed on coordination of the phosphorus atom furthermost from the nitrogen atom. For example, oxidation of this phosphorus atom with sulfur, to give P-N=C<u>H</u>-P=S, results in a singlet at δ9.02. In contrast, oxidation of the other phosphorus atom by sulfur, to give S=P-N=C<u>H</u>-P, results in no destruction of the observed imino proton-phosphorus coupling, resulting in a doublet at δ8.87, with a ^{4}J(H,P) coupling constant of 6.2 Hz.[18] This feature is of value in interpreting reaction mechanism and product assignment.

2.2.4.2 ^{13}C and ^{1}H NMR spectroscopy of the 'free' PNCHP ligand

The resolved ^{1}H signals and all ^{13}C NMR signals of the 'free' PNCHP ligand have been assigned using standard 2D correlation experiments and an APT experiment. The chemical shifts and assignments are given in **Table 2.7** with the numbering system used shown in **Figure 2.6**. The aromatic ^{13}C and ^{1}H NMR signals to stand out from the bulk of the aromatic signals, were those associated with the aromatic rings linked directly to the imino group. The aromatic carbon and proton belonging to position **7** of **Figure 2.6**, experienced the greatest shielding effect, whilst the aromatic position to feel the greatest deshielding was the proton at position **7'** and the carbon at position **2**.

[19] M. J. R Halstead, *Iminophosphine Complexes of Ni(II)*, B.Sc(Hons) report, 1991, Massey University.

2.2.4.3 Fac-[Mo(CO)$_3$(PNCHP-κ^3P,N,P)], fac-[Mo(CO)$_3$(PNHCH$_2$P-κ^3P,N,P)] and cis-[Mo(CO)$_4$(PNHCH$_2$P-κ^2P,P)]

^{1}H NMR data for the compounds is shown in **Table 2.8**. The *facial* isomer *fac*-[Mo(CO)$_3$(PNCHP-κ^3*P,N,P*)] displays a singlet peak at δ8.87, which is assigned to the imine proton of the PNCHP ligand. The chemical shift is δ0.31 towards higher frequency than the *meridional* isomer *mer*-[Mo(CO)$_3$(PNCHP-κ^3*P,N,P*)].[1] As expected, the *fac*-[Mo(CO)$_3$(PNHCH$_2$P-κ^3*P,N,P*)] compound displays no signals typical of an imine proton, but gives a pair of doublets (δ4.57 and 4.29 {^2J(H,H) = 12.3 Hz}), typical of the methylene protons in a -Ar-C<u>H$_2$</u>-NH- grouping.[20] It is noted that the methylene group of the 'free' PNHCH$_2$P ligand resonates at δ4.5.[21] and is observed as a broad singlet. Therefore, coordination of the PNHCH$_2$P ligand, in the complex [MCl$_2$(CO)$_2$(PNHCH$_2$P)] (M = Mo or W), results in the protons of the methylene group becoming inequivalent. In contrast, a singlet at δ4.07 is observed for the methylene protons of the complex *cis*-[Mo(CO)$_4$(PNHCH$_2$P-κ^2*P,P*)]. The area under the methylene protons peaks, in both of the above compounds, integrates to two protons relative to the twenty eight protons of the aromatic region, which is consistent with the composition of the ligand.

[20] R. M. Silverstein, G. C. Bassler and T. C. Morrill, *Spectrometric Identification of Organic compounds*, 1991, John Wiley & Sons, New York, p212.
[21] P. A. Duckworth, *Polydentate Phosphorus-Nitrogen Hybrid Ligands Containing the 2-Aminophenyl Group*, 1984, Ph.D. Thesis, University of Sydney.

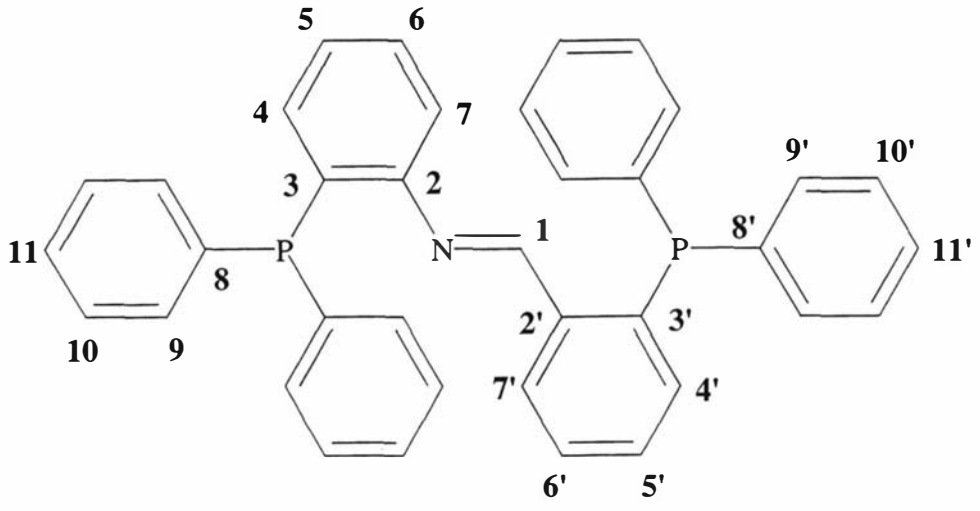

Figure 2.6 The PNCHP ligand showing the numbering system used in **Table 2.7**.

Table 2.7

^{13}C and ^{1}H NMR data[a,b] for the 'free' PNCHP ligand

Assignment	$\delta^{13}C$(multiplicity)	J(P,C)/Hz	$\delta^{1}H$(multiplicity)
1	157.9(d)	25.0	8.94(d), J(H,P) = 5.7 Hz
2	153.7(d)	18.0	
3	139.1(d)	17.0	
4	125.8(s)		7.03(m)
5	132.2(s)		6.74(m)
6/6'	130.7(s) or 129.5(s)		
7	117.1(s)		6.46(m)
8/8'	136.8(d) or 135.8(d)	11.0, 10.0	
9/9'	134.0(s) or 133.7(s)		
10/10'	128.5(d) or 128.1(d)	7.0, 7.0	
11/11'	128.8(s) or 128.3(s)		
2'	132.5(d)	11.0	
3'	137.8(d)	19.0	
4'	127.4(s)		
5'	132.7(s)		6.81(m)
7'	127.3(s)		7.96(m)

[a] Recorded at 68 MHz, chemical shifts are in ppm $CDCl_3$ referenced as 77.0 ppm, solvent $CDCl_3$. [b] Recorded at 270 MHz, chemical shifts are in ppm relative to $Si(CH_3)_4$, solvent $CDCl_3$. s = singlet, d = doublet, m = multiplet.

Table 2.8

Selected ^{1}H NMR data for the compounds [a]

Compound	δ C<u>H</u>=N (*J*(HP)/Hz)	δ Other, [integral]
PNCHP[18]	8.92 (d, 5.5 Hz)	
SPNCHP[18]	8.87 (d, 6.2 Hz)	
Cis-[Cr(CO)$_4$(PNCHP-κ^2*N,P*)][1]	[b]	
Cis-[Cr(CO)$_4$(SPNCHP-κ^2*N,P*)]	8.10(s)	
Fac-[Mo(CO)$_3$(PNCHP-κ^3*P,N,P*)]	8.87(s)	
Cis-[Mo(CO)$_4$(PNHCH$_2$P-κ^2*P,P*)][9]		-C<u>H$_2$</u>-N-, 4.07(s), [2H]
Fac-[Mo(CO)$_3$(PNHCH$_2$P-κ^3*P,N,P*)]		-C<u>H$_2$</u>-N-, 4.57(d, ^2J(H,H) = 12.3 Hz), [1H]; -C<u>H$_2$</u>-N-, 4.29(d, ^2J(H,H) = 12.3 Hz), [1H]).

[a] Recorded at 270 MHz, chemical shifts are in ppm relative to Si(CH$_3$)$_4$, solvent CDCl$_3$.
[b] Not resolved. s = singlet, d = doublet.

2.2.5 IR spectroscopic studies of the compounds

2.2.5.1 The compounds fac-[Mo(CO)$_3$(PNCHP-κ^3P,N,P)], fac-[Mo(CO)$_3$(PNHCH$_2$P-κ^3P,N,P)] and cis-[Mo(CO)$_4$(PNHCH$_2$P-κ^2P,P)]

Selected IR data for the compounds are given in **Table 2.9**. The solution IR spectrum of the *fac*-[Mo(CO)$_3$(PNCHP-κ^3*P,N,P*)] complex exhibits three ν(CO) bands (1932vs, 1843s, 1825s) typical of tricarbonyl complexes with a facial geometry.[22] The energies of the bands are some 20 cm^{-1} lower than the *mer* isomer (1956w, 1857vs, 1836sh), which is consistent with the competition for back-bonding between the *trans* carbonyl groups of the later. The analogous compound *fac*-[Mo(CO)$_3$(PNHCH$_2$P-κ^3*P,N,P*)] exhibits similar ν(CO) stretching (1927vs, 1826s, 1811s). Likewise, *cis*-[Mo(CO)$_4$(PNHCH$_2$P-κ^2*P,P*)], with bands at 2016m, 1917vs, 1904s, 1814w, is similar to the *cis*-[Mo(CO)$_4$(PNCHP-κ^2*P,P*)] compound (2019m, 1919vs, 1900vs, 1865m cm^{-1}).

2.2.5.2 The reactivity of cis-[Cr(CO)$_4$(PNCHP-κ^2N,P)] towards sulfur and methyliodide

The solution IR spectrum of the complex *cis*-[Cr(CO)$_4$(PNCHP-κ^2*N,P*)] shows four bands typical of a *cis*-[Cr(CO)$_4$L$_2$] species. The coordination of the imino nitrogen produces a shift of 39 cm^{-1} towards lower energy for the C=N stretch, relative to the free ligand. This is consistent with a lengthening of the C=N bond, which can be attributed to back-bonding from a chromium d-orbital to the π*-orbital of the imino functionality. A virtually identical spectrum is obtained for the *cis*-[Cr(CO)$_4$(SPNCHP-κ^2N,P)] complex with the addition of a medium to strong absorption at 717 cm^{-1} which is typical of ν(P=S) stretching.[23]

NMR experiments pointed towards the reaction product, of *cis*-[Cr(CO)$_4$(PNCHP-κ^2*N,P*)] and excess CH$_3$I, as a phosphonium salt, as discussed in section *2.2.3*. A solution

---

[22] a) D. M. Adams, Metal-Ligand and Related Vibrations: A Critical Survey of the Infrared and Raman Spectra of Metallic and Organometallic Compounds, 1967, Spottiswoode, Ballantyne and Co. Ltd, London. b) P. S. Braterman, Metal Carbonyl Spectra, 1975, Academic Press, London.

[23] K. Nakamoto, *Infrared and Raman Spectra of Inorganic and Coordination Compounds*, 1986, John Wiley & Sons, New York, p168.

IR spectrum of the final product displayed bands at 2052m, 1970m, 1922vs and 1858s cm^{-1}, which is indicative of the $[Cr(CO)_5I]^-$ anion (2068m, 1982m, 1928vs, 1873s).[24]

A hexachlorobutadiene mull of the methyliodide reaction product also displays peaks at 2963 and 2924 cm^{-1} which have been assigned to the asymmetric and symmetric ν(C-H) stretches of the methyl groups respectively. A medium to strong band at 1115 cm^{-1} has been assigned to the phosphorus-methyl stretch ν(P-CH_3).[25] The band at 1613 cm^{-1} has been assigned to the imine stretch ν(C=N) of **S.2.2-4** and is 31 cm^{-1} higher in energy than the starting material *cis*-[$Cr(CO)_4$(PNCHP-κ^2*N,P*)] and 9 cm^{-1} higher than the free PNCHP ligand.

Table 2.9

Selected IR data for the compounds

Compound	ν(C≡O)[a] [Other]	ν(C=N)[b]	ν(P-C)[b]
PNCHP[18]		1621m	1091m
Cis-[$Cr(CO)_4$(PNCHP-κ^2*N,P*)][1]	2001m, 1911s, 1893s, 1857m	1582m	1090m
Cis-[$Cr(CO)_4$(SPNCHP-κ^2*N,P*)]	2004m, 1913s, 1882vs, 1856s [ν(P=S) 717m]	1584-1559w[e]	1098m[e]
[(Me)PNCHP(Me)][$Cr(CO)_5$I]I	2052m, 1970m, 1922vs, 1858s [ν(P-Me) 1115s, $\nu(C\text{-}H)_{methyl}$ 2923m[c]]	1612[d]	
Fac-[$Mo(CO)_3$(PNCHP-κ^3*P,N,,P*)]	1932vs, 1843s, 1825s[b]	1571	1890
Cis-[$Mo(CO)_4$($PNHCH_2P$-κ^2*P,P*)]	2016m, 1917vs, 1904s, 1814w		
Fac-[$Mo(CO)_3$($PNHCH_2P$-κ^3*P,N,,P*)]	1927vs, 1826s, 1811s		

[a] In $CHCl_3$. [b] As nujol mull. [c] Most intense peak of a multiplet. [d] Tentative assignment. vs = very strong, s = strong, m = medium, w = weak, sh = shoulder. [e] 'Free' SPNCHP exhibits a ν(C=N) band at 1613 cm^{-1} and a ν(P-C) band at 1097 cm^{-1}.

[24] E. W. Ainscough, Andrew M. Brodie and Alan R. Furness, *J. C. S. Dalton*, 1973, 2360.
[25] See ref 20, p162

2.3 Conclusions

The *fac* isomer *fac*-[Mo(CO)$_3$(PNCHP-κ^3*P,N,P*] readily converts to the *mer* isomer. The first-order forward rate constants (k_1) for the *fac*-to-*mer* isomerism in acetone are 1.22×10^{-5}, 4.18×10^{-5}, 1.72×10^{-4} and 4.89×10^{-4} s^{-1} at 19.5, 29.7, 40.0 and 49.5 °C respectively, with thermodynamic activation parameters $\Delta H_1^{\ddagger}$ and $\Delta S_1^{\ddagger}$ of 95 kJ mol^{-1} and −14.1 J mol^{-1} K^{-1} respectively. The related compound to *fac*-[Mo(CO)$_3$(PNCHP-κ^3*P,N,P*], *fac*-[Mo(CO)$_3$(PNHCH$_2$P-κ^3*P,N,P*], does not convert to the *mer* isomer.

The PNCHP ligand in the complex *cis*-[Cr(CO)$_4$(PNCHP-κ^2*N,P*] coordinates through the nitrogen atom, and the phosphorus atom furthest away from the nitrogen, resulting in a six-membered chelate ring and a 'free' phosphorus donor. The 'free' phosphorus donor can be oxidised with sulfur and methylated with methyliodide, however, for the later to occur, a carbon monoxide atmosphere must be present.

2.4 Experimental

2.4.1 Materials

The preparation of the ligands PNCHP,[19] SPNCHP[18] and PNHCH$_2$P[21] have been reported elsewhere. *Cis*-[Cr(CO)$_4$(PNCHP-κ^2*N,P*)],[1] [Mo(CO)$_4$(C$_5$H$_{11}$N)$_2$][26] and [Mo(CO)$_3$(C$_7$H$_8$)][27] were prepared as previously described. For the kinetic and equilibrium studies - acetone was freshly distilled over 4A molecular sieves. Chloro solvents and acetonitrile were freshly distilled over CaH$_2$. All solvents were degassed with bubbling argon.

2.4.2 Fac-to-mer isomerisation of [Mo(CO)$_3$(PNCHP-κ^3P,N,P)]

Kinetic and equilibrium studies - Stock solutions of fac-[Mo(CO)$_3$(PNCHP)] were prepared by dissolving an appropriate amount of the solid complex directly before each experiment. Samples were transferred into a 1 cm path-length sealed quartz curvette placed in the constant temperature jacket of the spectrometer (± 3 %). Kinetic runs as a function of temperature (19.5-49.5°C) were performed with a HP 8452A uv-vis spectrometer at 700

[26] D. J. Darensbourg and R. L. Klump, *Inorg. Chem.*, 1978, **17**, 2680.

nm. Absorbance readings were taken until the reaction had progressed to equilibrium. Values of k_{obsd} were obtained from linear plots of $\ln(A-A_\infty)$ against time, using a minimum of 6 absorbance/time pairs. All plots gave correlation coefficients greater than 0.9993.The first-order rate constants were calculated using a linear regression method. Activation energy was calculated from an Arrhenius plot and activation enthalpy and entropy from an Eyring plot.

2.4.3 Cis-[Cr(CO)$_4$(PNCHP-κ^2N,P)] + excess S_8

Cis-[Cr(CO)$_4$(PNCHP-κ^2*N,P*)] (0.0500 g, 0.0701 mmol) and S_8 (0.0112 g, 0.0437 mmol) were combined in dichloromethane. The resulting mixture was stirred at room temperature until the sulfur suspension was taken into solution. The reaction mixture was then analysed by ^{31}P NMR (**Table 2.6**), IR (**Table 2.9**) and mass spectroscopy. Positive FAB mass spectrum: Found m/z (%) , assignment[calculated m/z for ^{52}Cr]: 745(2), [Cr(CO)$_4$(SPNCHP)]$^+$ [745]; 714(9), [Cr(CO)$_4$(PNCHP)H]$^+$ [714]; 685(20), [Cr(CO)$_3$(PNCHP)] [685]; 633(16), [Cr(SPNCHP)]$^+$ [633]; 601(100), [Cr(PNCHP)]$^+$ [601].

2.4.4 Cis-[Cr(CO)$_4$(SPNCHP-κ^2N,P)]

A mixture of [Cr(CO)$_4$(NBD)] (0.1370 g, 0.5348 mmol) and SPNCHP (0.3119 g, 0.5362 mmol) in 10 mL of dichloromethane/acetonitrile (1:1) was stirred at room temperature for 24 h. The greenish reaction mixture was taken to dryness *in vacuo* and the resulting dark green residue dissolved in chloroform, where, over several minutes the solution progressively reddened. This colour change phenomenon is reproducible. The red solution was filtered through kieselguhr to remove a small amount of insoluble material. The chloroform was removed *in vacuo*. The resulting red residue was crystallised from a dichloromethane/methanol system at 4 °C. *Cis*-[Cr(CO)$_4$(SPNCHP-κ^2*N,P*)] was isolated by filtration and washed with n-pentane yielding 0.1071 g, 26.9 %, of dark red coloured crystals. Positive FAB mass spectrum: Found m/z (%) , assignment[calculated m/z for ^{52}Cr]: 746(1), MH$^+$[746]; 649(11), MO$^+$-4CO[649]; 633(100), M$^+$-4CO[633].

---

[27] F. A. Cotton, J. A. McCleverty and J. E. White, *Inorganic Syntheses*, 1967, **9**, 121.

2.4.5 Cis-[Cr(CO)$_4$(PNCHP-κ^2N,P)] + CH_3I + CO

Cis-[Cr(CO)$_4$(PNCHP-κ^2*N,P*)] (0.2006 g, 0.2811 mmol) was dissolved in methyliodide (12 mL) and left under an atmosphere of carbon monoxide for c.a. 4 h, at which time a yellow precipitate emerged. The precipitate was isolated and washed with n-pentane to giving the product as a yellow powder (0.1782 g, 61.8 % {calculated as [Cr(CO)$_5$I][**S.2.2-4**]I}). Positive FAB mass spectrum: Found m/z (%) , assignment[calculated m/z for ^{52}Cr]: 706(100), ["PNCHP + 2CH$_3$ + I"]$^+$ [706]. Negative FAB mass spectrum: Found m/z (%) , assignment[calculated m/z for ^{52}Cr]: 319(12), [Cr(CO)$_5$I]$^-$ [319]; 127(100), I$^-$[127].

2.4.6 Fac-[Mo(CO)$_3$(PNCHP-κ^3P,N,P)]

An ice-cold solution of [Mo(CO)$_3$(CHT)] (0.0992 g, 365 mmol) dissolved in toluene was added to an ice-cold solution of PNCHP (0.200 g, 0.364 mmol) dissolved in the same solvent. The mixture was stirred for c.a. 1 h, keeping the temperature below 0 °C, followed by a further 23 h at room temperature. The resulting precipitate was isolated, washed with n-pentane, and dried *in vacuo*, yielding 0.215 g (73 %) of *fac*-[Mo(CO)$_3$(PNCHP-κ^3*P,N,P*)] as a crimson powder, mp 154-155 °C. Anal. Found: C, 65.89; H, 4.19; N, 1.85. Calcd for $C_{40}H_{29}MoNO_3P_2$: C, 65.85; H, 4.01; N, 1.92.

2.4.7 Fac-[Mo(CO)$_3$(PNHCH$_2$P-κ^3P,N,P)]

A mixture of [Mo(CO)$_3$(CHT)] (0.0985 g, 0.0371 mmol) and PNHCH$_2$P (0.207 g, 0.0371 mmol) in 25 mL of toluene was stirred at room temperature for 3.5 h. The resulting yellow suspension of *fac*-[Mo(CO)$_3$(PNHCH$_2$P)] was isolated by filtration and washed with n-pentane. The filtrate was stood overnight under argon. The yellow powder is surface active resulting in a green discolouration, hence filtration is best carried out under a stream of argon. Recrystallisation was from toluene (80 mL). *fac*-[Mo(CO)$_3$(PNHCH$_2$P)] (0.0263 g, 96.9 %) was isolated as yellow microcrystals and washed with n-pentane. (See **Tables 2.6**, **2.8** and **2.9**)

2.4.8 Fac-[Mo(CO)$_4$(PNHCH$_2$P-κ^2P,P)][9]

Cis-[Mo(CO)$_4$(piperidine)$_2$][28] and one equivalent of PNHCH$_2$P were combined together in dichloromethane and heated to reflux. The title compound was isolated as pale yellow crystals in 64% yield, mp 184-187 °C. Anal. Found: C, 60.75; H, 3.93; N, 1.65. Calcd for $C_{41}H_{31}MoNO_4P_2 \bullet CH_2Cl_2$: C, 59.57; H, 3.90; N, 1.65.

[28] D. J. Darensbourg and R. L. Kump, *Inorg. Chem.*, 1978, **17**, 2680.

3 Reactivity of the Group 6 Metal - Carbonyl Complexes with Acids

3.1 Introduction

3.1.1 Background information

When substituted zerovalent metal-carbonyl complexes react with a protic acid, initially one of two things can occur. One of these is protonation at the metal centre.[1,2] For example, when a series of compounds of the type $M(CO)_3(L_3)$, where L_3 is a terdentate ligand containing a 'S_3', 'PS_2', 'NS_2', 'N_2S', 'N_3' or 'NP_2' donor set and M is Mo or W, were reacted with CF_3SO_3H, all were protonated at the metal centre.[1] Such protonation can facilitate geometrical isomerisation,[2,3] as seen in the case where trace amounts of acid have been found to catalyse the *fac* to *mer* isomerisation of phosphane-substituted tricarbonyls of Mo or W *via* a seven-coordinate hydride intermediate.[2]

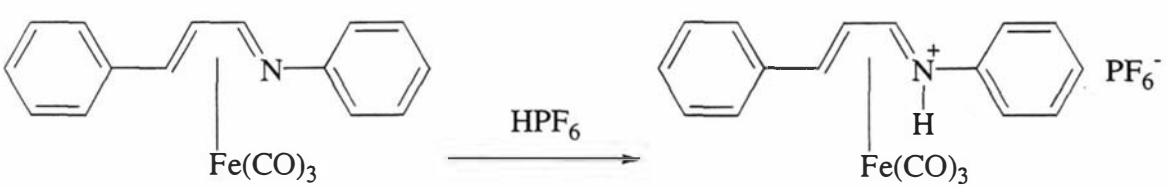

S.3.1-1 **S.3.1-2**

Scheme 3.1 Protonation of a coordinated ligand

Alternatively, protonation of a complex can occur at the ligand. For example, the complex $Fe(CO)_3L$ (**S.3.1-1**) (L = cinnamylideneaniline), shown in **Scheme 3.1**, reacts with HPF_6, resulting in protonation of the heteroatom to give **S.3.1-2**.[4] A kinetic study on

[1] O. P. Siclovan and R. J. Angelici, *Inorg. Chem.*, 1998, **37**, 432.
[2] J. M. Vila and B. L. Shaw, *J. Chem. Soc., Chem. Commun.*, 1987, 1178.
[3] C.N. Hsu and W.-Y. Yeh, *J. Chem. Soc., Dalton Trans.*, 1998, 125.
[4] A.M. Brodie, B.F.G. Johnson, P.L. Josty and J. Lewis, *J.C.S. Dalton*, 1972, 2031.

complexes of the type $Mo(CO)_4(P\text{-}N)$, where P-N is a pyridylphosphine bidentate ligand, in the presence of high concentrations of trifluroacetic acid, experience rapid protonation of the pyridyl group, resulting in the facilitation of ring-opening reactions. Protonation of a coordinated 'P_2N' terdentate ligand in *fac*-[$Mo(CO)_3(P_2N\text{-}\kappa^3P,N,P)$] facilitates carbonyl substitution reactions to give *cis*-[$Mo(CO)_4(P_2N\text{-}\kappa^2P,P)$].[5] Protonated PN-mixed donor multidentate ligands in particular, have been linked to the facilitation of a reductive elimination step in a hydroformylation catalyst[6] and as a proton messenger in an exceptional alkyne carbonylation catalyst.[7]

(a)

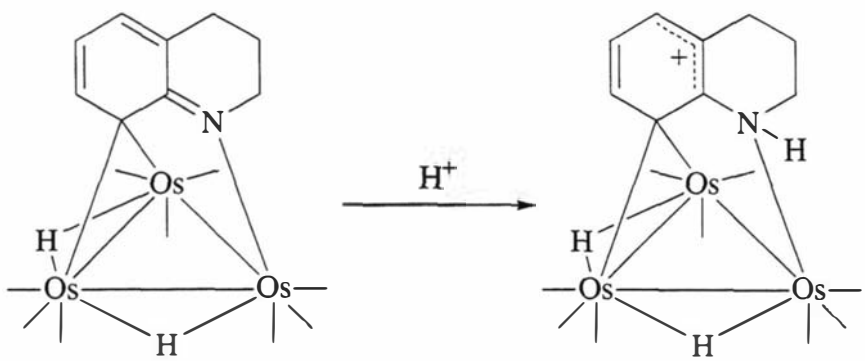

S.3.2-1

(b)

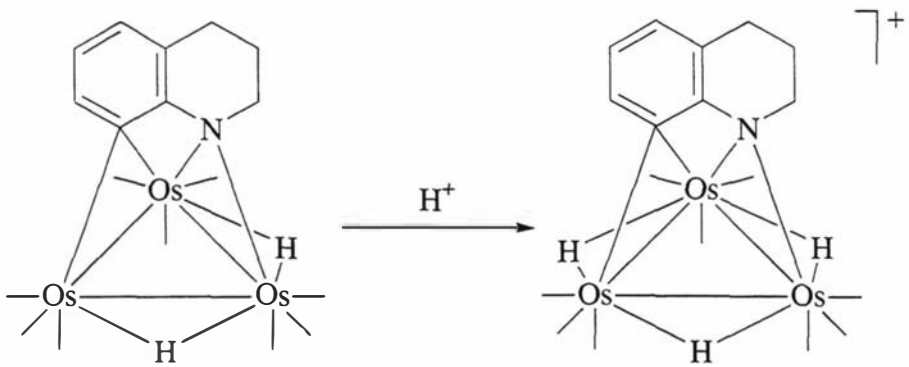

S.3.2-2

Scheme 3.2 Subtle changes in the nature of the ligand can influence the site of protonation: (a) ligand protonation; (b) metal protonation

[5] W.J. Knebel and R.J. Angelici, *Inorg. Chem.*,1974, **13**, 632.
[6] G. Francio, R. Scopelliti, C. G. Arena, G. Bruno, D. Drommi and F. Faraone, *Organometallics*, 1998, **17**, 338.
[7] E. Drent et al., *J. Organomet. Chem.*, 1994, **475**, 57

The ligand can influence the site of protonation. For example, the reaction of $[Os_3(CO)_9(\mu\text{-}H)(\mu_3\text{-}\eta^2\text{-}C_9H_9N)]$ (**S.3.2-1**), with CF_3SO_3H or CF_3CO_2H revealed protonation at the nitrogen of the coordinated tetrahydroquinoline (THQ). In sharp contrast, the closely related $[Os_3(CO)_{10}(\mu\text{-}H)(\mu_3\text{-}\eta^2\text{-}C_9H_9N)]$ (**S.3.2-2**) experiences protonation at the metal. Both situations are depicted in **Scheme 3.2**.[8]

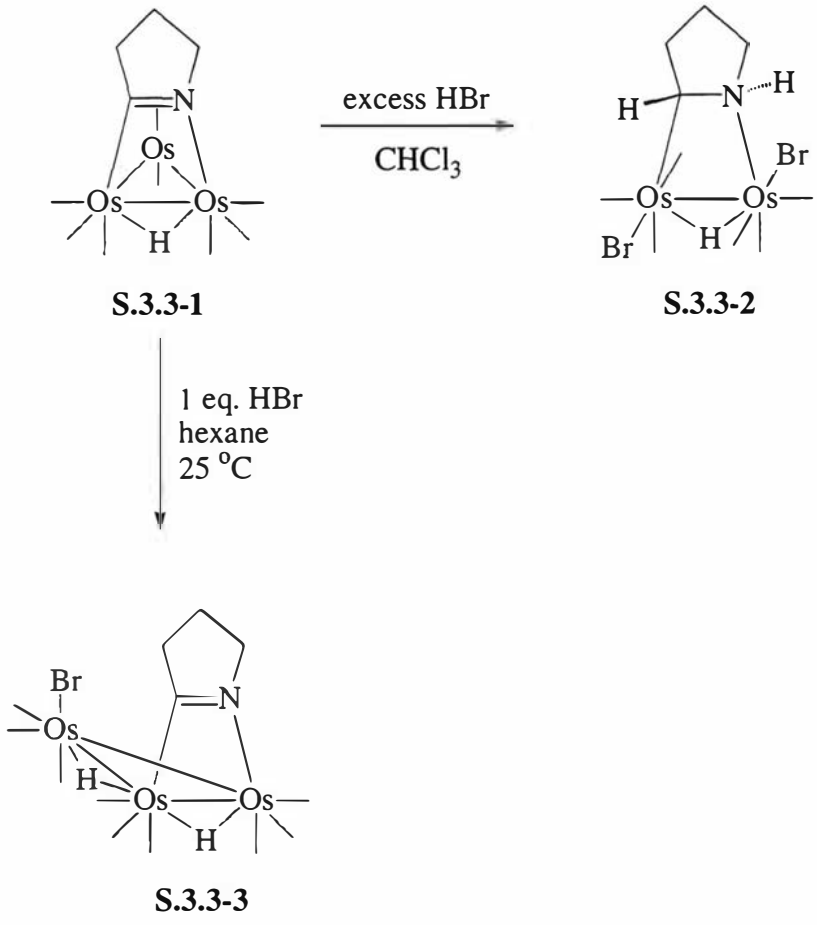

S.3.3-1 **S.3.3-2** **S.3.3-3**

Scheme 3.3 The acid-promoted hydrogenation of a carbon-nitrogen double bond

After the initial protonation step of a complex, activation for further reactivity can result. This is the case for an unusual example of acid-promoted hydrogenation of a carbon-nitrogen double bond, where the compound $[Os_3(CO)_9(\mu\text{-}H)(\mu_3\text{-}\eta^2\text{-}C{=}N(CH_2)_3)]$ (**S.3.3-1**) is reacted with excess HBr in chloroform to give $[Os_2(CO)_6Br_2(\mu\text{-}H)(\mu_3\text{-}\eta^2\text{-}CHNH(CH_2)_3)]$ (**S.3.3-2**), as shown by **Scheme 3.3**. It was postulated that **S.3.3-2** could be

[8] S. E. Kabir, D. S. Kolwaite and E. Rosenberg, *Organometallics*, 1996, **15**, 1979.

the result of the addition of 2 mol of HBr to the imidoyl bridged edge of $[Os_3(CO)_9(\mu\text{-}H)_2(\mu_3\text{-}\eta^2\text{-}\overline{C=N(CH_2)_3}Br]$ (**S.3.3-3**), also shown in **Scheme 3.3**.[9]

3.1.2 The present study

This chapter investigates the addition of various acids to group 6 metal-carbonyl complexes of PNCHP. It has previously been established that the 'free' PNCHP ligand cyclises when reacted with $HClO_4$ to form a racemic mixture of the phosphonium salt R- and S-$[PN(H)CHP]^+$ (**S.3.4-1R** and **S.3.4-1S**, respectively) as shown in **Scheme 3.4**.[10] Therefore, what would occur when the PNCHP ligand is coordinated, would protonation occur at the metal or at the ligand for complexes such as **F.3.1-1** and **F.3.1-2** shown in **Figure 3.1**?

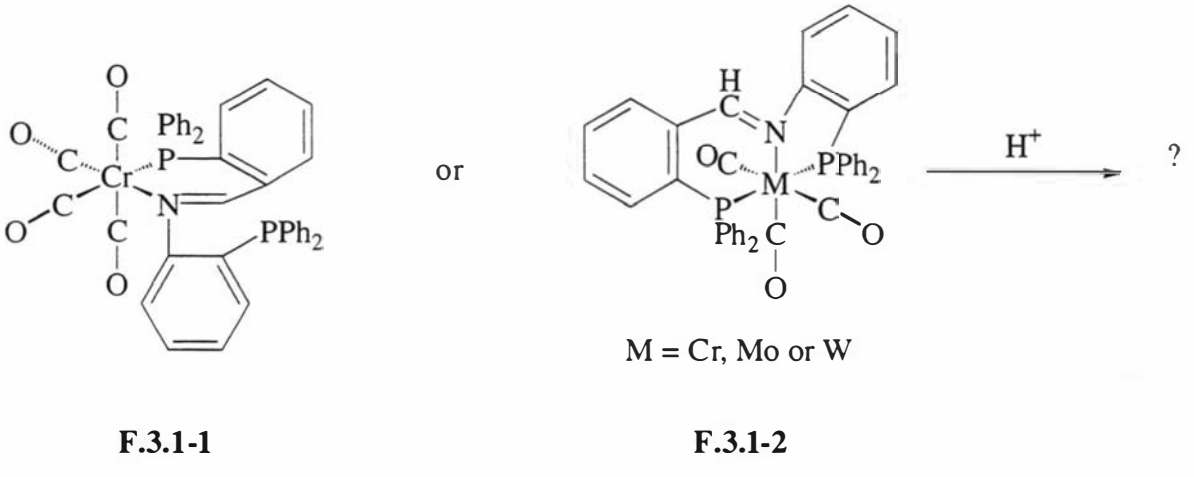

F.3.1-1 **F.3.1-2**

Figure 3.1 In what way do complexes containing the PNCHP ligand react towards acids?

[9] S. E. Kabir, E. Rosenberg, J. Stetson and M. Yin, *Organometallics*, 1996, **15**, 4473.
[10] M. J. R Halstead, *Iminophosphine Complexes of Ni(II)*, B.Sc(Hons) report, 1991, Massey University.

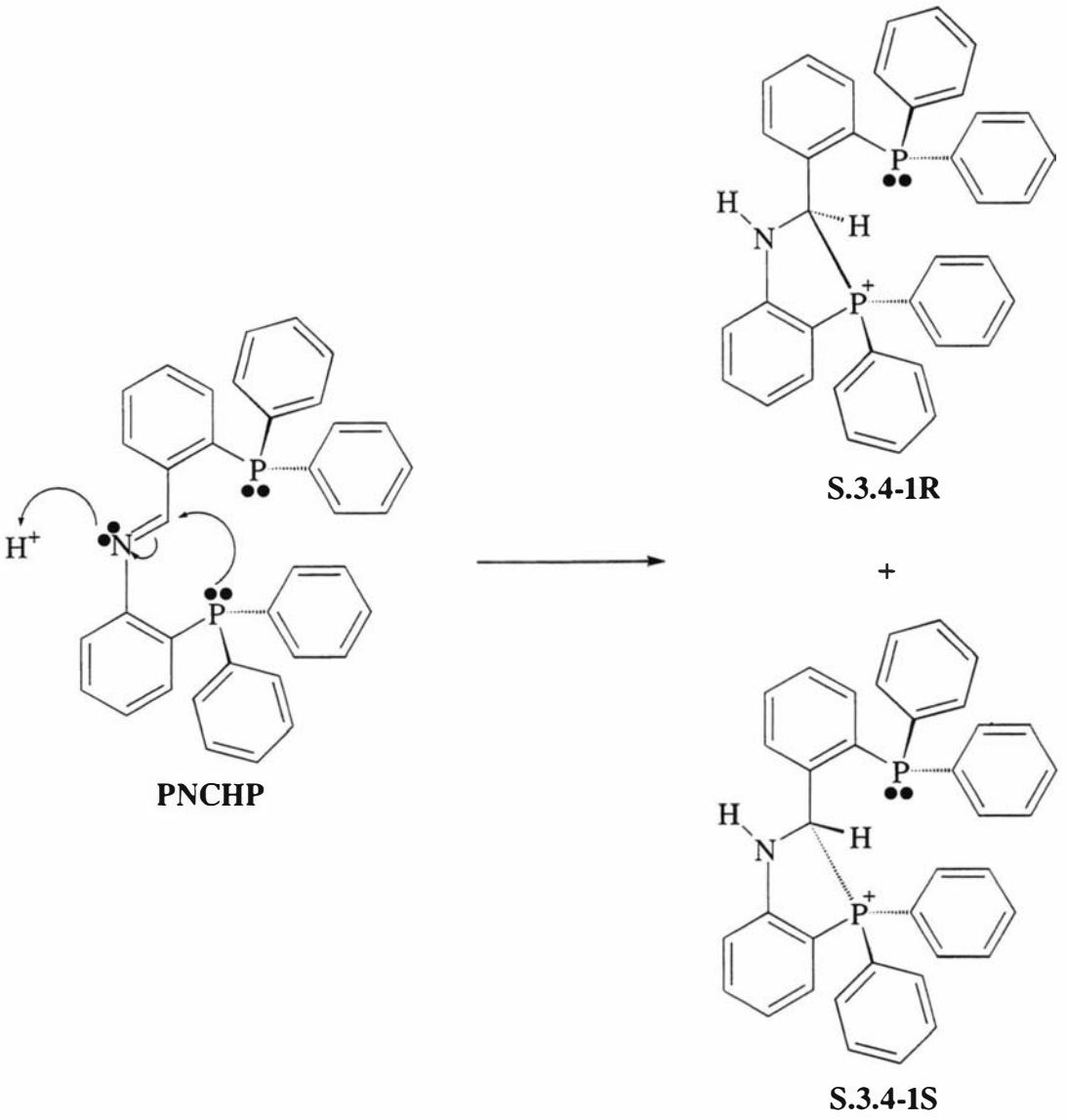

Scheme 3.4 The reaction of 'free' PNCHP with protic acids

3.2 Results and discussion

3.2.1 Synthesis

Evidence for the products discussed here is given in the succeeding sections. All the compounds have been fully characterised except for $[M(CO)_3\{PN(H)CHP\text{-}\kappa^2P,P\text{-}\eta^2(C{=}N)\}]BF_4$ (M = Cr or W), $[Mo(CO)_3\{PN(H)CHP\text{-}\kappa^2P,P\text{-}\eta^2(C{=}N)\}](CF_3CO_2)$, $[Mo(CO)_3\{PN(H)CHP\text{-}\kappa^2P,P\text{-}\eta^2(C{=}N)\}](CF_3SO_2)$ and *cis*-$[WCl_2(CO)_2(PNHCH_2P\text{-}\kappa^3P,N,P)]$, which have only been spectroscopically characterised due to difficulties in isolating the product.

Yellow dichloromethane/ethanol solutions of the PNCHP ligand rapidly decolourise on the addition of aqueous HBF_4 in slight excess. The product obtained is a racemic mixture of the cyclic-phosphonium salt $[PN(H)CHP]BF_4$, as shown in **Scheme 3.4**. The reaction is analogous to the reaction of PNCHP with $HClO_4$, which has been reported previously.[10]

Purple dichloromethane solutions of *mer*-$[M(CO)_3(PNCHP\text{-}\kappa^3P,N,P)]$ (**S.3.5-1M**, as shown in **Scheme 3.5**), where M is Mo or W,[11] react instantaneously with 50% HBF_4(in diethylether) or 32% $HBF_{4(aq)}$ (solubilised in dichloromethane by the addition of a little methanol), at room temperature, to give orange coloured $[M(CO)_3\{PN(H)CHP\text{-}\kappa^2P,P\text{-}\eta^2(C{=}N)\}]BF_4$ type species. An analogous reaction occurs for the dark green *mer*-$[Cr(CO)_3(PNCHP\text{-}\kappa^3P,N,P)]$ complex, although less readily. The Mo and W compounds are very stable unless exposed to any proton acceptor molecule like H_2O, diethylether or piperidine. For example, contact with diethylether will deprotonate $[M(CO)_3\{PN(H)CHP\text{-}\kappa^2P,P\text{-}\eta^2(C{=}N)\}]BF_4$ yielding the starting material *mer*-$[M(CO)_3(PNCHP\text{-}\kappa^3P,N,P)]$. When the metal is chromium a large excess of acid is required to drive the reaction to completion.

[11] S. M. F. Kennedy, *Structural Studies on a P_2N Triligate with Group 6 Metal Carbonyls*, B.Sc(Hons) report,1995, Massey University.

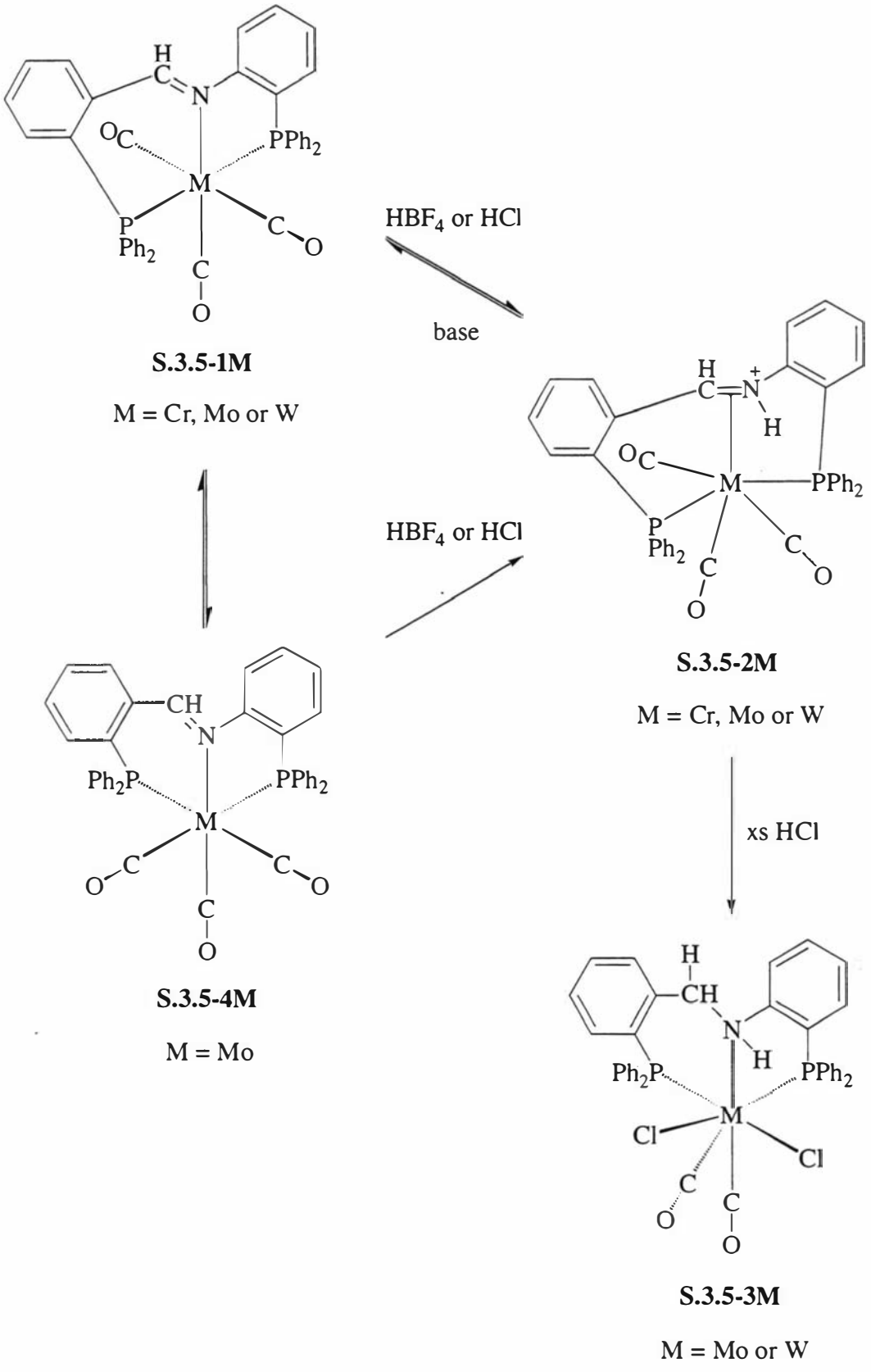

Scheme 3.5 Reactivity of the tricarbonyl complexes with the acids HBF_4 and HCl

The above chemistry on the *mer* isomer *mer*-[Mo(CO)$_3$(PNCHP-κ^3*P,N,P*)] (**S.3.5-1M**) starting material is reproduced when the *fac* isomer *fac*-[Mo(CO)$_3$(PNCHP-κ^3*P,N,P*)] (**S.3.5-4M**) is used instead. However, on deprotonation the *fac* isomer is not recovered, but the *mer* isomer instead. This suggests that a *mer* arrangement of the protonated PNCHP ligand is the favoured arrangement in the product. X-ray quality crystals of *mer*-[M(CO)$_3${PN(H)CHP-κ^2*P,P*-η^2(*C*=*N*)}]BF$_4$ proved extremely difficult to grow. Best results are achieved by slow evaporation of 1:1 dichloromethane/toluene solvent mixtures or from vapour diffusion using a dichloromethane/n-pentane solvent system. When BF$_3$.Et$_2$O is used in place of HBF$_4$ in all of the above reactions, the same products are observed, indicating the BF$_3$.Et$_2$O used contained residual amounts of HBF$_4$, even after purification, or that the BF$_3$.Et$_2$O is converted to HBF$_4$ in the course of the reaction.

Initially, the same species are also obtained when the HCl$_{(g)}$ is used in place of HBF$_4$, as shown in **Scheme 3.5**. However, unlike the HBF$_4$ product, [M(CO)$_3${PN(H)CHP-κ^2*P,P*-η^2(*C*=*N*)}]BF$_4$, the HCl product, [M(CO)$_3${PN(H)CHP-κ^2*P,P*-η^2(*C*=*N*)}]Cl (M = Mo or W), reacts with an additional mole of the respective acid yielding complexes of the type *cis*-[M(CO)$_2$Cl$_2$(PNHCH$_2$P-κ^3*P,N,P*)] (**S.3.5-3M**). In this case the metal has undergone a two-electron oxidation and the imine bond has been fully reduced to a secondary amine. This reaction is discussed in more detail in section *3.2.7*. In contrast, for M = Cr the reaction does not proceed past the initial protonation product.

The complex *cis*-[Cr(CO)$_4$(PNCHP-κ^2*N,P*)] was selected for reaction with H^+, to determine if the coordinated imino nitrogen would also protonate and, hence, the bonding mode of the imino group 'slip' to η^2(*C*=*N*) coordination in an analogous fashion to the tricarbonyl complexes discussed previuosly. Dichloromethane/ethanol solutions of *cis*-[Cr(CO)$_4$(PNCHP-κ^2*N,P*)][11] react with 32%HBF$_{4(aq)}$. However, unlike the tricarbonyl complexes, the protonated ligand detaches from the metal and the product isolated is a racemic mixture of the cyclic-phosphonium salt [PN(H)CHP]BF$_4$. This reaction is discussed in more detail in section *3.2.8*.

3.2.2 Description of the crystal structures

3.2.2.1 Crystal structure of mer-[W(CO)$_3${PN(H)CHP-κ^2P,P-η^2(N=C)}]BF$_4$

The structure of *mer*-[W(CO)$_3$(PN(H)CHP-κ^2*P,P*-η^2(*N*=*C*)}]$^+$ is shown in **Figure 3.2** with crystal data and structure refinement details being given in **Table 3.1** and bond lengths and angles given in **Table 3.2**. The complex contains a central tungsten atom (W) in a distorted octahedral geometry. Three carbonyl ligands (C(2)-O(2), C(3)-O(3) and C(4)-O(4)) are bound to the metal in a *meridional* arrangement, with the carbonyl-metal-carbonyl angles C(2)-W-C(4) (92.36(14) °), C(3)-W-C(4) (87.40(14) °) and C(2)-W-C(3) (176.05(13) °) close to the ideal angles of 90 ° and 180 °, respectively. The three remaining *meridional* sites are occupied by a protonated PNCHP ligand (PN(H)CHP). The PN(H)CHP ligand is coordinated unusually in that the protonated imino group (N-C(1)) is bound to the tungsten atom (W) *via* its π-bond, and not coordinated through the nitrogen, as expected for a neutral imine[12] and as found in the starting material *mer*-[W(CO)$_3$(PNCHP-κ^3*P,N,P*)].[11] The reason for this binding mode is that the nitrogen lone pair is involved in bonding to a proton and hence not available to bond to the metal. A least difference map was used to locate the 'proton'. The two phosphorus atoms (P(1) and P(2)) of PN(H)CHP are coordinated in a *trans* arrangement with a P(1)-W-P(2) angle of 173.22(3) °. A BF_4^- anion and two dichloromethane molecules reside at non-bonding distances from the complex.

The major contributor to the distortion of the octahedron is caused by the coordination of the imine π-bond in η^2 fashion. The P(1)-W-N and P(2)-W-C(1) angles are similar at 74.40(7) ° and 73.32(8) °, respectively. But at the same time, the angle N-W-C(4) (172.07(12) °) is closer to an ideal octahedron than the angle C1-W-C4 (149.87(13) °), implying that the nitrogen atom still sits above an the ideal coordination site of an octahedron, as it does in the starting material. Therefore, the major structural change upon protonation of the starting material is a move of the imino carbon C(1) from a non-bonding distance to a bonding distance. The situation can be visualised with the aid of **Figure 3.3**.

---

[12] *Comprehensive Coordination Chemistry*, G. Wilkinson (Editor-in Chief), Volume 2, 1987, Pergamon Press, Oxford, p715-735

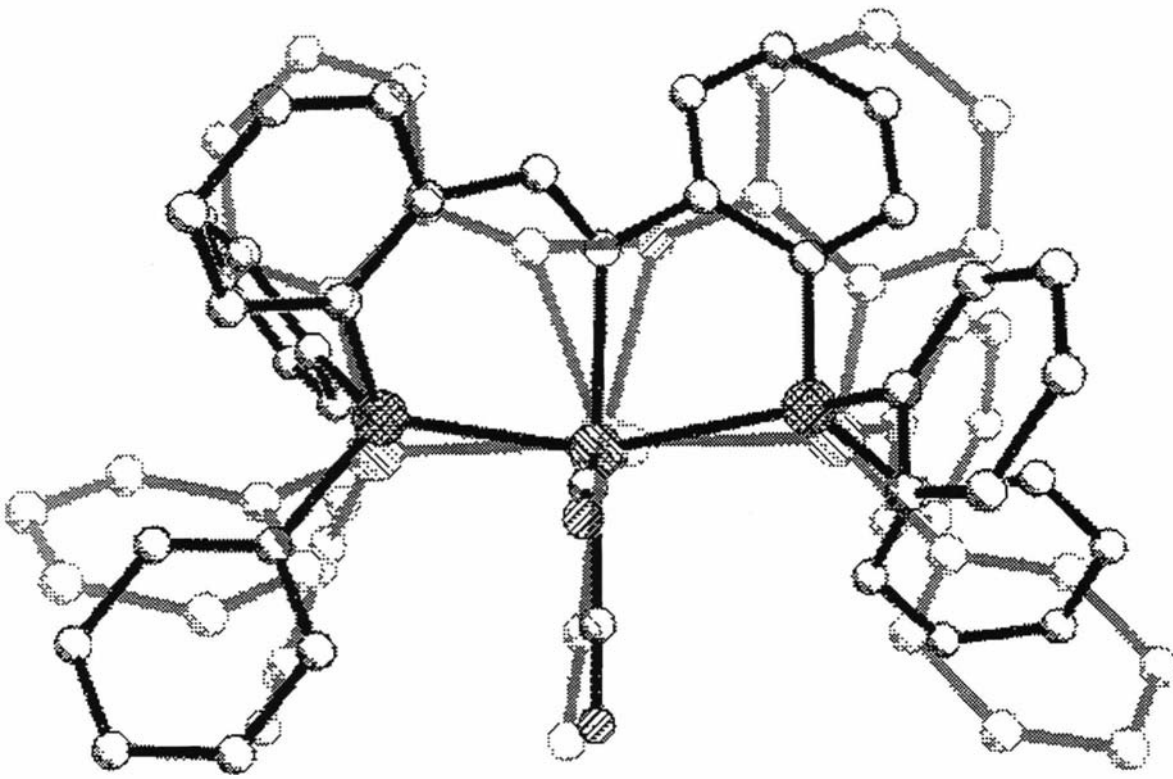

Figure 3.3 Crystal structures of the protonated complex *mer*-$[W(CO)_3\{PN(H)CHP\text{-}\kappa^2P,P\text{-}\eta^2(N{=}C)\}]^+$ (coloured gray) superimposed onto the non-protonated complex *mer*-$[Mo(CO)_3(PNCHP\text{-}\kappa^3P,N,P)]$ (coloured black) {an analogue of the starting material *mer*-$[W(CO)_3(PNCHP\text{-}\kappa^3P,N,P)]$} graphically illustrating the structural changes between the two

The positive charge carried by the complex is reflected in the slightly shortened carbonyl ligand C-O lengths C(2)-O(2) (1.141(4) Å), C(3)-O(3) (1.140(4) Å) and C(4)-O(4) (1.150(4) Å), when compared to the structurally similar and neutral complex *mer*-$[Mo(CO)_3(PNCHP\text{-}\kappa^3P,N,P)]$ at C(2)-O(2) (1.148(3) Å), C(3)-O(3) (1.152(3) Å) and C(4)-O(4) (1.162(3) Å), respectively.[11]

As touched on previously, an interesting feature of the complexes structure is the existence of η^2-imino coordination. Only one other example of an η^2-imine is catalogued at the Cambridge Crystallographic Data Centre and is found in the complex $[Ti(OAr\text{-}2,6\text{-}Pr^i{}_2)_2\{\eta^2\text{-}Bu^tNC(CH_2Ph)_2\}(py\text{-}4\text{-}Ph)]$.[13] The N-Ti (1.846(4) Å) and C-Ti (2.158(5) Å) are similar to the imino N-W distance (2.221(3) Å) and imino C(1)-W distance (2.219(3) Å) found in the title complex. The imine bond length N-C1 is 1.432(4) Å and is considerably

[13] L. D. Durfee, J. E. Hill, P. E. Fanwick and I. P. Rothwell, *Organometallics*, 1990, **9**, 75.

elongated when compared to the imine bond length of 1.257(3) Å found in *mer*-[Mo(CO)$_3$(PNCHP-κ^3*P,N,P*)],[11] but again very similar to the imine bond length of 1.421(7) Å found in the above titanium complex. The N-C length is also similar to μ_3-imines found coordinated to triosmiumcarbonyl clusters.[14] The lengthening is likely due to π back donation[15] from an appropriate tungsten d-orbital into the π^*_{imine} orbital.

In summary, protonation of the imino N atom has occurred resulting in a slippage of the imino coordination mode from κ^1 to η^2. This distortion of the octahedron appears to arise from the encroaching imino C atom which in the analogous Mo starting material is at non-bonding distances.

[14] a) M. Day, D. Espitia, K. I. Hardcastle, S. E. Kabir, and E. Rosenberg, *Organometallics*, 1991, **10**, 3550. b) C. J. Adams, M. I. Bruce, O. Kühl, B. W. Skelton and A. H. White, *J. Organomet. Chem.*, 1993, **445**, C6. c) R. D. Adams and N. M. Golembeski, *Inorg. Chem.*, 1978, **17**, 1969.

[15] J. E. Huheey, E. A. Keiter and R. L. Keiter, *Inorganic Chemistry: Principles of Reactivity and Structure*, Fourth Edition, 1993, HarperCollins College Publishers, New York, p662-663.

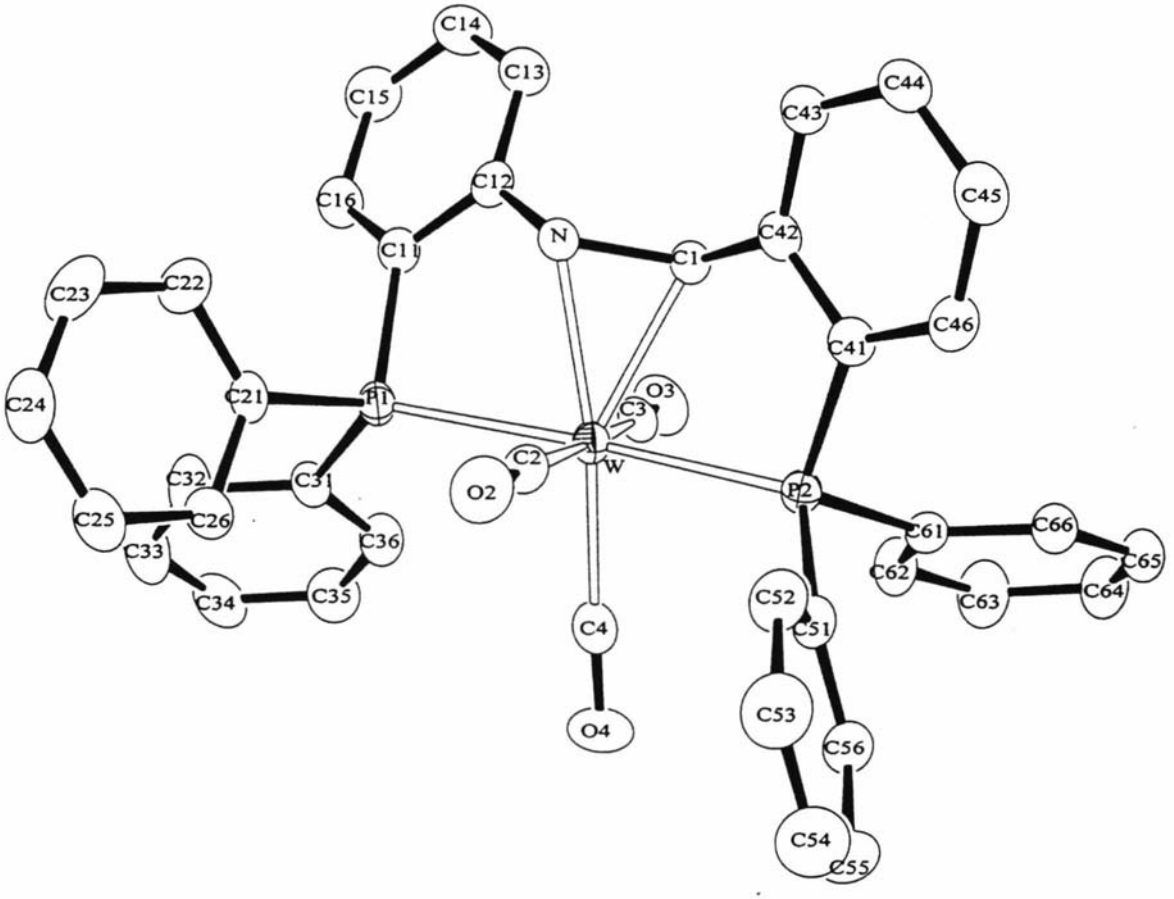

Figure 3.2 ORTEP diagram for the cation *mer*-$[W(CO)_3\{PN(H)CHP\text{-}\kappa^2P,P\text{-}\eta^2(N{=}C)\}]^+$ showing the numbering system used. Thermal ellipsoids are at the 50% probability level. Hydrogen atoms have been omitted for clarity

Table 3.1

Crystal data and structure refinement for *mer*-[$W(CO)_3${PN(H)CHP-κ^2*P*,*P*-η^2(*N*=*C*)}]BF_4.

Identification code	sk14
Empirical formula	C42 H33 B Cl4 F4 N O3 P2 W
Formula weight	1074.09
Temperature	203(2) K
Wavelength	0.71073 Å
Crystal system	Triclinic
Space group	P-1
Unit cell dimensions	a = 10.91880(10) Å α= 95.6520(10)°.
	b = 12.88350(10) Å β= 105.2640(10)°.
	c = 17.43280(10) Å γ = 111.0940(10)°.
Volume	2155.80(3) $Å^3$
Z	2
Density (calculated)	1.655 Mg/m^3
Absorption coefficient	3.058 mm^{-1}
F(000)	1058
Crystal size	0.23 x 0.17 x 0.11 mm^3
Theta range for data collection	1.24 to 27.48°.
Index ranges	-14<=h<=13, -16<=k<=16, 0<=l<=21
Reflections collected	9391
Independent reflections	9391 [R(int) = 0.0000]
Completeness to theta = 0.50°	0.0 %
Absorption correction	Semi-empirical from equivalents
Max. and min. transmission	0.7296 and 0.5397
Refinement method	Full-matrix least-squares on F^2
Data / restraints / parameters	9391 / 0 / 523
Goodness-of-fit on F^2	1.056
Final R indices [I>2sigma(I)]	R1 = 0.0279, wR2 = 0.0661
R indices (all data)	R1 = 0.0328, wR2 = 0.0693
Largest diff. peak and hole	1.504 and -1.323 e.$Å^{-3}$

Table 3.2

Selected bond lengths (Å) and angles (°) for the cation *mer*-[$W(CO)_3$(PNCHP-κ^2*P*,*P*-η^2(*N*=*C*)]$^+$ with estimated standard deviations in parentheses

Bond lengths:			
W-P(1)	2.4959(8)	N-C(12)	1.451(4)
W-P(2)	2.4703(8)	C(12)-C(11)	1.399(5)
W-N	2.221(3)	P(1)-C(11)	1.830(3)
W-C(1)	2.219(3)	P(1)-C(21)	1.818(3)
W-C(2)	2.045(3)	P(1)-C(31)	1.820(3)
W-C(3)	2.030(3)	C(1)-C(42)	1.491(4)
W-C(4)	2.029(4)	C(42)-C(41)	1.401(5)
C2-O(2)	1.141(4)	P(2)-C(41)	1.822(3)
C3-O(3)	1.140(4)	P(2)-C(51)	1.826(3)
C4-O(4)	1.150(4)	P(2)-C(61)	1.826(3)
N-C(1)	1.432(4)		
Bond angles:			
P(1)-W-P(2)	173.22(3)	P(2)-W-C(3)	100.30(9)
P(1)-W-N	74.40(7)	W-N-C(1)	71.10(16)
P(2)-W-C(1)	73.32(8)	W-C(1)-N	71.26(16)
C(2)-W-C(3)	176.05(13)	C1(2)-N-C(1)	120.7(3)
C(2)-W-C(4)	92.36(14)	N-C(1)-C(42)	120.3(3)
C(3)-W-C(4)	87.40(14)	W-P(1)-C(11)	98.43(11)
N-W-C(4)	172.07(12)	W-P(1)-C(21)	117.57(11)
C(1)-W-C(4)	149.87(13)	W-P(1)-C(31)	124.64(11)
P(1)-W-C(2)	89.76(9)	W-P(2)-C(41)	104.15(11)
P(1)-W-C(3)	86.76(9)	W-P(2)-C(51)	116.93(11)
P(2)-W-C(2)	83.56(9)	W-P(2)-C(61)	120.27(11)

3.2.2.2 Crystal structure of cis-[W(CO)$_2$Cl$_2$(PNHCH$_2$P-κ^3P,N,P)]

The structure of *cis*-[W(CO)$_2$Cl$_2$(PNHCH$_2$P-κ^3*P,N,P*)] is shown in **Figure 3.4** with crystal data and structure refinement details given in **Table 3.3** and bond lengths and angles given in **Table 3.4**. The complex contains a seven-coordinate tungsten atom (W) with two *cis* Cl atoms (Cl(1) and Cl(2)) and two *cis* CO groups (C(2)-O(2) and C(3)-O(3)) occupying four of the coordination sites, and a *fac* bound reduced-PNCHP (i.e. **PNHCH$_2$P**) ligand occupying the remaining three sites. The coordination geometry around the metal is predominantly a capped trigonal prism,[16] where Cl(1) acts as the capping ligand and Cl(2)-C(3), P(2)-C(2) and N-P(1) are edges defining the three tetragonal faces of the prism. However, a slight distortion from capped trigonal prism towards the more common capped octahedron geometry[17,18,19] exists, with the P(1), P(2), Cl(1), Cl(2), C(3) and N atoms occupying the six vertices of the octahedron and the C(2) atom capping it.

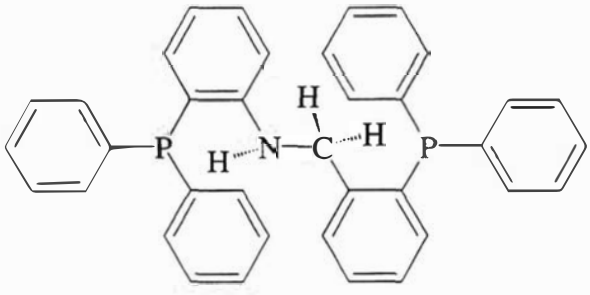

PNHCH$_2$P

There are no significant differences between the two W-CO or W-Cl bond lengths. However, the carbonyl ligand C(2)-O(2) (1.164(3) Å) is significantly longer than the other carbonyl ligand C(3)-O(3) (1.148(3) Å). The W-P(1) (2.4817(6) Å) bond length is slightly longer than bond length W-P(2) (2.4785(6) Å).

The angles C(1)-N-C(12) (109.0(2) °) and C(42)-C(1)-N (111.0(3) °), coupled with a C(1)-N bond distance of 1.455(4) Å, are supportive of the reduction of the imine bond of PNCHP to a secondary amine to give the ligand PNHCH$_2$P, shown above. The κ^3*P,N,P*

[16] P. K. Baker, M. C. Durrant, S. D. Harris, D. L. Hughes and R. L. Richards, *J. Chem. Soc., Dalton Trans.*, 1997, 509.
[17] Paul K. Baker, *Chemical Society Reviews*, 1998, **27**, 125.
[18] C. G. Young, S. Thomas and R. W. Gable, *Inorg. Chem.*, 1998, **37**, 1299.

coordination of the $PNHCH_2P$ ligand creates a five/six-membered fused ring system with the P(1)-W-N angle in the five membered ring measuring 75.73(7) ° and the P(2)-W-N angle in the six-membered ring at 85.58(7) °.

[19] P. K. Baker, A. I. Clark, M. G. B. Drew, M. C. Durrant and R. L. Richards, *Polyhedron*, 1998, **17**, 1407.

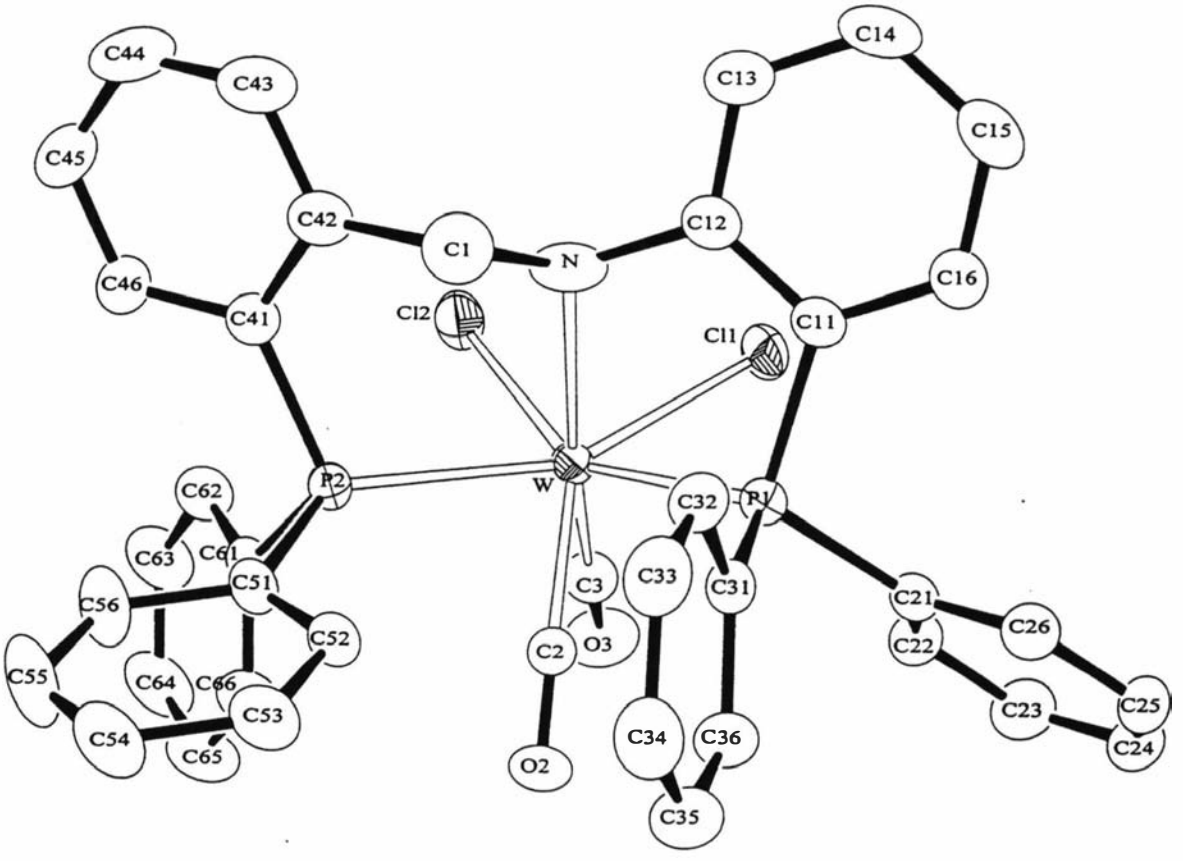

Figure 3.4 ORTEP diagram for the complex *cis*-[$W(CO)_2Cl_2(PNHCH_2P$-$\kappa^3P,N,P)$] showing the numbering system used. Thermal ellipsoids are at the 50% probability level. Hydrogen atoms have been omitted for clarity

Table 3.3

Crystal data and structure refinement for *cis*-[$W(CO)_2Cl_2(PNHCH_2P\text{-}\kappa^3P,N,P)$].

Identification code	sk10	
Empirical formula	C39 H30 Cl2 N O2 P2 W	
Formula weight	861.33	
Temperature	203(2) K	
Wavelength	0.71073 Å	
Crystal system	Triclinic	
Space group	P-1	
Unit cell dimensions	a = 11.0236(2) Å	α= 68.9950(10)°.
	b = 12.0855(2) Å	β= 85.7360(10)°.
	c = 16.6620(3) Å	γ = 71.9260(10)°.
Volume	1968.35(6) $Å^3$	
Z	2	
Density (calculated)	1.453 Mg/m^3	
Absorption coefficient	3.183 mm^{-1}	
F(000)	850	
Crystal size	0.45 x 0.40 x 0.23 mm^3	
Theta range for data collection	1.31 to 27.47°.	
Index ranges	-14<=h<=14, -15<=k<=15, -21<=l<=21	
Reflections collected	19519	
Independent reflections	8557 [R(int) = 0.0195]	
Absorption correction	Semi-empirical from equivalents	
Max. and min. transmission	0.5280 and 0.3284	
Refinement method	Full-matrix least-squares on F^2	
Data / restraints / parameters	8557 / 0 / 424	
Goodness-of-fit on F^2	1.019	
Final R indices [I>2sigma(I)]	R1 = 0.0206, wR2 = 0.0531	
R indices (all data)	R1 = 0.0218, wR2 = 0.0538	
Largest diff. peak and hole	1.360 and -0.748 $e.Å^{-3}$	

Table 3.4

Selected bond lengths (Å) and angles (°) for *cis*-[$W(CO)_2Cl_2(PNHCH_2P$-$\kappa^3P,N,P)$] with estimated standard deviations in parentheses

Bond lengths:			
W-P(1)	2.4817(6)	N-C(12)	1.543(4)
W-P(2)	2.4785(6)	C(12)-C(11)	1.393(4)
W-N	2.315(2)	P(1)-C(11)	1.824(3)
W-C(2)	1.961(2)	P(1)-C(21)	1.828(3)
W-C(3)	1.962(3)	P(1)-C(31)	1.832(3)
W-Cl(1)	2.5072(6)	C(1)-C(42)	1.514(5)
W-Cl(2)	2.5050(6)	C(42)-C(41)	1.413(4)
C(2)-O(2)	1.164(3)	P(2)-C(41)	1.826(3)
C(3)-O(3)	1.148(3)	P(2)-C(51)	1.839(3)
N-C(1)	1.455(4)	P(2)-C(61)	1.837(2)
Bond angles:			
P(1)-W-P(2)	123.16(2)	C(3)-W-Cl(1)	83.20(8)
P(1)-W-N	75.73(7)	C(3)-W-Cl(2)	83.92(8)
P(2)-W-N	85.58(7)	C(12)-N-C(1)	109.0(2)
C(2)-W-C(3)	70.58(10)	N-C(1)-C(42)	111.0(3)
Cl(1)-W-Cl(2)	80.73(2)	W-P(1)-C(11)	103.23(9)
W-N-C(1)	118.9(2)	W-P(1)-C(21)	119.66(9)
W-N-C(12)	114.94(18)	W-P(1)-C(31)	119.24(8)
C(2)-W-N	127.31(9)	W-P(2)-C(41)	110.64(8)
C(3)-W-N	162.03(10)	W-P(2)-C(51)	124.04(8)
C(2)-W-Cl(1)	129.55(7)	W-P(2)-C(61)	110.68(8)
C(2)-W-Cl(2)	135.08(7)		

3.2.2.3 Crystal structure of cis-[$Mo(CO)_2Cl_2(PNHCH_2P$-$\kappa^3P,N,P)$)]

A preliminary structure of the molecule *cis*-[$Mo(CO)_2Cl_2(PNHCH_2P$-$\kappa^3P,N,P)$] is shown by **Figure 3.5**. Atom connectivity and the complexes geometry is analogous to that of *cis*-[$W(CO)_2Cl_2(PNHCH_2P$-$\kappa^3P,N,P)$] discussed in directly above.

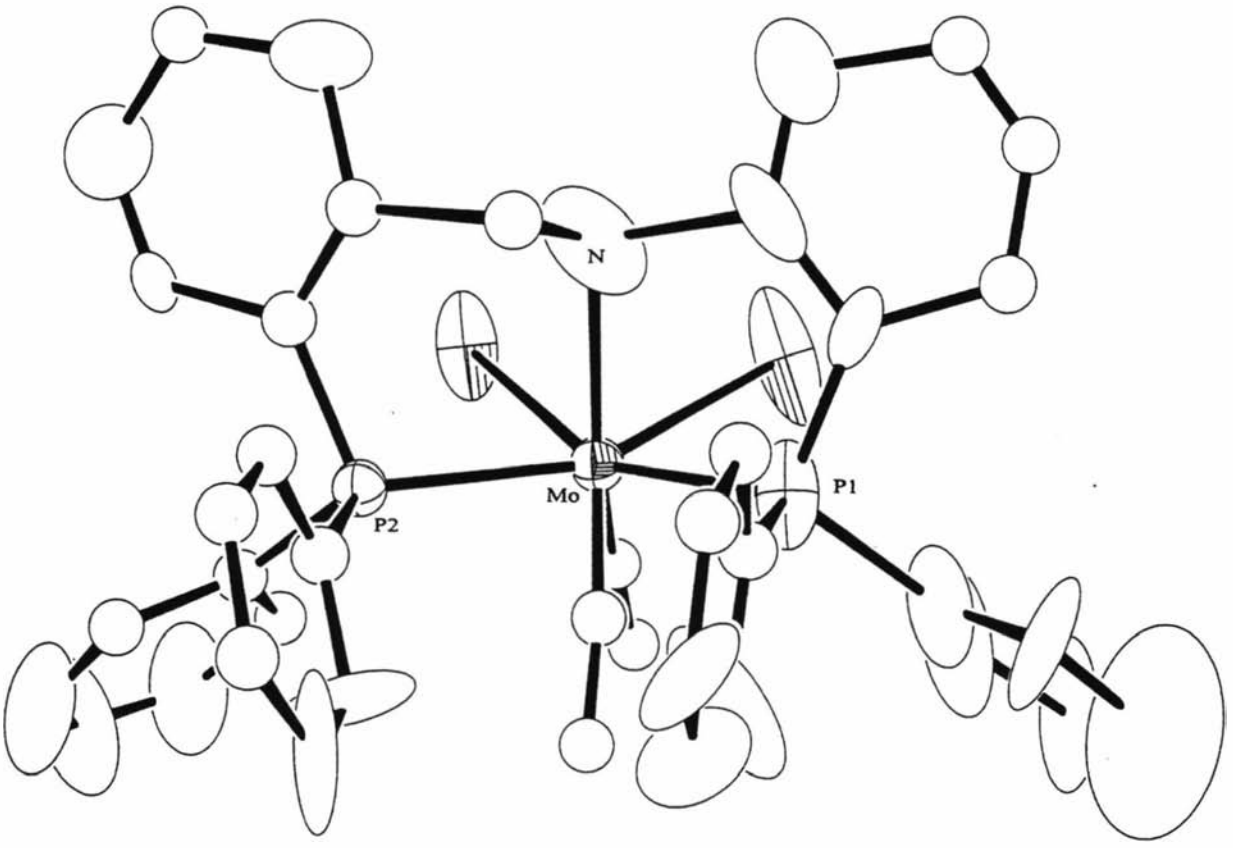

Figure 3.5 ORTEP diagram for the complex *cis*-[$Mo(CO)_2Cl_2(PNHCH_2P$-κ^3P,N,P)] showing the numbering system used. Thermal ellipsoids are at the 50% probability level. Hydrogen atoms have been omitted for clarity

3.2.2.4 Crystal structure of [PN(H)CP)]BF_4

The cation $[PN(H)CHP]^+$ is shown by **Figure 3.6** with crystal data and structure refinement details given in **Table 3.5** and bond lengths and angles given in **Table 3.6**. The structure shows that the phosphorus atom P(1) is quaternarised and is part of a five-membered heterocyclic ring. The other phosphorus atom P(2) is a tertiary phosphane, as it is in PNCHP. The angles around the N(1) and C(1)atoms (which was the imino group in PNCHP), C(12)-N(1)-C(1) (116.5(4) °), N(1)-C(1)-C(21) (115.8(4) °), C(21)-C(1)-P(1) (111.3(3) °) and N(1)-C(1)-P(1) (100.6(3) °), coupled with a N(1)-C(1) bond length of 1.444(6) Å, suggests that the N(1)-C(1) bond is more typical of a amine than an imine. The C(1) atom is tetrahedral and is a stereocentre, however, the compound crystallises as the racemate. Aryl C-P-C angles are significantly smaller for the P(2) atom than they are for the P(1) atom, with averages of 103.3 and 112.3 ° respectively, this is primarily due to the P(1) atom and one of its phenyl rings being involved in the five-membered heterocyclic ring, creating a strained C(11)-P(1)-C(1) angle of 93.0 °. As expected, the structure is similar to $[PN(H)CHP]ClO_4$.[10]

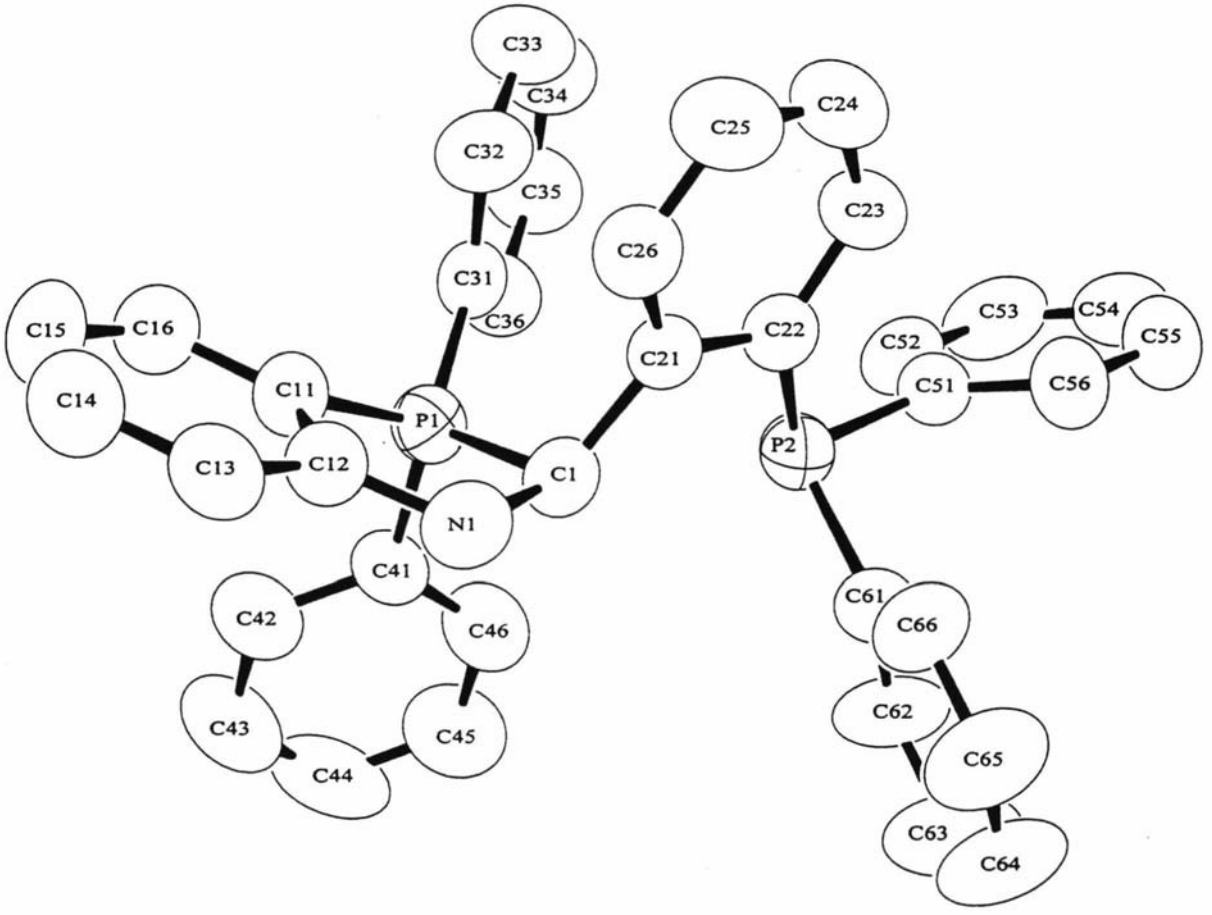

Figure 3.6 ORTEP diagram for the cation $[PN(H)CHP]^+$ showing the numbering system used. Thermal ellipsoids are at the 50% probability level. Hydrogen atoms have been omitted for clarity

Table 3.5.

Crystal data and structure refinement for $[PN(H)CHP)]BF_4$.

Identification code	amb6	
Empirical formula	C37 H30 B F4 N P2	
Formula weight	637.37	
Temperature	298(2) K	
Wavelength	0.71073 Å	
Crystal system	Monoclinic	
Space group	$P2_1/n$	
Unit cell dimensions	a = 8.950(2) Å	α= 90°.
	b = 19.188(4) Å	β= 99.39(3)°.
	c = 18.656(4) Å	γ = 90°.
Volume	3160.9(12) $Å^3$	
Z	4	
Density (calculated)	1.339 Mg/m^3	
Absorption coefficient	0.189 mm^{-1}	
F(000)	1320	
Crystal size	0.39 x 0.35 x 0.27 mm^3	
Theta range for data collection	1.53 to 24.97°.	
Index ranges	0<=h<=10, 0<=k<=22, -22<=l<=21	
Reflections collected	5925	
Independent reflections	5546 [R(int) = 0.0382]	
Absorption correction	Empirical via scans	
Max. and min. transmission	0.9506 and 0.9298	
Refinement method	Full-matrix least-squares on F^2	
Data / restraints / parameters	5546 / 4 / 407	
Goodness-of-fit on F^2	0.991	
Final R indices [I>2sigma(I)]	R1 = 0.0548, wR2 = 0.1368	
R indices (all data)	R1 = 0.2043, wR2 = 0.1886	
Largest diff. peak and hole	0.390 and -0.267 $e.Å^{-3}$	

Table 3.6

Selected bond lengths (Å) and angles (°) for [PN(H)CHP)]BF_4 with estimated standard deviations in parentheses

Bond lengths:			
P(1)-C(1)	1.856(5)	P(2)-C(51)	1.801(5)
P(1)-C(11)	1.764(5)	P(2)-C(61)	1.808(6)
P(1)-C(31)	1.764(5)	N(1)-C(1)	1.444(6)
P(1)-C(41)	1.786(5)	N(1)-C(12)	1.367(6)
P(2)-C(22)	1.804(5)	C(1)-C(21)	1.515(6)
Bond angles:			
C(1)-P(1)-C(31)	115.5(2)	C(21)-C(1)-N(1)	115.8(4)
C(1)-P(1)-C(11)	93.0(2)	P(1)-C(1)-N(1)	100.6(3)
C(11)-P(1)-C(31)	114.3(2)	C(1)-N(1)-C(12)	116.5(4)
C(1)-P(1)-C(41)	110.1(2)	C(22)-P(2)-C(51)	106.3(2)
C(11)-P(1)-C(41)	110.6(2)	C(22)-P(2)-C(61)	102.7(3)
C(31)-P(1)-C(41)	112.0(2)	C(51)-P(2)-C(61)	101.0(2)
P(1)-C(1)-C(21)	111.3(3)		

3.2.3 NMR spectroscopic studies

3.2.3.1 ^{31}P NMR spectroscopy of the compounds

Solution ^{31}P NMR data for the compounds to be discussed are listed in **Table 3.7**. The compounds $[M(CO)_3\{PN(H)CHP\text{-}\kappa^2P,P\text{-}\eta^2(N{=}C)\}]^+$, where M is Cr, Mo or W, each displayed two doublets, which are assigned to the two inequivalent phosphorus atoms of the protonated PNCHP ligand. The signal splitting is assigned to two-bond phosphorus-phosphorus spin coupling, with ^2J(P,P) constants unresolved for the chromium complex, 29 Hz for the molybdenum complex and 35 Hz for the tungsten complex. The magnitude of the coupling constants is indicative of two inequivalent phosphorus atoms in a *cis*

arrangement around zerovalent group 6 metal in solution (22-40 Hz).[20] The tungsten compound exhibits satellites peaks consistent with one-bond phosphorus coupling to the 14 % abundant spin ½ nucleus ^{183}W. The $^{1}J(P,W)$ coupling constants measured 229 Hz for the high frequency resonance and 253 Hz for the low frequency resonance.

Table 3.7

^{31}P-NMR data for selected compounds [a]

Compounds	δ		$^{2}J(P,P)$ /Hz	$^{1}J(W,P)$ /Hz	
$[PN(H)CHP]BF_4$	39.0	-16.2			
$[Cr(CO)_3\{PN(H)CHP\text{-}\kappa^2P,P\text{-}\eta^2(N{=}C)\}]BF_4$	41.8	35.9	[b]		
$[Mo(CO)_3\{PN(H)CHP\text{-}\kappa^2P,P\text{-}\eta^2(N{=}C)\}]BF_4$	62.1	48.0	35		
$[W(CO)_3\{PN(H)CHP\text{-}\kappa^2P,P\text{-}\eta^2(N{=}C)\}]BF_4$ [c]	37.1	31.4	29	229	253
cis-$[MoCl_2(CO)_2(PNHCH_2P\text{-}\kappa^3P,N,P)]$	66.7	44.8	22		
cis$[WCl_2(CO)_2(PNDCHDP\text{-}\kappa^3P,N,P)]$	49.9	25.2	21	221	244
cis-$[Cr(CO)_4(PNCHP\text{-}\kappa^2N,P)] + HBF_4$	38.8	-16.1			

[a] Solvent is $CDCl_3$ unless indicated. [b] Not resolved. [c] See **Figure 3.7** for CP/MAS data

In the chromium complex $[Cr(CO)_3\{PN(H)CHP\text{-}\kappa^2P,P\text{-}\eta^2(N{=}C)\}]^+$, one of the PN(H)CHP ligands phosphorus signals is 5.9 ppm to higher frequency than the other, 14.1 ppm higher in the molybdenum complex and 5.7 ppm higher in the tungsten complex for the solution spectra. In the starting materials *mer*-$[M(CO)_3(PNCHP\text{-}\kappa^3P,N,P)]$ (M = Cr, Mo or W), these differences (Δδ) are also present, at 4.9 ppm, 5.3 ppm, 8.4 ppm, respectively, with the higher frequency resonance most likely due to the to the phosphorus

[20] a) S. D. Perera, B. L. Shaw and M. Thorton-Pett, *J. Chem. Soc. Dalton Trans.*, 1992, 1469. b) U. U. Ike, S. D. Perera, B. L. Shaw and M. Thorton-Pett, *J. Chem Soc. Dalton Trans.*, 1995, 2057. c) S. O. Grim, R. C. Barth, J. D. Mitchell and J. D. Gaudio, *Inorg. Chem.*, 1977, **16**, 1776.

atom involved in the five-membered chelate ring.[21] However, if the coordination mode of the imino group in solution is the same as it is in the solid state, i.e., η^2, a fused five/six-membered ring system would no longer exist, but two five-membered rings instead, hence the signal at higher frequency can no longer be caused solely by the involvement of a phosphorus in a five-membered ring. From the crystal structure of *mer*-$[W(CO)_3\{PN(H)CHP\text{-}\kappa^2P,P\text{-}\eta^2(N{=}C)\}]^+$, discussed in section *3.2.2.1*, it is noted that the two inequivalent phosphorus atoms of the PNCHP ligand are both involved in five-membered chelate rings, so one may not expect such a significant difference in chemical shift of the two phosphorus atoms, considering that in the 'free' ligand the $\Delta\delta$ value between the two phosphorus atoms is small at 0.6 ppm. However, in the compound *cis*-$[W(CO)_4(PNCHP\text{-}\kappa^2P,N,P)]$, where both phosphorus atoms are mutually involved in a nine-membered chelate ring and may be thought of to be in very similar chemical environments, the $\Delta\delta$ value is large at 19.2 ppm, suggesting that the chelate ring sizes that each phosphorus atom is involved in is not the only factor determining the large difference in chemical shift of each of the phosphorus atoms in the $[M(CO)_3(PN(H)CHP)]^+$ complexes. This implies that the solution structure could still be essentially the same as the solid state structure with respect to the binding mode of the imino group.

Compared to the *mer*-$[M(CO)_3(PNCHP\text{-}\kappa^3P,N,P)]$ starting materials, the protonated products *fac*-$[M(CO)_3\{PN(H)CHP\text{-}\kappa^2P,P\text{-}\eta^2(N{=}C)\}]^+$ have, in general, had their ^{31}P NMR signals shifted to a higher frequency, which is consistent with a deshielding of the phosphorus caused by the positive charge. The most notable difference is the reduction of the $^2J(P,P)$ coupling constant, from c.a. 90 hz to c.a. 30 Hz, on going from the starting material to the protonated product. This is consistent with a change from a *trans* arrangement of phosphorus atoms around the metal to a *cis* arrangement in solution.[22]

As mentioned above for the compound $[W(CO)_3\{PN(H)CHP\text{-}\kappa^2P,P\text{-}\eta^2(N{=}C)\}]BF_4$, the solution ^{31}P NMR results gave information typical of a *cis* arrangement of phosphorus atoms. In contrast, the X-ray structure showed *trans* phosphorus atoms. In an attempt to confirm the apparent geometric differences between the solution and solid state structures, a CP/MAS ^{31}P NMR study was undertaken on the compound and, for

[21] a) S. Berger, S. Braun and H-O. Kalinowski, *NMR Spectroscopy of the Non-Metallic Elements*, 1997, John Wiley & Sons Ltd, Chichester, 837. b) G. Dyer and J. Roscoe, *Inorg. Chem.*, 1996, **35**, 4098, and refs. within.

[22] *Multinuclear NMR*, J. Mason (Editor), 1987, Plenum Press, New York, p394

comparison, the known *trans*-phosphorus compound *mer*-[$W(CO)_3$(PNCHP-κ^3*P,N,P*)]. The CP/MAS ^{31}P NMR spectra, shown in **Figure 3.7**, for both compounds under study are interpreted as two overlapping groups of signals from each of the two inequivalent phosphorus atoms. Each phosphorus atom exhibits a group of signals due to the ^{31}P chemical shift anisotropy.[23] No ^2J(P,P) coupling is evident in the solid state, based on a smallest magnitude between adjacent peaks of 1250 Hz being unreasonable as a ^2J(P,P) coupling constant, considering the largest ^2J(P,P) splitting magnitudes found in solution are 88 Hz. Despite the lack of ^2J(P,P) coupling constant information to resolve the geometry similarities/differences between [$W(CO)_3${PN(H)CHP-κ^2*P,P*-η^2(*N*=*C*)}]BF_4 and *mer*-[$W(CO)_3$(PNCHP-κ^3*P,N,P*)], the overall spectral characteristics of the protonated tungsten complex [$W(CO)_3${PN(H)CHP-κ^2*P,P*-η^2(*N*=*C*)}]BF_4 were virtually identical to the starting material *mer*-[$W(CO)_3$(PNCHP-κ^3*P,N,P*)], reflecting the same structural arrangement in both compounds. This result suggests that the solid state structure of [$W(CO)_3${PN(H)CHP-κ^2*P,P*-η^2(*N*=*C*)}]BF_4 and *mer*-[$W(CO)_3$(PNCHP-κ^3*P,N,P*)] is similar, which is expected if the crystal structure discussed in section *3.2.2.1* represents the bulk of the sample. Therefore, it does appear that there is a difference between the solid state and solution structures of [$W(CO)_3${PN(H)CHP-κ^2*P,P*-η^2(*N*=*C*)}]BF_4 or that the ^2J(P,P) coupling constant of 29 Hz in solution is a new lower limit for *trans* phosphorus atoms, if so, there would be no difference between the solid and solution structures. IR evidence discussed in section *3.2.4* seems to favour the later.

[23] M. M. Maricq and J. S. Waugh, *J. Chem. Phys.*, 1979, **70**, 3300.

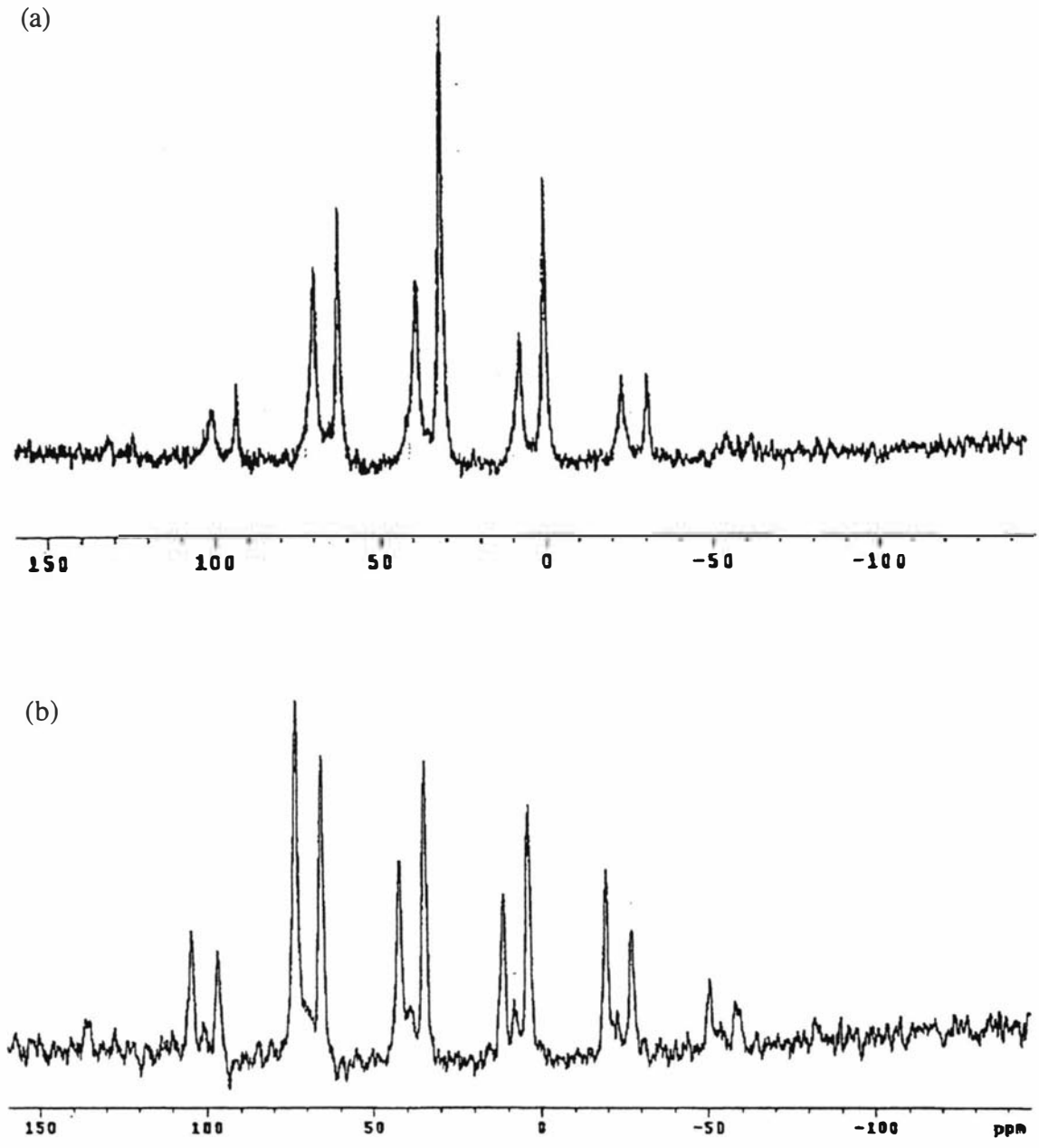

Figure 3.7 (CP MAS) ^{31}P NMR spectra of the compounds (a) *mer*-[W(CO)$_3${PN(H)CHP-κ^2*P*,*P*-η^2(*N*=*C*)}]BF$_4$ and (b) *mer*-[W(CO)$_3$(PNCHP-κ^3*P*,*N*,*P*)]

The discussion so far has centred on the protonation of *mer*-[$M(CO)_3$(PNCHP-κ^3*P,N,P*)]. In addition, the same product is obtained when the geometrical isomer of *mer*-[$M(CO)_3$(PNCHP-κ*P,N,P*)], that is, *fac*-[$Mo(CO)_3$(PNCHP-κ^3*P,N,P*)], is protonated. ^{31}P NMR monitoring of the deprotonation reaction, by piperidine in dichloromethane as solvent, in both cases, results in the recovery of only the *mer* starting material as depicted by **S.3.5-1M**, **S.3.5-2M** and **S.3.5-4M** in **Scheme 3.5**.

^{31}P NMR monitoring of the reactions that resulted in the [$M(CO)_3${PN(H)CHP-κ^2*P,P*-η^2(*N*=*C*)}]$^+$ compounds, showed no intermediates or other products except for the reaction of *mer*-[$Cr(CO)_3$(PNCHP-κ^3*P,N,P*)] with HBF_4. In this case, a substantial second product was observed, in about 30 % concentration (by peak area integration), which displayed singlet signals at δ39.0 and δ-15.5. The spectrum observed for the second product is suggestive of the formation of the cyclic-phosphonium salt [PN(H)CHP]BF_4 (δ39.0(s), δ-16.2(s)).

[PN(H)CNP]BF_4 is also the product when *cis*-[$Cr(CO)_4$(PNCHP-κ^2*N,P*)] is reacted with HBF_4. The reaction is discussed in detail in section *3.2.8*. Again the signals are at δ38.8 and δ-16.1. The higher frequency signal is consistent with a phosphorus atom involved in the five-membered ring[21] and lower frequency signal typical of non-coordinated tertiary arylphosphanes.[24]

The compound [$MoCl_2(CO)_2$(PNHCH$_2$P-κ^3*P,N,P*)] exhibits a signal at δ66.7 and δ44.8, both split as doublets by phosphorus-phosphorus spin coupling with a ^2J(P,P) coupling constant of 22 Hz. The chemical shifts are again typical of transition metal-coordinated phosphanes.[25] The tungsten analogue [$WCl_2(CO)_2$(PNDCHDP-κ^3*P,N,P*)] displays a signal at δ49.9 and δ25.2 and like the molybdenum compound, both signals are split as doublets with a ^2J(P,P) coupling constant, of 21 Hz, typical of *cis* phosphorus atoms. In addition, the tungsten compound also displays the expected ^{183}W (14.4 %) satellite peaks, with a ^1J(W,P) coupling constant of 221 Hz for the high frequency signal and a 244 Hz one for the lower.

[24] See ref 21a, p702
[25] See ref 21a, p835

3.2.3.2 ^1H NMR spectroscopy of the compounds

Selected proton NMR data for the compounds is given in **Table 3.8**. When the PNCHP ligand is reacted with HBF_4, the disappearance of the imine proton signal at δ8.92 occurs. This is consistent with formation of the product $[PN(H)CHP]BF_4$ (**F.3.8-1**), shown in **Figure 3.8**. All other signals observed were in the aromatic region (δ8.02-6.53) of the spectrum, which suffered from poor resolution due to the number of inequivalent aromatic protons of the compound, hence, the signal of the methine proton of $[PN(H)CHP]BF_4$ (**F.3.8-1**) was not assigned. An identical proton NMR spectrum was obtained for the reaction product of *cis*-$[Cr(CO)_4(PNCHP\text{-}\kappa^2N,P)]$ with HBF_4, therefore, the product of the reaction was assigned as $[PN(H)CHP]BF_4$ (**F.3.8-1**) and confirmed by a single crystal X-ray diffraction study, as discussed in section *3.2.2.4*.

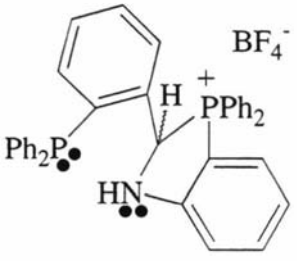

F.3.8-1

Figure 3.8 The cyclic phosphonium salt $[PN(H)CHP]BF_4$

The compounds $[Mo(CO)_3\{PN(H)CHP\text{-}\kappa^2P,P\text{-}\eta^2(N{=}C)\}]BF_4$ and $[W(CO)_3\{PN(H)CHP\text{-}\kappa^2P,P\text{-}\eta^2(N{=}C)\}]BF_4$ exhibited similar spectra. The imino proton signal of $[Mo(CO)_3\{PN(H)CHP\text{-}\kappa^2P,P\text{-}\eta^2(N{=}C)\}]BF_4$ had shifted 0.67 ppm to higher frequency, and split from a singlet to a doublet (J = 8.6Hz), relative to the non-protonated complex mer-$[Mo(CO)_3(PNCHP)]$. In the tungsten case the shift was similar at 0.62 ppm with a 7.7 Hz J(P,H) coupling constant. Protonation of the metal was discounted by monitoring the reaction of *mer*-$[W(CO)_3(PNCHP\text{-}\kappa^3P,N,P)]$ in deuterated chloroform with one equivalent of CF_3SO_2H at temperatures form -60 °C to ambient temperature (c.a 20 °C). Results showed no evidence of a signal(s) in the metal-hydride region.[1,2]

The compounds *cis*-[$MoCl_2(CO)_2(PNHCH_2P$-κ^3*P,N,P*)] and *cis*-[$WCl_2(CO)_2(PNHCH_2P$-κ^3*P,N,P*)] displayed similar spectra. The chief characteristic of both compounds was a doublet of doublets/triplet grouping centred at about δ4.47 and integrating to two protons. The chemical shift is typical of methylene protons in a R_2N-CH_2-Ar environment (δ3.65).[26] In addition, the methylene protons in the related complex *fac*-[$Mo(CO)_3(PNCHP$-κ^3*P,N,P*)] are inequivalent and are seen as two doublets (δ4.57 and δ4.29, ^2J(H,H) = 12.3 Hz). The assignment of the signals as those due to the methylene group of $PNHCH_2P$ is supported by the spectrum of the deuterium analogue *cis*-[$WCl_2(CO)_2$(PNDCHDP)], as discussed in section *3.2.7*.

[26] R. M. Silverstein, G. C. Bassler and T. C. Morrill, *Spectrometric Identification of Organic Compounds*, 1991, John Wiley & Sons, Inc., New York, p212.

Table 3.8

^{1}H-NMR data for selected compounds [a]

Compounds	δ(multiplicity,[b] *J*), integral, assignment
PNCHP	8.92(d, 5.5 Hz), 1H, C<u>H</u>=N;
[PN(H)CHP]BF_4	8.02-6.53, Ar-H + N<u>H</u>
[Mo(CO)$_3${PN(H)CHP-κ^2*P,P*-η^2(*N*=*C*)}]BF_4	9.22(d, 8.6 Hz), 1H, C<u>H</u>=N; 8.29-5.85(m) 29H, Ar-H + N<u>H</u>;
[W(CO)$_3${PN(H)CHP-κ^2*P,P*-η^2(*N*=*C*)}]BF_4	9.12(d, 7.7 Hz), 1H, C<u>H</u>=N; 8.37-5.78(m) 29H, Ar-H + N<u>H</u>;
cis-[$MoCl_2(CO)_2$(PNHCH_2P-κ^3*P,N,P*)]	4.60(dd, 3.6 Hz and 12.1 Hz), 1H, C<u>H</u>$_2$; 4.37(t, 12.1 Hz), 1H, C<u>H</u>$_2$; 7.94-5.70, 29H, Ar-H + N<u>H</u>;
cis-[$WCl_2(CO)_2$(PNHCH_2P-κ^3*P,N,P*)]	4.70(dd, 3.1 Hz and 11.8 Hz), 1H, C<u>H</u>$_2$; 4.18 (t, 11.8 Hz), 1H, C<u>H</u>$_2$; 8.24-6.55(m) 29H, Ar-H + N<u>H</u>
cis-[$WCl_2(CO)_2$(PNDCHDP-κ^3*P,N,P*)]	4.69(dd, 3.1 Hz and 12.4 Hz), 0.6H, CH_2; 4.18(t, 12.4 Hz), 0.6H, CH_2; 8.23-6.54 29H, Ar-H + N<u>H</u>
cis-[Cr(CO)$_4$(PNCHP-κ^2*N,P*)] + HBF_4	8.02-6.53, Ar-H
mer-[W(CO)$_3$(PNCHPκ^3*P,N,P*)] + CF_3SO_2H	9.90(d, 7.7 Hz), 1H, C<u>H</u>=N; 8.27-5.52 29H, Ar-H + N<u>H</u>;

[a] Recorded at 270 MHz, chemical shifts are in ppm relative to $Si(CH_3)_4$, solvent $CDCl_3$. [b] s = singlet, d = doublet, t = triplet, m = multiplet, br = broad.

3.2.4 IR spectroscopic studies

The infrared spectroscopic data are given in **Table 3.9**. For all the $[M(CO)_3\{PN(H)CHP\text{-}\kappa^2P,P\text{-}\eta^2(N{=}C)\}]^+$ complexes the metal-carbonyl stretching frequencies, in solution, have increased in energy by about 100 cm^{-1} relative to the neutral starting materials, *fac-* or *mer*-$[M(CO)_3(PNCHP\text{-}\kappa P,N,P)]$. The energy increase of the metal-carbonyl stretching frequencies is consistent with loss of electron density from the π^*_{CO} orbitals, which in turn can be attributed to the protonated PNCHP ligand. Other positively-charged zerovalent group 6-tricarbonyl species show identical trends. For example, the neutral complex, *fac*-$[Mo(CO)_3(bipy)\{PN(Me)CH_2CH_2NMe(OMe)\}]$ (**F.3.9-1**), displays bands at 1916, 1818 and 1790 cm^{-1} which are shifted to 2016, 1930 and 1872 cm^{-1} when **F.3.9-1** loses OMe to give the positively charged phosphenium complex, *fac*-$[Mo(CO)_3(bipy)\{PN(Me)CH_2CH_2NMe\}]^+$ (**F.3.9-2**), as shown in **Figure 3.9**.[27] Note however, that the shifts observed give no indication of the site of protonation. For example, metal-protonation of *fac*-$[W(CO)_3(PNP)]$ (**F.3.9-3**) to give *fac*-$[W(H)(CO)_3(PNP)]^+$ (**F.3.9-4**),[1] also shown in **Figure 3.9**, results in similar shifts (from 1922, 1823 and 1797 cm^{-1} to 2032, 1950 and 1919 cm^{-1}).

It was identified in section *3.2.3.* that the solid state structure of $[W(CO)_3\{PN(H)CHP\text{-}\kappa^2P,P\text{-}\eta^2(N{=}C)\}]^+$ may be similar to the solution structure. The ν(CO) bands of the solid state structure are some 10 cm^{-1} greater in energy than the ν(CO) bands of solution structure with the solid state spectra containing an additional band at 1842(w) cm^{-1}, however, the intensity and relative positions of the bands are identical for both compounds, as shown in **Figure 3.10**. The extra band and the 10 cm^{-1} difference between the two spectra can be attributed to band splitting in the solid state and solvent effects, respectively.[28] Therefore, IR evidence suggests that the cation $[W(CO)_3\{PN(H)CHP\text{-}\kappa^2P,P\text{-}\eta^2(N{=}C)\}]^+$ possesses the same structural identity in solution and the solid state, assuming the compound has remained totally insoluble in the nujol used as a mulling agent. The possibility that the solution structure is a five-coordinate tricarbonyl species,[29] such as *cis*-$[M(CO)_3(PN(H)CHP\text{-}\kappa^2P,P)]^+$, was ruled out by carrying

[27] H Nakazawa, Y. Yamaguchi and K. Miyoshi, *J. Organomet. Chem.*, 1994, **465**, 193.
[28] a) D. M. Adams, *Metal-Ligand and Related Vibrations: A Critical Survey of the Infrared and Raman Spectra of Metallic and Organometallic Compounds*, 1967, Spottiswoode, Ballantyne and Co. Ltd, London, p107-111. b) P. S. Braterman, *Metal Carbonyl Spectra*, 1975, Academic Press, London.
[29] G. J. Kubas, *J. C. S. Chem. Comm.*, 1980, p145.

out the protonation reactions under an atmosphere of CO whilst monitoring the metal-carbonyl stretching region. Results showed that the $[M(CO)_3\{PN(H)CHP\text{-}\kappa^2P,P\text{-}\eta^2(N{=}C)\}]^+$ complexes maintained their identity under such conditions with no sign of any other species.

Table 3.9

IR data for selected compounds

Compound	$\nu(C{\equiv}O)$[a]
$[PN(H)CHP]BF_4$	$\nu(N\text{-}H)$[b] 3303w
$[Cr(CO)_3\{PN(H)CHP\text{-}\kappa^2P,P\text{-}\eta^2(N{=}C)\}]BF_4$	2032w, 2021m, 1961m, 1918vs
$[Mo(CO)_3\{PN(H)CHP\text{-}\kappa^2P,P\text{-}\eta^2(N{=}C)\}]BF_4$	2035w, 1971s, 1924vs
$[W(CO)_3\{PN(H)CHP\text{-}\kappa^2P,P\text{-}\eta^2(N{=}C)\}]BF_4$	2030m, 1959s, 1912vs (2038m, 1968s, 1921vs, 1842w)[b] $\nu(N^+\text{-}H)$[b] 3176w
cis-$[MoCl_2(CO)_2(PNHCH_2P\text{-}\kappa^3P,N,P)]$	1974vs, 1861s, $\nu(N\text{-}H)$[b] 3198w
cis-$[WCl_2(CO)_2(PNHCH_2P\text{-}\kappa^3P,N,P)]$	1956vs, 1839m

[a] In $CHCl_3$. [b] Recorded as a nujol mull.

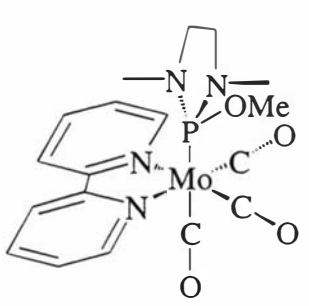

F.3.9-1

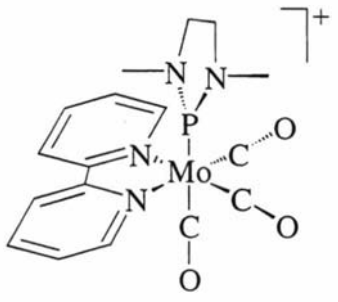

F.3.9-2

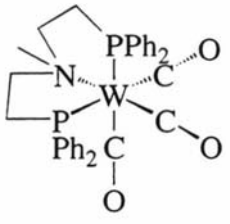

F.3.9-3

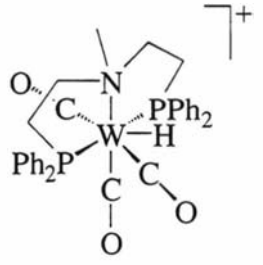

F.3.9-4

Figure 3.9 Neutral (left) and their related positively charged tricarbonyl complexes (right)

The compounds $[MCl_2(CO)_2(PNHCH_2P\text{-}\kappa^3P,N,P)]$, where M is Mo or W, displayed ν(CO) bands typical of divalent-*cis*-dicarbonyl species.[30,31] In addition, $[MoCl_2(CO)_2(PNCH_2P\text{-}\kappa^3P,N,P)]$ displayed a weak vibration at 3198 cm^{-1} which is assigned to the nitrogen-hydrogen stretch,ν(NH). The appearance of N-H stretch supports the hydrogenation of the imine.

[30] P. K. Baker, A. I. Clark, M. G. B. Drew, M. C. Durrant and R. L. Richards, *Polyhedron*, 1998, **17**, 1407.
[31] See ref 17 and refs within.

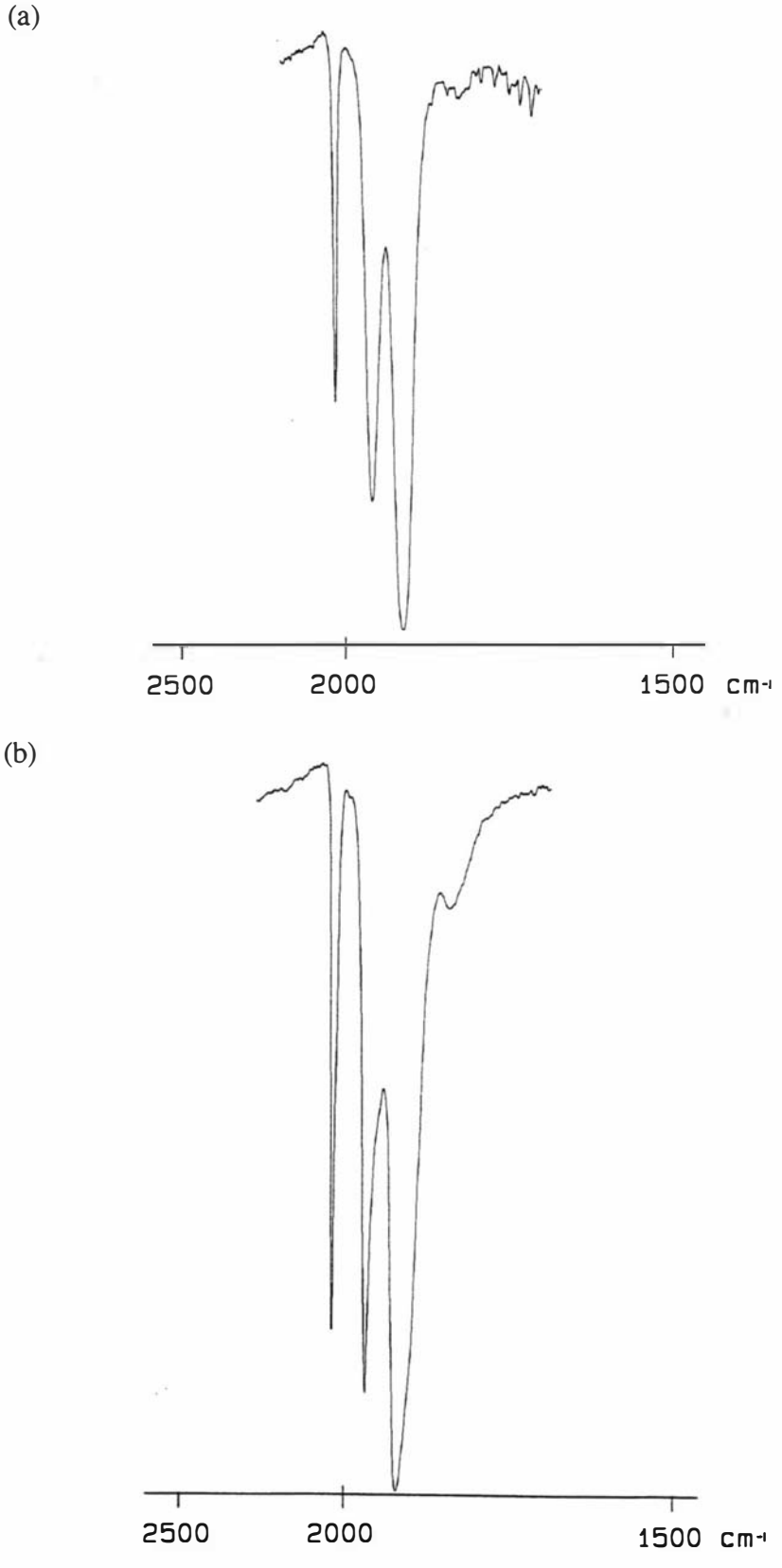

Figure 3.10 Metal carbonyl IR spectra of the compound $[M(CO)_3\{PN(H)CHP\text{-}\kappa^2P,P\text{-}\eta^2(N{=}C)\}]BF_4$ in chloroform (a) and as a nujol mull (b)

3.2.5 Electronic spectroscopic studies

The metal to ligand charge transfer (MLCT) bands $M \rightarrow \pi^*_{imine}$ at 628 nm (1800 $M^{-1}cm^{-1}$), 574 nm (1900 $M^{-1}cm^{-1}$) and 580 nm, for the complexes *mer*-[$Cr(CO)_3$(PNCHP-κ^3*P,N,P*)], *mer*-[$Mo(CO)_3$(PNCHP-κ^3*P,N,P*)] and *mer*-[$W(CO)_3$(PNCHP-κ^3*P,N,P*)] respectively,[11] are destroyed on protonation , giving rise to the orange coloured [$M(CO)_3${PN(H)CHP-κ^2*P,P*-η^2(*N*=*C*)}]$^+$ species. The disappearance of the charge transfer band displayed by the starting materials is consistent with protonation of the imino nitrogen atom.

3.2.6 Mass spectroscopic studies

Generally all the compounds of **Table 3.10** exhibited molecular ion peaks with isotope patterns in good agreement with calculations. The metal-carbonyl compounds showed additional peaks consistent with sequential loss of all the CO ligands. The most stable fragment, i.e. with a relative intensity of 100 %, was found at m/z = 550 and assigned to the protonated PNCHP ligand [PN(H)CHP]$^+$. A mass spectrum of the reaction mixture of *cis*-[$Cr(CO)_4$(PNCHP-κ^2*N,P*)] with HBF_4, showed the expected [PN(H)CHP]$^+$ ion, along with its various chromium-carbonyl fragments.

Table 3.10

FAB mass spectral data for selected compounds

Compound	Found m/z (%), assignment[calculated m/z for ^{52}Cr, ^{98}Mo or ^{184}W].
$[PN(H)CHP]BF_4$	566(26), $PNCHPH^+$ + O[566]; 550(100), $PNCHPH^+$[550].
$[Cr(CO)_3\{PN(H)CHP\text{-}\kappa^2P,P\text{-}\eta^2(N{=}C)\}]BF_4$	[a]
$[Mo(CO)_3\{PN(H)CHP\text{-}\kappa^2P,P\text{-}\eta^2(N{=}C)\}]BF_4$	732(23), M^+-BF_4[732]; 704(48), M^+-BF_4•CO[704]; 676(13), M^+-BF_4•2CO[676]; 648(46), M^+-BF_4•3CO[648]; 566(67), MO^+-BF_4•3CO•Mo[566]; 550(100), M^+-BF_4•3CO•Mo[550].
$[W(CO)_3\{PN(H)CHP\text{-}\kappa^2P,P\text{-}\eta^2(N{=}C)\}]BF_4$	818(75), M^+-BF_4[818]; 762(40), M^+-BF_4•2CO[762]; 734(31), M^+-BF_4•3CO[734]; 550(100), MH^+-BF_4•3CO•W[550].
cis-$[MoCl_2(CO)_2(PNHCH_2P\text{-}\kappa^3P,N,P)]$	740(11), M^+-Cl[740]; 719(25), M^+-2CO[719].
cis-$[Cr(CO)_4(PNCHP\text{-}\kappa^2N,P)]$ + HBF_4	793(16), $[Cr_2(CO)_5(PNCHP)]^+$[793]; 742(15), $[Cr(CO)_5(PNCHP)]^+$[742]; 653(21), $[Cr_2(PNCHP)]^+$[653]; 602(31), $[Cr(PN(H)CHP)]^+$[602]; 550(100), $PN(H)CHP^+$[550].

[a] Non isolatable.

3.2.7 The reduction of coordinated PNCHP by HCl and DCl

The imino group of the 'free' PNCHP ligand undergoes a standard reduction with $LiAlH_4$ to give $PNHCH_2P$ (shown in section *3.2.2.2*).[32] On the other hand, the coordinated PNCHP ligand in the complex $[M(CO)_3(PNCHP\text{-}\kappa^3P,N,P)]$, where M is Mo or W, can be reduced atypically with HCl or DCl. The reduction can be visualised as occurring in an

[32] P. A. Duckworth, *Polydentate Phosphorus-Nitrogen Hybrid Ligands Containing the 2-Aminophenyl Group*, 1984, Ph.D. Thesis, University of Sydney.

analogous fashion to the hydrogenation of an alkene by H_2 or D_2.[33] That is, by oxidative-addition of HCl, in the case of the imine group of PNCHP and H_2 in the case of the alkene, followed by a migration of the hydrogen to the unsaturated bond. However, unlike the hydrogenation of an alkene which receives both of its hydrogens *via* metal coordinated hydrogens, the imino group receives one of the hydrogens by direct protonation as shown by **Scheme 3.6**. The direct protonation of the nitrogen atom is supported by monitoring the reaction of *mer*-[$W(CO)_3$(PNCHP-κ^3*P,N,P*)] with CF_3SO_2H by ^{1}H NMR at temperatures from -60 °C to room temperature. Results showed no evidence of protonation of the metal, as discussed in section *3.2.3.2*. Monitoring of the reaction of [$Mo(CO)_3$(PNCHP-κ^3*P,N,P*)] and excess HCl, also showed no hydride intermediate(s) on the NMR time scale. When DCl is used in place of HCl, the area under the peaks of the ^{1}H NMR signals at δ4.70 (dd, J = 3.1 and 11.8 Hz) and 4.18 (t, J = 11.8 Hz), assigned to the -CH_2- group of $PNHCH_2P$, are reduced by approximately half. This is consistent with one deuterium atom protonating the imino nitrogen atom and one deuterium atom migrating to the imino carbon, as shown by **Scheme 3.6**. Monitoring of the same reaction by ^{31}P NMR spectroscopy revealed a new species with signals at δ64.1 and 55.9 and a ^2J(P,P) coupling constant of 24.9 Hz, as well as the final product. The concentration of the new species remained low (c.a. 5 % by peak area integration) and constant throughout the reaction and could possibly be a byproduct and not an intermediate of the reduction reaction.

[33] See Ref 15, p706-709

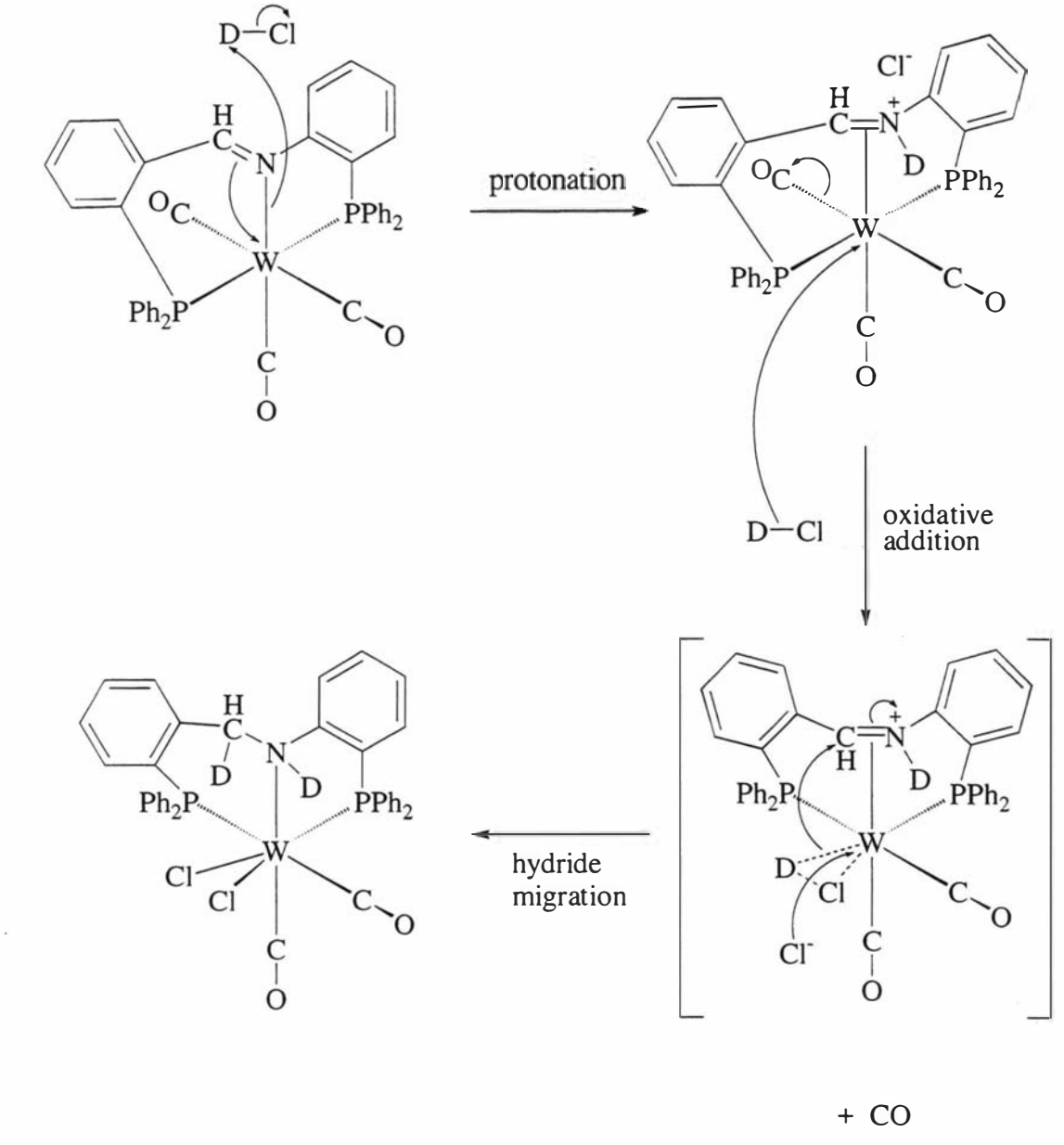

Scheme 3.6 A plausible mechanism for the acid-promoted hydrogenation of a carbon-nitrogen double bond in the complex *mer*-[W(CO)$_3$(PNCHP-κ^3*P*,*N*,*P*)]

3.2.8 The reaction of cis-[Cr(CO)$_4$(PNCHP-κ^2N,P)] with HBF$_4$

The previous section discussed the reaction of a proton with a terdentate PNCHP complex. In contrast, this section endeavours to detail the reaction of a proton with a bidentate PNCHP complex. When *cis*-[Cr(CO)$_4$(PNCHP-κ^2N,P)] (**S.3.7-1**) is reacted with HBF$_4$, the cyclic-phosphonium salt [PN(H)CHP]BF$_4$ (**S.3.7-2**) is isolated from the reaction mixture, as highlighted in section *3.2.1*. The reaction was monitored by ^{31}P NMR, ^{1}H NMR and IR spectroscopy.

From ^{31}P NMR spectra it is evident that the cyclic-phosphonium salt [PN(H)CHP]BF$_4$ (**S.3.7-2**) is formed in < 90% concentration immediately, as shown by **Scheme 3.7**. Another species with ^{31}P NMR singlet resonances at δ56.4 and δ39.4 forms more slowly than the first observed product [PN(H)CHP]BF$_4$ (**S.3.7-2**) and is significant in the fact that it eventually reaches concentrations of around 50 % at the expense of the [PN(H)CHP]BF$_4$ (**S.3.7-2**) signals. Also forming at a much slower rate is a minor species at δ54.7 and δ53.8 which reaches concentrations no greater than 10%. ^{1}H NMR spectra do not show any observable imino proton signals for the above species.

It appears that one of the two slower forming species observed by ^{31}P NMR spectroscopy, gives rise to IR bands at 2063(m), 1986(w) and 1942(s) cm^{-1}, which is consistent with a neutral chromium(0) pentacarbonyl species (**S.3.7-4**).[34] Dissociation of [PN(H)CHP]$^+$ from the metal will leave a "Cr(CO)$_4$" species, it is speculated that the pentacarbonyl species (**S.3.7-4**) arises from reaction of a "Cr(CO)$_4$" moiety with another molecule of its self or *cis*-[Cr(CO)$_4$(PNCHP-κ^2N,P)]. The identity of the pentacarbonyl species **S.3.7-4** being [Cr(CO)$_5$(PN(H)CHP-κ^1*P*)]BF$_4$, i.e. L = [PN(H)CHP]$^+$, is not favoured, as no reaction is observed when pure [PN(H)CHP]BF$_4$ (**S.3.7-2**) is combined with [Cr(CO)$_5$(THF)] in THF.

In summary, it is speculated that protonation occurs at the nitrogen, as depicted by **S.3.7-3**, followed by a cyclisation driven dissociation of the ligand to give the first observable species [PN(H)CHP]BF$_4$ (**S.3.7-2**), a similar protonation occurs in the reaction of [W(CO)$_3$(PN(H)CHP-κ*P,N,P*)] with H$^+$ as discussed in section *3.2.2.1* above.

[34] See ref 31a, p135.

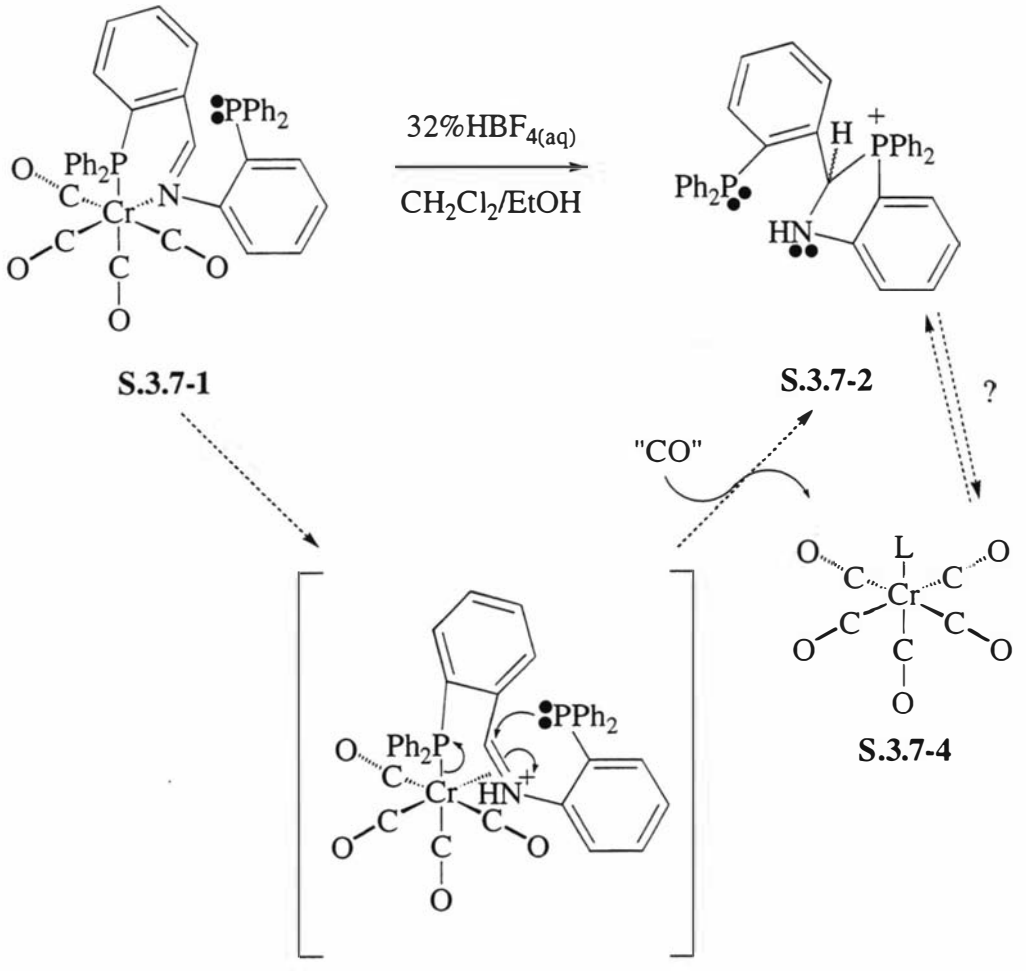

Scheme 3.7 The reaction of *cis*-[Cr(CO)$_4$(PNCHP-κ^2*N,P*)] with HBF_4

3.3 Conclusions

A stable protonated zerovalent group 6 metal-carbonyl complex with the ligand PNCHP can only be obtained when [M(CO)$_3$(PNCHP-κ^3*P,N,P*)] (M = Mo or W), containing a terdentate PNCHP, is reacted with a strong protic acid to give [M(CO)$_3${PN(H)CHP-κ^2*P,P*-η^2(*N*=*C*)}]$^+$. In the course of this reaction, the metal-to-ligand bonding slips from a metal-to-σ nitrogen(imino) bond of the starting material, to the metal-to-π (imino) bond found in the product. When M = Cr the equilibrium heavily favours the starting materials. For the complex *cis*-[Cr(CO)$_4$(PNCHP-κ^2*N,P*)], where the PNCHP

ligand is not bound in a terdentate fashion, H^+ causes decomposition with production of the cyclic phosphonium salt $[PN(H)CHP]^+$. Therefore, the stability of the $[M(CO)_3\{PN(H)CHP\text{-}\kappa^2P,P\text{-}\eta^2(N{=}C)\}]^+$ (M = Mo or W) complexes can be attributed to the filling of the vacant coordination site, left by the protonation of the nitrogen, by the imino π-bond, in combination with the 'strapping down' of this coordinated π-bond *via* the phosphorus atoms on either side.

The complex $[M(CO)_3\{PN(H)CHP\text{-}\kappa^2P,P\text{-}\eta^2(N{=}C)\}]Cl$ (M = Mo or W) formed when the acid is HCl, reacts further with excess HCl to give the halocarbonyl complex, *cis*-$[MCl_2(CO)_2(PNHCH_2P\text{-}\kappa^3P,N,P)]$ as the final product. In this case, the metal has been oxidised from M(0) to M(II) and the coordinated PNCHP ligand has undergone reduction across the -HC=N- bond to give $-H_2C\text{-}NH-$. This reaction is unusual in that both hydrogens originate from HCl, with M playing an important role as discuused above. As discussed in the chapter introduction, a similar style reaction occurs when the imino compound $[Os_3(CO)_9(\mu\text{-}H)(\mu_3\text{-}\eta^2\text{-}C{=}N(CH_2)_3)]$ (**S.3.3-1**) is reacted with excess HBr in chloroform to give the amino compound $[Os_2(CO)_6Br_2(\mu\text{-}H)(\mu_3\text{-}\eta^2\text{-}CHNH(CH_2)_3)]$ (**S.3.3-2**), as shown by **Scheme 3.3**. It was postulated by the authors of the study that both hydrogens, added across the imine bond to give the amine, were likely to have arrived *via* osmium-hydrides, as reduction *via* a direct protonation of the imino nitrogen was disfavoured. In view of the results discussed within this chapter, a mechanism for the reduction of the imino-osmium species involving a protonated imino species seems favourable.

3.4 Experimental

3.4.1 [PN(H)CHP]BF_4

PNCHP (0.2205 g, 0.4012 mmol) was dissolved in dichloromethane (10 mL) followed by addition of ethanol (20 mL). 32% HBF_4 (0.137 g, 0.534 mmol) was then added resulting in rapid decolourisation of the yellow solution. The volume of solvent was reduced by about half *in vacuo* and solution kept at 5 °C to aid crystallisation. $[PN(H)CHP]BF_4$ (0.2018 g, 79 %) was isolated as square colourless crystals, washed with absolute ethanol and dried *in vacuo*. M.p: 226-235 °C (dec). Anal. Calcd for $C_{37}H_{30}BF_4NP_2$: C, 69.72; H, 4.74; N, 2.20; P, 9.72. Found: C, 69.54; H, 4.78; N, 2.09; P, 9.72.

3.4.2 [Cr(CO)$_3$(PNCHP-κ^3P,N,P)] + HBF$_{4(aq)}$

Mer-[Cr(CO)$_3$(PNCHP-κ^3*P,N,P*)] (0.035 g, 0.051 mmol) was dissolved in dichloromethane (10 mL) followed by addition of methanol (6 mL) giving a dark green solution. To this solution was added 7 drops of 32% HBF$_{4(aq)}$ and the green solution stirred for 0.5 h at room temperature. The solvent was removed in vacuo giving orange and green solids. Redissolving in chloroform gave an orange solution. A solution infrared spectrum was recorded (**Table 3.11**). The orange solution gradually turned green inside the solution cell over a few minutes.

3.4.3 Mer-[Mo(CO)$_3$(PNCHP-κ^3P,N,P)] + HBF$_{4(aq)}$

Mer-[Mo(CO)$_3$(PNCHP-κ^3*P,N,P*)] (0.012 g, 0.016 mmol) was dissolved in dichloromethane followed by addition of a little methanol to solubilise the aqueous acid. Two drops of 32% HBF$_{4(aq)}$ was then added, turning the purple solution orange instantaneously. The NMR and IR spectra were then recorded (see entry for [Mo(CO)$_3$(PN(H)CHP)]BF$_4$ in **Tables 3.9**, **3.10** and **3.11**). The tungsten analogue *mer*-[W(CO)$_3$(PNCHP-κ^3P,N,P)] was synthesised in a similar fashion.

3.4.4 Mer-[Mo(CO)$_3$(PNCHP-κ^3P,N,P)] + BF$_3$.Et$_2$O

Mer-[Mo(CO)$_3$(PNCHP-κ^3*P,N,P*)] (0.0506 g, 0.0694 mmol) was dissolved in dichloromethane followed by addition of freshly distilled BF$_3$.Et$_2$O (2 drops), turning the initial purple solution orange. The NMR and IR spectra were then recorded (see entry for [Mo(CO)$_3$(PN(H)CHP)]BF$_4$ in **Tables 3.9**, **3.10** and **3.11**).

3.4.5 Mer-[Mo(CO)$_3$(PNCHP-κ^3P,N,P)] + CF$_3$COOH

Mer-[Mo(CO)$_3$(PNCHP-κ^3*P,N,P*)] (0.0400 g, 0.0548 mmol) was dissolved in dichloromethane (2 mL) then a few drops of methanol added. Trifluoroacetic acid was added drop-wise until an orange coloured solution was obtained and a solution infrared spectrum recorded immediately (see **Table 3.11**).

3.4.6 Fac-[Mo(CO)$_3$(PNCHP-κ^3P,N,P)] + BF$_3$.Et$_2$O

Fac-[Mo(CO)$_3$(PNCHP-κ^3*P,N,P*)] (0.011 g, 0.015 mmol) was dissolved in dichloromethane (4 mL) followed by addition of $BF_3.Et_2O$ (1 drop), turning the initial purple solution orange. The NMR and IR spectra were then recorded (see entry for [Mo(CO)$_3$(PN(H)CHP)]BF_4 in **Tables 3.9**, **3.10** and **3.11**).

3.4.7 Mer-[W(CO)$_3$(PNCHP-κ^3P,N,P)] + BF$_3$.Et$_2$O

Mer-[W(CO)$_3$(PNCHP-κ^3*P,N,P*)] (0.100 g, 0.122 mmol) was dissolved in dichloromethane (4 mL) followed by addition of toluene (2 mL). 2 drops of $BF_3.Et_2O$ were added, turning the initial purple solution orange. The solution was stood for several days in a freezer at c.a -10 °C, open to the atmosphere. [W(CO)$_3$(PN(H)CHP-κ^3*P,N,P*)]BF_4 (0.045 g, 40.7 %) was isolated as red crystalline blocks by filtering through a glass frit pre-rinsed with $CH_2Cl_2/BF_3.Et_2O$ to preserve the filtrate, then washed with chloroform followed by n-pentane. Anal. Calcd for $C_{40}H_{30}BF_4NO_3P_2W$: C, 53.07; H, 3.34; N, 1.55; F, 8.39. Found: C, 52.67; H, 3.37; N, 1.45; F, 7.97.

3.4.8 Mer-[W(CO)$_3$(PNCHP-κ^3P,N,P)] + CF$_3$SO$_3$H

mer-[W(CO)$_3$(PNCHP-κ^3*P,N,P*)] (0.0100 g, 0.0122 mmol) was dissolved in 0.6 mL of $CDCl_3$ containing 0.0012 mL of CF_3SO_2H (0.012 mmol), and the ^{1}H NMR spectrum collected (**Table 3.10**).

3.4.9 Cis-[MoCl$_2$(CO)$_2$(PNHCH$_2$P-κ^3P,N,P)]

Mer-[Mo(CO)$_3$(PNCHP-κ^3*P,N,P*)] (0.1035 g, 0.1419 mmol) was dissolved in dichloromethane (4 mL) then $HCl_{(g)}$ bubbled through the solution, resulting in a colour change to orange. The solution was then sealed under an atmosphere of $HCl_{(g)}$ and left to stand overnight, resulting in a yellow solution. [$MoCl_2(CO)_2$(PNHCH$_2$P-κ^3*P,N,P*)] (0.0567 g, 51.6 %) was isolated as orange crystals which slowly blackened when exposed to light. M.p: 160 °C (dec). Anal. Calcd for $C_{39}H_{31}Cl_2MoNO_2P_2.CH_2Cl_2$: C, 55.90; H, 3.87; N, 1.63. Found: C, 55.94; H, 3.69; N, 1.61.

3.4.10 cis-[$WCl_2(CO)_2$(PNDCHDP-κ^3P,N,P)] and cis-[$WCl_2(CO)_2$(PNHCH$_2$P-κ^3P,N,P)]

D_2SO_4 was dripped on to anhydrous $NaCl_{(s)}$ and the resulting $DCl_{(g)}$ bubbled into a purple dichloromethane solution of *mer*-[$W(CO)_3$(PNCHP-κ^3*P,N,P*)] (0.050 g, 0.061 mmol) until the solution turned orange. The solution was sealed under an atmosphere of DCl until a colour change to yellow resulted (c.a. 2 days). The solution was then vapour diffused with n-hexane, giving large yellow crystals of [$WCl_2(CO)_2$(PNDCHDP-κ^3*P,N,P*)] after a couple of days. The crystals were isolated, washed quickly with dichloromethane follow by n-pentane (×3) and dried *in vacuo* to yield 0.0376 g, 71.3 %. Anal. Calcd for $C_{39}H_{31}Cl_2NO_2P_2W \bullet CH_2Cl_2$: C, 50.71; H, 3.51; N, 1.48; Cl, 14.96. Found: C, 50.89; H, 3.49; N, 1.48; Cl, 14.86. The 'HCl' analogue was synthesised in a similar fashion.

3.4.11 Cis-[$Cr(CO)_4$(PNCHP-κ^2N,P)] + $HBF_{4(aq)}$

Cis-[$Cr(CO)_4$(PNCHP-κ^2*N,P*)] (0.1006 g 0.1410 mmol) was dissolved in dichloromethane/ethanol (7 mL/1.5 mL) and 5 drops of 32% HBF_4 added. The mixture was stirred overnight open to the air resulting in very pale yellow crystals. The crystals were isolated and washed with ethanol then diethylether to give 0.0238 g (26.5 %) of [PN(H)CHP]BF_4.

4 The Palladium & Platinum Complexes

4.1 Introduction

4.1.1 A brief overview of palladium and platinum chemistry

Palladium and platinum have played major roles in the development of coordination chemistry and catalysis. The kinetic inertness of platinum complexes has facilitated studies of geometrical isomerism and reaction mechanisms. The less stable palladium analogues, in both a thermodynamic and kinetic sense, have been suited to catalysis. The most common oxidation states of palladium and platinum are II and IV, and the most common mode of coordination in these two oxidation states are four-coordinate square planar and six-coordinate octahedral arrangements respectively.[1]

The PNCHP ligand should be suited to coordination in a square planar environment due to its co-planar qualities, that is, its potentially conjugated π-system and inherent rigidity. PNCHP has shown preference for terdentate coordination, in a *mer* fashion, at the expense of the expulsion of other ligands in the coordination shell and when so coordinated, shows no sign of dissociation.[2] Therefore, the platinum(II) complex, $[Pt(PNCHP\text{-}\kappa^3P,N,P)Cl]^+$, should be straight forward to prepare since its nickel(II) analogue, $[Ni(PNCHP\text{-}\kappa^3P,N,P)Cl]^+$, has been made previously.[3] With this platinum complex in hand, chloride substitution at the square-planar centre by various potential ligands should be readly investigated. Of particular interest is substitution with strong bidentate ligands such as 1,10-phenanthroline (phen), 2,2'-bipyridine (bipy) and bis(diphenylphosphino)ethane (diphos). The questions to be answered are:

---

[1] F. A. Cotton, G. Wilkinson, C. A. Murillo and M. Bochmann, *Advanced Iinorganic Chemistry*, 6th Ed., 1999, John Wiley & Sons, Inc., New York.

[2] S. M. F. Kennedy, *Structural Studies on a P_2N triligate with Group 6 Metal Carbonyls*, 1995, BSc(Hons) Thesis, Massey University.

[3] M. J. R. Halstead, *Iminophosphine Complexes of Nickel(II)*, 1991, BSc(Hons) Thesis, Massey University.

- Would these extremely good ligands compete with the also strong PNCHP ligand for coordination sites?

- Would the "bidentate" ligand be forced to bind through a fifth coordination site?

- Would these "bidentate" ligands act in the unusual monodentate fashion?

- A natural extension to the previous questions is, what binding mode would the traditionally terdentate ligand, 2,2':6',2"-terpyridine, adopt in such a situation?

With reference to the above questions, the occurrences of monodentate "bidentate" ligands and five-coordinate platinum(II) complexes are discussed in the next section with particular emphasis on 1,10-phenanthroline ligands.

4.1.2 Five-coordinate platinum(II) complexes

Stable five-coordinate complexes of platinum(II) were almost unknown until about 1973. During the following years a number of chelating nitrogen ligands, when combined with a π-acceptor ligand such as an olefin or an acetylene, were found to stabilise five-coordination for the platinum(II) ion.[4,5] The presence of a ligand with π-acceptor character enables the metal to back-bond into the ligand's π* orbital, and hence, increase the positive charge at the metal centre thereby making an interaction with a fifth donor atom favourable. Strong σ donors, on the other hand, reduce the positive charge on the metal, making five-coordination less favourable.[6] The role of the π-acceptor ligand has been supported by *ab initio* Hartree-Fock SCF molecular orbital calculations on a series of compounds of the type $[Pt(L)(bipy)F_2]$ (where L is C_2H_4, CO, PH_3 or ONMe, and bipy is 2,2'-bipyridine). The results showed that five-coordination stems from the ability of the L ligand to reduce the electron density on the metal centre. The C_2H_4 ligand, because of its side-on coordination, is very efficient at lowering the electron density so that the metal can

[4] V. G. Albano and D. Braga, *Organometallics*, 1987, **6**, 517, and refs within.
[5] F. P. Fanizzi, F. P. Intini, L. Maresca, G. Natile, M. Lanfranchi and A. Tiripicchio, *J. Chem. Soc. Dalton Trans.*, 1991, 1007, and refs within.

receive electron charge from an extra donor atom. PH_3 and ONMe, unlike C_2H_2, are poor π-acceptors; The structure of the CO complex is intermediate between the two extremes. As a consequence, the 2,9-dimethyl-1,10-phenanthroline (dmphen) ligand is, in the series of compounds depicted in **Figure 4.1**, doubly bonded in $[Pt(C_2H_4)(dmphen)I_2]$ (**F.4.1-1**), singly bonded in $[Pt(PPh_3)(dmphen)I_2]$ (**F.4.1-4**) and $[Pt(N(O)Ph)(dmphen)I_2]$ (**F.4.1-5**), and intermediately bonded in $[Pt(CO)(dmphen)I_2]$ (**F.4.1-2**).[7]

The majority of the five-coordinate complexes of palladium(II) and platinum(II) also appear to have structures closer to square pyramidal than trigonal bipyramidal. The metal atoms generally lie slightly above the basal plane, as expected from calculations, and the apical bond lengths are longer than those in the base.[8]

Pictured in **Figure 4.1** are representations of the X-ray determined molecular structures of several platinum(II) and palladium(II) complexes containing 1,10-phenanthroline ligands bound through one nitrogen donor atom in the square-plane of the metal. The interest of these complexes lies in the nature of second nitrogen atom. Examination of the structures from **F.4.1-1** through to **F.4.1-8** sees the metal-to-second nitrogen atom orientation progress from clearly bonding to essentially non-bonding. Defining the phenanthroline ligand, in such complexes as **F.4.1-1** to **F.4.1-8**, as mono- or bidentate is not always immediately easy and is open to discussion.[9] The second nitrogen atom will obviously always be in the vicinity of the apical site of the square-pyramid since the bite angle of the phenanthroline ligand and the requirement of reasonable bond angles about the equatorial nitrogen donor atom sets an upper limit on the Pt-N(axial) length.

---

[6] H. Nikol, H.-B. Bürgi, K. I. Hardcastle and H. B. Gray, *Inorg. Chem.*, 1995, **34**, 6319.
[7] F. P. Fanizzi, L. Maresca, G. Natile, M. Lanfranchi, A. Tiripicchio and G. Pacchioni, *J. Chem. Soc., Chem. Commun.*, 1992, 333.
[8] R. J. Cross, *Advances in Inorganic Chemistry*, 1989, **34**, 234.
[9] B. Milani, G. Corso, E. Zangrando, L. Randaccio and G. Mestroni, *Eur. J. Inorg. Chem.*, 1999, 2085.

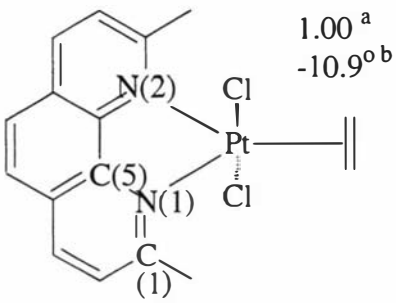

F.4.1-1

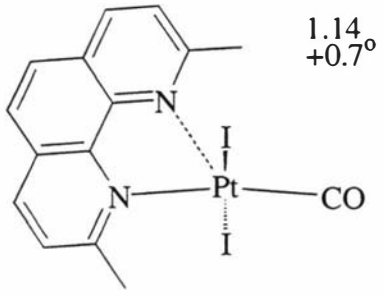

F.4.1-2

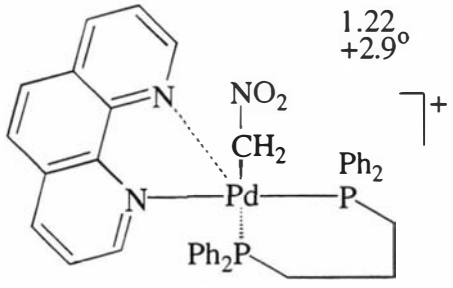

F.4.1-3

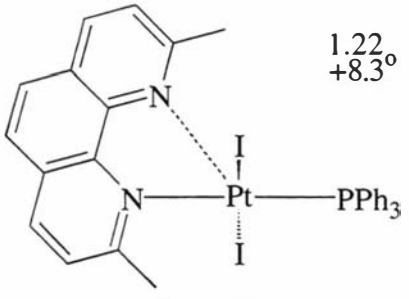

F.4.1-4

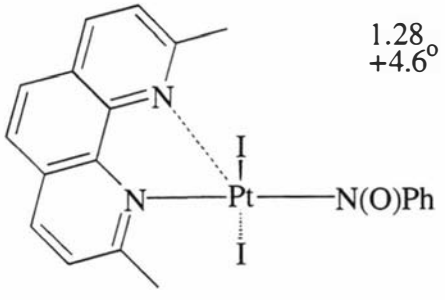

F.4.1-5

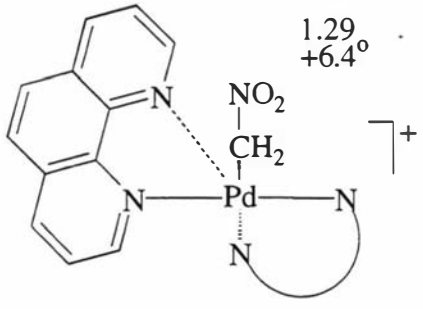

F.4.1-6

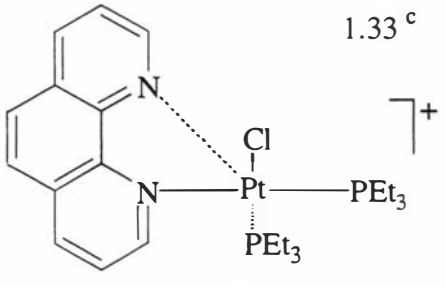

F.4.1-7

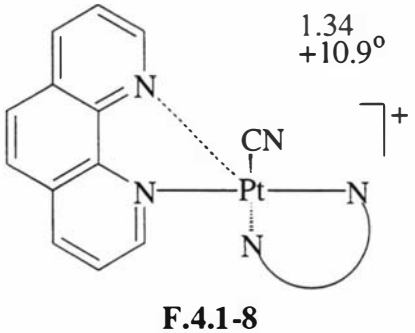

F.4.1-8

[a] [M-N(2)]/[M-N(1)], where M = Pd or Pt. [b] [M-N(1)-C(5)]-[M-N(1)-C(1)].
[c] angles not available. N-N = 1,10-phenanthroline.

Figure 4.1 The progression of bi- to monodentate (**F.4.1-1** to **F.4.1-8**) coordination modes of phenanthroline ligands in potentially five-coordinate Pd(II) and Pt(II) species

The following arguments have been used together to gain acceptance for the above compounds as either four- (square planar) or five-coordinate (square pyramidal):

i) The ratio of the axial/equatorial bond lengths of accepted five-coordinate complexes such as [Pd(2-phenylisophosphinindoline)$_2$Br$_2$] (ratio = 1.13)[10] and [Pd(PMe$_2$Ph)$_3$Cl$_2$] (ratio = 1.21)[11] can be used for comparison. For example, in **F.4.1-2** the axial/equatorial bond length ratio is 1.14 and typical of five-coordination, whilst the ratio in **F.4.1-8** is 1.34 and suggestive of a monodentate phenanthroline ligand.

ii) The average N---N bite for complexes where 1,10-phenanthroline acts as a bidentate ligand is 2.66 Å, but for 'free' phenanthroline and the similar 2,2'-bipyridine, the bite is considerably longer at 2.97 and 2.84 Å respectively.[12] For **F.4.1-8** the N---N bite is 2.85 Å and is supportive of a monodentate phenanthroline ligand.

iii) The degree of bonding interaction between the second end of the phenanthroline ligand and the metal (M) can also be evaluated from the difference between the M-N(1)-C(5) and M-N(1)-C(1) angles.[13] For example, this difference in the five-coordinate complex **F.4.1-3** is +2.9 °, whilst in the four-coordinate complex **F.4.1-8** the difference is significantly larger at +10.9 °.

iv)The N(1)-Pt-N(2) angle can also be used to evaluate the interaction. A low value is expected when the ligand is monodentate owing to the more distant position of the uncoordinated end of the phenanthroline ligand.[12]

4.1.3 Carbon monoxide (CO) insertion

Palladium(II) complexes have seen widespread use in catalysis, for example hydroformylation, alkoxycarbonylation and polyketone production.[14] A key step in these

---

[10] O. S. C. Headley, R. S. Nyholm, C. A. McAuliffe, L. Sindellari, M. L. Tobe and L. M. Venanzi, *Inorg. Chem. Acta*, 1970, **4**, 93.
[11] G. J. Kruger, W. J. Louw and D. J. A. de Waal, *J. Chem. Soc. Dalton Trans.*, 1976, 2364.
[12] G. W. Bushnell, K. R. Dixon and M. A. Khan, *Can. J. Chem.*, 1974, **52**, 1367, and refs. within
[13] L. Cavallo, R. Cini, J. Kobe, L. G. Marzilli and G. Natile, *J. Chem. Soc., Dalton Trans.*, 1991, 1867.
[14] A. Buijs, G. P. C. M. Dekker, C. J. Elsevier, W. J. J. Smeets, A. L. Spek, C. H. Stam, P. W. N. M. van Leeuwen, K. Vrieze and Y. F. Wang, *Organometallics*, 1992, **11**, 1937, and ref 1 within.

catalytic processes is the carbonylation reaction. Most experimental studies on square planar palladium(II) complexes indicate that CO insertion by a mechanism involving four-coordinate intermediates is more favourable than by a mechanism involving five-coordinate intermediates, even when the stabilising ligands are terdentate.[15] For example, studies on the insertion of CO into the palladium-methyl (Pd-Me) bond, showed the creation of a vacant coordination site in the square plane to be a common theme. The creation of the vacant coordination site is achieved by synthesising complexes containing weakly coordinating solvents and/or anions and/or bi- or terdentate ligands which ring-open.[15,16] For example, the compound [Pd(PNN-κ^3*P,N,N*)Me]Cl, which contains a similar ligand to PNCHP, PNN (**F.4.2.1**), as shown in **Figure 4.2**, undergoes CO insertion under mild conditions. The terdentate bound PNN ring-opens to bind in a bidentate fashion, as shown in **Scheme 4.1**.[17]

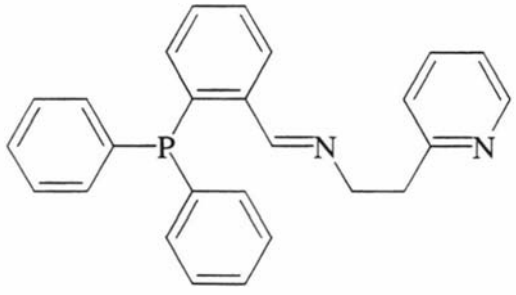

F.4.2-1

Figure 4.2 A 'PN_2' ligand successfully employed in CO insertion into the Pd-Me bond

[15] J. H. Groen, A. de Zwart, M. J. M. Vlaar, J. M. Ernsting, P. W. N. M. van Leeuwen, K. Vrieze, H. Kooijman, W. J. J. Smaates, A. L. Spek, P. H. M. Budzelaar, Q. Xiang and R. P. Thummel, *Eur. J. Inorg. Chem.*, 1998, 1129.
[16] J. H. Groen, M. J. M. Vlaar, P. W. N. M. van Leeuwen, K. Vrieze, H. Kooijman and A. L. Spek, *J. Organomet. Chem.*, 1998, **551**, 67, and refs. within.
[17] P. Wehman, R. E. Rülke, V. E. Kaasjager, P. C. J. Kamer, H. Kooijman, A. L. Spek, C. J. Elsevier, K. Vrieze and P. W. N. M. van Leeuwen, *J. Chem. Soc., Chem. Commun.*, 1995, 331.

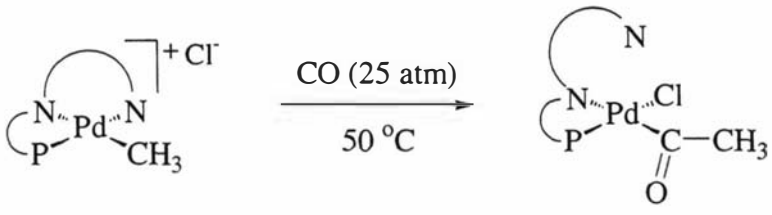

S.4.1-1 **S.4.1-2**

Scheme 4.1 The ring-opening reaction of the ligand **F.4.2-1**

It is only in recent years that substantial investigations into the behaviour of catalytic systems with chelating ligands have been undertaken.[18] Therefore it seemed worthwhile to synthesise [Pd(PNCHP)Me]X, where X^- is Cl^- or $BF4^-$, that is analogues of **S.4.1-1,** so as to evaluate the potential of a 'P_2N' tridentate ligand in CO insertion reactions.

4.2. Results and discussion

4.2.1 Synthesis

The syntheses of the palladium(II) and platinum(II) complexes containing the PNCHP ligand are depicted in **Scheme 4.2.** The identity of the products are highlighted here and evidence discussed in the sections to follow. PNCHP coordinates to platinum(II) and palladium(II) in a terdentate fashion by displacing 1,5-cyclooctadiene (COD) and one chloride from [M(COD)Cl_2] to yield complexes of the type [M(PNCHP-κ^3*P,N,P*)Cl]Cl (**S.4.2-1**) as shown in **Scheme 4.2.** Attempts to isolate complexes where PNCHP behaves as a bidentate ligand by only displacing the COD ligand from [M(COD)Cl_2] to obtain, for example, [M(PNCHP-κ^2*P,P*)Cl_2], were unsuccessful. However, several intermediates, which were suggestive of mono- and bidentate PNCHP species, were observed when monitoring the synthesis of [M(PNCHP-κ^3*P,N,P*)Cl]Cl by ^{31}P NMR.

[18] K. J. Cavell, *Coord. Chem. Rev.*, 1996, **155**, 209.

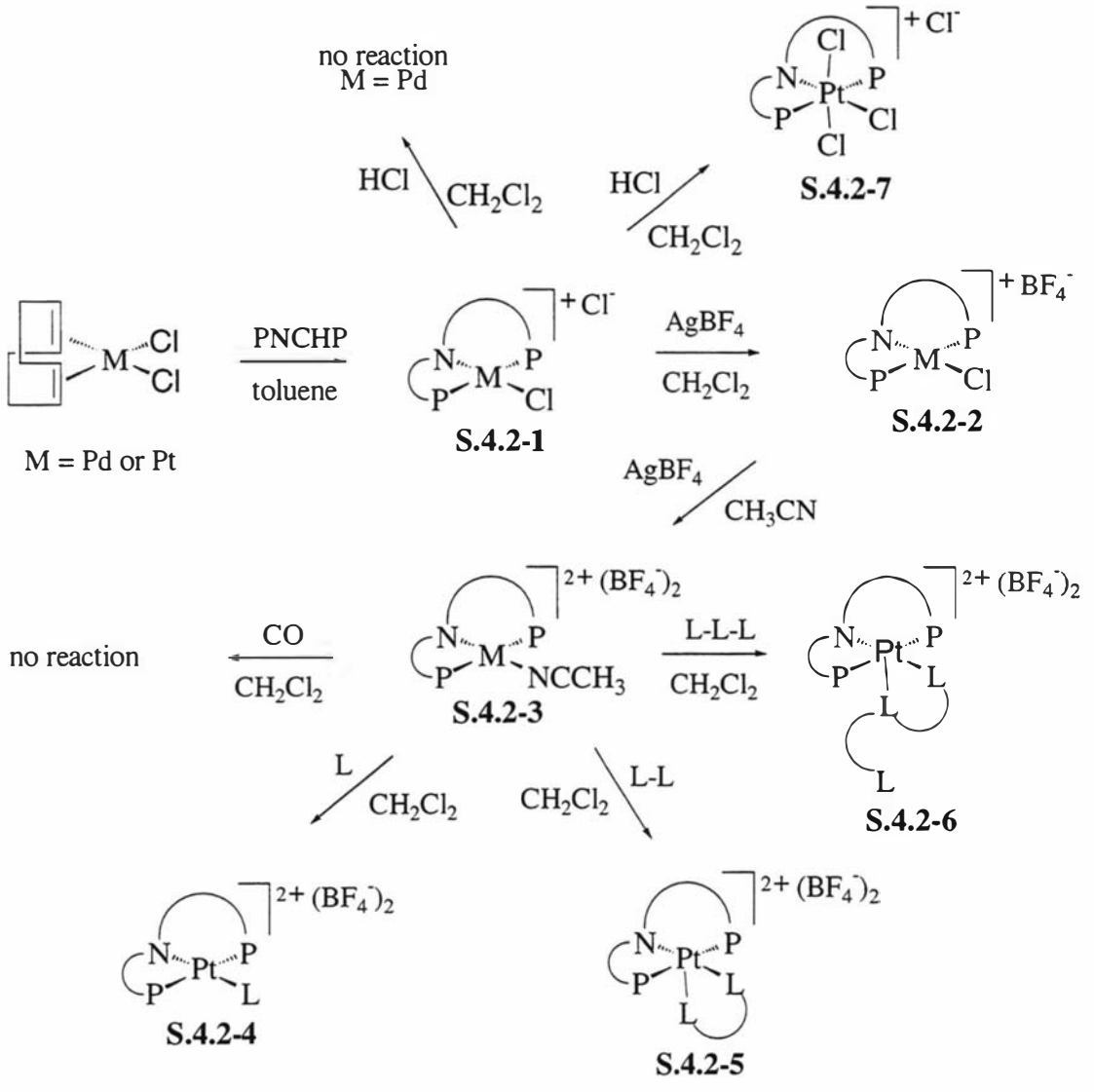

Legend to Scheme 4.2

PNCHP = P N P

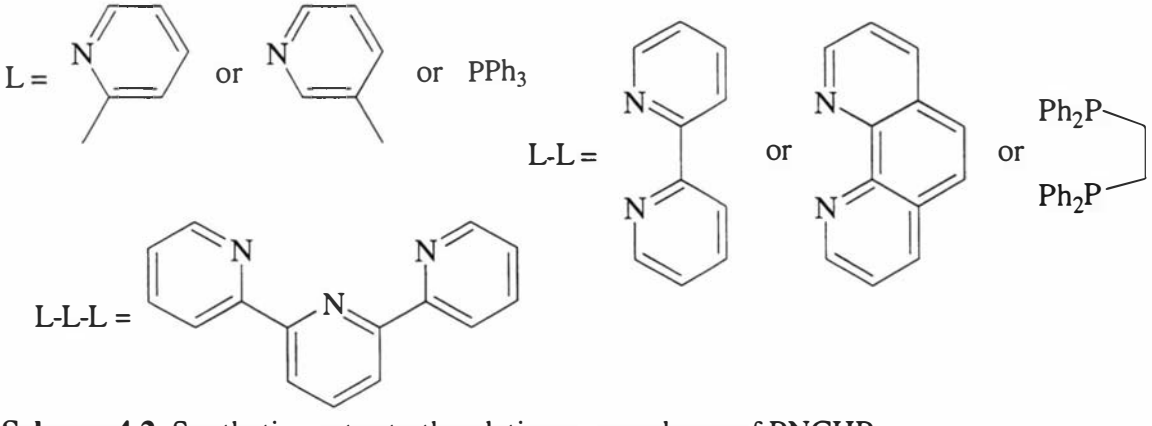

Scheme 4.2 Synthetic routes to the platinum complexes of PNCHP

The chlorides of [Pt(PNCHP-κ^3*P,N,P*)Cl]Cl can be successively exchanged for BF_4^- ions in the presence of acetonitrile (MeCN) to give [Pt (PNCHP-κ^3*P,N,P*)Cl]BF_4 (**S.4.2-2**) then [Pt(PNCHP-κ^3*P,N,P*)(MeCN)]$(BF_4)_2$ (**S.4.2-3**). Reacting **S.4.2-3**, when M is Pt, with 2-picoline, 3-picoline or triphenylphosphane (L) results in the substitution of the acetonitrile ligand to give four coordinate complexes of the type [Pt(PNCHP-κ^3*P,N,P*)(L-κ^1)]$^{2+}$ (**S.4.2-4**). Analogous substitution reactions also occur with 2,2'-bipyridine (bipy), 1,10-phenanthroline (phen) or bis(diphenylphosphino)ethane (diphos) (L-L), however, the complexes that result are of the type [Pt(PNCHP-κ^3*P,N,P*)(L-κ^2)]$^{2+}$ where the metal is now five-coordinate. The compound [Pt(PNCHP-κ^3*P,N,P*)(diphos)]$(BF_4)_2$ was the only compound found, in this chapter, to be unstable in the solid state. Reaction of **S.4.2-3** with the potentially terdentate ligand 2,2':6',2"-terpyridine (terpy) also gives rise to a five-coordinate complex. Carbon monoxide (CO), on the other hand, did not react with **S.4.2-3**, which may be expected considering the +2 charge of the complex.

Attempted oxidation of [M(PNCHP-κ^3*P,N,P*)Cl]Cl with HCl was only modestly successful when M is platinum and unsuccessful when M is palladium. The product when M is platinum was assigned the platinum(IV) species [$PtCl_3$($PNHCH_2P$)]Cl (**S.4.1-7**). This trend with respect to ease of oxidation of palladium versus platinum is well documented.[19]

Syntheses of the palladium-methyl compounds containing PNCHP are depicted in **Scheme 4.3.** Reacting [Pd(COD)(Me)Cl] with the PNCHP ligand yields the compound [Pd(PNCHP-κ^3*P,N,P*)(Me)]Cl (**S.4.3-1**). The chloride of **S.4.3-1** is easily exchanged for BF_4^- on reaction with $AgBF_4$, affording the compound [Pd(PNCHP-κ^3*P,N,P*)(Me)]BF_4 (**S.4.3-2**). When **S.4.3-2** is subjected to 7 atm of carbon monoxide (CO) at room temperature, no evidence for CO addition, substitution or insertion is observed. In view of an unsuccessful CO insertion reaction, or for that matter any reactivity at all, it can be concluded, that under the reaction conditions used, the PNCHP ligand is not a suitable coligand. This is probably due to PNCHP unable to ring-open, thereby allowing an incoming CO ligand to bind to a coordination site in the square plane *cis* to the methyl group, which is considered to be an important step in the mechanism of successful CO insertions involving other terdentate ligands,[15,17] for example see **Scheme 4.1**.

[19] F. R. Hartley, *The Chemistry of Platinum and Palladium: With Particular Reference to Complexes of the Elements*, 1973, Applied Science Publishers Ltd, London, p2.

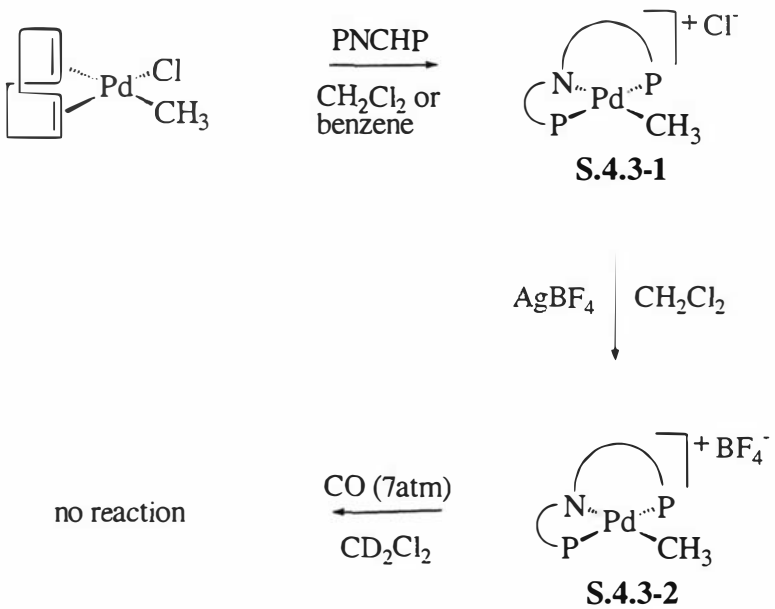

Scheme 4.3 Synthetic routes to the palladium(II) complexes of PNCHP

4.2.2 Description of the crystal structures

4.2.2.1 Crystal structure of [Pt(PNCHP-κ^3P,N,P)Cl]Cl.2CH_2Cl_2

The structure of the cation [Pt(PNCHP-κ^3*P,N,P*)Cl]$^+$ is shown in **Figure 4.3** with crystal data and structure refinement details given in **Table 4.1** and bond lengths and angles given in **Table 4.2**. The compound contains a four coordinate platinum atom with the two phosphorus atoms (P(1) and P(2)) and nitrogen atom (N) of PNCHP and one chloride (Cl(1)) atom making up the four donor atoms. A second chloride (ionic) and two molecules of dichloromethane are also present but omitted from **Figure 4.3** for clarity. The coordination geometry around the platinum atom is slightly distorted square planar. The distortion of the square plane can be attributed to the five-membered ring formed by P(1) and N coordinated to Pt with a P(1)-Pt-N angle of 84.43(19) °, significantly tighter than the 90 ° expected for an ideal square planar complex. Calculation of a plane involving the four donor atoms shows a deviation from coplanarity of 0.0254(15) Å, which is slightly less than 0.052(1) Å found in the nickel analogue. Bond lengths and angles within the PNCHP

ligand are normal[20] except for the unusually short imine bond N-C(1) of 1.117(9) Å. In the 'free' PNCHP ligand, the C=N bond measures 1.296(8) Å, and is similar in the related compounds, $[Pt(PNCHP-\kappa^3P,N,P)(PPh_3)]^{2+}$ (1.290(6) Å) and $[Pt(PNCHP-\kappa^3P,N,P)(phen)]^{2+}$, to be discussed later. In addition, the analogous bond length in the nickel analogue measures 1.25(1) Å and is typical of a C=N.[20] A relatively long imine bond of 1.33(1) Å is found in the similar complex [Pt(PNCHO)Cl][21] (**F.4.4-1**), shown in **Figure 4.4**. Therefore, the short C=N bond length found for $[Pt(PNCHP-\kappa^3P,N,P)Cl]^+$ is probably an artefact of the structures solution. The Pt-Cl bond length of 2.2892(12) Å is considerably shorter than the Pt-Cl bond length of 2.386(4) Å in **F.4.4-1**. This is likely due to the positive charge of $[Pt(PNCHP-\kappa^3P,N,P)Cl]^+$ versus the neutrality of **F.4.4-1**.

[20] *International Tables for X-ray Crystallography*, Volume III, Kynock Press, Birmingham, England, 1962.
[21] A. J. Jircitano and K. B. Mertes, *Inorg. Chim. Acta*, 1985, **103**, L15.

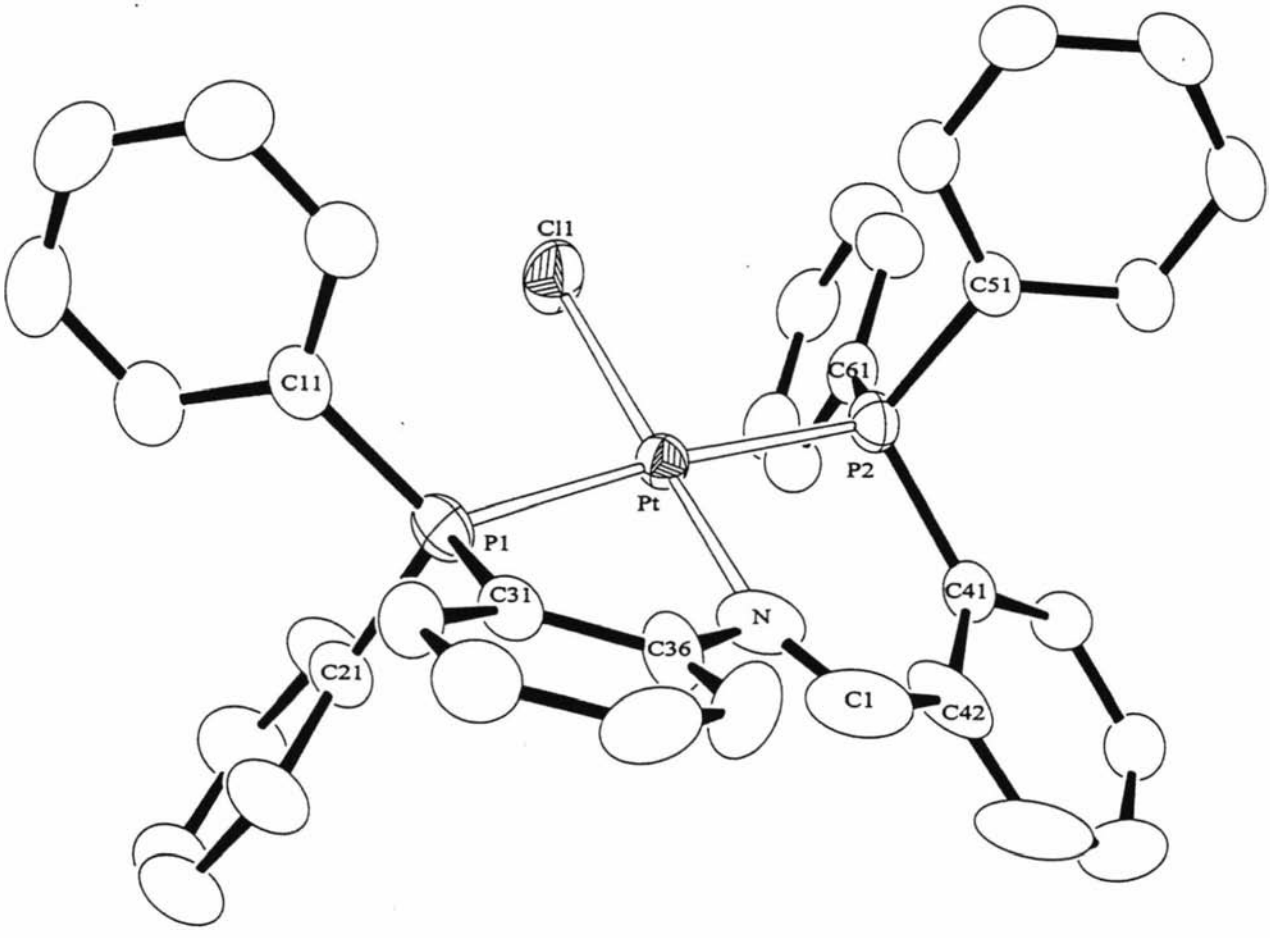

Figure 4.3 ORTEP diagram for the cation $[Pt(PNCHP\text{-}\kappa^3P,N,P)Cl]^+$ showing the numbering system used. Thermal ellipsoids are at the 50% probability level. Hydrogen atoms have been omitted for clarity

Table 4.1

Crystal data and structure refinement for [Pt(PNCHP-κ^3*P,N,P*)Cl]Cl•2CH_2Cl_2.

Identification code	sk13	
Empirical formula	C39 H33 Cl6 N P2 Pt	
Formula weight	985.39	
Temperature	203(2) K	
Wavelength	0.71073 Å	
Crystal system	Triclinic	
Space group	P-1	
Unit cell dimensions	a = 10.72070(10) Å	α = 114.840(2)°.
	b = 13.8244(2) Å	β = 91.4020(10)°.
	c = 14.5320(2) Å	γ = 96.5590(10)°.
Volume	1935.45(4) $Å^3$	
Z	2	
Density (calculated)	1.691 Mg/m^3	
Absorption coefficient	4.152 mm^{-1}	
F(000)	968	
Crystal size	0.40 x 0.23 x 0.14 mm^3	
Theta range for data collection	1.55 to 25.00°.	
Index ranges	-12<=h<=12, -16<=k<=16, -17<=l<=17	
Reflections collected	16406	
Independent reflections	6783 [R(int) = 0.0237]	
Completeness to theta = 0.50°	0.0 %	
Absorption correction	Semi-empirical from equivalents	
Max. and min. transmission	0.5941 and 0.2875	
Refinement method	Full-matrix least-squares on F^2	
Data / restraints / parameters	6783 / 0 / 437	
Goodness-of-fit on F^2	1.065	
Final R indices [I>2sigma(I)]	R1 = 0.0299, wR2 = 0.0731	
R indices (all data)	R1 = 0.0323, wR2 = 0.0746	
Largest diff. peak and hole	1.654 and -1.227 $e.Å^{-3}$	

Table 4.2

Selected bond lengths (Å) and angles (°) for the cation [Pt(PNCHP-κ^3*P,N,P*)Cl]$^+$ with estimated standard deviations in parentheses

Bond lengths:			
Pt-P(1)	2.2949(11)	P(1)-C(11)	1.806(5)
Pt-P(2)	2.2848(11)	P(1)-C(21)	1.820(5)
Pt-N	2.028(5)	P(1)-C(31)	1.816(5)
Pt-Cl(1)	2.2873(12)	P(2)-C(41)	1.813(5)
N-C(1)	1.117(9)	P(2)-C(51)	1.816(4)
N-C(36)	1.698(8)	P(2)-C(61)	1.815(5)
C1-C(42)	1.532(11)	C-C (phenyl)	1.352(9)-1.421(7)
Bond angles:			
N-Pt-Cl(1)	173.72(19)	N-C(1)-C(42)	116.0(7)
P(1)-Pt-P(2)	174.81(4)	C(1)-C(42)-C(41)	132.8(5)
P(1)-Pt-N	84.43(19)	C(1)-C(42)-C(43)	108.2(5)
P(2)-Pt-N	91.42(19)	Pt-P(1)-C(11)	120.28(15)
P(1)-Pt-Cl(1)	93.06(4)	Pt-P(1)-C(21)	114.37(15)
P(2)-Pt-Cl(1)	91.38(4)	Pt-P(1)-C(31)	101.35(15)
Pt-N-C(1)	141.6(7)	Pt-P(2)-C(41)	106.12(14)
Pt-N-C(36)	113.4(4)	Pt-P(2)-C(51)	113.17(14)
C(1)-N-C(36)	104.9(7)	Pt-P(2)-C(61)	116.78(14)
N-C(36)-C(31)	113.8(4)	P1-C(31)-C(36)	117.0(3)
N-C(36)-C(35)	126.9(4)	P(2)-C(41)-C(42)	120.0(4)

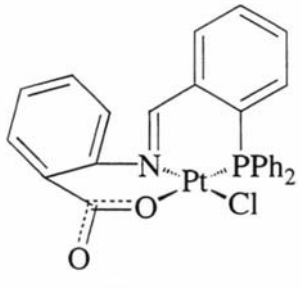

F.4.4-1

Figure 4.4 A square planar platinum(II) complex related to [Pt(PNCHP-κ^3*P,N,P*)Cl]$^+$

4.2.2.2 Crystal structure of [Pt(PNCHP-κ^3P,N,P)(PPh$_3$)](BF$_4$)$_2$•2CH$_2$Cl$_2$

The dication [Pt(PNCHP)(PPh$_3$)]$^{2+}$ is depicted in **Figure 4.5**, with crystal data and structure refinement details given in **Table 4.3** and bond lengths and angles given in **Table 4.4**. The structure shows the two phosphorus atoms (P(1) and P(2)) and nitrogen atom (N) of PNCHP and the phosphorus atom of a triphenyphosphane (P(3)) coordinated to a central platinum atom (Pt). The coordination geometry of the platinum is slightly distorted square planar for reasons discussed in section 4.2.2.1. Calculation of a plane involving the platinum atom and the four donor atoms shows a significant deviation from coplanarity of 0.0773(12) Å, much greater (0.0254(15) Å) than in the structure discussed previously. The Pt-P bond lengths to PNCHP (Pt-P(1), 2.3151(12) Å and Pt-P(2), 2.3247(12) Å), listed in **Table 4.2**, are similar (2.332(2)-2.347(2) Å) to other square-planar d^8 complexes of platinum for compounds with two phosphanes *trans* to each other.[22] Pt-P and Pt-N bond lengths are similar to those found in the complexes *cis*-[Pt(PNH$_2$)]$^{2+}$ (**F.4.6-1**) and *trans*-[Pt(PNH$_2$)]$^{2+}$ (**F.4.6-2**) (PNH$_2$ = o-aminophenyldiphenylphosphane) shown in **Figure 4.6**.[23] However, the bond lengths Pt-P(1) and Pt-P(2) are significantly longer (Δ0.0202 and 0.0399 Å, respectively) than those found in the previously discussed complex [Pt(PNCHP-κ^3*P,N,P*)Cl]$^+$. One might expect the reverse trend to be present after considering the charges of the complexes, +2 and +1 respectively. However, the lengthening of the Pt-P(1) and Pt-P(2) bonds can be explained using steric arguments involving the mutually *cis* coordinated triphenylphosphane ligand. Effectively there are three bulky triphenylphosphino moieties in close proximity causing the elongation. To further support the steric arguments, the Pt-P(1) and Pt-P(2) bond axis are bent away from the sterically demanding triphenyphosphane ligand (cone angle = 145 °), as noted by the significant decrease in the P(2)-Pt-N angle of 83.14 °. In the related complex [Pt(PNCHP-κ^3*P,N,P*)Cl]$^+$, which contains a chloride, a much less bulky ancillary ligands than triphenylphosphane, this angle does not deviate much from the ideal angle of 90 ° (91.42(19) °). The Pt-N bond length of 2.109(15) Å is significantly shorter by 0.063 Å than the analogous bond length in the [Pt(PNCHP-κ^3*P,N,P*)Cl]$^+$ (2.046(5) Å) complex. This is

[22] L. M. Engelhardt, J. M. Patrick, C. L. Raston, P. Twiss and A. H. White, *Aust. J. Chem.*, 1984, **37**, 2193.
[23] M. K. Cooper, J. M. Downes, H. J. Goodwin and M. McPartlin, *Inorg. Chim. Acta*, 1983, **76**, L157.

most likely due to a combination of the greater *trans* influence[24] of the phosphorus over the chloride and greater charge of the complex relative to $[Pt(PNCHP)Cl]^+$.

[24] D. Dowerah, L. J. Radonovich and N, F. Woolsey, *Organometallics*, 1990, **9**, 614-620.

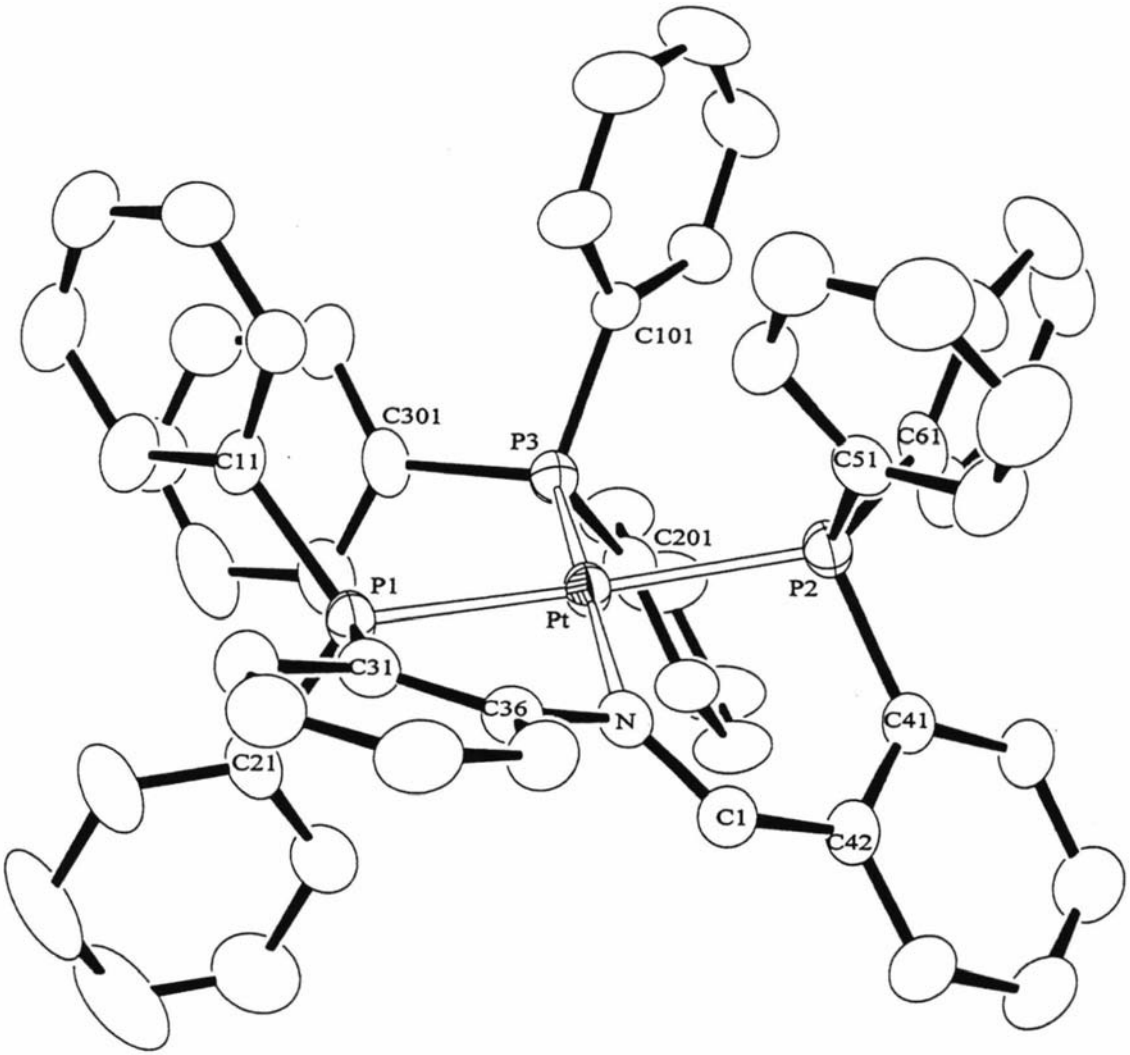

Figure 4.5 ORTEP diagram for the dication $[Pt(PNCHP\text{-}\kappa^3P,N,P)(PPh_3]^{2+}$ showing the numbering system used. Thermal ellipsoids are at the 50% probability level. Hydrogen atoms have been omitted for clarity

Table 4.3

Crystal data and structure refinement for [Pt(PNCHP-κ^3*P,N,P*)(PPh$_3$)](BF$_4$)$_2$•2CH$_2$Cl$_2$.

Identification code	sk12	
Empirical formula	C57 H48 B2 Cl4 F8 N P3 Pt	
Formula weight	1350.38	
Temperature	203(2) K	
Wavelength	0.71073 Å	
Crystal system	Monoclinic	
Space group	P2(1)/c	
Unit cell dimensions	a = 13.17220(10) Å	α = 90°.
	b = 21.81280(10) Å	β = 91.9420(10)°.
	c = 19.7670(2) Å	γ = 90°.
Volume	5676.24(8) Å^3	
Z	4	
Density (calculated)	1.582 Mg/m^3	
Absorption coefficient	2.810 mm^{-1}	
F(000)	2684	
Crystal size	0.61 x 0.32 x 0.22 mm^3	
Theta range for data collection	1.39 to 27.49°.	
Index ranges	-16<=h<=16, -27<=k<=28, -20<=l<=25	
Reflections collected	31955	
Independent reflections	12425 [R(int) = 0.0285]	
Completeness to theta = 0.50°	0.0 %	
Absorption correction	Semi-empirical from equivalents	
Max. and min. transmission	0.5768 and 0.2790	
Refinement method	Full-matrix least-squares on F^2	
Data / restraints / parameters	12425 / 0 / 675	
Goodness-of-fit on F^2	1.118	
Final R indices [I>2sigma(I)]	R1 = 0.0449, wR2 = 0.0996	
R indices (all data)	R1 = 0.0603, wR2 = 0.1095	
Largest diff. peak and hole	2.053 and -1.372 e.Å^{-3}	

Table 4.4

Selected bond lengths (Å) and angles (°) for the dication [Pt (PNCHP-κ^3*P,N,P*)(PPh_3)]$^{2+}$ with estimated standard deviations in parentheses

Bond lengths:			
Pt-P(1)	2.3151(12)	P(2)-C(41)	1.817(6)
Pt-P(2)	2.3247(12)	P(2)-C(51)	1.808(6)
Pt-N	2.107(4)	P(2)-C(61)	1.812(5)
N-C(1)	1.290(6)	Pt-P(3)	2.2688(13)
N-C(36)	1.450(6)	P(3)-C(101)	1.803(5)
C(1)-C(42)	1.461(7)	P(3)-C(201)	1.816(5)
P(1)-C(11)	1.812(5)	P(3)-C(301)	1.818(5)
P(1)-C(21)	1.798(6)	C-C (phenyl)	1.352(10)-1.410(8)
P(1)-C(31)	1.815(5)		
Bond angles:			
P(1)-Pt-P(2)	160.96(5)	Pt-P(1)-C(31)	98.69(17)
P(1)-Pt-N	82.23(11)	Pt-P(2)-C(41)	105.87(17)
P(2)-Pt-N	83.37(11)	Pt-P(2)-C(51)	103.77(18)
Pt-N-C(1)	126.3(4)	Pt-P(2)-C(61)	126.95(18)
Pt-N-C(36)	116.3(3)	P1-C(31)-C(36)	117.3(4)
C(1)-N-C(36)	116.9(4)	P(2)-C(41)-C(42)	119.2(4)
N-C(36)-C(31)	117.3(4)	N-Pt-P(3)	175.68(12)
N-C(36)-C(35)	122.1(5)	P(1)-Pt-P(3)	98.80(5)
N-C(1)-C(42)	128.0(5)	P(2)-Pt-P(3)	96.49(5)
C(1)-C(42)-C(41)	125.0(5)	Pt-P(3)-C(101)	111.36(17)
C(1)-C(42)-C(43)	115.0(5)	Pt-P(3)-C(201)	110.82(18)
Pt-P(1)-C(11)	116.80(17)	Pt-P(3)-C(301)	118.37(17)
Pt-P(1)-C(21)	120.86(19)		

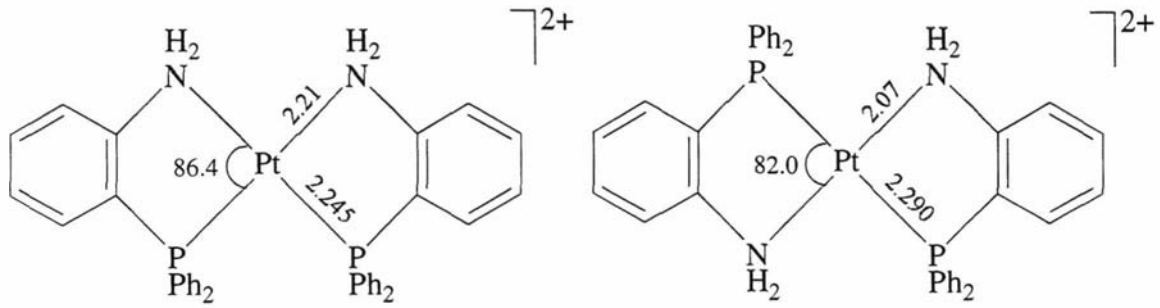

F.4.6-1 **F.4.6-2**

Figure 4.6 Bond lengths and angles in square planar platinum(II) species containing the 'PN' hybrid ligand o-aminophenyldiphenylphosphane

4.2.2.3 Crystal structure of [Pt(PNCHP-κ^3P,N,P)(phen)](BF$_4$)$_2$•CH$_2$Cl$_2$

The dication [Pt(PNCHP-κ^3*P,N,P*)(phen)]$^{2+}$ is shown in **Figure 4.7**, with crystal data and structure refinement details given in **Table 4.5** and bond lengths and angles given in **Table 4.6**. The platinum atom (Pt) is five-coordinate with slightly distorted square pyramidal geometry. The PNCHP ligand occupies three sites of the complexes basal plane, coordinating through the two phosphorus atoms (P(1) and P(2)) and the nitrogen atom (N). The remaining coordination site of the basal plane is filled by one of the nitrogen atoms (N(1)) of the 1,10-phenanthroline (phen) ligand. The 1,10-phenanthroline's second nitrogen atom (N(2)) is located at the apex of the square pyramid. There is no significant difference between the Pt-N(imine) (2.038(2) Å) and Pt-N1(phen) (2.043(2) Å) bond lengths, which are *trans* to one another in the basal plane. The phen ligands axial N(2)-Pt distance of 2.529(3) Å is considerably longer than the equatorial N(1)-Pt distance of 2.035(3) Å, the latter is a typical length for platinum(II)-1,10-phenanthroline species.[25] As explained in section *4.1.2*, it is normal for axial bonding lengths to be longer than equatorial bond lengths.

Due to the 1,10-phenanthroline's rigid structure the second nitrogen atom is, without choice, always in the vicinity of the metal. Therefore it is difficult to decide whether the axial nitrogen atom-to-metal distance N(2)-Pt constitutes a weak bond, or is

[25] A. Hazell and A. Mukhopadhyay, *Acta Cryst.* 1980, B**36**, 1647.

non-bonding. The author has called the N(2)-Pt distance bonding for the following reasons combined, and in view of the background given in section *4.1.2*:

i) The platinum atom is displaced from the basal by 0.1052(8) Å towards the N2 atom.

ii) The ratio of the axial/equatorial bond lengths of 1.24 are closer to values for accepted five coordinate species,[12] for example, a ratio of 1.17 is found for the five coordinate species $[Ni(CN)_5]^{2-}$ and 1.14 in the five coordinate $[PtI_2(CO)(dmphen)]$, where the phenanthroline ligand is bound as a axial-to-equatorial bidentate ligand, whilst in the accepted four coordinate $[PtCl(phen)(PEt_3)_2]^+$, where the phen ligand is considered monodentate, the ratio is 1.33.[26] The structure of $[Pt(PNCHP\text{-}\kappa^3P,N,P)(phen)]^{2+}$ (**F.4.8-1**) shown in **Figure 4.8** may be compared with those in **Figure 4.1**.

iii) The N1-Pt-N2 angle of 74.54(8) ° lies fairly close to the average phen N-M-N angle of 79.5 when the ligand is clearly bidentate.[12] For comparison these same angles in the complexes $[PtCN(phen)_2]^+$ and $[PtCl(phen)(PEt_3)_2]^+$, where the phen ligand is monodentate, are 69.7(2) and 68.2 ° respectively.[27,28]

iv) The difference between the Pt-N(1)-C(5) and Pt-N(1)-C(1) angles of -2.2 °, is indicative of a phenanthroline ligand bound to both the basal plane and the apical site of the metal atom, thereby, coordinated as a bidentate ligand (refer to the angle difference [M-N(1)-C(5)] - [M-N(1)-C(1)] given in **Figure 4.1**).

v) Lastly, the considered non-bonding axial phen nitrogen-to-platinum lengths in $[PtCN(phen)_2]^+$ and $[PtCl(phen)(PEt_3)_2]^+$ are 2.761(5) and 2.843(20) Å respectively, which are significantly longer than the 2.529(3) Å found in the title complex.

---

[26] K. N. Raymond, T. G. Spiro and A. Terzis, *Inorg. Chem.*, 1970, **9**, 2415
[27] O. Wernberg and A. Hazell, *J. Chem. Soc. Dalton Trans.*, 1980, 973
[28] G. W. Bushnell, K. R. Dixon and M. A. Khan, *Can. J. Chem.*, 1978, **56**, 450.

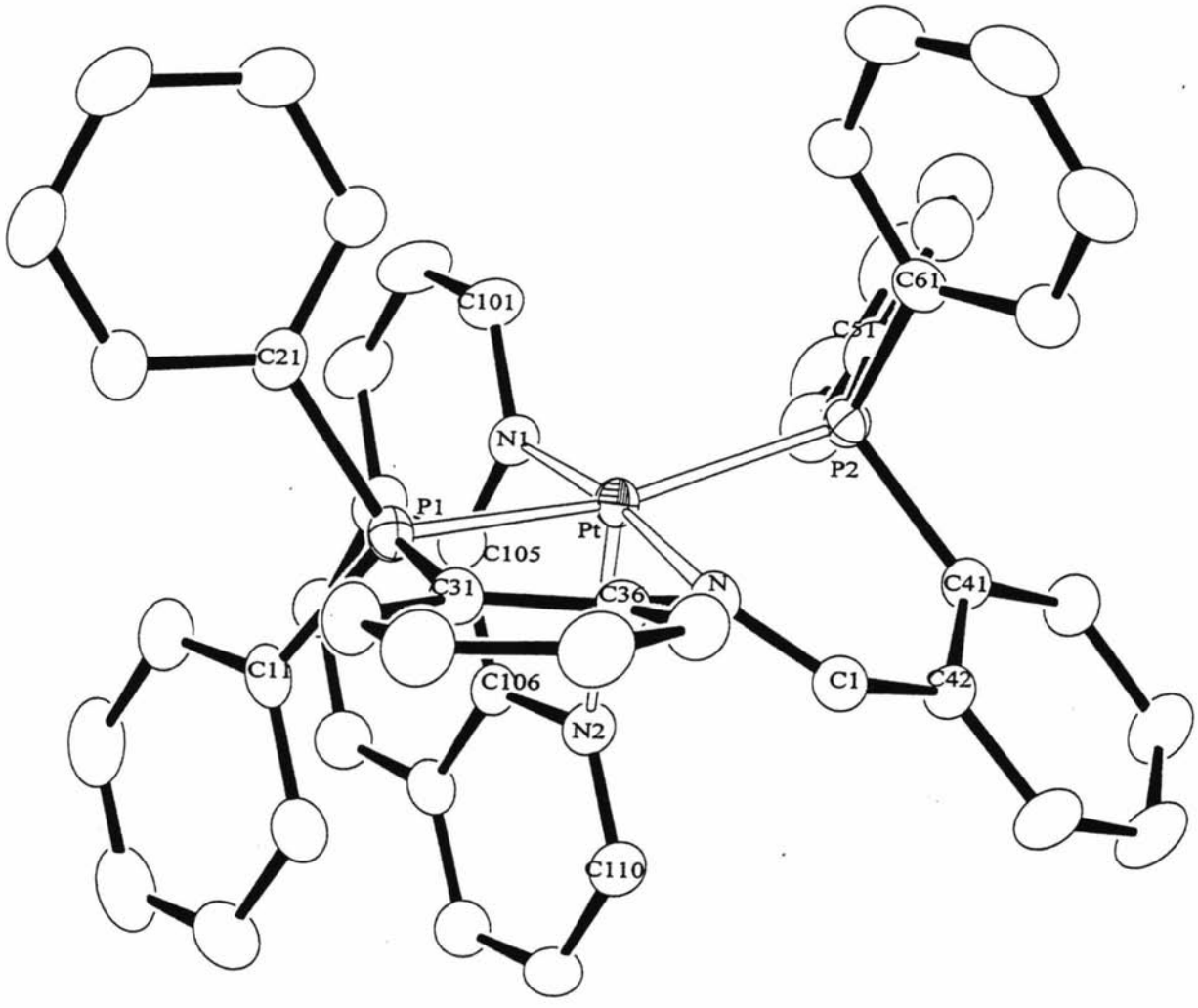

Figure 4.7 ORTEP diagram for the dication [Pt(PNCHP-κ^3*P,N,P*)(phen)]$^{2+}$ showing the numbering system used. Thermal ellipsoids are at the 50% probability level. Hydrogen atoms have been omitted for clarity

Table 4.5

Crystal data and structure refinement for [Pt(PNCHP-κ^3*P,N,P*)(phen)]$(BF_4)_2 \bullet CH_2Cl_2$.

Identification code	sk11	
Empirical formula	C50 H39 B2 Cl2 F8 N3 P2 Pt	
Formula weight	1183.39	
Temperature	203(2) K	
Wavelength	0.71073 Å	
Crystal system	Triclinic	
Space group	P-1	
Unit cell dimensions	a = 10.33380(10) Å	α = 87.0120(10)°.
	b = 12.9595(2) Å	β = 88.3890(10)°.
	c = 18.5480(2) Å	γ = 76.2110(10)°.
Volume	2408.78(5) $Å^3$	
Z	2	
Density (calculated)	1.632 Mg/m^3	
Absorption coefficient	3.160 mm^{-1}	
F(000)	1168	
Crystal size	0.40 x 0.27 x 0.24 mm^3	
Theta range for data collection	1.10 to 26.35°.	
Index ranges	-12<=h<=12, -16<=k<=15, -23<=l<=23	
Reflections collected	20996	
Independent reflections	9682 [R(int) = 0.0130]	
Completeness to theta = 0.50°	0.0 %	
Absorption correction	Semi-empirical from equivalents	
Max. and min. transmission	0.5176 and 0.3646	
Refinement method	Full-matrix least-squares on F^2	
Data / restraints / parameters	9682 / 0 / 598	
Goodness-of-fit on F^2	1.020	
Final R indices [I>2sigma(I)]	R1 = 0.0207, wR2 = 0.0547	
R indices (all data)	R1 = 0.0220, wR2 = 0.0559	
Largest diff. peak and hole	1.065 and -1.090 $e.Å^{-3}$	

Table 4.6

Selected bond lengths (Å) and angles (°) for dication $[Pt(PNCHP\text{-}\kappa^3P,N,P)(phen)]^{2+}$ with estimated standard deviations in parentheses

Bond lengths:			
Pt-P(1)	2.2997(6)	P(1)-C(31)	1.809(3)
Pt-P(2)	2.2947(6)	P(2)-C(41)	1.815(3)
Pt-N	2.038(2)	P(2)-C(51)	1.814(3)
N-C(1)	1.295(3)	P(2)-C(61)	1.813(3)
N-C(36)	1.450(3)	C-C (phenyl)	1.376(6)-1.417(4)
C(1)-C(42)	1.468(3)	Pt-N(1)	2.043(2)
P(1)-C(11)	1.806(3)	Pt-N(2)	2.526(2)
P(1)-C(21)	1.810(3)		
Bond angles:			
P(1)-Pt-P(2)	161.34(2)	Pt-P(2)-C(51)	120.01(9)
P(1)-Pt-N	84.66(6)	Pt-P(2)-C(61)	109.02(8)
P(2)-Pt-N	86.84(6)	P(1)-C(31)-C(36)	116.27(19)
Pt-N-C(1)	124.55(17)	P(2)-C(41)-C(42)	119.14(18)
Pt-N-C(36)	117.62(15)	N-Pt-N(1)	172.52(8)
C(1)-N-C(36)	116.2(2)	P(1)-Pt-N(1)	91.98(6)
N-C(36)-C(31)	118.4(2)	P(2)-Pt-N(1)	98.25(6)
N-C(36)-C(35)	121.0(2)	N-Pt-N(2)	99.03(8)
N-C(1)-C(42)	128.7(2)	P(1)-Pt-N(2)	94.69(5)
C(1)-C(42)-C(41)	125.7(2)	P(2)-Pt-N(2)	103.04(5)
C(1)-C(42)-C(43)	114.9(2)	N(1)-Pt-N(2)	74.54(8)
Pt-P(1)-C(11)	116.62(8)	Pt-N(1)-C(101)	121.74(18)
Pt-P(1)-C(21)	116.77(9)	Pt-N(1)-C(105)	119.01(17)
Pt-P(1)-C(31)	99.88(8)	Pt-N(2)-C(110)	133.68(18)
Pt-P(2)-C(41)	105.76(8)	Pt-N(2)-C(106)	104.77(16)

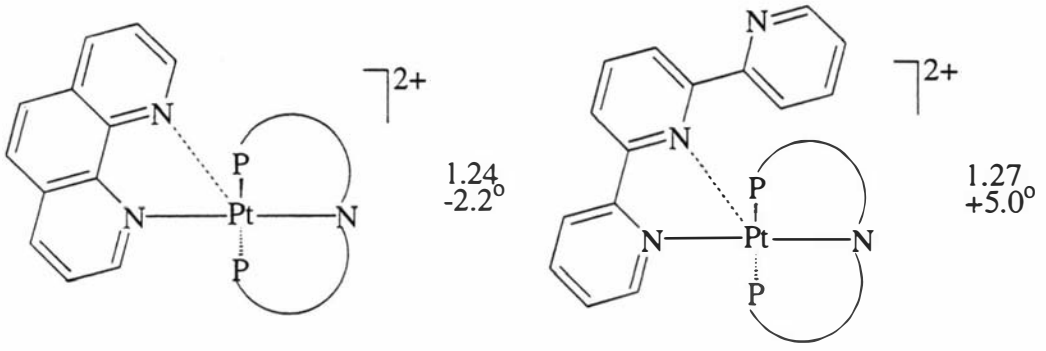

F.4.8-1 **F.4.8-2**

Figure 4.8 Five-coordinate platinum(II) complexes containing the ligand PNCHP

It is worthwhile to note the stacking of the 1,10-phenanthroline ligand with the phenyl ring starting at C11. The corresponding mean planes make a dihedral angle of 6.25(14) °, with the shortest non-bonding distance C(14)----C(108) of 2.71(10) Å. This feature is, interestingly, analogous to the situation found from the X-ray analysis of $[Pd(dppp)(tmphen)(CH_2NO_2)]^{+}$, shown in **Figure 4.9**, where the dihedral angle is 11.5(1) ° and shortest non-bonding distance (N1-C(39)) is 3.10 Å.[9]

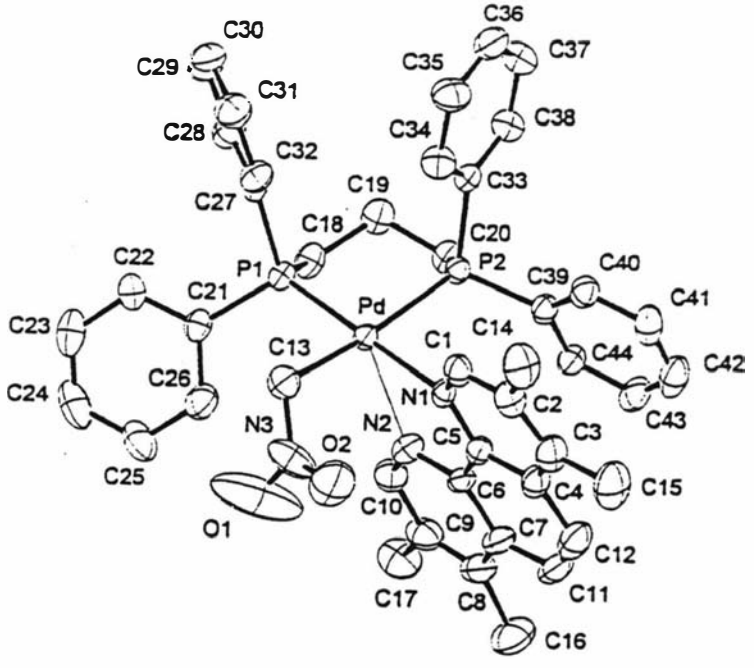

Figure 4.9 Stacking of the phenyl rings containing the atoms C(39) and N(1) in the complex $[Pd(dppp)(tmphen)(CH_2NO_2)]^{+}$

4.2.2.4 Crystal structure of [Pt(PNCHP-κ^3P,N,P)(terpy)]BF_4

The structure of [Pt(PNCHP-κ^3*P,N,P*)(terpy)]$^{2+}$ is shown in **Figure 4.10**, with crystal data and structure refinement details given in **Table 4.7** and bond lengths and angles given in **Table 4.8**. The complex [Pt(PNCHP-κ^3*P,N,P*)(terpy)]$^{2+}$ is analogous to the previously discussed [Pt(PNCHP-κ^3*P,N,P*)(phen)]$^{2+}$. The geometry around the platinum atom is square pyramidal with the two phosphorus atoms (P(1) and P(2)) and one nitrogen atom (N) of PNCHP occupying three equatorial sites, with the fourth site occupied by one of the terminal nitrogen atoms (N(1)) of the 2,2',6'2"-terpyridine (terpy) ligand. The middle nitrogen atom (N(2)) of the terpy occupies the axial site. The axial Pt-N(2) distance of 2.625(7) is, as expected, longer than the equatorial Pt-N1 distance of 2.062(6), as listed in **Table 4.4**. The Pt-N(2) distance is considered as a weak interaction for the following reasons:

i) The same arguments put forth to describe the nature of the axial Pt-N(2) bond in [Pt(PNCHP)(phen)]$^{2+}$ also hold here For example, the platinum atom is displaced from the basal by 0.0349(8) Å towards the N(2) atom, and the axial/equatorial ratio of 1.27 and difference between the M-N(1)-C(105) and M-N(1)-C(101) angles of +5.0 ° are all indicative of a Pt-N(2) interaction. These values, also given in **F.4.8-2** of **Figure 4.8,** may be compared with the values given in **Figure 4.1**, where it can be seen that structure of [Pt(PNCHP-κ^3*P,N,P*)(terpy)]$^{2+}$ (**F.4.8-2**) fits into the series at about the mid point.

ii) In addition, unlike the phen ligand in the previuos structure, the pyridyl ring containing the axial bound nitrogen atom is free to rotate around the C(106)-C(107) axis and therefore is not required to orientate itself for bonding with the metal, which it does.

The two rings containing the N(1) and N(2) atoms lie in one plane. In contrast, the mean plane of the pyridyl ring containing the non-bonding nitrogen atom N13(a_4) is 47.47(0.63) ° to the mean plane of the middle pyridyl ring. There are no significant differences in bond lengths of the three pyridyl rings. Due to the molecule sitting on a two-fold axis, bond lengths of the PNCHP ligand cannot be confidently discussed.

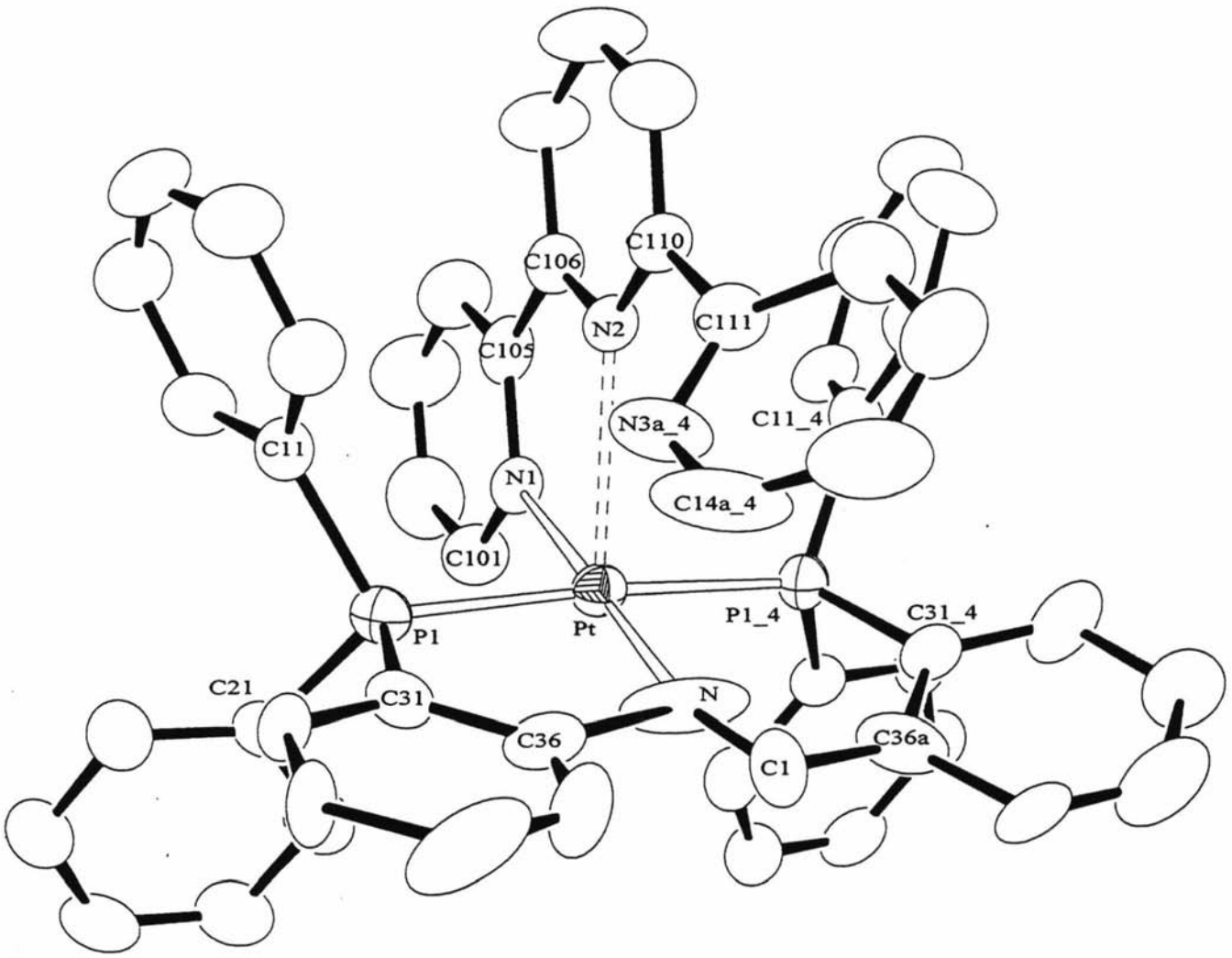

Figure 4.10 ORTEP diagram for the dication [Pt(PNCHP-κ^3*P,N,P*)(terpy)]$^{2+}$ showing the numbering system used. Thermal ellipsoids are at the 50% probability level. Hydrogen atoms have been omitted for clarity

Table 4.7

Crystal data and structure refinement for [Pt(PNCHP-κ^3*P,N,P*)(terpy)]BF_4.

Identification code	sk15a	
Empirical formula	C52 H40 B2 F8 N4 P2 Pt	
Formula weight	1151.53	
Temperature	200(2) K	
Wavelength	0.71073 Å	
Crystal system	Monoclinic	
Space group	P2(1)/m	
Unit cell dimensions	a = 11.2894(3) Å	$\alpha = 90°$.
	b = 16.0209(5) Å	$\beta = 107.978(1)°$.
	c = 13.6843(4) Å	$\gamma = 90°$.
Volume	2354.32(8) $Å^3$	
Z	2	
Density (calculated)	1.624 Mg/m^3	
Absorption coefficient	3.122 mm^{-1}	
F(000)	1140	
Crystal size	0.36 x 0.16 x 0.11 mm^3	
Theta range for data collection	1.56 to 25.56°.	
Index ranges	-13<=h<=13, -18<=k<=18, -16<=l<=16	
Reflections collected	19782	
Independent reflections	4368 [R(int) = 0.0992]	
Completeness to theta = 0.50°	0.0 %	
Absorption correction	Semi-empirical from equivalents	
Max. and min. transmission	0.7252 and 0.3995	
Refinement method	Full-matrix least-squares on F^2	
Data / restraints / parameters	4368 / 0 / 415	
Goodness-of-fit on F^2	1.006	
Final R indices [I>2sigma(I)]	R1 = 0.0449, wR2 = 0.1013	
R indices (all data)	R1 = 0.0619, wR2 = 0.1084	
Largest diff. peak and hole	2.330 and -0.923 $e.Å^{-3}$	

Table 4.8

Selected bond lengths (Å) and angles (°) for the dication [Pt (PNCHP-κ^3*P,N,P*)(terpy)]$^{2+}$ with estimated standard deviations in parentheses

Bond lengths:			
Pt-P(1)	2.3049(16)	Pt-N(1)	2.062(6)
Pt-P(1_4)	2.3049(16)[a]	Pt-N(2)	2.625(7)
Pt-N	2.017(8)	C(101)-N(1)	1.351(11)
N-C(1)	1.090(11)[b]	N(1)-C(105)	1.375(11)
N-C(36)	1.871(6)[b]	C(105)-C(106)	1.488(13)
C(1)-C(36)a	1.871(15)[b]	C(106)-N(2)	1.338(11)
P(1)-C(11)	1.818(6)	N(2)-C(110)	1.329(11)
P(1)-C(21)	1.832(6)	C(111)-N(3a_4)	1.282(13)
P(1)-C(31)	1.806(6)	N(3a_4)-C(14a_4)	1.364

Bond lengths:			
P(1)-Pt-P(1_4)	175.27(8)	P(1)-C(31)-C(36)	113.7(2)
P(1)-Pt-N	89.81(4)[b]	N-Pt-N(1)	178.0(3)[b]
P(1_4)-Pt-N	89.81(4)[a,b]	P(1)-Pt-N(1)	90.11(4)
Pt-N-C(1)	147.1(6)[b]	P(1_4)-Pt-N(1)	90.11(4)[a]
Pt-N-C(36)	108.9(3)[b]	C(101)-N(1)-Pt	118.0(6)
C(1)-N-C(36)	103.7(7)[b]	Pt-N(1)-C(105)	123.0(5)
N-C(36)-C(31)	120.0(3)[b]	C(101)-N(1)-C(105)	119.0(7)
N-C(36)-C(35)	119.8(9)[b]	N(1)-C(105)-C(106)	119.5(7)
N-C(1)-C(36a)	117.2(13)[b]	C(105)-C(106)-N(2)	118.9(8)
C(1)-C(36a)-C(31_4)	132(2)[b]	C(106)-N(2)-Pt	106.04
C(1)-C(36a)-C(35a)	114.3(17)[b]	Pt-N(2)-C(110)	133.93
Pt-P(1)-C(11)	114.7(2)	N(2)-C(110)-C(111)	119.1(8)
Pt-P(1)-C(21)	117.7(2)	C(110)-C(111)-N(3a_4)	116.9(8)
Pt-P(1)-C(31)	106.4(2)		

[a] Atoms generated by C2 rotation. [b] Group sits on the two-fold axis

4.2.3 ^{31}P NMR spectroscopy for the PNCHP complexes

4.2.3.1 ^{31}P NMR spectra for the platinum PNCHP complexes

The ^{31}P NMR data for all the compounds is collected in **Table 4.9**. All the platinum(II) compounds displayed similar spectra, showing two doublets with satellites. A representative spectrum for [Pt(PNCHP-κ^3*P,N,P*)Cl]Cl is shown in **Figure 4.11**. The features of the spectra were assigned to the two inequivalent phosphorus atoms of the PNCHP ligand with ^2J(P,P) coupling between the two inequivalent phosphorus nuclei and ^1J(Pt,P) coupling due to the spin ½ nucleus ^{195}Pt, found in 33 % abundance. In general, for all the platinum(II) compounds one of the phosphorus atoms has a high frequency resonance in the range δ45.9 to δ28.7 and the other a low frequency resonance in the range δ19.5 to δ12.3. The former is most likely caused by the phosphorus atom involved in the five membered ring, due to the ring contribution (ΔR) effect.[29,30] The ^2J(P,P) coupling constants ranged from 306 to 422 Hz which is indicative of a *trans* arrangement of inequivalent phosphorus atoms.[31] The coupling constants of larger magnitude were exhibited by the monocation complexes, whilst those of smaller magnitude were displayed by the dicationic complexes. ^1J(P,Pt) coupling constants ranged from 2353 to 2789 Hz and were typical of *trans*-platinum(II) complexes.[32] The ^1J(P,Pt) coupling constants associated with the higher frequency resonances, ie those from δ45.9 to δ28.7, were on average 30 Hz higher than their lower frequency counterparts at δ19.5 to δ12.3, further supporting the assignments of the signals at high frequency as the phosphorus atom most likely involved in the five membered ring, again due to the ring contribution (ΔR) effect.[33]

---

[29] a) S. Berger, S. Braun and H-O. Kalinowski, *NMR Spectroscopy of the Non-Metallic Elements*, 1997, John Wiley & Sons Ltd, Chichester, p837. b) G. Dyer and J. Roscoe, *Inorg. Chem.*, 1996, **35**, 4098, and refs. within.
[30] G. Dyer and J. Roscoe, *Inorg. Chem.*, 1996, **35**, 4098, and refs. within.
[31] *Multinuclear NMR*, J. Mason (Editor), 1987, Plenum Press, New York, p394.
[32] See ref 31a, p974.
[33] See ref 31a, p977.

4.2.3.1.2 ^{31}P NMR spectra for the complexes containing an ancillary phosphorus ligand

Two of the complexes contained other phosphorus signals due to their phosphane ancillary ligands. This naturally complicated the ^{31}P NMR spectrum. For the complex $[Pt(PNCHP\text{-}\kappa^3P,N,P)(PPh_3)](BF_4)_2$, where the ancillary ligand is triphenylphosphane, an additional resonance at δ5.1, with ^2J(P,P) coupling constants of 18 and 21 Hz and a ^1J(P,Pt) of 3397 Hz, was observed. The nature of the relatively large ^1J(P,Pt) coupling constant for the triphenylphosphane ligand, relative to those of the PNCHP ligand, is due to the poorer *trans* directing capabilities of the nitrogen when compared to the phosphorus atom. The chemical shift was similar to other triphenylphosphane platinum(II) compounds[34] and the ^2J(P,P) coupling constant was typical of phosphorus atoms in a *cis* arrangement.[31] The spectrum of the complex where diphos is the ancillary ligand is shown in **Figure 4.12**. In the 'free' diphos ligand the phosphorus atoms are equivalent. However, in the complex the two phosphorus atoms of diphos have become inequivalent with one resonance at δ42.6 and the other at δ38.3. The chemical shifts and ^1J(P,Pt) spin-spin coupling observed support both diphos phosphorus atoms being coordinated to the platinum atom. However, the coupling constants are markedly different. The ^1J(P,Pt) coupling constant of 3088 Hz is typical of diphos coordinated in square planar platinum(II) complexes[35,36] and consistent with P trans to N. On the other hand, the ^1J(P,Pt) coupling constant of 117 Hz is atypical; it is assigned to one of the diphos phosphorus atoms coordinated to the apical site of a square pyramid. A trigonal bipyramidal structure has been ruled out because the diphos signals would be expected to be equivalent since the ^2J(P,P) coupling constants indicate that the two phosphorus atoms of PNCHP are *trans* to one another. The number of ^2J(P,P) coupling constants expected for the assigned geometry of the complex containing the diphos ligand are seven (six *cis* and one *trans*) where each phosphorus atom of the diphos and PNCHP ligands couples to three inequivalent phosphorus atom neighbours in *cis* positions and the phosphorus atoms of PNCHP coupling to each other in *trans* positions. Unfortunately due to the small size and large number of *cis* coupling constants the spectrum, was not resolved well enough for coupling assignments to be made.

---

[34] D. V. Khasnis, M. Lattman and U. Siriwardane, *Inorg. Chem.*, 1989, **28**, 681.
[35] H. E. Bryndza, J. C. Calabrese, M. Marsi, D. C. Roe, W. Tam and J. E. Bercaw, *J. Am. Chem. Soc.*, 1986, **108**, 4805.
[36] G. Banditelli, A. L. Bandini and B. Bovio, *Inorg. Chim. Acta*, 1985, **96**, 213.

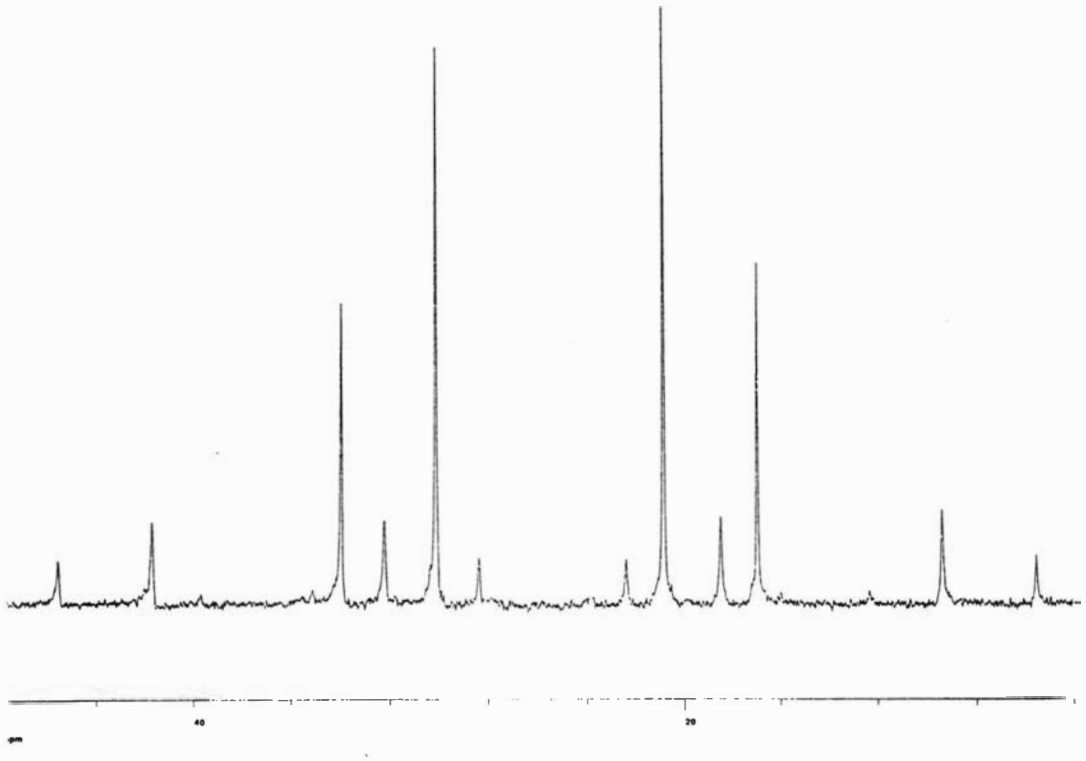

Figure 4.11 The ^{31}P NMR spectrum of the compound [Pt(PNCHP)Cl]Cl

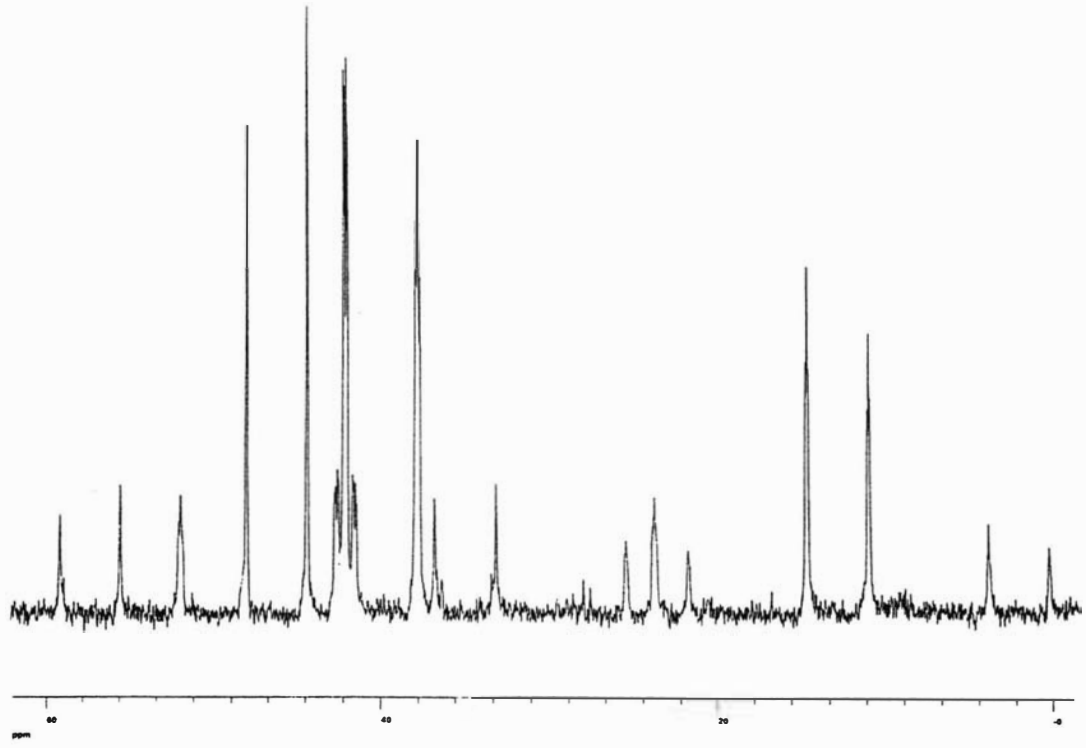

Figure 4.12 The ^{31}P NMR spectrum of the compound [Pt(PNCHP)(diphos)]$(BF_4)_2$

Table 4.9

^{31}P-NMR data for selected compounds [a]

Platinum compounds [b]	δ		^{2}J(PMP) /Hz	^{1}J(MP) /Hz	
	P_a	P_b		P_a	P_b
[Pt(PNCHP)Cl]Cl	32.0	18.8	421	2542	2495
[Pt(PNCHP)Cl]OTf	31.8	18.8	422	2531	2489
[Pt(PNCHP)(MeCN)](OTf)$_2$	34.8	17.5	356	2354	2322
[Pt(PNCHP)(2-pico)](BF$_4$)$_2$[c]	33.4	18.5	363	2493	2490
[Pt(PNCHP)(3-pico)](BF$_4$)$_2$[c]	34.4	19.3	366	2499	2505
[Pt(PNCHP)(phen)](BF$_4$)$_2$	29.9	14.4	354	2789	2757
[Pt(PNCHP)(bipy)](BF$_4$)$_2$	29.7	15.2	363	2731	2722
[Pt(PNCHP)(terpy)](BF$_4$)$_2$	28.7	13.6	306	2698	2669
[Pt(PNCHP)(PPh$_3$)](BF$_4$)$_2$	38.5	19.5	337	2496	2367
	5.1		21, 18	3397	
[Pt(PNCHP)(diphos)](BF$_4$)$_2$	45.9	12.3	396	2435	2353
	42.6	38.3	[d]	117	3088
Palladium compounds [b]					
[Pd(PNCHP)Cl]Cl	37.3	22.6	478		
[Pd(PNCHP)Me]Cl	33.6	27.5	392		

[a] Recorded at 109 MHz, chemical shifts are in ppm relative to 85% H_3PO_4, solvent $CHCl_3$ unless stated otherwise. [b] For all the complexes, the PNCHP ligand was coordinated in a κ^3*P,N,P* fashion. [c] In CH_3CN. [d] Unresolved.

It is interesting to compare the ^{31}P NMR spectra of [Pt(PNCHP-κ^3*P,N,P*)Cl]Cl with the similar compound [Pt($Ph_2PC_3P(Ph)C_2PPh_2$-κ^3*P,P,P*)Cl]Cl (**F.4.12-1**), shown in **Figure 4.13**, which contains a κ^3P,P,P analogue of the κ^3*P,N,P* ligand PNCHP.[37] Even though **F.4.12-1** contains a five- and six-membered ring system analogous to [Pt(PNCHP-κ^3*P,P,P*)Cl]Cl and is structurally similar, the chemical shifts were quite different. Excluding the middle phosphorus atom and *cis* coupling constants, **F.4.12-1** displayed two doublets at δ49.8 (δ32.0 for [Pt(PNCHP-κ^3*P,N,P*)Cl]Cl) and δ4.05 (δ18.8) with ^{2}J(P,P) = 379 (421) Hz, and 1J(P,Pt) = 2347 (2542) and 2241 (2495) Hz respectively. The difference

[37] R. D. Waid and D. W. Meek, *Inorg. Chem.* 1984, **23**, 778.

in the chemical shifts may be due to the π-conjugation in the chain linking the two phosphorus atoms in PNCHP, where the link is saturated in the $\kappa^3 P,P,P$ ligand.

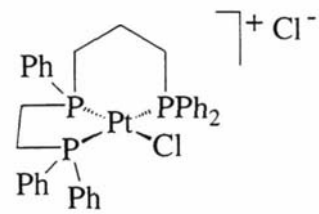

F.4.12-1

Figure 4.13 The compound $[Pt(Ph_2PC_3P(Ph)C_2PPh_2\text{-}\kappa^3 P,P,P)Cl]Cl$, a phosphorus analogue of $[Pt(PNCHP\text{-}\kappa^3 P,N,P)Cl]Cl$

4.2.3.1 ^{31}P NMR spectra for the palladium PNCHP complexes

The spectra of the palladium complexes (see **Table 4.9**) mimicked those of the platinum compounds, but contained no phosphorus-to-metal coupling. All spectra displayed two signals, split as doublets, assigned to the inequivalent phosphorus atoms of PNCHP. Like the platinum compounds, chemical shifts were indicative of phosphorus-transition metal coordination. The splitting was assigned to ^2J(P,P) coupling. The ^2J(P,P) coupling constants were typical of the PNCHP ligand bound to palladium(II) with its two phosphorus atoms *trans* to one another. Chemical shifts and coupling constants for the palladium complexes were significantly larger than their platinum analogues, which is again typical.[31]

4.2.4. ^1H NMR spectroscopy

4.2.4.1 Introduction

This discussion on the ^1H NMR spectroscopic properties of the platinum and palladium compounds of PNCHP will concentrate on the imine proton (-C<u>H</u>=N-) and protons of the ancillary ligands (L) (where the ancillary ligand is defined as any ligand other than PNCHP). Discussion of the aromatic protons, except where possible, is not undertaken due to the number of inequivalent aromatic protons and their poor resolution at 270 MHz. The platinum compounds will be discussed first, followed by those of palladium.

4.2.4.2 Imine proton NMR spectra of the PNCHP complexes

All the platinum(II) compounds listed in **Table 4.10** displayed a signal in the range δ10.87 ([Pt(PNCHP)Cl]Cl) to 8.62 ([Pt(PNCHP)(PPh_3)](BF_4)$_2$). The signal was assigned to the imine proton of PNCHP.[39] Each signal gave a singlet with ^{195}Pt satellites, except when the ancillary ligand contained a phosphorus donor atom, as in the case of [Pt(PNCHP)(PPh_3)](BF_4)$_2$, where the imine proton was observed as a doublet of doublets with J(H,P) coupling constants of 11.60 and 1.07 Hz, and a ^{195}Pt satellite coupling constant ^3J(H,Pt) at 63.93 Hz. The ^3J(H,Pt) coupling constants for the remaining compounds, i.e. those containing no ancillary ligand with a phosphorus atom donor, were significantly larger, ranging from 90.3 to 108.0 Hz. When the ancillary ligand was diphos the imine proton signal was buried in the aromatic region of the spectrum, that is less than δ7.95, and hence not assigned. Therefore, in general when the ancillary ligand was changed from a halogen to a nitrogen to a phosphorus donor ligand, the trend in chemical shift of the imine proton was a move to lower frequency coupled with a decrease in the magnitude of the ^3J(H,Pt) coupling constants. The shift to lower frequency can be explained using the relative *trans* influence of the ancillary ligands' donor atom. For example, when the ancillary donor atom is phosphorus (high in the *trans* influence series), as it is in [Pt(PNCHP)(PPh_3)](BF_4)$_2$ and [Pt(PNCHP)(diphos)](BF_4)$_2$, the imine proton exhibits its lowest frequency shifts. The aromatic region shifted in the same direction as the imine proton signal. With the area under the imine proton peak assigned as one proton (1H), the

area under the remaining peaks gave excellent agreement with the number of aromatic protons expected.

4.2.4.3 Proton NMR spectra of the ancillary ligand in the PNCHP complexes

The methyl and methylene protons of the ancillary ligand in the complexes $[Pt(PNCHP)(L)]^{2+}$ (L = 2-pico, 3-pico, diphos and MeCN) were easily assigned. The aromatic α-proton of 2-picoline was assigned to the doublet at δ8.83 on the basis that it exhibited ^{195}Pt satellites and a peak area integral of 1H. The analogous α-protons of 3-picoline remained obscured by other aromatic protons in the region δ8.46-7.45 and hence not assigned.

The most important feature in the room temperature spectra of the compound $[Pt(PNCHP)(phen)](BF_4)_2$ is the equivalence of the two pyridyl rings of the 1,10-phenanthroline (phen) ligand. In the solid state the compound possesses no elements of symmetry. This raises the question of whether this structure persists in solution. The presence of a dynamic process has been demonstrated by recording the spectra at low temperature. For the complex at room temperature all signals are sharp. The signals due to the phen ligand were easily assigned using standard 2D ^1H-^1H correlation experiments, and are given in **Table 4.10**; they are similar to that of the 'free' ligand.[38] The decrease in temperature causes a progressive broadening of all the proton signals, suggesting the phen ligand and the PNCHP ligand play a role in the fluxional processes. Unfortunately, at the lowest temperature reached, T = -80 °C, the signals detected are still too broad to allow a clear assignment. Detailed variable temperature NMR studies of the cations $[Pt(PNCHP)(bipy)]^{2+}$, $[Pt\ (PNCHP)(terpy)]^{2+}$ and $[Pt\ (PNCHP)(diphos)]^{2+}$ were not undertaken. However, the molecular structure of $[Pt(terpy)(PNCHP)]^{2+}$ shown in section *4.2.2.4* is analogous to the phen case, therefore it is not unreasonable to suggest that the same fluctional processes are occurring in solution for these compounds.

The four palladium compounds [Pd(PNCHP)(L)]X, where L is Cl or CH_3 and X^- is Cl^- or BF_4^-, were investigated. All gave singlet signals in the range δ10.61 - 10.20 assigned to the imine proton of the PNCHP ligand. The area under the peaks of the aromatic protons gave the expected 28 protons for all the complexes relative to the one proton assignment of

[38] R. H. Martin et al., *Tetrahedron Suppl.*, 1966, **8**, 181.

the imine signal. The palladium-methyl compounds gave an additional triplet signal at δ0.56 (^2J(H,Pt)6.53 Hz) and 0.58 (^2J(H,Pt)5.93 Hz) for the chloro and tetrafluoroborate salts respectively, with peak areas integrating to the expected three protons of the methyl group.

Table 4.10
^{1}H-NMR data for selected complexes [a,f]

Platinum Compounds	δC<u>H</u>=N[b]	^{3}J(H,Pt)/Hz	Ar-<u>H</u>[∫]	δL[c][∫]{assign.}	J(L,P)/Hz
[Pt(PNCHP)Cl]Cl[d]	10.87	106.45	9.55(m)[1H] 8.91(m)[1H] 7.86-7.22[26H]		
[Pt(PNCHP)Cl]BF_4[e]	9.72	107.88	8.42(m)[1H] 8.16(m)[1H] 7.93-7.53[26H]		
[Pt(PNCHP)(MeCN)]$(BF_4)_2$[e]	9.42	111.85	8.41(m)[1H] 8.15(m)[1H] 8.09-7.57[26H]	2.20(t)[3H] {C<u>H</u>$_3$CN}	1.22
[Pt(PNCHP)Cl]OTf	9.80	108.19	8.70(m)[1H] 8.24(m)[1H] 7.89-7.27[26H]		
[Pt(PNCHP)(2-pico)]$(BF_4)_2$[e]	9.48	92.16	8.47-7.05[31H]	8.83(d)[1H] {-<u>H</u>C-N=CMe-} 2.24(br)[3H] {-C<u>H</u>$_3$}	5.49 and (^{3}J(H,Pt) = 41.81)
[Pt(PNCHP)(3-pico)]$(BF_4)_2$[e]	9.46	90.33	8.46-7.45[31H] 7.05(m)[1H]	1.97(br)[3H] {-C<u>H</u>$_3$}	
[Pt(PNCHP)(phen)]$(BF_4)_2$[h]	9.42	91.55	8.54m)[1H] 8.04-6.94[35]	8.70(dd)[2H] {H(c)}[h,i] 8.36(dd)[2H] {H(a)} 7.89(s)[2H] {H(d)} 7.54(dd)[2H] {H(b)}	J(c,b)=4.7 J(c,b)=1.2 J(a,b)=8.1 J(b,c)=1.4 J(b,a)=8.2 J(b,c)=5.0
[Pt(PNCHP)(bipy)]$(BF_4)_2$	8.95	90.94	8.24(m)[1H] 8.04-7.08[35]		
[Pt(PNCHP)(terpy)]$(BF_4)_2$[h]	9.04	95.67	8.58-6.51[39]		
[Pt(PNCHP)(PPh_3)]$(BF_4)_2$[j]	8.62(dd)	63.93 ($<^{4}$J(H,P) = 11.60 and 1.07)	8.15(m)[1H] 7.97(m)[1H] 7.89(m)[1H] 7.70-6.71(m)[40]		
[Pt(PNCHP)(diphos)]$(BF_4)_2$[j]	[k]		7.95-5.94[49H]	3.02(m)[4H] {-C<u>H</u>$_2$C<u>H</u>$_2$-}	

Table 4.10 continued...

Palladium Compounds

[Pd(PNCHP)Cl]Cl	10.61	9.48(m)[1H] 8.80(m)[1H] 7.91-7.14[26]		
[Pd(PNCHP)Me]Cl	10.29	9.20(m)[1H] 8.65(m)[1H] 7.84-7.18[26H]	0.56(t)[3H]	6.53
[Pd(PNCHP)Me]BF_4	10.20	9.12(m)[1H] 8.59(m)[1H] 7.83-7.20[26H]	0.58(t)[3H]	5.93

[a] Recorded at 270 MHz, chemical shifts are in ppm relative to $Si(CH_3)_4$, solvent $CDCl_3$ unless stated otherwise; s = singlet, d = doublet, t = triplet, m = multiplet. [b] The integral is assigned to 1H. [c] Only assigned peaks of L are listed in this column, see previous column for others. [d] For all the complexes, the PNCHP ligand was coordinated in a κ^3*P,N,P* fashion. [e] In d^6-acetone. [f] For all the complexes, the PNCHP ligand was coordinated in a κ^3*P,N,P* fashion.[g] Contaminated with [PtCl(PNCHP)]OTf. [h] In d^2-dichloromethane, referenced to $Si(CH_3)_4$. [j] See **Figure 4.14** for key to the assignments. [j] In d^3-acetonitrile, referenced to $Si(CH_3)_4$. [k] Unresolved.

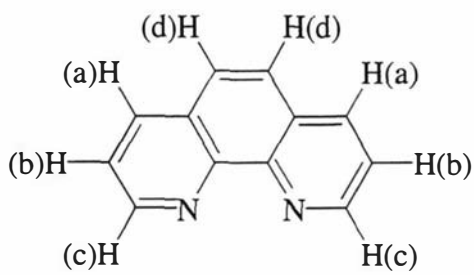

Figure 4.14 Key to the ^{1}H NMR assignments of the 1,10-phenanthroline ligand in the compound [Pt(PNCHP)(phen)]$(BF_4)_2$

4.2.5 IR spectroscopy

IR data for selected compounds is listed in **Table 4.11**. The κ^3*P,N,P* coordinated PNCHP ligand displayed C=N and P-C vibrations around 1595 and 1100 cm^{-1} respectively for all the platinum(II) complexes. The ν(C=N) band was shifted to lower energy by c.a. 26 cm^{-1} relative to the 'free' ligand,[39] which is consistent with other PNCHP complexes where the imino nitrogen atom is coordinated.[2] The P-C vibration is assigned to a peak some 10 cm^{-1} higher in energy relative to the 'free' ligand and group 6 metal carbonyl complexes.[2] Comparison of the spectrum of the monocation $[Pt(PNCHP\text{-}\kappa^3P,N,P)Cl]^+$ with that of the dication $[Pt(PNCHP\text{-}\kappa^3P,N,P)(CH_3CN)]^{2+}$ showed no observable differences. The tetrafluoroborate salts exhibited a very broad band around 1060 cm^{-1} typical of B-F stretching frequencies.[40] The strong stretches present due to the triflate salts were more difficult to assign due to the S=O and C-F stretching occurring in the same region.[41] Both compounds $[Pt(PNCHP)(L)](BF_4)_2$, (L = 2- or 3-picoline) displayed asymmetrical methyl stretches at 2960 (ν_{as}) cm^{-1}, with a symmetrical stretching band at 2940 (ν_s) and 2930 (ν_s) cm^{-1}, respectively.

[39] X. Fan, *Structural Studies on the Interactions of a P_2N Tridentate ligand with Copper(I), Silver(I) and Sulfur,* MPhil Thesis, Massey University, 1995.
[40] K. Nakamoto, *Infrared and Raman Spectra of Inorganic and Coordination Compounds*, 1986, John Wiley & Sons, New York, p132.
[41] R. M. Silverstein, G. Clayton and T. C. Morrill, *Spectrometric Identification of Organic Compounds*, 1991, John Wiley & Sons, Inc., New York

Table 4.11

IR data of selected compounds[a]

Compound	ν(C=N)[b]	ν(P-C)	ν(B-F)	other
[Pt(PNCHP)Cl]Cl	1594(w)	1099(m)		
[Pt (PNCHP)Cl]BF_4	1596(w)	1101(s)	1058(s)	
[Pt (PNCHP)(MeCN)]$(BF_4)_2$	1598(w)	1100(m)	1057(s)	ν(C≡N), 2340(w)
[Pt (PNCHP)Cl]OTf	1595(w)	1101(m)		ν(S=O), 1030(s); ν(C-F), 637(s)
[Pt (PNCHP)(2-pico)]$(BF_4)_2$	[c]	1103(m)	1061	$\nu_{as}(CH_3)$, 2960(w); $\nu_s(CH_3)$, 2940(w)
[Pt (PNCHP)(3-pico)]$(BF_4)_2$	[c]	[c]	1060	$\nu_{as}(CH_3)$, 2960(w); $\nu_s(CH_3)$, 2930(w)

[a] $\tilde{\upsilon}/cm^{-1}$, nujol or hexachlorobutadiene mull. [b] Tentative assignment. [c] Not assigned. s = strong, m = medium and w = weak.

4.2.6 Mass spectroscopy

All the compounds generally exhibited molecular ion peaks with isotope patterns in good agreement with calculations. The most stable fragment, i.e. an absorption of 100 %, for the platinum(II) compounds was found at m/z = 744 and assigned to $[Pt(PNCHP)]^+$. The doubly charged complexes $[Pt(PNCHP)(L)]^{2+}$, where L is any neutral ancillary ligand, gave the expected m/z peaks for z = 2.

Table 4.12

FAB mass spectral data for selected compounds

Platinum compounds	Found m /z (%) , assignment[calculated m/z for ^{195}Pt].
[Pt(PNCHP)Cl]Cl	780(100), MH^+-Cl[780]; 743(50), M^+-H•2Cl[743].
$[Pt(PNCHP)(MeCN)](BF_4)_2$	872(35), M^+-BF_4[872]; 744(100), M^+-CH_3CN•BF_4[744]; 393(18), M^{2+}-$2BF_4$[393].
$[Pt(PNCHP)(2\text{-pico})](BF_4)_2$	924(14), M^+-BF_4[924]; 837(21), M^+-$2BF_4$[837]; 744(100), M^+-$C_6H_7N2BF_4$[744]; 419(42), M^{2+}-$2BF_4$[419].
$[Pt(PNCHP)(3\text{-pico})](BF_4)_2$	924(22), M^+-BF_4[924]; 837(32), M^+-$2BF_4$[837]; 744(100), M^+-C_6H_7N•$2BF_4$[744]; 419(69), M^{2+}-$2BF_4$[419].
$[Pt(PNCHP)(bipy)](BF_4)_2$	987(20), M^+-BF_4[987]; 901(15), MH^+-$2BF_4$[901]; 744(100), M^+-$C_{10}H_8N_2BF_4$[744]; 450(33), M^{2+}-$2BF_4$[450].
$[Pt(PNCHP)(PPh_3)](BF_4)_2$	1093(28), M^+-BF_4[1093]; 1006(57), M^+-$2BF_4$[1006]; 744(100), M^+-$C_{18}H_{15}P$•$2BF_4$[744]; 503(36), M^{2+}-$2BF_4$[503].
$Pt(PNCHP)Cl_4$	850(26), M^+-Cl[850]; 780(100), MH^+-2Cl[780]; 743(17), M^+-H•3Cl[743].
Palladium compounds	**Found m /z (%) , assignment[calculated m/z for ^{106}Pd].**
[Pd(PNCHP)Cl]Cl	692(99), M^+-Cl[692]; 656(20), M^+-H•2Cl[657].
[Pd(PNCHP)Me]Cl	670(100), MH^+-Cl[670], 655(19), MH^+-Cl•CH_3[655]

4.3. Conclusions

For the square planar d^8 metals platinum(II) and palladium(II), the PNCHP ligand coordinates to three sites of the square plane, through the two phosphorus atoms and the imino nitrogen atom. The fourth site of the square plane can be occupied by mono-, bi- or tridentate ligands. In the case of the bi- and tridentate ligands, like 1,10-phenantroline and 2,2',6',2''-terpyridine, both types act in a bidentate fashion, with the second donor atom occupying the apical site of a square pyramid. To the author's knowledge, these five-coordinate species are the first that are platinum dications. The fact that the typically tridentate ligand 2,2',6',2''-terpyridine is forced to bind bidentate fashion suggests that the PNCHP ligand is a relatively strong ligand. This is supported by the non-reactivity of [Pd(Me)(PNCHP-κ^3*P,N,P*)] towards CO to give an insertion product, which requires the tridentate ligand to ring-open in successful systems.

4.4 Experimental

4.4.1 Materials

[Pt(COD)Cl_2], [Pd(COD)Cl_2] and [Pd(COD)(Me)Cl] were prepared as previously described.[14]

4.4.2 [Pt(PNCHP-κ^3P,N,P)Cl]Cl•CH_2Cl_2

A mixture of [Pt(COD)Cl_2] (0.100 g, 0.267 mmol) and PNCHP (0.147g, 0.267 mmol) in benzene (12 mL) was stirred at room temperature for 40 min, giving a yellow precipitate. The mixture was heated to reflux for 30 min and allowed to cool. The resulting yellow precipitate was isolated by fitration, washed with diethylether and air dried to yield [Pt(PNCHP-κ^3*P,N,P*)Cl]Cl•CH_2Cl_2 (0.146 g, 60.7 %) as a yellow powder. The compound can be crystallised from dichloromethane/n-hexane. M.p: 294-296 °C (dec). Anal. Found: C, 48.78; H, 2.75; N, 1.52. Calcd for $C_{37}H_{29}Cl_2NP_2Pt$•CH_2Cl_2: C, 49.34; H, 3.25; N, 1.56.

4.4.3 [Pt(PNCHP-κ^3P,N,P)Cl]BF_4•0.75CH_2Cl_2

A mixture of [Pt(PNCHP-κ^3*P,N,P*)Cl]Cl•CH_2Cl_2 (0.300 g, 0.333 mmol) and $AgBF_4$ (0.071 g, 365 mmol) in dichloromethane (12 mL) was exposed to ultrasound for 1

h, resulting in yellow and white precipitates. The mixture was filtered through kieselguhr and the trapped yellow precipitate dissolved and washed through into the filtrate using acetonitrile, leaving the insoluble white precipitate behind. The filtrate was taken to dryness *in vacuo* and the resulting yellow residue crystallised from dichloromethane/n-hexane overnight. [Pt(PNCHP-κ^3*P,N,P*)Cl]BF_4•0.75CH_2Cl_2 (0.248 g, 79.9 %) was isolated as orange crystals, washed with a dichloromethane/n-pentane mixture and air-dried. M.p: 198-200 °C. Anal. Found: C, 48.55; H, 3.29; N, 1.56. Calcd for $C_{37}H_{29}BClF_4NP_2Pt$•0.75CH_2Cl_2: C, 48.72; H, 3.30; N, 1.51.

4.4.4 [Pt(PNCHP-κ^3P,N,P)(MeCN)](BF$_4$)$_2$

A mixture of [Pt(PNCHP-κ^3*P,N,P*)Cl]BF_4•0.75CH_2Cl_2 (0.401 g, 0.431 mmol) and $AgBF_4$ (0.0899 g, 401 mmol) in acetonitrile (c.a. 15 mL) was heated to reflux for 27 h, giving a dark-orange solution. The solvent was removed *in vacuo* and the resulting orange residue crystallised from dichloromethane/n-hexane to yield [Pt(PNCHP-κ^3*P,N,P*)(MeCN)]$(BF_4)_2$ (0.369 g, 96.0 %). Anal. Found: C, 47.89; H, 3.45; N, 2.81. Calcd for $C_{39}H_{32}B_2F_8N_2P_2Pt$: C, 47.50; H, 3.33; N, 2.81.

4.4.5 [Pt(PNCHP-κ^3P,N,P)Cl]OTf

[Pt(PNCHP-κ^3*P,N,P*)Cl]Cl•CH_2Cl_2 (0.145 g, 0.161 mmol) and AgOTf (0.0459 g, 0.179 mmol) were combined in dichloromethane (12 mL) and mixed in an ultrasound water-bath. The resulting white precipitate was isolated by filtration through a plug of keiselguhr and the filtrate taken to dryness *in vacuo.* The yellow orange solid was dissolved in a minimum amount of dichloromethane and subjected to vapour diffusion using diethylether. A semi-solid emerged as a result which was solidified by addition of n-hexane. [Pt(PNCHP-κ^3*P,N,P*)Cl]OTf (0.0978 g, 65.2 %) was isolated as a yellow powder. Anal. Found: C, 47.54; H, 2.95; N, 1.55. Calcd for $C_{38}H_{29}ClF_3NO_3P_2SPt$: C, 47.82; H, 3.15; N, 1.51.

4.4.6 [Pt(PNCHP-κ^3P,N,P)(MeCN)](OTf)$_2$

[Pt(PNCHP-κ^3*P,N,P*)Cl]OTf (0.100 g, 0.108 mmol) and AgOTf (0.0284 g, 0.111 mmol) were combined in acetonitrile (12 mL) and mixed in an ultrasound water-bath for 2 h. The resulting white precipitate was isolated by filtration through a plug of keiselguhr.

The filtrate was taken to dryness *in vacuo* and cold n-hexane added to give [Pt(PNCHP-κ^3*P,N,P*)(MeCN)]2OTf (0.0817g 69.8 %) as a yellow solid. Analytical data was not obtained due to difficulties in recrystallising this compound.

4.4.7 [Pt(PNCHP-κ^3P,N,P)(2-pico)](BF$_4$)$_2$

A mixture of [Pt(PNCHP-κ^3*P,N,P*)Cl]BF_4•0.75CH_2Cl_2 (0.162 g, 0.174 mmol) and $AgBF_4$ (0.0360 g, 0.185 mmol) in acetonitrile (12 mL) was heated to reflux for 30 min, giving a white precipitate. 2-picoline (2-pico) (0.0183 mL, 0.185 mmol) was added to the reaction mixture and refluxing continued for a further 30 min. The white precipitate was removed by filtration through kieselguhr and the filtrate taken to dryness *in vacuo*. The resulting yellow residue converted to a white and brown mixture over the weekend. The white product was separated from the insoluble brown product by dissolving in dichloromethane, followed by filtration. Crystallisation was initiated by addition of n-hexane to the filtrate. [Pt(PNCHP-κ^3*P,N,P*)(2-pico)]$(BF_4)_2$ (0.1354 g, 72.4 %) was isolated as white microcrystals, washed with diethylether and dried *in vacuo*. Anal. Found: C, 51.04; H, 3.48; N, 2.79. Calcd for $C_{43}H_{36}B_2F_8N_2P_2Pt$: C, 51.06; H, 3.59; N, 2.78.

4.4.8 [Pt(PNCHP-κ^3P,N,P)(3-pico)](BF$_4$)$_2$•CH$_2$Cl$_2$

A mixture of [Pt(PNCHP-κ^3*P,N,P*)Cl]BF_4•0.75CH_2Cl_2 (0.154 g, 0.165 mmol) and $AgBF_4$ (0.0343 g, 0.176 mmol) in acetonitrile (12 mL) was heated to reflux for c.a. 25 min, giving a white precipitate. 3-picoline (3-pico) (0.016 mL, 0.18 mmol) was added to the reaction mixture and refluxing continued for a further 30 min. The white precipitate was removed by filtration through kieselguhr and the filtrate taken to dryness *in vacuo*. The resulting yellow residue was taken into solution with acetonitrile, followed by addition of diethylether to precipitate out the desired product. [Pt(PNCHP-κ^3*P,N,P*)(3-pico)]$(BF_4)_2$•CH_2Cl_2 (0.1006 g, 56.5 %) was isolated as a very pale yellow powder, washed with diethylether and air-dried. Anal. Found: C, 47.88; H, 3.31; N, 3.05. Calcd for $C_{43}H_{36}B_2F_8N_2P_2Pt$•$CH_2Cl_2$: C, 48.20; H, 3.49; N, 2.56.

4.4.9 [Pt(PNCHP-κ^3P,N,P)(phen)](BF$_4$)$_2$

A mixture of [Pt(PNCHP-κ^3*P,N,P*)(MeCN)]$(BF_4)_2$ (0.114 g, 0.119 mmol) and 1,10-phenanthroline (phen) (0.024 g, 0.133 mmol) in benzene (15 mL) was heated to

reflux for 1 h, giving an orange toffee-like solid. The solvent was removed in vacuo and the resulting orange residue taken up into dichloromethane and heated to reflux overnight. The orange solution was subject to vapour diffusion using n-hexane giving [Pt(PNCHP-κ^3*P,N,P*)(phen)]$(BF_4)_2$ (0.126 g, 96.4 %) as chunky orange crystals. Anal. Found: C, 51.05; H, 2.95; N, 3.52. Calcd for $C_{49}H_{37}B_2F_8N_3P_2Pt$: C, 50.75; H, 3.32; N, 3.55.

4.4.10 [Pt(PNCHP-κ^3P,N,P)(bipy)]$(BF_4)_2$

A yellow solution of [Pt(PNCHP-κ^3*P,N,P*)Cl]BF_4•0.75CH_2Cl_2 (0.194 g, 0.209 mmol) and $AgBF_4$ (0.0436 g, 0.224 mmol) in acetonitrile (12 mL) was heated to reflux for 20 h. The resulting orange solution was filtered through kieselguhr. 2,2'-bipyridine (bipy) (0.033 g, 0.21 mmol), dissolved in acetonitrile, was added to the filtrate and refluxing continued for a further 1 h, giving an intense orange solution. The solution was allowed to cool, followed by solvent removal *in vacuo*. Additional white precipitate was removed by filtration through kieselguhr and washed with acetonitrile, the filtrate plus washings were taken to dryness *in vacuo*. The resulting yellow residue was crystallised from dichloromethane/n-hexane. [Pt(PNCHP-κ^3*P,N,P*)(bipy)]$(BF_4)_2$ (0.141 g, 62.7 %) was isolated as orange crystals, washed with n-pentane and air-dried. M.p: 259-260 °C.

4.4.11 [Pt(PNCHP-κ^3P,N,P)(terpy)]$(BF_4)_2$

[Pt(PNCHP-κ^3*P,N,P*)(MeCN)]$(BF_4)_2$ (0.100 g, 0.105 mmol) and 2,2',6',2''-terpyridine (terpy) (0.0244 g, 0.105 mmol) were dissolved together in dichloromethane (c.a. 12 mL) and heated to reflux for c.a. 3 h. The reaction mixture was filtered and set up to vapour diffuse in n-hexane. [Pt(PNCHP-κ^3*P,N,P*)(terpy)]$(BF_4)_2$ (0.0919 g, 76.9 %) was isolated as orange crystals, washed with n-pentane and air dried. Anal. Found: C, 53.97; H, 3.50; N, 4.85. Calcd for $C_{52}H_{40}B_2F_8N_3P_2Pt$: C, 54.28; H, 3.42; N, 4.87.

4.4.12 [Pt(PNCHP-κ^3P,N,P)(PPh$_3$)]$(BF_4)_2$

A mixture of [Pt(PNCHP-κ^3*P,N,P*)Cl]BF_4•0.75CH_2Cl_2 (0.101 g, 0.108 mmol) and $AgBF_4$ (0.0226 g, 0.116 mmol) in acetonitrile (12 mL) was heated to reflux for c.a. 25 min, giving a white precipitate. PPh_3 (0.0306 g, 0.117 mmol) was added to the reaction mixture and refluxing continued for a further 30 min. This mixture was filtered through kieselguhr and the trapped yellow precipitate dissolved and washed through into the filtrate with

dichloromethane, leaving the original white precipitate behind. The filtrate solvent was evaporated *in vacuo* and the resulting yellow residue precipitated from dichloromethane/n-hexane overnight. [Pt(PNCHP-κ^3*P,N,P*)(PPh_3)](BF_4)$_2$ (0.103 g, 80.8 %) was isolated as a very pale yellow powder, washed with n-pentane and air-dried. The powder can be crystallised from a CH_2Cl_2/n-hexane vapour diffusion to yield colourless crystals. Anal. Found: C, 53.36; H, 3.80; N, 1.18. Calcd for $C_{55}H_{44}B_2F_8NP_3Pt$: C, 53.15; H, 3.66; N, 1.11.

4.4.13 [Pt(PNCHP-κ^3P,N,P)(diphos)](BF$_4$)$_2$

[Pt(PNCHP-κ^3*P,N,P*)(MeCN)](BF_4)$_2$ (0.100 g, 0.104 mmol) and bis(diphenylphosphino)ethane (diphos) (0.0420 g, 0.105 mmol) were dissolved together in dichloromethane (12 mL) and heated to reflux for 3 h. A small amount of the by-product [Pt(diphos)$_2$](BF_4)$_2$ (0.015 g, 24.5 %), as a yellow precipitate, was removed by filtration and the filtrate set up to vapour diffuse with n-hexane. [Pt(PNCHP-κ^3*P,N,P*)(diphos)](BF_4)$_2$ was isolated as a yellow powder which on exposure to air, slowly turns green. Anal. Found: C, 52.60; H, 3.79; N, 0.58. Calcd for $C_{63}H_{53}B_2F_8NP_4Pt$: C, 52.51; H, 3.86; N, 0.94.

4.4.14 The reaction of [Pt(PNCHP-κ^3P,N,P)Cl]Cl with HCl

[Pt(PNCHP-κ^3*P,N,P*)Cl]Cl (0.0498 g, 0.0611 mmol) was dissolved in dichloromethane and heated to reflux under bubbling $HCl_{(g)}$. The solution was filtered and n-hexane added to the yellow filtrate to initiate crystallisation. The product (0.0116 g, 21.4 %-based on Pt(PNCHP)Cl_4) was isolated as a yellow solid and the mass spectrum recorded (**Table 4.12**).

4.4.15 [Pd(PNCHP-κ3P,N,P)Cl]Cl•0.5CH$_2$Cl$_2$

A mixture of [Pd(COD)Cl_2] (0.100 g, 0.350 mmol) and PNCHP (0.193 g, 0.351 mmol) in benzene (12 mL) was heated to reflux for 1 h. The resulting yellow precipitate was isolated by fitration, washed with n-pentane and air dried to yield [Pd(PNCHP-κ3*P,N,P*)Cl]Cl•0.5CH_2Cl_2 (0.235 g, 86.9 %) as a yellow powder. Anal. Found: C, 58.41; H, 3.99; N, 1.78. Calcd for $C_{37}H_{29}Cl_2NP_2Pd$•0.5CH_2Cl_2: C, 58.54; H, 3.93; N, 1.82.

4.4.16 [Pd(PNCHP-κ^3P,N,P)Cl]BF_4

A mixture of [Pd(PNCHP-κ^3*P,N,P*)Cl]Cl•0.5CH_2Cl_2 (0.202 g, 0.263 mmol) and $AgBF_4$ (0.054 g, 0.277 mmol) in dichloromethane (12 mL) was exposed to ultrasound for 1 h resulting in yellow and white precipitates. This mixture was filtered through kieselguhr and the trapped yellow precipitate dissolved and washed through into the filtrate with acetonitrile, leaving the insoluble white precipitate behind. The filtrate was taken to dryness *in vacuo* and the resulting yellow residue crystallised from dichloromethane/n-hexane. [Pd(PNCHP-κ^3*P,N,P*)Cl]BF_4 (0.169 g, 82.6 %) was isolated as large yellow crystals, washed with a dichloromethane/n-pentane mixture and air-dried. Anal. Found: C, 56.68; H, 3.70; N, 1.90. Calcd for $C_{37}H_{29}BClF_4NP_2Pd$: C, 57.10; H, 3.76; N, 1.80.

4.4.17 [Pd(PNCHP-κ^3P,N,P)Me]Cl - Method A

A mixture of [Pd(COD)(Me)Cl] (0.101 g, 0.381 mmol) and PNCHP (0.208 g, 0.378 mmol) in dichloromethane (12 mL) was stirred at room temperature for 1 h, giving a yellow solution. N-hexane was added until a slight cloudiness was observed. Very pale yellow microcrystals resulted after standing overnight. These were isolated by fitration, washed with n-pentane and air dried to yield [Pd(PNCHP-κ^3*P,N,P*)Me]Cl (0.239 g, 89.4 %). Anal. Found: C, 64.30; H, 4.64; N, 2.01. Calcd for $C_{38}H_{32}ClNP_2Pd$: C, 64.60; H, 4.57; N, 1.98.

Method B

A mixture of [Pd(COD)(Me)Cl] (0.154 g, 0.581 mmol) and PNCHP (0.319 g, 0.580 mmol) in toluene (12 mL) was heated for 30 min, giving a white-tan precipitate. The solid was isolated by fitration, washed with n-pentane and air dried to yield [Pd(PNCHP-κ^3*P,N,P*)Me]Cl (0.364 g, 88.8 %) as an off-white powder.

4.4.18 [Pd(PNCHP-κ^3P,N,P)Me]BF_4 - Method A

A mixture of [Pd(PNCHP-κ^3*P,N,P*)Me]Cl (0.136 g, 0.193 mmol) and $AgBF_4$ (0.038 g, 0.195 mmol) in dichloromethane (12 mL) was exposed to ultrasound for 3 h resulting in yellow and white precipitates. This mixture was filtered through kieselguhr and the trapped yellow precipitate dissolved and washed through into the filtrate with acetonitrile, leaving the insoluble white precipitate behind. The filtrate solvent was

evaporated *in vacuo* and the resulting yellow residue crystallised from dichloromethane/n-hexane. [Pd(PNCHP-κ^3*P,N,P*)Me]BF_4 was isolated as pale yellow crystals, washed with a dichloromethane/n-pentane mixture and dried *in vacuo.*

Method B

[Pd(PNCHP-κ^3*P,N,P*)Me]Cl (164 g, 0.232 mmol) and $AgBF_4$ (0.0447 g, 0.230 mmol) were combined in dichloromethane (c.a. 12 mL) and heated to reflux for 1 h. The reaction mixture was filtered through kieselguhr. N-pentane was vapour diffused into the filtrate over a weekend. [Pd(PNCHP-κ^3*P,N,P*)Me]BF_4•0.5CH_2Cl_2 (0.114 g, 61.9 %) was isolated as pale yellow microcrystals, washed with n-pentane and dried *in vacuo.* Anal. Found: C, 58.15; H, 4.18; N, 1.83. Calcd for $C_{38}H_{32}BF_4NP_2Pd$•0.5CH_2Cl_2: C, 58.17; H, 4.18; N, 1.76.

4.4.19 The reaction of [Pd(PNCHP-κ^3P,N,P)Me]BF_4.0.5CH_2Cl_2 with CO (7 atm)

[Pd(PNCHP-κ^3*P,N,P*)Me]BF_4.0.5CH_2Cl_2 (0.030 g, 0.037 mmol) was dissolved in d^2-dichloromethane (c.a. 4 mL) and stirred at room temperature, overnight under 7 atmospheres of carbonmonoxide. After work-up the starting material was recovered, there being no reaction with CO.

5 The Rhodium Complexes

5.1 Introduction

5.1.1 A brief overview of rhodium(I) chemistry

A major aspect of the chemistry of rhodium(I) is the formation of tertiary phosphane complexes.[1] Of these, complexes of the type $[RhXL_3]$, inspired by Wilkinson's catalyst, are the most populous class. In this case, L is a neutral ligand and usually possesses some π-bonding capacity and X can be virtually any uninegative ion, however, anions of low coordinating power do not form complexes of this stoichiometry and structure. All are sixteen electron compounds and are formally coordinatively unsaturated.[2] There are few ionic $[RhL_3]X$ complexes apart from the case where $X = ClO_4$.[3]

Five-coordinate rhodium(I) species are commonly produced by addition of neutral ligands to four-coordinate species.[4] They are also the intermediates in substitution reactions of square planar rhodium(I) complexes, which are often rapid and proceed by an associative pathway.[5]

Generally, the rhodium(I) chemistry of polydentate ligands is similar to the monodentate case discussed above. In addition, polydentate ligands have been shown to:

(i) Offer a more predictable coordination number and stoichiometry, as the chelate effect minimises the tendency of one or more phosphane groups to be displaced during a chemical reaction.

---

[1] F. A. Cotton, G. Wilkinson, C. A. Murillo and M. Bochmann, *Advanced Inorganic Chemistry* (Sixth Edition), 1999, John Wiley & Sons, Inc, New York, p1044

[2] *Comprehensive Coordination Chemistry*, G. Wilkinson (Editor-in Chief), Volume 4, 1987, Pergamon Press, Oxford, p913

[3] R. Bau, S. L. Miles, C. A. Reed and Y. W. Yared, *J. Am. Chem. Soc.*, 1977, **99**, 7076.

[4] See ref. 1, p1041

[5] See ref. 1 p1041-1042

(ii) Increase the basicity of the rhodium atom.

(iii) Allow more control on the stereochemistry of the complexes.

(iv) Impart detailed structural and bonding information in the form of metal-phosphorus and phosphorus-phosphorus coupling constants, e.g. in the case of polydentate phosphanes.[6,7]

For example, the linear tridentate phosphane ligand $PhP(CH_2CH_2CH_2PPh_2)_2$ has been found to endow its rhodium(I) complexes with much stronger nucleophilic characteristics then its *tris*-(triarylphosphine) monodentate counterparts, thereby reacting readily with neutral and cationic acids to yield stable five-coordinate intermediates.[8]

5.1.2 A brief overview of rhodium(III) chemistry

Most of the rhodium(I) square planar complexes undergo oxidative addition reactions yielding octahedral rhodium(III) complexes.[9] The most populous class are the $[RhX_3L_3]$ species, where meridional isomers are normally the rule.[10]

The oxidative addition of carbon halides to low valent metal complexes is of paramount interest. It is a key step in a number of industrially important catalytic processes, such as, carbonylation of methanol to acetic acid, cross coupling and carbonylation reactions. It has been found that for oxidative additions of carbon halide substrates to complexes of rhodium(I) (and iridium(I)), the additions are generally enhanced by increasing the electron density on the metal atom. The activation of dichloromethane requires relatively strong donor ligands, for example, the ligand *bis*-(dimethylphosphino)ethane in the complex $[Rh\{Me_2PCH_2CH_2PMe_2\}_2]Cl$.[11] Coordination of ligands with three or four nitrogen donor atoms to rhodium(I) also gives strong

[6] T. E. Nappier, Jr., D. W. Meek, R. M. Kirchner and J. A. Ibers, *J. Am. Chem. Soc.*, 1973, **95**, 4194.
[7] D. W. Meek, J. L. Peterson and J. A. Tiethof, *Inorg. Chem.*, 1976, **15**, 1365.
[8] P. Blum, G. G. Christoph, A. Elia, W.-C. Liu and D. W. Meek, *Inorg. Chem.*, 1979, **18**, 894.
[9] See ref. 1, p1042
[10] See ref. 2, p1028
[11] J. M. Ernsting, H. F. Haarman, M. Kranenburg, H. Kooijman, A. L. Speck, P. W. N. M. van Leeuwen N. Veldman and K. Vrieze, *Organometallics*, 1997, **16**, 887, and refs within

nucleophilic species that can activate dichloromethane.[11,12] Whilst the arylphosphane moieties of the PNCHP ligand are less basic than the alklyphosphane ligands employed to activate carbon halides, the nitrogen donor in combination with the chelating abilities of the ligand should increase the basicity of the rhodium atom.

5.1.3 The rhodium complexes of $PNHCH_2P$

A small number of rhodium(I) complexes containing the ligand **$PNHCH_2P$**, a ligand similar and related to PNCHP, have been synthesised by Edwards.[13] The complexes are depicted in **Figure 5.1**. The $PNHCH_2P$ ligand was obtained by a reduction of the imino group of PNCHP to a secondary amine using $LiAlH_4$. The compound $[Rh(CO)(PNHCH_2P\text{-}\kappa^3P,N,P)]PF_6$ (**F.5.1-1**) was synthesised by reacting the $PNHCH_2P$ ligand with $[NBu_4^n][Rh(CO)_2Cl_2]$ in the presence of excess NH_4PF_6. The triphenylphosphane analogue $[Rh(PPh_3)(PNCH_2P\text{-}\kappa^3P,N,P)]PF_6$ (**F.5.1-2**) was synthesised from $[Rh(solvent)_2(PPh_3)_2](PF_6)$, formed *in situ*, then addition of $PNHCH_2P$. Unexpectedly, the reaction of $PNHCH_2P$ with $[Rh(COD)Cl]_2$ did not give $[RhCl(PNCH_2P\text{-}\kappa^3P,N,P)]$, but, the five-coordinate $[Rh(COD)(PNHCH_2P\text{-}\kappa^3P,N,P)]Cl$ (**F.5.1-3**) compound instead.

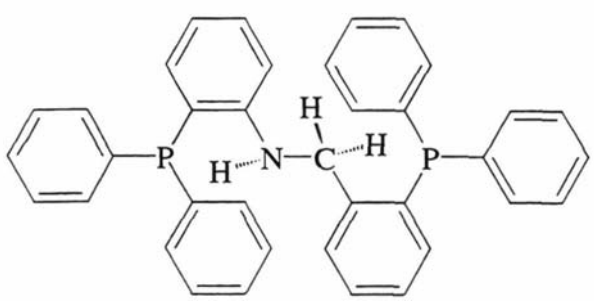

$PNHCH_2P$

[12] J. C. Calabrese, W. C. Fultz, R. L. Harlow, T. B. Marder and D. Milstein, *J. Chem. Soc., Chem. Commun.*, 1987, 1543.
[13] M. L. Edwards, *Rhodium(I) Complexes of a Tridentate Hybrid Phosphine-amine ligand: Catalytic Implications of Trans-Phosphorus Geometry*, 1984, BSc(Hons) Thesis, University of Sydney.

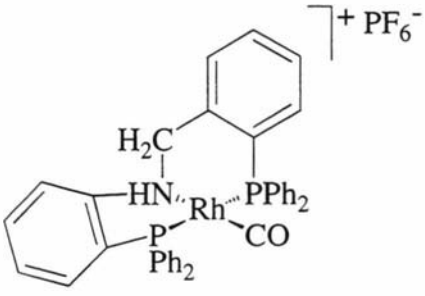

F.5.1-1

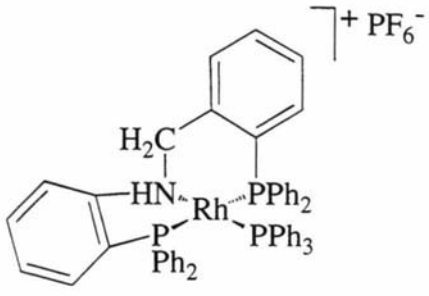

F.5.1-2

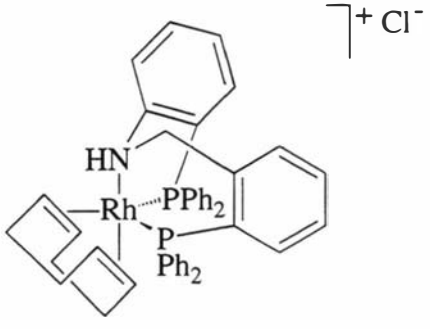

F.5.1-3

Figure 5.1 The rhodium(I) complexes of the 'P_2N' ligand $PNHCH_2P$

5.1.4 Other rhodium complexes containing 'P_2N' ligands

The 'P_2N' ligand 2,6-bis(diphenylphosphanylmethyl)pyridine (**PNP**) has played a key role in model studies aimed at elucidating the reaction mechanism of the rhodium complex-catalysed hydroamination of ethylene.[14,15,16]

[14] C. Hahn, E. Herdtweck, M. Spiegler and R. Taube, *Eur. J. Inorg. Chem.*, 1999, 435.
[15] C. Hahn, J. Sieler and R. Taube, *Polyhedron*, 1998, **17**, 1183.
[16] Hahn, E. Herdtweck, M. Spiegler and R. Taube, *Eur. J. Inorg. Chem.*, 1998, 1425.

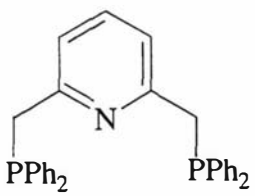

PNP

The added versatility of coordination modes displayed by 'P_2N' ligands is illustrated by the ligand 2-(bis(diphenylphosphino)methyl)pyridine (**S.5.1-1**),[17] as shown by **Scheme 5.1**. In the complex [Rh(nbd)(**S.5.1-1**-κ^3*P,N,P*)]PF_6 (**S.5.1-2**) the ligand **S.5.1-1** is terdentate, but on reacting with CO, the dimer $[Rh_2(CO)_2$(**S.5.1-1**)$](PF_6)_2$ (**S.5.1-3**) is obtained, where **S.5.1-1** is now bridging two rhodium atoms. Addition of Cl^- to the dimer results in the compound [RhCl(CO)(**S.5.1-1**-κ^2*P,N*)] (**S.5.1-4**), which has a bidentate **S.5.1-1** ligand.[18]

[17] M. P. Anderson, B. M. Mattson and Louis H. Pignolet, *Inorg. Chem.*, 1983, **22**, 2644.
[18] M. P. Anderson, C. C. Tso, B. M. Mattson and L. H. Pignolet, *Inorg. Chem.* 1983, **22**, 3267.

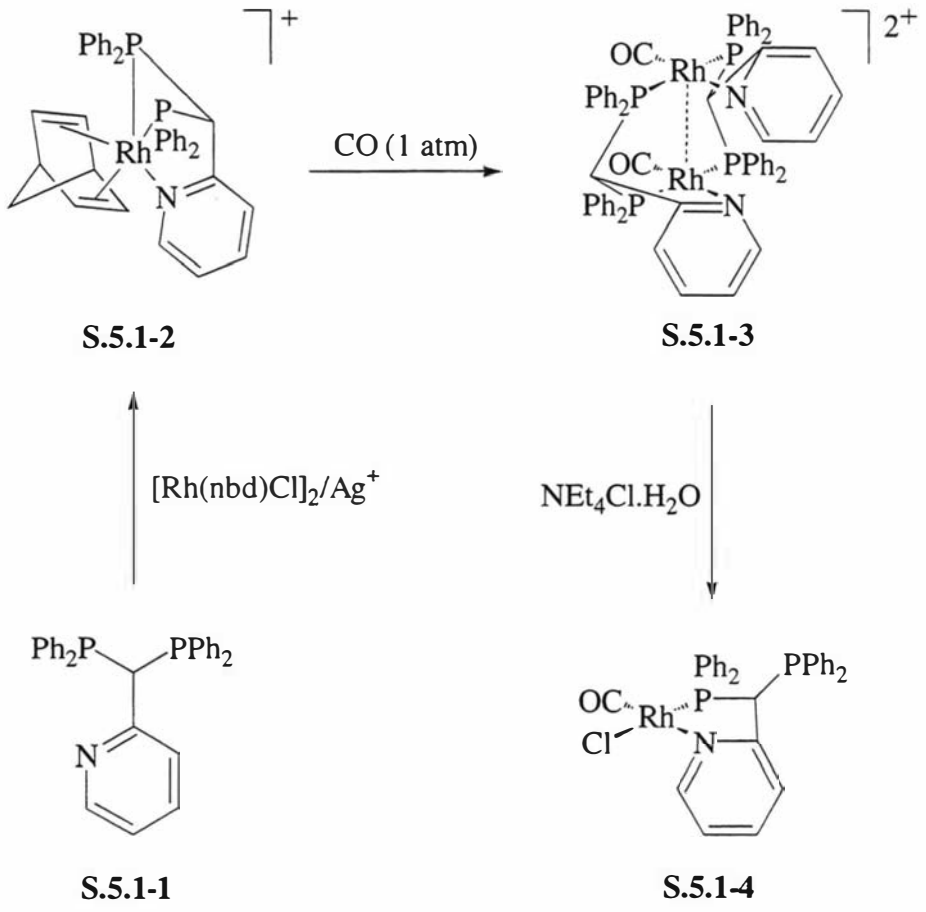

S.5.1-2 **S.5.1-3**

S.5.1-1 **S.5.1-4**

Scheme 5.1 A reaction scheme displaying the coordination mode versatility of the 'P_2N' ligand 2-(bis(diphenylphosphino)methyl)pyridine

The 'P_2N' ligands **F.5.2-1** and **F.5.2-2**, L, react with [{RhCl(COD)}$_2$] to give more common complexes of type [RhCl(L)] (**F.5.2-3**), as shown in **Figure 5.2**.[19]

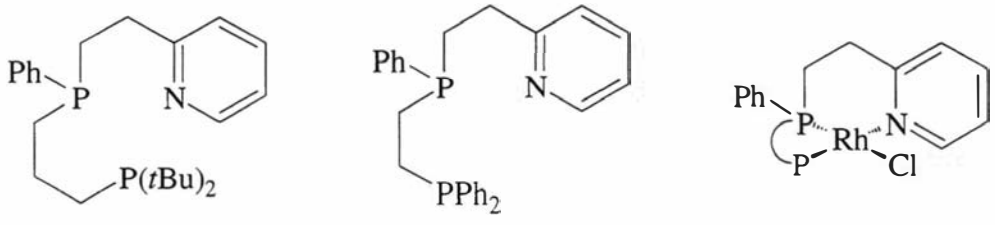

F.5.2-1 **F.5.2-2** **F.5.2-3**

Figure 5.2 Some 'P_2N' ligands and their rhodium(I) complexes

[19] A. Heβler, J. Fischer, S. Kucken and O. Stelzer, *Chem. Ber.*, 1994, **127**, 481.

The ligand α,α'-bis(bis-(2-(diphenylphosphino)ethyl)amino)-*m*-xylene (**F.5.2-1**) can be viewed as two 'P_2N' type ligands linked together. This thinking is justified, as the rhodium complexes of (**F.5.2-1**) are mirrored in each half of the ligand. Reaction of $[\{Rh(COD)Cl\}_2]$ with (**F.5.3-1**) forms the complex $[Rh_2$(**F.5.2-1**)$Cl_2]$ (**F.5.2-2**). Addition of CO to (**F.5.2-2**) gives complex $[Rh_2$(**F.5.2-1**)$Cl_2(CO)_2]$ (**F.5.2-3**), where each rhodium is five-coordinate.[20]

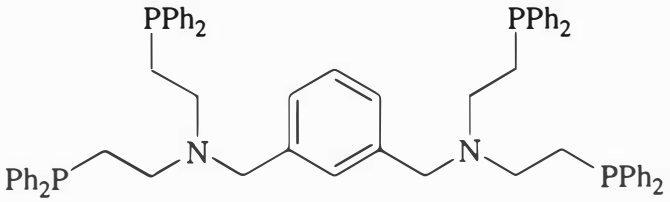

F.5.2-1

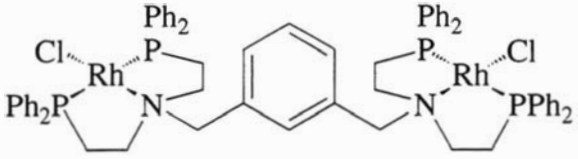

F.5.2-2

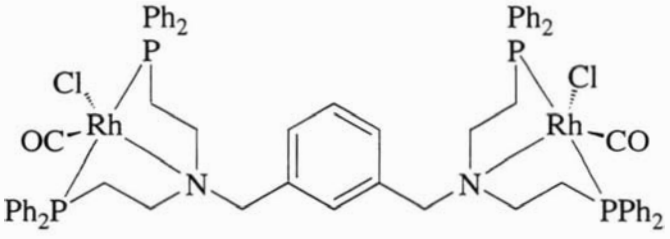

F.5.2-3

Figure 5.2 A 'P_4N_2' ligand behaving as two 'P_2N' ligands with respect to its rhodium(I) complexes

[20] P. Paul and B. Tyagi, *Polyhedron*, 1996, **15**, 675.

5.1.5 The present study

The coordination chemistry of the PNCHP ligand with rhodium(I) will be presented. Addition, substitution, and oxidative addition reactions on the resulting rhodium(I) complexes will be discussed. The chemistry will be compared and contrasted to relevant rhodium(I) species in the literature.

5.2 Results and discussion

5.2.1 Synthesis

Synthesis of the compounds is shown by **Scheme 5.2**. All the compounds were fully characterised apart from **S.5.2-2**, **S.5.2-3**, **S.5.2-4**, **S.5.2-6**, **S.5.2-7**, **S.5.2-8** and **S.5.2-11**, which were only characterised spectroscopically or, in the case of **S.5.2-6**, by a single-crystal X-ray diffraction experiment. All syntheses and manipulations of the rhodium complexes were carried out in an inert atmosphere box/or using standard Schlenk techniques due to their air-sensitive nature. The dark green (λ_{max} = 651 nm, ε_{max} = 2500 $M^{-1}cm^{-1}$) parent complex [RhCl(PNCHP-κ^3*P,N,P*)] (**S.5.2-1**) is prepared by the reacting two equivalents of the PNCHP ligand with the chloro-bridged dimer [{Rh(COD)Cl}$_2$] in benzene. An extremely interesting contrast to the synthesis of [RhCl(PNCHP-κ^3*P,N,P*)] is the attempted synthesis of the analogue [RhCl(PNHCH$_2$P-κ^3*P,N,P*)] by Edwards[13] (where PNHCH$_2$P is PNCHP with the imine functional group reduced to a secondary amine). In this case, when [{Rh(COD)Cl}$_2$] is reacted with PNHCH$_2$P, the five-coordinate compound [Rh(COD)(PNHCH$_2$P-κ^3*P,N,P*)]Cl (**F.5.1-3**) results.[13] In **F.5.1-3**, the PNHCH$_2$P ligand adopts a *facial* geometry. It is now known, that the PNCHP ligand prefers a *meridional* geometry, as discussed in section *2.2.1* of Chapter 2, hence, the PNCHP analogue of **F.5.1-3** would be expected to be unstable. The ligand PNHCH$_2$P has been observed in a *meridional* geometry with palladium(II) and platinum(II) metals.[21]

[21] P. A. Duckworth, *Polydentate Phosphorus-Nitrogen Hybrid Ligands Containing the 2-Aminophenyl Group*, 1984, Ph.D. Thesis, University of Sydney.

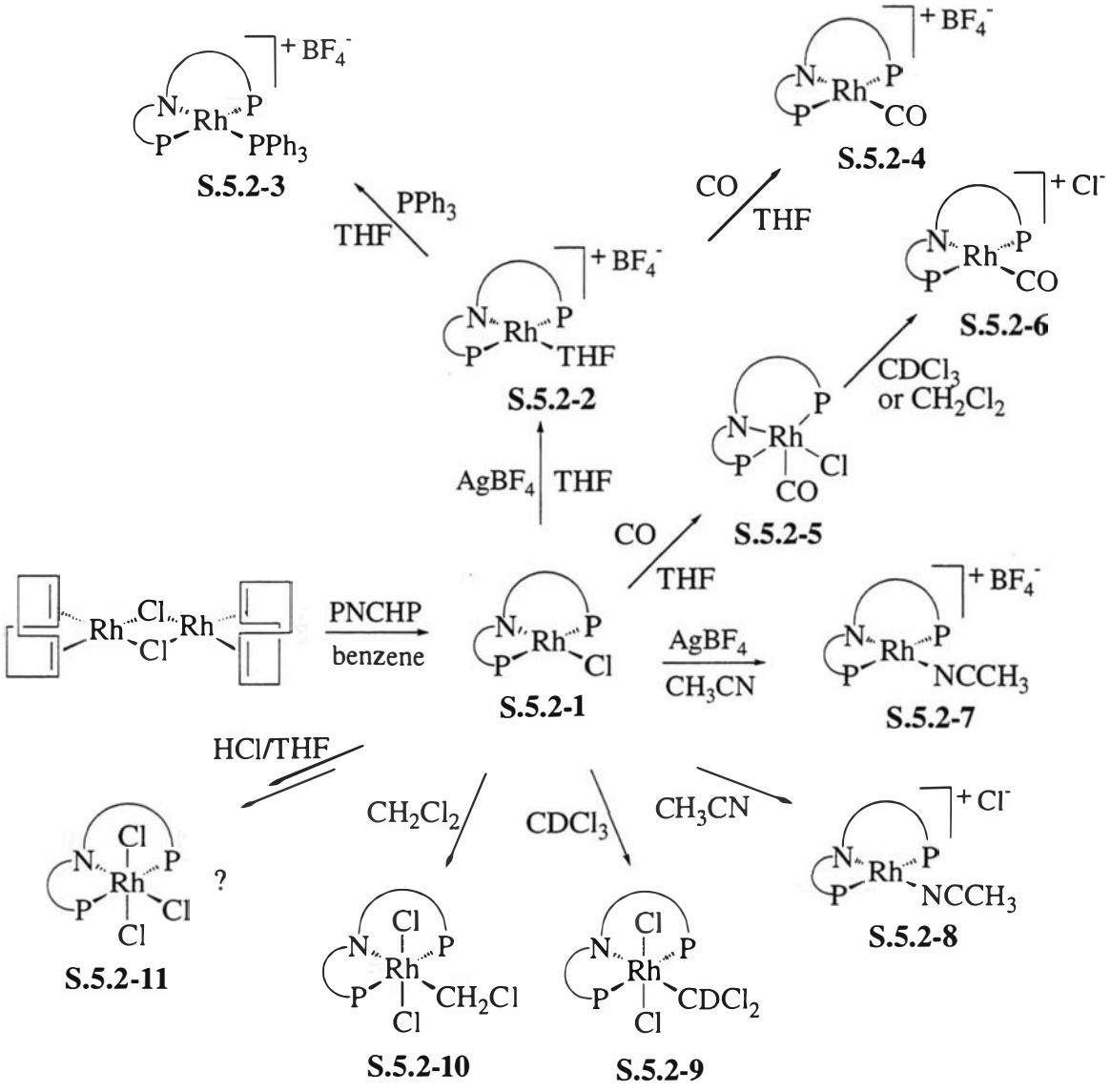

Legend to Scheme 5.2

PNCHP = P N P

Scheme 5.2 Synthetic routes to the rhodium complexes of PNCHP

The [RhCl(PNCHP-κ^3*P,N,P*)] complex readily undergoes oxidative addition reactions and can also readily add additional small neutral ligands to form five coordinate species, both detailed below. The dark-green solution of the complex [RhCl(PNCHP-κ^3*P,N,P*)] turns brown-orange almost instantaneously when exposed to air. The colour change also occurs in the solid state but requires several hours to go to completion. One of the products identified is formulated as $[RhCl(PNCHP)O_2]_2$, as identified by mass spectroscopy. This is in stark contrast to the similar compound [RhCl(PhP($CH_2CH_2CH_2PPh_2$)$_2$-κ^3*P,P,P*)] (**F.5.3-1**), shown in **Figure 5.3**, which is stable indefinitely in air. This difference is most likely solely due to the presence of a nitrogen donor atom in the former, which has the effect of increasing the electron density of the metal, hence, increases the metals susceptibility to oxidative addition of O_2 and/or H_2O.

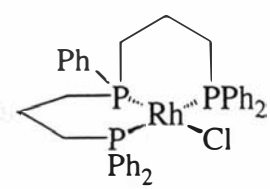

F.5.3-1

Figure 5.3 A 'P_3' analogue of the complex **S.5.2-1** in **Scheme 5.2**

[RhCl(PNCHP-κ^3*P,N,P*)] reacts with CO to give the neutral, five-coordinate, compound [Rh(CO)Cl(PNCHP-κ^3*P,N,P*)] (**S.5.2-5**), as a dark-green precipitate. On dissolving the precipitate, the ionic, four-coordinate compound [Rh(CO)(PNCHP-κ^3*P,N,P*)]Cl (**S.5.2-6**) is obtained as orange crystals. Its identity was confirmed by an X-ray study. In solution, the two carbonyl compounds exist as an equilibrium mixture, with the ionic compound heavily favoured, as discussed in sections *5.2.3* and *5.2.5*. The air-sensitivity of the complex [Rh(CO)(PNCHP-κ^3*P,N,P*)]$^+$ is dramatically diminished compared to the parent complex [RhCl(PNCHP-κ^3*P,N,P*)], with estimated half-lives in solution of several days and several seconds, respectively. The difference in reactivity can be rationalised by the relative 'electron richness' of the metal centres, for example, the CO ligands π-acid features enable it to shift electron density from the rhodium, thereby decreasing the metals nucleophilcity, and hence reactivity towards dioxygen.

Acetonitrile (MeCN) will substitute for the chloride of [RhCl(PNCHP-κ^3*P,N,P*)], with or without the aid of $AgBF_4$, to give the brown-orange cationic complex [Rh(MeCN)(PNCHP-κ^3*P,N,P*)]$^+$ (**S.5.2-7**) and (**S.5.2-8**), respectively. However, the reaction produces considerably less side products with $AgBF_4$ present to assist the removal of the chloride ion. [Rh(MeCN)(PNCHP-κ^3*P,N,P*)]BF_4 was initially made with a view to synthesising the complex [Rh(PPh_3)(PNCHP-κ^3*P,N,P*)]$^+$, as the attempted direct substitution of the chloride of [RhCl(PNCHP-κ^3*P,N,P*)] with PPh_3 resulted in numerous unidentified products as determined by ^{31}P NMR spectroscopy. Unfortunately, substitution of the MeCN by PPh_3 produced only marginally fewer reaction products. However, the desired [Rh(PPh_3)(PNCHP-κ^3*P,N,P*)]$^+$ (**S.5.2-3**) can be obtained as the sole product via the dark-red compound [Rh(THF)(PNCHP-κ^3*P,N,P*)]BF_4 (**S.5.2-2**), prepared by reacting [RhCl(PNCHP-κ^3*P,N,P*)] with $AgBF_4$ in THF. Unlike MeCN, THF will not displace the chloride from [RhCl(PNCHP-κ^3*P,N,P*)] without $AgBF_4$ present.

The parent compound [RhCl(PNCHP-κ^3*P,N,P*)] was proven not only to be extremely reactive with O_2 in air but with common halogenated solvents as well. When [RhCl(PNCHP-κ^3*P,N,P*)] is dissolved in $CDCl_3$ or CH_2Cl_2 the yellow oxidative-addition products [Rh($CDCl_2$)Cl_2(PNCHP)] (**S.5.2-9**) and [Rh(CH_2Cl)Cl_2(PNCHP)] (**S.5.2-10**) are obtained, respectively. The propensity of the rhodium atom to oxidatively add halogenated solvents is again likely due to the presence of the N donor atom of the PNCHP ligand, which has the effect of increasing the nucleophilicity of the metal. This point can be illustrated by comparing the reactivities of [RhCl(PhP($CH_2CH_2CH_2PPh_2$)$_2$-κ^3*P,P,P*)], containing a 'P_3' ligand,[22] and [RhCl(2,6-(C(R^1)=NR^2)$_2$$C_5H_3N$)$_2$-$\kappa^3$*N,N,N*)], where R^1 and R^2 are various alkyl groups, containing a 'N_3' ligand.[11] The 'P_3' complex shows no reported evidence of reacting with CH_2Cl_2, whilst the 'N_3' complex reacts in seconds. As expected, the PNCHP ('P_2N') complex lies between these two extremes, requiring a few hours for the reaction to go to completion.

The product of the reaction between [RhCl(PNCHP-κ^3*P,N,P*)] and excess HCl is tentatively formulated as $RhCl_3$(PNCHP). The formation of this compound proceeds *via* an intermediate, as observed by NMR. Rhodium(I)-phosphine complexes have been observed to form hydrido species on reacting with HCl,[22] however, there was no evidence for a hydrido intermediate in the reaction of [RhCl(PNCHP-κ^3*P,N,P*)].

5.2.2 Crystal structure of [Rh(CO)(PNCHP-κ^3P,N,P)]Cl

The cation [Rh(CO)(PNCHP-κ^3*P,N,P*)]$^+$ is shown in **Figure 5.4**, with crystal data and structure refinement details given in **Table 5.1** and bond lengths and angles given in **Table 5.2.** The cation has imposed mirror symmetry, with the N(1)-Rh-C(100)-O(100) group lying on the mirror plane. Further, the N(1) atom is disordered over two unresolved sites, hence, bond lengths and angles involving the N(1) atom will not be compared. The geometry of the coordination polyhedron about the rhodium atom is approximately square planar. The PNCHP ligand occupies three of the coordination sites by bonding through the two phosphorus atoms (P(2) and P(2)') and the one nitrogen atom (N(1)) with the fourth site occupied by a carbon monoxide ligand (C(100)-O(100)). Rh(1)-P(2) (2.2863(11) Å), Rh(1)-CO (1.824(8) Å), Rh(1)-N(1) (2.084(7) Å) and C-O (1.122(11) Å distances are similar to other rhodium(I)-monocarbonyl cations with mixed P and N donor sets.[18,23] The bond angle P(2)-Rh-P(2)' (168.31(7) °) shows a significant deviation from the 180 ° expected for an ideal square-planar geometry. In contrast, the C-Rh(1)-N(1) bond angle is 180.000(2) °.

[22] J. Ibers, R. M. Kirchner, D. W. Meek and T. E. Nappier, Jr., *J. Am. Chem. Soc.*, 1973, **95**, 4194.
[23] A. Heβler, J. Fischer, S. Kucken and O. Stelzer, *Chem. Ber.*, 1994, **127**, 481.

Table 5.1

Crystal data and structure refinement for [Rh(CO)(PNCHP-κ^3*P,N,P*)]Cl.

Identification code	sk16a
Empirical formula	C38 H31 Cl N O P2 Rh
Formula weight	717.94
Temperature	200(2) K
Wavelength	0.71073 Å
Crystal system	Monoclinic
Space group	C2/c
Unit cell dimensions	a = 20.09360(10) Å α = 90°.
	b = 19.38590(10) Å β = 92.2270(10)°.
	c = 8.94180(10) Å γ = 90°.
Volume	3480.49(5) Å^3
Z	4
Density (calculated)	1.370 Mg/m^3
Absorption coefficient	0.689 mm^{-1}
F(000)	1464
Crystal size	0.42 x 0.19 x 0.17 mm^3
Theta range for data collection	1.46 to 27.46°.
Index ranges	-24<=h<=25, -21<=k<=24, -10<=l<=11
Reflections collected	10561
Independent reflections	3804 [R(int) = 0.0227]
Completeness to theta = 0.50°	0.0 %
Absorption correction	Semi-empirical from equivalents
Max. and min. transmission	0.8918 and 0.7606
Refinement method	Full-matrix least-squares on F^2
Data / restraints / parameters	3804 / 0 / 192
Goodness-of-fit on F^2	1.119
Final R indices [I>2sigma(I)]	R1 = 0.0571, wR2 = 0.1833
R indices (all data)	R1 = 0.0631, wR2 = 0.1901
Largest diff. peak and hole	2.029 and -0.528 e.Å^{-3}

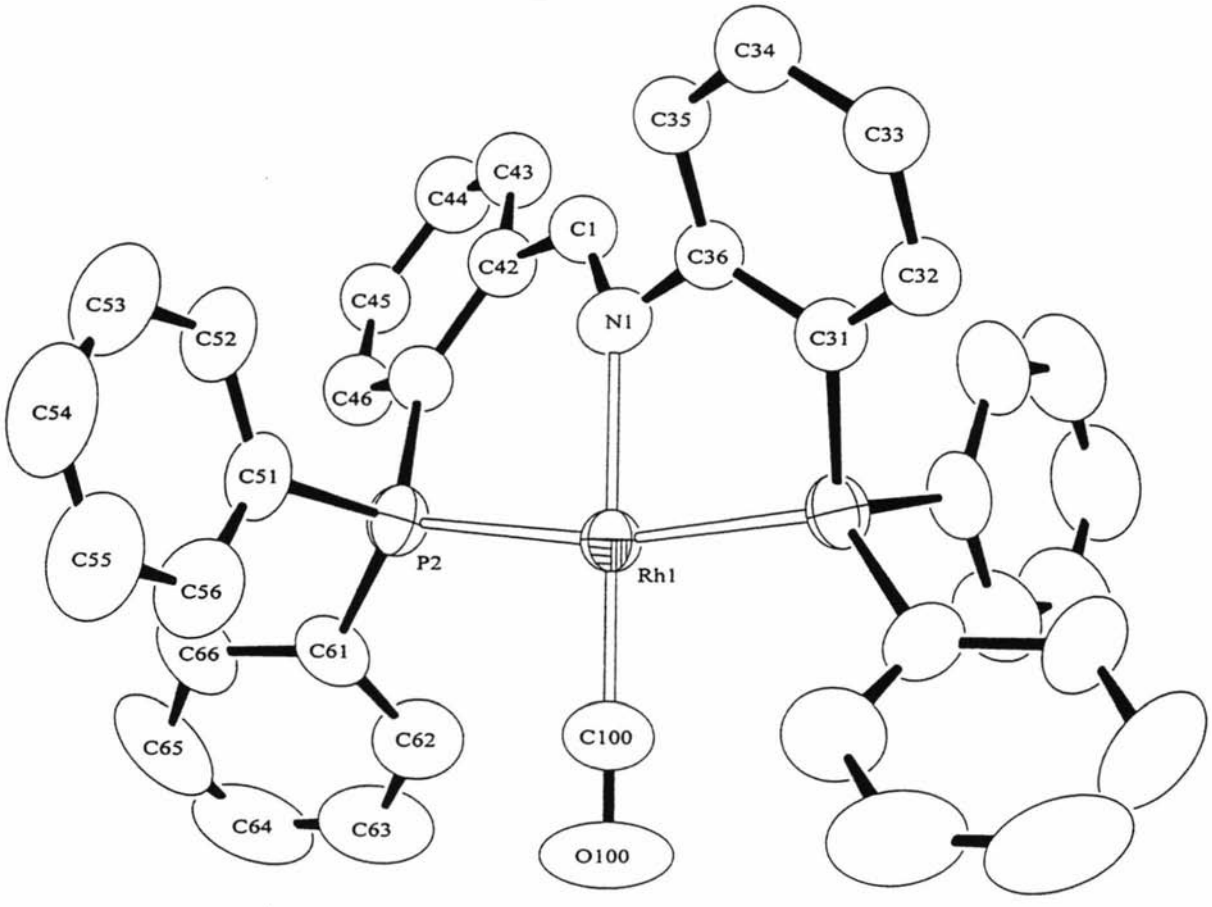

Figure 5.4 ORTEP diagram for the cation [Rh(CO)(PNCHP-κ^3*P,N,P*)]$^+$ showing the numbering system used. Thermal ellipsoids are at the 50% probability level. Hydrogen atoms have been omitted for clarity

Table 5.2

Selected bond lengths (Å) and angles (°) for [Rh(CO)(PNCHP-κ^3*P,N,P*)]Cl with estimated standard deviations in parentheses

Bond lengths:			
Rh(1)-P(2)	2.2863(11)	P(2)-C(61)	1.808(5)
Rh(1)-N(1)	2.084(7)	N(1)-C(36)	1.781(4)
Rh(1)-C(100)	1.824(8)	N(1)-C(1)	1.106(10)
C(100)-O(100)	1.122(11)	C(1)-C(42)	1.454(15)
P(2)-C(31)'	1.808(17)	C(42)-C(31)'	1.43(2)
P(2)-C(51)	1.815(5)	C(36)-C(31)	1.39
Bond angles:			
P(2)-Rh(1)-P(2)'	168.31(7)	Rh(1)-P(2)-C(61)	122.47(18)
N(1)-Rh(1)-C(100)	180.000(2)	Rh(1)-N(1)-C(1)	149.7(5)
P(2)-Rh(1)-N(1)	84.16(3)	Rh(1)-N(1)-C(36)	103.7(3)
Rh(1)-P(2)-C(31)'	103.8(4)	C(1)-N(1)-C(36)	106.6(7)
Rh(1)-P(2)-C(51)	110.22(15)	N(1)-C(1)-C(42)	114.0(8)

5.2.3 ^{31}P NMR spectroscopy

The parent compound [RhCl(PNCHP-κ^3*P,N,P*)] exhibits an ABX type spectrum resulting from mutual coupling of the two inequivalent phosphorus nuclei, at δ32.0 and 27.1, of the PNCHP ligand, and a phosphorus coupling to the ^{103}Rh (100 %) nucleus having S = ½. The coupling constant ^2J(P,P) is 408 Hz and the coupling constant ^1J(P,Rh) is 142 and 148 Hz, respectively. The coupling constants and chemical shifts are typical of other complexes with nitrogen/phosphorus donor atoms, where phosphorus atoms of PPh_2 are *trans* to each other.[24]

Substitution of the chloride in [RhCl(PNCHP-κ^3*P,N,P*)] for carbon monoxide (CO) or triphenylphosphane (PPh_3) results in a large shift of at least 12 ppm to higher frequency for one of the PNCHP phosphorus nuclei, the other shifting relatively little. The higher

[24] P. Paul and B. Tyagi, *Polyhedron*, 1996, **15**, 675, and refs within.

frequency signal is most likely caused by the phosphorus atom involved in the five-membered chelate ring due to the ring contribution (ΔR) effect.[25,26] The closely related complexes [Rh(CO)(PNHCH$_2$P-κ^3*P,N,P*)]$^+$ and [Rh(PPh$_3$)(PNHCH$_2$P-κ^3*P,N,P*)]$^+$, where PNHCH$_2$P is PNCHP with the imine functional group reduced to a secondary amine, have similar spectroscopic properties to the PNCHP compounds above.[13] This is to be expected, as the greatest influence on the spectral properties of the phosphorus nuclei is exerted by the *trans* ligand, all other things being equal, which has not changed. Comparison of the chloride and tetrafluoroborate salts of [Rh(CO)(PNCHP-κ^3*P,N,P*)]$^+$ show virtually no differences, indicating that at ambient temperatures the chloride remains ionic in solution as it does in the solid state. However, a trace of a second species in the spectrum of the chloride salt (which is unresolved due to its presence in small concentration and partial spectral overlap with the major species) supports the presence of an equilibrium between the four-coordinate [Rh(CO)(PNCHP-κ^3*P,N,P*)]Cl and the five-coordinate [Rh(CO)(PNCHP-κ^3*P,N,P*)Cl], which is discussed in full in section *5.2.5*.

The products of the reactions between [RhCl(PNCHP-κ^3*P,N,P*)] and HCl, $CDCl_3$ or CH_2Cl_2, display a relatively large increase in the ^{2}J(P,P) coupling constant and a large reduction of the ^{1}J(P,Rh) coupling constant. This feature is indicative of a increase in the rhodium oxidation state from +1 to +3.[27] Chemical shifts and the ^{2}J(P,P) coupling constants of the products point to the two phosphorus atoms of PNCHP coordinated in a *transiod* arrangement with the nitrogen atom also bound.

[25] S. Berger, S. Braun and H-O. Kalinowski, *NMR Spectroscopy of the Non-Metallic Elements*, 1997, John Wiley & Sons Ltd, Chichester, p837.
[26] G. Dyer and J. Roscoe, *Inorg. Chem.*, 1996, **35**, 4098, and refs. within.
[27] Multi J. Mason (Editor), *Multinuclear NMR*, 1987, Plenium Press, New York, p394.

Table 5.3

^{31}P-NMR data for selected compounds[a]

Compound[i]	δ_{PNCHP}		^2J(P,P)/Hz	^1J(RhP)/Hz	
	P_a	P_b		P_a	P_b
[RhCl(PNCHP)]	32.0	27.1	408	142	148
[RhCl(PNCHP)][b]	33.6	27.3	390	144	144
[Rh(PNCHP)(CO)]Cl	44.4	31.5	283	123	127
[Rh(PNCHP)(MeCN)]Cl[b]	36.6	30.7	331	138	138
[Rh(PNCHP)(CO)]BF_4[c]	44.5	32.0	281	123	126
[Rh(PNCHP)(MeCN)]BF_4[b]	36.6	30.8	331	138	138
[Rh(PNCHP)(THF)]BF_4[c]	33.6	29.7	338	146	148
[Rh(PNCHP)(PPh_3)]BF_4[c]	44.3	32.6	296	143	138
	47.1[h]		41, 32	164	
[Rh(PNCHP)Cl] + HCl[c,e]	43.6	35.6	487	103	103
[Rh(PNCHP)Cl] + HCl[c,f]	34.8	25.4	586,592	88	88
[Rh(PNCHP)Cl] + $CDCl_3$	28.4	26.9	[g]	59	60
[Rh(PNCHP)(CH_2Cl)Cl_2][d]	40.2	27.3	505	101	103

[a] Recorded at 109 MHz, chemical shifts are in ppm relative to 85% H_3PO_4, solvent $CDCl_3$, unless stated otherwise. [b] In CH_3CN. [c] In THF. [d] In CH_2Cl_2. [e] Spectrum recorded immediately after initial exposure to HCl. [f] Spectrum recorded after 15 min exposure to HCl. [g] Not resolved. [h] Rh-PPh$_3$. [i] For all the compounds, the PNCHP ligand was coordinated in a κ^3*P,N,P* fashion.

5.2.4 ^{1}H NMR spectroscopy

^{1}H NMR data are given in **Table 5.4**. Assignments of the imino proton and ancillary ligand protons were made only, as the aromatic protons were generally poorly resolved. The chemical shifts for the imino proton ranged from δ10.25, as found for [Rh(CO)(PNCHP-κ^3*P,N,P*)]Cl, to below δ7.44 (a search form +7.44 ppm to +30 ppm revealed no imino proton) as found for [RhCl(PNCHP-κ^3*P,N,P*)]. The imino proton was observed as a doublet for all the compounds except for the product of the reaction between [RhCl(PNCHP-κ^3*P,N,P*)] and $CDCl_3$, where it was observed as a singlet. The imino proton splitting was assigned to coupling with the spin ½, ^{103}Rh nucleus (100%). The ^3J(Rh,H) coupling constants ranged from 2.1, as found for [Rh(CO)(PNCHP-κ^3*P,N,P*)]Cl, to 3.7 Hz,

as found for [Rh(MeCN)(PNCHP-κ^3P,N,P)]BF_4. Chemical shifts and coupling constants showed no trends when comparing the rhodium(I) compounds with those of rhodium(III). The compound [Rh(MeCN)(PNCHP-κ^3P,N,P)]BF_4also reacts with $CDCl_3$. but gives several unidentified products.

The complex [Rh(MeCN)(PNCHP-κ^3P,N,P)]BF_4 displays a singlet at δ2.25, with the area under the peak measuring 3H, hence the signal was assigned to the methyl group of the coordinated acetonitrile ligand.[28] Two signals, at δ3.85 and 3.46, with multiple splitting, are exhibited by the complex [$RhCl_2(CH_2Cl)$(PNCHP-κ^3P,N,P)]BF_4. Each of these signals has been assigned to one of the -$C\underline{H}_2Cl$ protons. The chemical shift is similar to other Rh(III)-CH_2Cl complexes,[29,30] however in those cases, the methylene protons were equivalent.

Table 5.4

^{1}H-NMR data for selected compounds[a]

Compound	δ(N=CH)	^3J(RhH)/Hz	
[RhCl(PNCHP)][b]	[c]		
[Rh(PNCHP)(CO)]Cl	10.25(d)	2.1	
[Rh(PNCHP)(CO)]BF_4	9.10(d)	2.1	
[Rh(PNCHP)(MeCN)]BF_4[b]	8.49(d)	3.7	2.25(s), 3H, Rh-NCC$\underline{H}_3$
[Rh(PNCHP)Cl] + HCl[d]	8.68(d)	2.6	
[Rh(PNCHP)Cl] + HCl[e]	[c]		
[Rh(PNCHP)Cl] + $CDCl_3$	8.73(s)		
[Rh(PNCHP)(CH_2Cl)Cl_2]	8.78(d)	3.2	3.85(m), 1H, Rh-C$\underline{H}_2$Cl 3.46(m), 1H, Rh-C$\underline{H}_2$Cl

[a] Recorded at 270 MHz, chemical shifts are in ppm relative to $Si(CH_3)_4$, solvent $CDCl_3$ unless otherwise stated. [b] In C_6D_6. [c] Unable to assigned due to low solubility. [d] Reacted with HCl gas for several seconds. [e] Reacted with HCl gas for several minutes. s = singlet, d = doublet, m = multiplet.

[28] C. Hahn, J. Sieler and R. Taube, *Polyhedron*, 1998, **17**, 1183.
[29] J. M. Ernsting, H. F. Haarman, M. Kranenburg, H. Kooijman, A. L. Speck, P. W. N. M. van Leeuwen N. Veldman and K. Vrieze, *Organometallics*, 1997, **16**, 887.
[30] K. Kashiwabara, A, Morikawa, T. Suzuki, K. Isobe and K. Tatsumi, *J. Chem. Soc., Dalton Trans.*, 1997, 1075.

5.2.5 IR spectroscopy

Selected infrared data is given in **Table 5.5**. The ionic compound [Rh(CO)(PNCHP-κ^3*P,N,P*)]Cl, in chloroform, exhibits a strong absorption ν(CO) at 2009 cm^{-1}, characteristic of terminal carbonyls,[31,32] where as the related compound [Rh(CO)(PNHCH$_2$P-κ^3*P,N,P*)]PF_6[13] displays the band at 2000 cm^{-1} which is consistent with the imino nitrogen of PNCHP having better π-acid qualities than the amino nitrogen of PNHCH$_2$P. Also present in the solution spectrum of [Rh(CO)(PNCHP-κ^3*P,N,P*)]Cl is a very weak band at 1960 cm^{-1}, which has been assigned to the absorption ν(CO) of the neutral five-coordinate [Rh(CO)(PNCHP-κ^3*P,N,P*)Cl]. The nujol mull spectrum of [Rh(CO)(PNCHP-κ^3*P,N,P*)Cl], exhibits a strong band at 1959 cm^{-1}, typical of five-coordinate-rhodium(I)-terminal-monocarbonyl complexes.[31,33] The 50 cm^{-1} shift to lower energy of the ν(CO) band, is consistent with the coordination of the chloride, giving a five coordinate species, and hence, reduction of the positive charge on the metal. Thus an equilibrium between the two isomers seems likely in solution. A similar pair of compounds is found for the [Rh(CO)(PhP{CH$_2$CH$_2$PPh$_2$}$_2$-κ^3*P,P,P*)]Cl (**F.5.5-1**) (2020cm^{-1}) / [Rh(CO)(PhP{CH$_2$CH$_2$PPh$_2$}$_2$-κ^3*P,P,P*)Cl] (**F.5.5-2**) (1956cm^{-1}) system, as shown in **Figure 5.5**, although in this case, the equilibrium favours the neutral, five-coordinate complex [Rh(CO)Cl(PhP{CH$_2$CH$_2$PPh$_2$}$_2$-κ^3*P,P,P*)].[31]

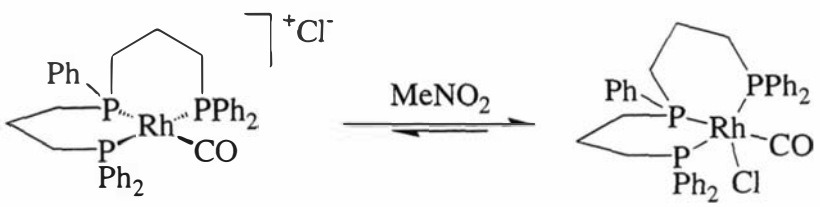

F.5.5-1 **F.5.5-2**

Figure 5.5 Four- and five-coordinate complexes in equilibrium

[31] D. W. Meek and T. E. Nappier, *J. Am. Chem. Soc.*, 1972, **94**, 306.
[32] N. Rahmouni, A. A. Bahsoun, M-T. Youinou, J. A. Osborn, J. Fischer and A. Ezzamarty, *Polyhedron*, 1998, **17**, 3083.
[33] P. Paul and B. Tyagi, *Polyhedron*, 1996, **15**, 675.

Table 5.5

IR data for selected compounds[a]

Compound	Band/cm^{-1} (intensity)	Assignment
[RhCl(PNCHP-κ^3P,N,P)][a]	1583(w)	ν(C=N)[b]
	1097(m)	ν(P-C)
[RhCl(CO)(PNCHP-κ^3P,N,P)][a]	1959(s)	ν(C≡O)
	1593(w)	ν(C=N)[b]
	1095(m)	ν(P-C)
[Rh(CO)(PNCHP-κ^3P,N,P)]Cl[c]	2009(s)	ν(C≡O)
[RhCl(PNCHP-κ^3P,N,P)] + HCl[d]	1602(w)	ν(C=N)[b]
	1097(m)	ν(P-C)

[a] Nujol mull. [b] Tenative assignment. [c] In $CHCl_3$. [d] Reacted with HCl gas for several minutes.

5.2.6 Mass spectroscopy

The typical fragmentation pattern of the compounds listed in **Table 5.6** consisted of the [Rh(PNCHP)(L)]$^+$ ion fragment at 100% abundance, where L is the ancillary ligand. The next most stable fragment was [Rh(PNCHP)]$^+$, where the ancillary ligand L had been lost. Isotope calculations, based on ^{103}Rh, of the molecular ion peaks gave excellent agreement with the isotope patterns found.

Table 5.6

FAB mass spectral data for selected compounds

Compound	Found m/z (%), assignment[calculated m/z for ^{103}Rh].
[RhCl(PNCHP)]	687(100), M^+[687]; 652(47), [M-Cl]$^+$ [652].
[RhCl(PNCHP)(CO)]	680(100), [M-Cl]$^+$ [680].
[Rh(PNCHP)(MeCN)]Cl	693(84), M^+[693]; 652(65), [M-CH_3CN]$^+$ [652].
[Rh(PNCHP)(CO)]BF_4	680(100), M^+[680]; 652(7), [M-CO]$^+$.
[Rh(PNCHP)(MeCN)]BF_4	779(57), [M-H]$^+$ [779], 693(87), [M-BF_4]$^+$ [693]; 652(100), [M^+-BF_4CH_3CN[652].
[Rh(PNCHP)(PPh_3)]BF_4	914(40), M^+[914]; 652(8), [M-PPh_3]$^+$ [652]; 262(39), PPh_3[262].
[Rh(PNCHP)(CH_2Cl)Cl_2]	736(76), [M-Cl]$^+$ [736].

[a] Non isolatable. [b] Other peaks correspond to various combination of $RhLBr_xCl_y$ compounds, however the isotope patterns are in poor agreement.

5.3 Conclusions

The complex [RhCl(PNCHP-κ^3*P,N,P*)] is extremely reactive. The enhanced reactivity of this compound, relative to [RhCl(P_3)] systems (P_3 = mono, bi or terdentate phosphanes), is attributed to the presence of the coordinated imino nitrogen, which has the effect of increasing the nucleophilicity of the rhodium atom. The complex will react rapidly, at room temperature, with common halogenated solvents, activating the halo-carbon bond. Exposure to air results in a large number of products. Dissolving [RhCl(PNCHP-κ^3*P,N,P*)] in coordinating solvents results in substitution of the chloride atom, as does exposure to carbon monoxide. The resulting cation [Rh(CO)PNCHP-κ^3*P,N,P*)]$^+$ does not show the high reactivity of the [RhCl(PNCHP-κ^3*P,N,P*)] complex, due to the carbon monoxide's ability to remove electron density from the metal, that is, decreasing the nuclephilicity of the rhodium atom. The above illustrates that relatively small changes in the ligand shell can markedly affect the reactivity of the rhodium centre.

5.4 Experimental

All work with rhodium was carried out in an inert atmosphere glove-box, unless stated otherwise. The complex [{RhCl(COD)}$_2$] was prepared as previously reported.[34]

5.4.1 [RhCl(PNCHP-κ^{3}P,N,P)]

A mixture of [{RhCl(COD)}$_2$] (0.239 g, 0.485 mmol) and PNCHP (0.528 g, 0.961 mmol) in c.a. 10 mL of benzene was stirred at room temperature for 1 h. The resulting dark green precipitate of [RhCl(PNCHP-κ^3*P,N,P*)] (0.661 g, 100 %) was isolated by filtration, washed with n-pentane. Anal. Found: C, 64.54; H, 4.29; N, 1.86. Calcd for $C_{37}H_{29}ClNP_2Rh$: C, 64.60; H, 4.25; N, 2.04.

5.4.2 [Rh(CO)(PNCHP-κ^{3}P,N,P)Cl].C$_4$H$_8$O

[RhCl(PNCHP-κ^3*P,N,P*)] (0.154 g, 0.224 mmol) dissolved in 20 mL of THF was loaded into a Schlenk tube, whilst in a dry-box. All further manipulations were carried out using standard Schlenk techniques. CO (g) was bubbled through the dark green solution for 30 min, resulting in a dark green precipitate. The solvent was removed *in vacuo*, yielding [RhCl(CO)(PNCHP-κ^3*P,N,P*)] (0.160 g, 79%) as dark green microcrystals. Anal. Found: C, 63.10; H, 4.65; N, 1.82. Calcd for $C_{38}H_{29}ClNOP_2Rh{\bullet}C_4H_8O$: C, 62.49; H, 4.73; N, 1.77.

5.4.3 [Rh(CO)(PNCHP-κ^{3}P,N,P)]Cl

[Rh(CO)(PNCHP-κ^3*P,N,P*)Cl] (0.030 g, 0.042 mmol) was dissolved in dichloromethane (2 mL) and stood until the green colour of the starting material discharged. N-hexane vapour was then slowly diffused into the yellow solution resulting in orange crystals of [Rh(CO)(PNCHP-κ^{3}P,N,P)]Cl after several days. A single crystal was selected for an X-ray study, as reported in section *5.2.2*.

5.4.4 [Rh(CO)(PNCHP-κ^{3}P,N,P)]BF$_4$

[RhCl(PNCHP-κ^3*P,N,P*)] (0.100 g, 0.145 mmol) and $AgBF_4$ (0.028 g, 0.145 mmol) dissolved in THF (10 mL) were combined and stirred at room temperature overnight. The

[34] G. Giordano and R. H. Crabtree, *Inorg. Synth.*, 1979, **19**, 218.

reaction mixture was filtered and the filtrate loaded into a Schlenk tube fitted with a rubber septum cap. Carbon monoxide was bubbled through the filtrate for 15 min, turning the dark orange-red coloured solution a light orange. The solvent was removed *in vacuo* and residue returned to the dry-box where it was redissolved in THF and the ^{31}P nmr spectrum recorded (**Table 5.3**).

5.4.5 [Rh(L)(PNCHP-κ³P,N,P)]X (L = MeCN or THF, X = Cl⁻ or BF₄⁻)

A dark green solution of [RhCl(PNCHP-κ³*P,N,P*)] (0.100 g, 0.145 mmol) dissolved in L (4 mL) and $AgBF_4$[†] (0.0283 g, 0.145 mmol) dissolved in acetonitrile (2 mL) were combined producing a red-brown coloured solution instantaneously. The solution was stirred for 1 h, then the white precipitate (AgCl) removed by filtration to give a rust (red for L =THF) coloured filtrate containing [Rh(L)(PNCHP-κ³P,N,P)]X. The solvent was removed *in vacuo* and the compound redissolved in solvents appropriate for spectroscopic characterisation, see **Tables 5.3**, **5.4** and **5.6**.

[†] Omitted for X = Cl^-

5.4.6 [Rh(PPh₃)(PNCHP-κ³P,N,P)]BF₄

[RhCl(PNCHP-κ³*P,N,P*)] (0.050 g, 0.075 mmol) and $AgBF_4$ (0.014 g, 0.0072 mmol) dissolved in THF were combined and stirred at room temperature for 5 min. The reaction mixture was filtered and PPh_3 (0.0191 g, 0.0728 mmol) added to the dark-red filtrate resulting in a colour change to brown-yellow. The reaction mixture was run through a plug of alumina, eluting with THF, to yield a yellow solution. The solvent volume was removed and spectroscopic characterisation carried out, see **Tables 5.3** and **5.6**.

5.4.7 [RhCl(PNCHP-κ³P,N,P)] + xsHCl

[RhCl(PNCHP-κ³*P,N,P*)] (50 mg, 0.073 mmol) and THF (4 mL) were loaded in a Schlenck tube, whilst in a dry-box. HCl (g) was bubbled through the dark green solution for 1 min, resulting in a colour change to orange. The reaction mixture was sealed under an atmosphere of HCl and stood overnight. From then on, no further precautions were taken to exclude air. The product (0.0152 g, 27% as $RhCl_3$(PNCHP)) was isolated as orange crystalline needles, and washed with n-pentane (see **Tables 5.3**, **5.4** and **5.5**).

5.4.8 [$RhCl_2(CDCl_2)$(PNCHP-κ^3P,N,P)].½$CDCl_3$

[RhCl(PNCHP-κ^3*P,N,P*)] (50 mg, 0.073 mmol) was dissolved in $CDCl_3$, giving a orange solution after several minutes. Yellow microcrystals of [$RhCl_2(CDCl_2)$(PNCHP-κ^3P,N,P)].0.5$CDCl_3$ emerged upon slow evaporation of the solvent. Anal. Found: C, 52.82; H, 3.50; N, 1.91; Cl, 22.95. Calcd for $C_{38}H_{29}ClNOP_2Rh$•½$CDCl_3$: C, 53.34; H, 3.55; N, 1.62; Cl, 22.49.

5.4.9 [$RhCl_2(CH_2Cl)$(PNCHP-κ^3P,N,P)]•⅔CH_2Cl_2

[RhCl(PNCHP-κ^3*P,N,P*)] (0.030 g, 0.042 mmol) was dissolved in dichloromethane (2 mL) and stood until the green colour of the starting material discharged. N-hexane vapour was then slowly diffused into the yellow solution resulting in the title compound as a yellow powder. Anal. Found: C, 55.25; H, 3.87; N, 1.65; Cl, 18.10. Calcd for $C_{38}H_{31}Cl_3NP_2Rh$•⅔CH_2Cl_2: C, 55.99; H, 3.92; N, 1.69; Cl, 18.50.

6 The Triosmium Cluster Complexes

6.1 Introduction

Doubly bridging ligands which donate more than six electrons to trinuclear clusters of ruthenium and osmium are uncommon and even fewer examples exist where the ligand is triply bridging.[1] The ligand PNCHP or 2-$PPh_2(C_6H_4N{=}CHC_6H_4)$2-$PPh_2$ (**F.6.1-1**), can be viewed as an extension of the ligand 2-$PPh_2(C_6H_4N{=}CHPh)$ (**F.6.1-2**) which is found, minus the imino hydrogen, as a triply bridging seven electron donor in the complex $[Ru_3(\mu\text{-}H)(CO)_6(\mu_3\text{-}CPh{=}NC_6H_4PPh_2)(\mu\text{-}dppm)]$ (**F.6.1-3**),[2] as shown in **Figure 6.1**. The ligand PNCHP has the potential to donate an additional two electrons to the cluster, making the ligand a rare example of a triply bridging nine electron donor. The only other example is found in the complex $[Os_3(\mu\text{-}H)(CO)_6(\mu_3\text{-}PPh_2CH_2P(Ph)C_6H_4CNR)(PPh_3)]$ (**F.6.1-4**). However, in this case the ligand is not reacted directly with the triosmium cluster but formed from a subsequent C-C coupling reaction.[3] This chapter reports, the reaction products of PNCHP with $[Os_3(CO)_{10}(CH_3CN)_2]$ followed by addition of trimethylamineoxide *in situ* in order to encourage the higher degrees of substitution desired. PNCHP was also reacted with $[Os_3(CO)_{11}(CH_3CN)]$ and $[Os_3(CO)_{10}(CH_3CN)_2]$ in the absence of trimethylamineoxide. In these cases the PNCHP's three inequivalent lone pairs of electrons, from the two phosphorus atoms and one nitrogen atom, are available to substitute for the acetonitrile ligand(s), hence, potential for several coordination isomers exist.[4]

---

[1] *Comprehensive Organometallic Chemistry II: A Review of the Literature 1982-1984*, Editors-in-Chief E. W. Abel, F. Gordon A. Stone and G. Wilkinson, Pergamon, 1995 Elsevier Science Ltd, p700 and p709 and refs. within.

[2] C. J. Adams, M. I. Bruce, O. Kühl, B. W. Skelton and A. H. White, *J. Organomet. Chem.*, 1993, **445**, C6.

[3] K. L. Lu, H. J. Chen, P. Y. Lu, S. Y. Li, F. E. Hong, S. M. Peng and G. H. Lee, *Organometallics*, 1994, **13**, 585.

[4] E. W. Ainscough, A. M. Brodie, A. K. Burrell, S. M. F. Kennedy, J. M. Waters and in part P. D. Buckley, *Synthesis, Structure and Kinetics of Group 6 Metal Carbonyl Complexes Containing a New 'P_2N' Mixed Donor Multidentate Ligand*, *J. Chem. Soc., Dalton Trans.*, (in print).

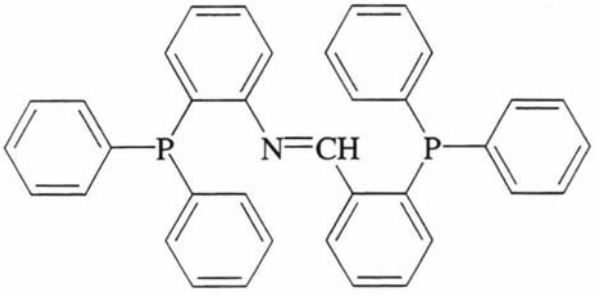

F.6.1-1

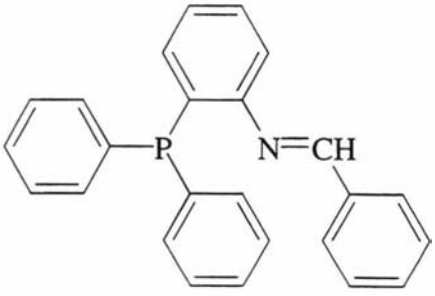

F.6.1-2

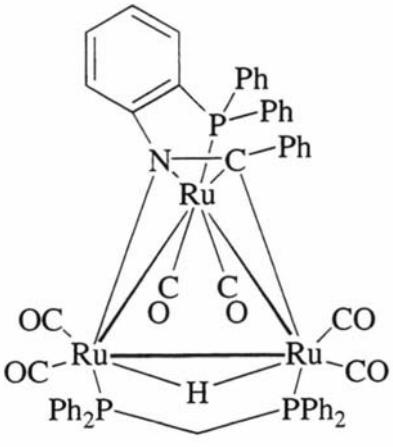

F.6.1-3

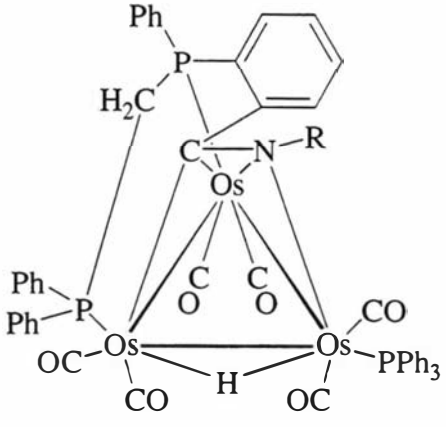

F.6.1-4

Figure 6.1 The trimetallic clusters of the ligand 2-$PPh_2(C_6H_4N{=}CHPh)$,a close relation of PNCHP

6.2 Results and discussion

6.2.1 Synthesis

The osmium cluster compounds described in this report are depicted in **Figure 6.2**. The PNCHP bridged dicluster species $[\{Os_3(CO)_{11}\}_2(PNCHP)]$ (**F.6.2-1**) was synthesised by reacting a half mole equivalent of the ligand PNCHP with $[Os_3(CO)_{11}(MeCN)]$. The dimer is also obtained as a major product when attempting to synthesise the monomers, and coordination isomers of $[Os_3(CO)_{11}(PHCNP)]$ (**F.6.2-2a**) and (**F.6.2-2b**), by reacting one mole equivalent of the ligand PNCHP with $[Os_3(CO)_{11}(MeCN)]$. The monomer **F.6.2-**

2a was isolated by TLC, however, the monomer **F.6.2-2b** could not be separated from the dimer **F.6.2-1**. The cluster 1,1-$[Os_3(CO)_{10}(PNCHP)]$ (**F.6.2-3**) was synthesised by reacting the ligand PNCHP with $[Os_3(CO)_{10}(MeCN)_2]$. When **F.6.2-3** is reacted *in situ* with one or two equivalents of trimethylamineoxide, $[Os_3(\mu\text{-}H)(CO)_7(\mu_3\text{-}PNCP)]$ (**F.6.2-4**) is obtained as the major product with two coordination isomers of $[Os_3(\mu\text{-}H)(CO)_8(\mu_2\text{-}PNCP)]$ (**F.6.2-5a**) and (**F.6.2-5b**) as minor products. **F.6.2-5a** and **F.6.2-5b** are also observed in the ageing of **F.6.2-3**.

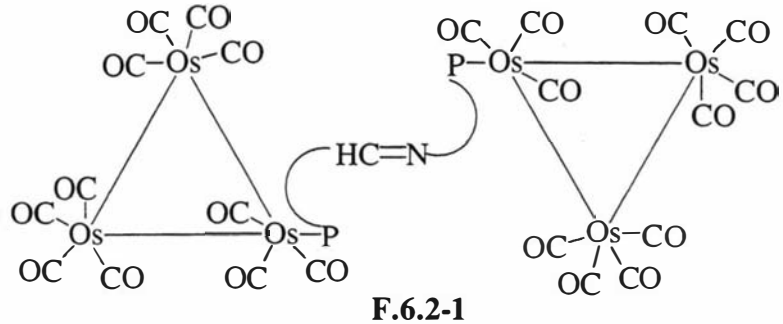

F.6.2-1

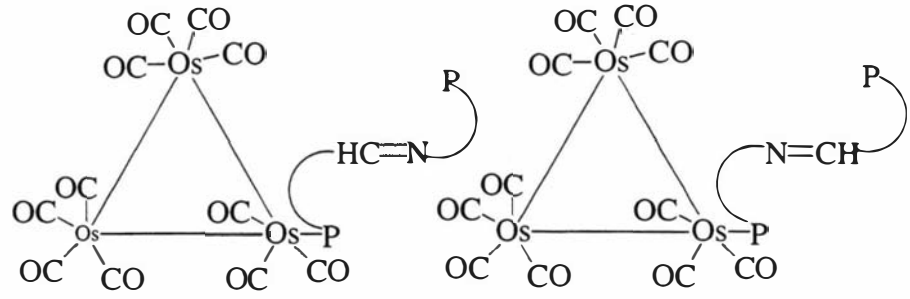

F.6.2-2a F.6.2-2b

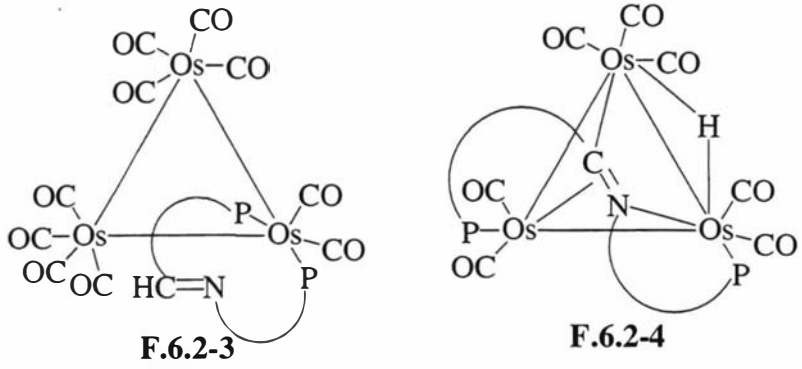

F.6.2-3 F.6.2-4

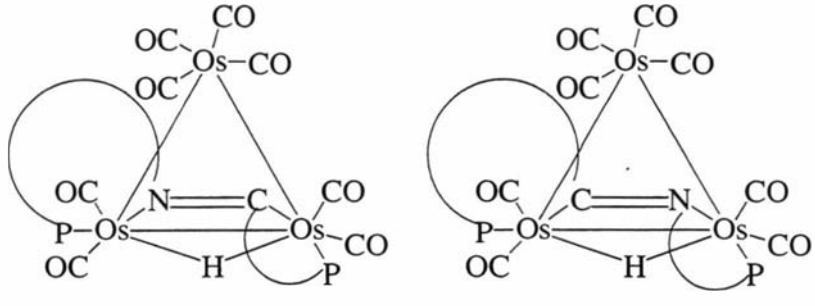

F.6.2-5a F.6.2-5b

Figure 6.2 The complexes showing the various coordination modes of PNCHP, where PNCHP is depicted by P-N=CH-P

6.2.2 Description of the crystal structures

*6.2.2.1 Crystal structure of [{$Os_3(CO)_{11}$}$_2$(PNCHP)](**F.6.2-1**)•CH_2Cl_2*

The ORTEP diagram of [{$Os_3(CO)_{11}$}$_2$(PNCHP)] (**F.6.2-1**) is shown by **Figure 6.3**, with crystal data and structure refinement details given in **Table 6.1** and bond lengths and angles given in **Table 6.2**. X-ray analyses of **F.6.2-1** shows two independent molecules in the asymmetric unit. One of these is affected by disorder of the osmium triangle as discussed in section. *6.4.2*. Both molecules in all other respects are essentially the same except for the imine bond lengths C(127)-C(127_2) (1.276(15) Å) and C(227)-C(227_2) (1.327(16) Å. It is unlikely that this difference is a real effect and probably arises from the pseudo-symmetry which is present. The structure shows two "$Os_3(CO)_{11}$" moieties bridged by one PNCHP via the P atoms. The P atoms are coordinated in equatorial positions relative to the osmium triangle. A centre of inversion lies at the mid-point of the imine bond therefore it was not possible to distinguish the imino N from the imino C. Eleven carbonyl ligands occupy the remaining coordination sites to give a slightly distorted octahedral geometry for each osmium. Os-P, Os-CO and Os-Os bond lengths are identical to those reported for [$Os_3(CO)_{11}(PPh_3)$][5] and similar to another reported iminophosphino-$Os_3(CO)_{11}$ species and the comparable complex [{$Os_3(CO)_{11}$}$_2$(dppa)] (dppa is bis(diphenylphosphino)acetylene).[9,10]

[5] M. I. Bruce, C. A. Hughes, M. J. Liddell, B. W. Skelton and A. H. White, *J. Organomet. Chem.*, 1988, **347**, 157.

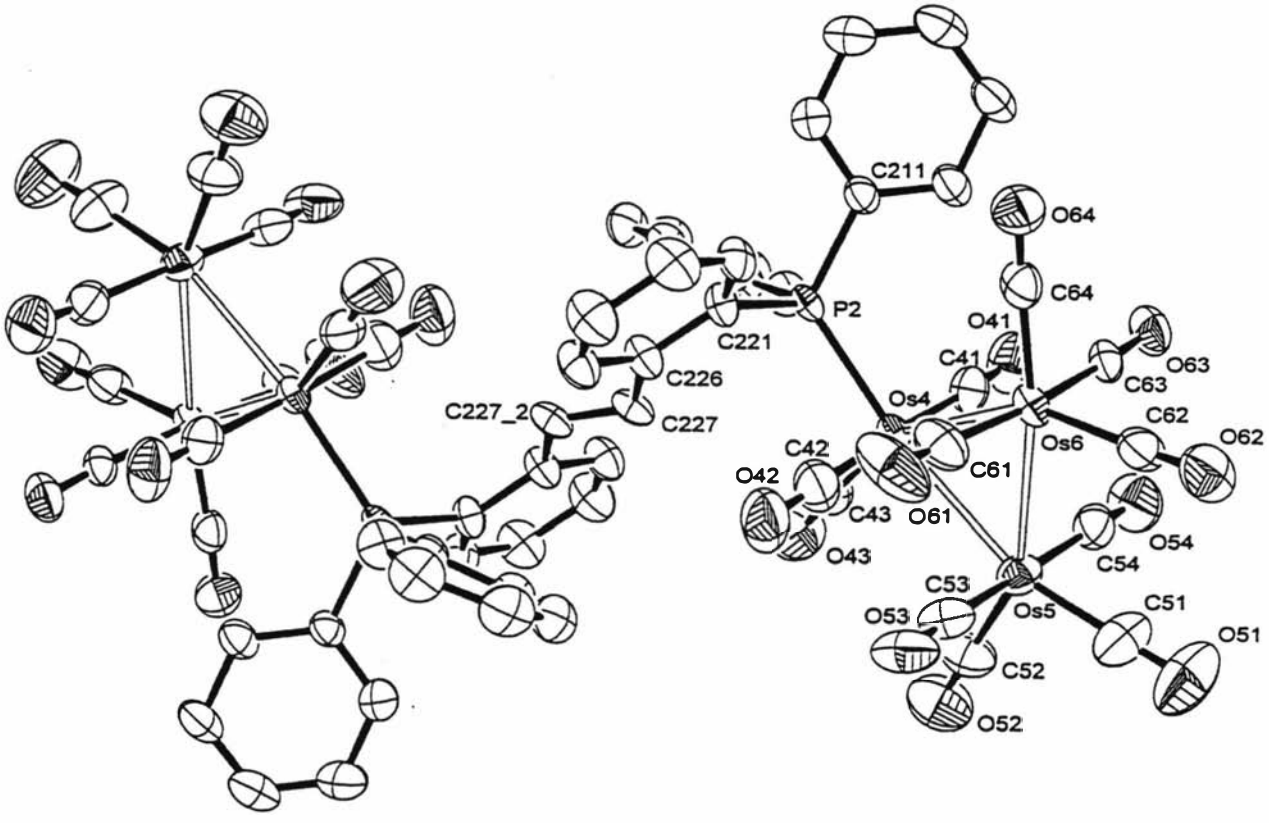

Figure 6.3 ORTEP diagram for one molecule of $[\{Os_3(CO)_{11}\}_2(PNCHP)]$ (**F.6.2-1**) showing the numbering system used. Thermal ellipsoids are at the 50% probability level. Hydrogen atoms have been omitted for clarity

Table 6.1

Crystal data and structure refinement for [{$Os_3(CO)_{11}$}$_2$(PNCHP)](**F.6.2-1**)•CH_2Cl_2.

Identification code	sk2a	
Empirical formula	C60.51 H32 Cl3 O20.50 Os6 P2	
Formula weight	2396.49	
Temperature	203(2) K	
Wavelength	0.71073 Å	
Crystal system	Triclinic	
Space group	P-1	
Unit cell dimensions	a = 11.14790(10) Å	α = 105.3140(10)°.
	b = 17.003 Å	β = 104.9670(10)°.
	c = 19.5194(2) Å	γ = 98.2070(10)°.
Volume	3358.00(5) Å^3	
Z	2	
Density (calculated)	2.370 Mg/m^3	
Absorption coefficient	11.545 mm^{-1}	
F(000)	2192	
Crystal size	0.56 x 0.30 x 0.18 mm^3	
Theta range for data collection	1.14 to 27.46°.	
Index ranges	-13<=h<=14, -21<=k<=21, -25<=l<=24	
Reflections collected	31036	
Independent reflections	14322 [R(int) = 0.0533]	
Absorption correction	Semi-empirical from equivalents	
Max. and min. transmission	0.2304 and 0.0596	
Refinement method	Full-matrix least-squares on F^2	
Data / restraints / parameters	14322 / 976 / 906	
Goodness-of-fit on F^2	0.930	
Final R indices [I>2sigma(I)]	R1 = 0.0478, wR2 = 0.1289	
R indices (all data)	R1 = 0.0667, wR2 = 0.1473	
Extinction coefficient	0.00061(7)	
Largest diff. peak and hole	2.954 and -3.044 e.Å^{-3}	
(Peek is located close to C(13) and hole is close to Os(5))		

Table 6.2

Selected bond lengths (Å) and angles (°) for [{$Os_3(CO)_{11}$}$_2$(PNCHP)] (**F.6.2-1**)•CH_2Cl_2 with estimated standard deviations in parentheses

Bond lengths:			
Os(4)-Os(5)	2.8990(5)	Os(4)-P(2)	2.374(2)
Os(5)-Os(6)	2.8844(4)	Os-CO	1.881(9)-1.960(11)
Os(4)-Os(6)	2.9191(5)	C(227)-C(227_2)	1.327(16)
Bond angles:			
P2-Os-CO_{eq}	99.2(3)	OC_{ax}-Os-CO_{eq}	87.7(4)-95.1(4)
OC_{eq}-Os-CO_{eq}	100.7(4)-102.7(5)		

*6.2.2.2 Crystal structure of [Os_3(μ-H)$(CO)_7$(μ$_3$-PNCP)](**F.6.2-4**).1½CH_2Cl_2*

The ORTEP diagram of [Os_3(μ-H)$(CO)_7$(μ$_3$-PNCP)](**F.6.2-4**) is shown by **Figure 6.4**, with crystal data and structure refinement details given in **Table 6.3** and bond lengths and angles given in **Table 6.3**. Complex **F.6.2-4** has at its centre an osmium triangle with the three Os-Os bond lengths at 2.8523(2) (Os(1)-Os(2)), 2.7644(2) (Os(1)-Os(3)) and 2.8290(2) Å (Os(2)-Os(3)). An electron count of 48 electrons for the complex is supportive of three Os-Os bonds.[6] The imine bond N-C of the PNCP ligand caps the osmium triangle across its mid-point with the N atom lying directly above the Os(1)-Os(3) vector, relative to the plane of the osmium triangle, and the C atom likewise above the Os(2)-Os(3) vector. The imine-to-osmium triangle bonding distances are 2.130(3) (N-Os(1)), 2.210(3) (N-Os(2)), 2.050(4) (C(1)-Os(2)) and 2.253(4) Å (C-Os(3)). The P atoms P(1) and P(2) are coordinated to Os(3) and Os(1) respectively in equatorial positions and have P-Os bond lengths of 2.3368(10) and 2.3326(10) Å which are typical for an osmium-arylphosphane

[6] Ref. [1] p689.

bond.[3,7,8,9,10] Therefore the PNCP ligand is formally a 9-electron donor. To our knowledge only one other 9-electron donor ligand to Os or Ru has been reported.[3,11] The remaining coordination sites on the osmium triangle are filled by seven carbonyl ligands to give a distorted octahedral geometry around each Os atom. The Os-CO bond lengths ranged from 1.881(4)-1.933(5) Å. The imine bond N-C at a length of 1.414(5) Å has lengthened considerably relative to 1.296(8) Å found in the free-ligand.[12] However, this lengthening is expected as a result of the interaction of the imine bond with the osmium cluster.[13,14,15] In the PNCHP free-ligand the phosphane moieties are *trans* to the imine bond,[12] however they are *cis* in **F.6.2-4**. The hydride that was observed by ^{1}H NMR could not be located in the X-ray structure, but a cavity along the Os(1)-Os(3) edge, as determined by the angles C(600)-Os(3)-Os(1) (113.23(14)°), C700-Os3-Os1 (108.68(13)) and C(100)-Os(1)-Os(3) (118.47(13)°), suggests a suitable position for H. In addition the longest Os-Os bond is at this edge which is consistent with a bridging H[16] and in the analogous system $[Ru_3(\mu\text{-}H)(CO)_6(\mu_3\text{-}CPh{=}NC_6H_4PPh_2)(\mu\text{-dppm})]$[14] the H is proposed to bridge what would effectively be the Os(1)-Os(3) edge in **F.6.2-4**.

---

[7] D. Braga, F. Grepioni, C. Gradella, B. F. G. Johnson, J. Lewis and M. Monari, *J. Chem. Soc. Dalton Trans.*, 1990, 2863.
[8] A. J. Deeming, S. Donovan-Mtunzi, K. I. Hardcastle, K. Henrick, S. E. Kabir and M. McPartlin, *J. Chem. Soc. Dalton Trans.*, 1988, 579.
[9] C. J Adams, P. Braunstein, M. I. Bruce, S. C. Cea, W. R. Cullen, P. A. Duckworth, P. A. Humphrey, O. Kühl, B. W. Skelton, E. R. T. Tiekink and A. H. White, *J. Organomet. Chem.*, 1994, **467**, 251.
[10] A. J. Amoroso, B. F. G. Johnson, J. Lewis, A. D. Massey, P. R. Raithby and W. T. Wong, *J. Organomet. Chem.*, 1992, **440**, 219.
[11] For example see Ref. [1] p709.
[12] X. Fan, *Structural Studies on the Interactions of a P_2N Tridentate ligand with Copper(I), Silver(I) and Sulfur,* MPhil Thesis, Massey University, 1995.
[13] M. Day, D. Espitia, K. I. Hardcastle, S. E. Kabir, and E. Rosenberg, *Organometallics*, 1991, **10**, 3550.
[14] C. J. Adams, M. I. Bruce, O. Kühl, B. W. Skelton and A. H. White, *J. Organomet. Chem.*, 1993, **445**, C6.
[15] R. D. Adams and N. M. Golembeski, *Inorg. Chem.*, 1978, **17**, 1969.
[16] See ref.[5] and refs. within.

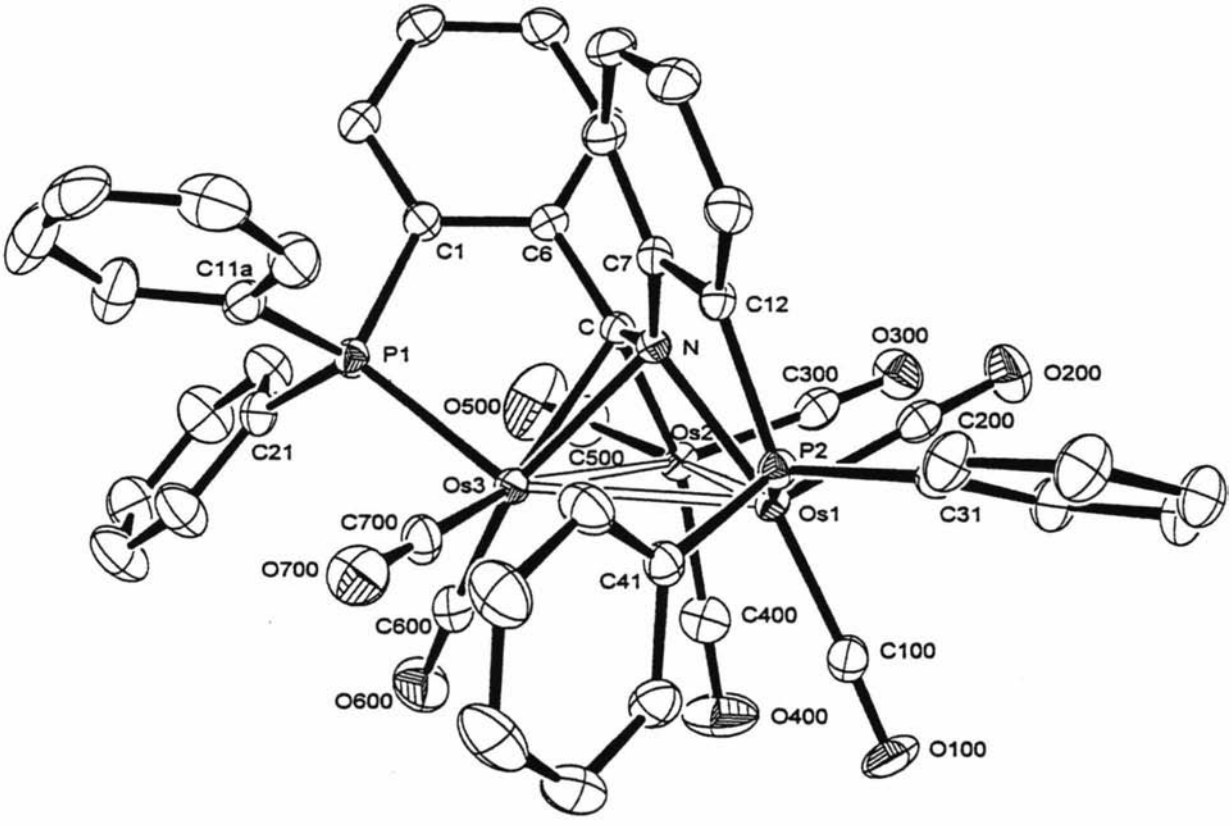

Figure 6.4 ORTEP diagram for the complex $[Os_3(\mu\text{-H})(\mu_3\text{-PNCP})(CO)_7]$ (**F.6.2-4**) showing the numbering system used. Thermal ellipsoids are at the 50% probability level. Hydrogen atoms have been omitted for clarity

Table 6.3

Crystal data and structure refinement for $[Os_3(\mu\text{-}H)(\mu_3\text{-}PNCP)(CO)_7]$(**F.6.2-4**)•1½$CH_2Cl_2$.

Identification code	sk17	
Empirical formula	C45 H30 Cl2 N O7 Os3 P2	
Formula weight	1400.14	
Temperature	200(2) K	
Wavelength	0.71073 Å	
Crystal system	Triclinic	
Space group	P-1	
Unit cell dimensions	a = 11.50110(10) Å	α = 70.5570(10)°.
	b = 11.7702(2) Å	β = 86.44(1)°.
	c = 17.2844(2) Å	γ = 78.6220(10)°.
Volume	2162.98(5) $Å^3$	
Z	2	
Density (calculated)	2.150 Mg/m^3	
Absorption coefficient	9.039 mm^{-1}	
F(000)	1310	
Crystal size	0.40 x 0.36 x 0.28 mm^3	
Theta range for data collection	1.25 to 27.46°.	
Index ranges	-14<=h<=14, -15<=k<=15, -22<=l<=22	
Reflections collected	21157	
Independent reflections	9351 [R(int) = 0.0195]	
Absorption correction	Semi-empirical from equivalents	
Max. and min. transmission	0.1863 and 0.1227	
Refinement method	Full-matrix least-squares on F^2	
Data / restraints / parameters	9351 / 0 / 536	
Goodness-of-fit on F^2	1.153	
Final R indices [I>2sigma(I)]	R1 = 0.0230, wR2 = 0.0584	
R indices (all data)	R1 = 0.0261, wR2 = 0.0607	
Largest diff. peak and hole	1.185 and -1.424 $e.Å^{-3}$	

Table 6.4

Selected bond lengths (Å) and angles (°) for $[Os_3(\mu\text{-}H)(\mu_3\text{-}PNCP)(CO)_7]$(**F.6.2-4**)•1½$CH_2Cl_2$. with estimated standard deviations in parentheses

Bond lengths:			
Os(1)-Os(2)	2.7644(2)	Os(1)-N	2.130(3)
Os(1)-Os(3)	2.8523(2)	Os(2)-C	2.050(4)
Os(2)-Os(3)	2.8290(2)	Os(3)-N	2.210(3)
Os(3)-P(1)	2.3368(10)	Os(3)-C	2.253(4)
Os(1)-P(2)	2.3326(10)	Os-CO	1.881(4)-1.933(5)
		C-N	1.414(5)

Bond angles:			
N-Os(1)-P(2)	80.65(9)	P(2)-Os(1)-Os(3)	96.74(2)
C-Os(3)-P(1)	80.23(10)	P(1)-Os(3)-Os(1)	145.30(3)
Os(1)-N-Os(3)	82.16(11)	C(100)-Os(1)-Os(3)	118.47(13)
Os(2)-C-Os(3)	82.06(13)	C(600)-Os(3)-Os(1)	113.23(14)
		C(700)-Os(3)-Os(1)	108.68(13)

*6.2.2.3 Crystal structure of [$Os_3(\mu\text{-}\dot{H})(CO)_8(\mu_2\text{-}PNCP)$] (**F.6.2-5a**)*

The ORTEP diagram [$Os_3(\mu$-H)$(CO)_8(\mu_2$-PNCP)] (**F.6.2-5a**) is shown by **Figure 6.5**, with crystal data and structure refinement details given in **Table 6.5** and bond lengths and angles given in **Table 6.6**. Complex **F.6.2-5a** can be viewed as a 'one carbonyl-group removal' step away from the previously discussed structure of **F.6.2-4**. Therefore the PNCP ligand binds to the osmium triangle in a similar fashion to **F.6.2-4** except that the distances 3.680(9) (N-Os3) and 3.610(9) Å (C(1)-Os(3)) are clearly non-bonding. In this case the PNCP ligand acts formally as a 7-electron donor. Again, the imine bond N-C(1) has lengthened relative to the free ligand (from 1.296(8) to 1.334(12)Å) but not to the extent found in **F.6.2-4** (1.414(5) Å), this is expected for a μ_2-imidoyl group compared with a μ_3-imidoyl group in terms of the electron density available for back-bonding into the antibonding orbital of the N=C bond.[15] The N and C1 were unable to be distinguished from one another due to a half occupancy of each atom disordered over the two sites, hence a swapping of the N and C1 labels of **Figure 6.5** gives the isomer **F.6.2-5b**. This was supported by the ^{1}H NMR spectrum where two hydride signals are observed in a 1:1 ratio (**Table 6.7**). The hydride was not located but is proposed to be found bridging the Os1-Os2 bond for the same reasons discussed for **F.6.2-4** above.

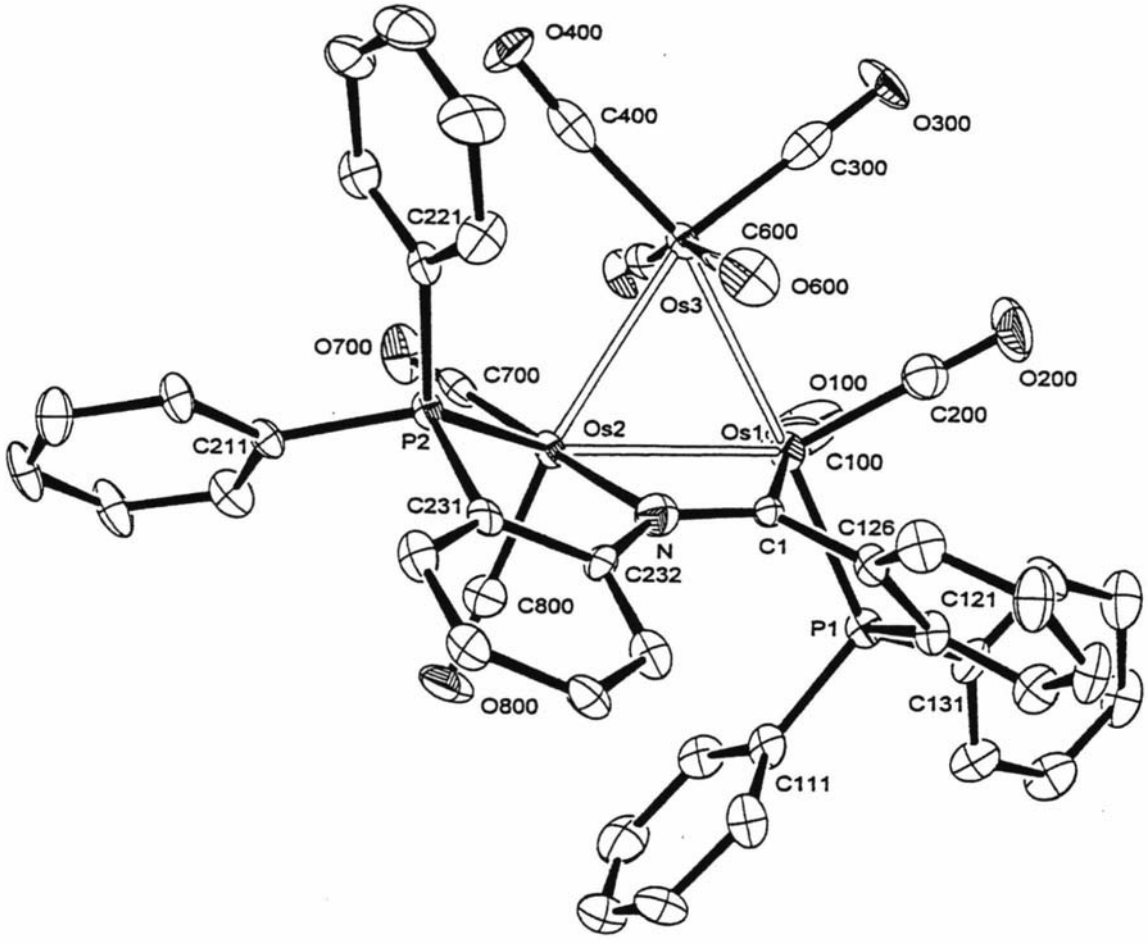

Figure 6.5 ORTEP diagram for the complex $[Os_3(\mu\text{-}H)(\mu_2\text{-}PNCP)(CO)_8]$. (**F.6.2-5a**) showing the numbering system used. Thermal ellipsoids are at the 50% probability level. Hydrogen atoms have been omitted for clarity

Table 6.5

Crystal data and structure refinement for $[Os_3(\mu\text{-}H)(\mu_2\text{-}PNCP)(CO)_8]$. (**F.6.2-5a**).

Identification code	osa	
Empirical formula	C45 H29 N O8 Os3 P2	
Formula weight	1344.23	
Temperature	171(2) K	
Wavelength	0.71073 Å	
Crystal system	Triclinic	
Space group	p-1	
Unit cell dimensions	a = 11.289(3) Å	α = 84.433(3)°.
	b = 11.709(3) Å	β = 77.697(3)°.
	c = 17.143(5) Å	γ = 70.918(4)°.
Volume	2091.3(9) $Å^3$	
Z	2	
Density (calculated)	2.135 Mg/m^3	
Absorption coefficient	9.223 mm^{-1}	
F(000)	1256	
Crystal size	0.68 x 0.48 x 0.30 mm^3	
Theta range for data collection	1.95 to 26.42°.	
Index ranges	-13<=h<=14, -14<=k<=14, -21<=l<=21	
Reflections collected	26697	
Independent reflections	8407 [R(int) = 0.0664]	
Absorption correction	Semi-empirical from equivalents	
Max. and min. transmission	0.1684 and 0.0619	
Refinement method	Full-matrix least-squares on F^2	
Data / restraints / parameters	8407 / 0 / 517	
Goodness-of-fit on F^2	1.003	
Final R indices [I>2sigma(I)]	R1 = 0.0428, wR2 = 0.1010	
R indices (all data)	R1 = 0.0640, wR2 = 0.1102	
Largest diff. peak and hole	3.201 and -3.955 e.$Å^{-3}$	

Both peak and hole are found close to Os(2)

Table 6.6

Selected bond lengths (Å) and angles (°) for $[Os_3(\mu\text{-}H)(\mu_2\text{-}PNCP)(CO)_8]$ (**F.6.2-5a**) with estimated standard deviations in parentheses

Bond lengths:			
Os(1)-Os(2)	2.9377(9)	Os(2)-N	2.130(8)
Os(1)-Os(3)	2.8565(8)	Os(1)-C(1)	2.130(9)
Os(2)-Os(3)	2.9218(7)	Os-CO	1.874(11)- 1.940(11)
Os(1)-P(1)	2.322(3)	C(1)-N	1.334(12)
Os(2)-P(2)	2.320(2)		
Bond angles:			
N-Os(2)-P(2)	79.6(2)	P(1)-Os(1)-Os(2)	112.30(6)
C(1)-Os(1)-P(1)	74.1(2)	P(2)-Os(2)-Os(1)	140.36(6)

6.2.3 NMR spectroscopic studies

6.2.3.1 The compound $[Os_3(\mu\text{-}H)(CO)_7(\mu_3\text{-}PNCP)]$

NMR spectroscopic data are given in **Table 6.7**. The hydride of $[Os_3(\mu\text{-}H)(CO)_7(\mu_3\text{-}PNCP)]$ (**F.6.2-4**) resonates at δ-14.76 as a doublet of doublets. The coupling constants of 34.0 and 5.6 Hz have been assigned to $^2J(HP)$ hydride coupling to inequivalent P atoms. The hydride has been postulated, based on crystallographic evidence, to lie almost *trans* to one P atom and *cis* to the other as depicted in **Figure 6.2**. Therefore the larger coupling constant has been assigned to the H involved in the *trans*-like H-Os-P angle and the smaller coupling constant to the H in the *cis* H-Os-P angle.[13] ^{31}P NMR signals at 33.4(s) and 14.6(s) ppm support both phosphorus atoms being coordinated in solution.[17]

[17] *NMR spectroscopy of the non-metallic elements*, S. Berger, S. Braum and H-O. Kalinowski, 1997 John Wiley & Sons Ltd, p835.

6.2.3.2 The [$Os_3(\mu\text{-}H)(CO)_8(\mu_3\text{-}PNCP)$] compounds

[$Os_3(\mu\text{-}H)(CO)_8(\mu_2\text{-}PNCP)$] exists as two isomers (**Figure 6.2** (**F.6.2-5a**) and (**F.6.2-5b**)) since it shows two hydride signals. They are at δ-14.52 and δ-14.97 and both have a doublet of doublets splitting pattern with ^{2}J(HP) coupling constants of 35.3 and 4.5 Hz and 41.4 and 5.1 Hz respectively. The integral ratio of the two hydride signals is 1:1 in the ^{1}H NMR spectrum of the same crystals used for the crystallographic study. This ratio is reproducible. However, the ^{1}H NMR spectrum recorded on a sample eluted from the chromatography band from which the crystals are grown (i.e. crude **F.6.2-5a/F.6.2-5b**) show an integral ratio of 3:1 in favour of the signal at δ-14.97 and again this is reproducible. Therefore it is proposed that the product prefers to crystallise with the isomers in a 1:1 ratio. The ^{31}P NMR of the crystals used for the x-ray diffraction study show four peaks, at δ32.9(s), δ31.2(s), δ26.3(s) and δ19.1(s). The peaks at δ32.9 and δ26.3 have been tentatively assigned to one of the hydride isomers and the peaks at δ31.2 and δ19.1 to the other hydride isomer. The closely related compound **F.6.2-4** has similar ^{31}P NMR signals at δ33.4 and δ14.6.

6.2.3.3 The compound [{$Os_3(CO)_{11}$}$_2$(PNCHP)]

The ^{1}H NMR spectrum of [{$Os_3(CO)_{11}$}$_2$(PNCHP)] (**F.6.2-1**) exhibits a singlet resonance at δ8.63 compared with the free ligand value of δ8.92(d) which has been assigned to the imine proton. Other peaks present in the region δ7.8 to δ5.6 were assigned to the twenty eight aromatic protons as confirmed by peak area integration. As expected, two singlets were observed in the ^{31}P NMR spectrum at δ0.87 and δ-1.8, both consistent with coordinated P atoms.

6.2.3.4 The [$Os_3(CO)_{11}$(PNCHP)] compounds

The coordination isomer **F.6.2-2a** displays an imine proton singlet at δ8.35 while **F.6.2-2b** displays a doublet at δ9.07. It has been previously documented that the imino proton of the 'free' PNCHP ligand is split by the PNCHP phosphorus nucleus (^4J(PH) = 5.5 Hz). However, when the same phosphorus is bound to sulfur, as in PNCHP=S, the imine

proton is a singlet, suggesting that coordination of the phosphorus four bonds removed from the nitrogen means that P-H coupling is no longer observed. When sulfur is bound to the other phosphorus atom, as in S=PNCHP, a doublet imine proton is still observed.[12] Both compounds show two peaks in their ^{31}P NMR spectra, as shown in **Table 6.7**, consistent with one coordinated and one non-coordinated P atom. Although **F.6.2-2b** could not be separated from **F.6.2-1**, **F.6.2-2a** could be isolated pure. Subtraction of the NMR signals for pure **F.6.2-1** from that of the **F.6.2-1/ F.6.2-2b** mixture enabled the assignments to be made for **F.6.2-2b**.

6.2.3.5 The compound $[Os_3(CO)_{10}(PNCHP)]$

The ^{31}P NMR signal shifts for **F.6.2-3** (**Table 6.7**), relative to the free-PNCHP ligand, were consistent with the coordination of both P atoms to the osmium triangle. The ^{1}H NMR signal at δ5.83 assigned to the imino-proton is at a considerably higher frequency than normally found for the coordinated ligand.[4] Unlike many osmium-carbonyl clusters, the ^{13}C NMR spectrum of **F.6.2-3** showed the carbonyl ligands to be non-fluxional at room temperature and the cluster to have very low symmetry due to the complexity and number of ^{13}C resonances in the metal-carbonyl region of the spectrum.

Table 6.7

NMR spectroscopic data of the compounds

Complex	^{1}H NMR/δ[a]			^{31}P NMR/δ[b]
	Os-H	CH=N	J(P,H)/Hz	
$[\{Os_3(CO)_{11}\}_2(PNCHP)]$ (**F.6.2-1**)		8.63(s)	6.4	0.87(s), -1.8(s)
$[Os_3(CO)_{11}(PCHNP)]$ (**F.6.2-2a**)		8.35(s)		-1.9(s), -14.5(s)
$[Os_3(CO)_{11}(PNCHP)]$ (**F.6.2-2b**)		9.07(d)		-0.19(s), -15.3(s)
1,1-$[Os_3(CO)_{10}(PNCHP)]$ (**F.6.2-3**)		5.83(s)[c]		27.0(s), 18.8(s)
$[Os_3(\mu\text{-H})(CO)_7(\mu_3\text{-PNCP})]$ (**F.6.2-4**)	-14.76(dd)		34.0, 5.7	33.4(s), 14.6(s)
$[Os_3(\mu\text{-H})(CO)_8(\mu_2\text{-PNCP})]$ (**F.6.2-5a**) and (**F.6.2-5b**)[d]	-14.52(dd) -14.97(dd)		35.3, 4.5 41.4, 5.1	32.9(s), 31.2(s) 26.3(s), 19.1(s)

[a] Recorded at 270 MHz, chemical shifts are in ppm relative to $Si(CH_3)_4$, solvent $CDCl_3$.
[b] Recorded at 109 MHz, chemical shifts are in ppm relative to 85% H_3PO_4, solvent $CHCl_3$.
[c] Tentative assignment. [d] 1:1 mixture of two geometric isomers. s = singlet, d = doublet.

6.2.4 IR spectroscopic studies

Inspection of the infrared spectroscopic data, given in **Table 6.8**, shows a typical lowering of the carbonyl stretching energies from **F.6.2-1** through **F.6.2-5** consistent with the increasing degree of carbonyl substitution in the complex by the PNCHP ligand. **F.6.2-1** exhibited bands typical of $Os_3(CO)_{11}L$ species[5,9] which is confirmed by its X-ray structure. Likewise for **F.6.2-2a** which gave a spectrum with no significant differences from **F.6.2-1**. Most $[M_3(CO)_{10}(L\text{-}L)]$ clusters, where M is Os or Ru and L-L is a bidentate ligand, tend to be found as 1,2-isomers.[18] However **F.6.2-3** was assigned the 1,1-isomer with equatorial bound phosphorus atoms, due to the similarity of its metal-carbonyl stretching region to other such species and dissimilarity to other isomers of $Os_3(CO)_{10}L_2$.[7,8,19,20,21,22,23]

[18] Ref. [1] p 715
[19] A. J. Deeming, S. Donovan-Mtunzi and S.E. Kabir, *J. Organomet. Chem.*, 1987, **333**, 253.
[20] G. Süss-Fink and H. Jungbluth, *J. Organomet. Chem.*, 1988, **352**, 185.
[21] A. J Deeming, S. Donovan-Mtunzi, S. E. Kabir and P. J. Manning, *J. Chem. Soc., Dalton Trans.*, 1985, 1037.
[22] A. J. Deeming and M. B. Smith, *J. Chem. Soc., Chem. Commun.*, 1993, 844.
[23] D. Heijdenrijk, J. T. B. H. Jastrzebski, G. van Koten, T. Mahabiersing, C. H. Stam, K. Vrieze and R. Zoet, *Organometallics*, 1988, **7**, 2108.

Table 6.8

IR spectroscopic data of the compounds

Complex	ν(CO)/cm^{-1} [a]			
[{$Os_3(CO)_{11}$}$_2$(PNCHP)] (**F.6.2-1**)	2107m	2078w	2054s	2032s
	2019vs	1988m	1984sh	1952sh
[$Os_3(CO)_{11}$(PCHNP)] (**F.6.2-2a**)	2108m	-	2057s	2033s
	2020vs	1989m	1980sh	1958sh
[$Os_3(CO)_{11}$(PNCHP)] (**F.6.2-2b**)	[b]			
1,1-[$Os_3(CO)_{10}$(PNCHP)] (**F.6.2-3**)	2093m	2056m	2034s	2009vs
	1995sh	1985s	1961sh	1940sh
[$Os_3(\mu$-H)$(CO)_7(\mu_3$-PNCP)] (**F.6.2-4**)	2038vs	2009vs	1984m	1968m
	1952s	1935sh	1923sh	
[$Os_3(\mu$-H)$(CO)_8(\mu_2$-PNCP)] (**F.6.2-5a/b**)[c]	2058s	1994vs	1967m	1960sh
	1937w	1927sh		

[a] In $CHCl_3$. [b] Contaminated with **F.6.2-1**. [c] 1:1 mixture of two geometric isomers.

6.2.5 Mass spectroscopic studies

FAB-mass spectral data, given in **Table 6.9**, for all the complexes recorded, showed the expected molecular ion peaks with the appropriate isotopic abundances and fragmentation patterns corresponding to the loss of successive carbonyl ligands.

Table 6.9

FAB mass spectroscopic data of the compounds

Compound	Found(%), assignment[calculated for ^{192}Os]
$[\{Os_3(CO)_{11}\}_2(PNCHP)]$ (**F.6.2-1**)	2307(21), M^+[2307]; 1949(37), M^+-13CO[1949].
$[Os_3(CO)_{11}(PCHNP)]$ (**F.6.2-2a**)	[a]
$[Os_3(CO)_{11}(PNCHP)]$ (**F.6.2-2b**)	1431(26), MH^+[1431]; 550(100), MH^+-(3Os + 10CO)[550].
1,1-$[Os_3(CO)_{10}(PNCHP)]$ (**F.6.2-3**)	1400(100), M^+-H[1400]; 1316(26), M^+-[H+3CO][1316]; 1290(22), MH^+-4CO[1290].
$[Os_3(\mu\text{-}H)(CO)_7(\mu_3\text{-}PNCP)]$ (**F.6.2-4**)	1317(100), M^+-CO[1317].
$[Os_3(\mu\text{-}H)(CO)_8(\mu_2\text{-}PNCP)]$ (**F.6.2-5a**) and (**F.6.2-5b**)	1345(100), M^+[1345]; 1317(70), M^+-CO[1317]; 1289(49), M^+-2CO[1289]; 1261(34), M^+-3CO[1261]; 1233(29), M^+-4CO[1233]; 1204(16), M^+-[H+5CO][1204]; 1177(22), M^+-6CO[1177].

[a] Non isolatable.

6.3 Conclusions

The triosmium clusters $[Os_3(CO)_{11}(CH_3CN)]$ and $[Os_3(CO)_{10}(CH_3CN)_2]$ react with 2-(diphenylphosphino)-N-[2-(diphenylphosphino)benzylidene]benzeneamine (PNCHP) to give $[\{Os_3(CO)_{11}\}_2(PNCHP)]$ (**F.6.2-1**), two coordination isomers of $[Os_3(CO)_{11}(PHCNP)]$ (**F.6.2-2a**) and (**F.6.2-2b**), and 1,1-$[Os_3(CO)_{10}(PNCHP)]$ (**F.6.2-3**) respectively. When

F.6.2-3 is reacted with one equivalent of trimethylamineoxide the major product is $[Os_3(\mu\text{-}H)(CO)_7(\mu_3\text{-}PNCP)]$ (**F.6.2-4**) with two geometrical isomers of $[Os_3(\mu\text{-}H)(CO)_8(\mu_2\text{-}PNCP)]$ (**F.6.2-5a**) and (**F.6.2-5b**) being minor products. The clusters have been fully characterised by spectroscopic means and the structures of **F.6.2-1**·CH_2Cl_2, **F.6.2-4**·1½CH_2Cl_2 and **F.6.2-5a** established by single crystal X-ray analyses. In **F.6.2-1** PNCHP bridges equatorially two osmium triangles. In **F.6.2-4** the imine hydrogen of PNCHP has migrated to the osmium cluster and PNCP acts as a triply bridging nine electron donor, while in **F.6.2-5a** PNCP acts as a doubly bridging seven electron donor ligand.

6.4. Experimental

*6.4.1 $[\{Os_3(CO)_{11}\}_2(PNCHP)]$ (**F.6.2-1**)*

$[Os_3(CO)_{11}(CH_3CN)]$ (0.251 g, 0.273 mmol) dissolved in dichloromethane (c.a. 15 mL) and PNCHP (0.0749 g, 0.136 mmol) dissolved in the same solvent (c.a. 3 mL) were combined and the mixture stirred at room temperature for 2.5 h. N-hexane vapour was diffused into the reaction mixture to initiate crystallisation. The product, $[\{Os_3(CO)_{11}\}_2(PNCHP)]$ (0.198 g, 63 %) was isolated as large orange crystals, washed with n-pentane, and air-dried. M.p: 176 °C (dec). (Found: C, 30.32; H, 0.96; N, 0.61; $C_{59}H_{29}NO_{22}Os_3P_2$ requires: C, 30.71; H, 1.27; N, 0.61).

*6.4.2 $[Os_3(CO)_{11}(PCHNP)]$ (**F.6.2-2a**)*

$[Os_3(CO)_{11}(CH_3CN)]$ (0.100 g, 0.109 mmol) dissolved in dichloromethane (c.a. 10 mL) and PNCHP (0.0597 g, 0.109 mmol) in c.a. 3 mL of the same solvent were combined and the heated under reflux for 30 min. The solvent was removed *in vacuo* giving yellow-orange microcrystals, which were purified by TLC, eluting with dichloromethane/n-hexane (2:1). Two major bands were obtained with Rf values of 0.91 and 0.53 respectively. The first band afforded a 5/1 mixture of $[\{Os_3(CO)_{11}\}_2(PNCHP)]$ (**F.6.2-1**)/ $[Os_3(CO)_{11}(PNCHP)]$ (**F.6.2-2b**)} (0.0384 g, 12 %) as a yellow powder, the second band gave $[Os_3(CO)_{11}(PNCHP)]$ (**F.6.2-2a**) (0.0252 g 16 %) as a yellow powder, after isolation by filtration, washing with n-pentane and air-drying. M.p: 203 °C (dec).

*6.4.3 1,1-[$Os_3(CO)_{10}$(PNCHP)] (**F.6.2-3**)*

$[Os_3(CO)_{10}(CH_3CN)_2]$ (0.0955 g, 0.102 mmol) dissolved in dichloromethane (c.a. 10 mL) and PNCHP (0.0562 g, 0.102 mmol) in c.a. 3 mL of the same solvent were combined. The mixture was stirred at room temperature for 2 h. The solvent volume was reduced *in vacuo* and the reaction mixture purified by TLC, eluting with dichloromethane/n-hexane (3:1). The major band was extracted into dichloromethane and the product precipitated with hexamethyldisiloxane as an orange powder, washed with n-pentane, and air-dried to give 1,1-$[Os(CO)_{10}(PNCHP)]$ (0.0280 g, 27%). The compound is very soluble in all common solvents. (Found: C, 37.48; H, 2.19; N, 0.89; $C_{49}Cl_2H_{31}NO_{10}OsP_2$ requires: C, 37.44; H, 2.29; N, 1.04). ^{13}C-NMR δCO ($CDCl_3$): 193.22(d), 5.49 Hz; 193.18(s); 190.46(d) 7.32 Hz; 190.16(s); 188.59(d), 6.72 Hz; 186.72(d), 6.71 Hz; 179.68(d), 3.67 Hz; 178.49(d), 2.44 Hz; 172.67(d), 2.44 Hz; 170.32(s).

*6.4.4 [$Os_3(\mu$-H)$(CO)_7(\mu_3$-PNCP)] (**F.6.2-4**)*

$[Os_3(CO)_{10}(CH_3CN)_2]$ (0.0960 g, 0.103 mmol) and PNCHP (0.0561 g, 0.102 mmol) were combined in dichloromethane (45 mL) and stirred at room temperature for 110 min, to form 1,1-$[Os_3(CO)_{10}$(PNCHP)] *in situ.* Freshly sublimed trimethylamineoxide (0.0155 g, 0.206 mmol) in acetonitrile (c.a. 5 mL) was added dropwise to the red-orange solution over 135 min. The reaction mixture was stirred for a further 22 h then taken to dryness *in vacuo.* The product was crystallised from dichloromethane/n-hexane by vapour diffusion to give the product as large orange crystals (0.0404 g, 30%). M.p: 182 °C (dec). (Found: C, 38.82; H, 2.13; N, 1.15; $C_{45}Cl_2H_{31}NO_7Os_3P_2$ requires: C, 38.66; H, 2.19; N, 0.98).

*6.4.5 [$Os_3(\mu$-H)$(CO)_8(\mu_2$-PNCP)] (**F.6.2-5a/b**)*

$[Os_3(CO)_{10}(CH_3CN)_2]$ (0.0910 g, 0.0976 mmol) and PNCHP (0.0538 g, 0.0979 mmol) were combined in dichloromethane (c.a. 12 mL) and heated to reflux for 30 min. Freshly sublimed trimethylamineoxide (0.0147 g, 0.196 mmol) in dichloromethane (c.a. 5 mL) was added dropwise to the red reaction mixture, resulting in a colour change to very dark-brown after 1 h. After a further 1 h when the reaction mixture became red again, it

was allowed to cool. It was passed through a small alumina column (200-400mesh) to remove any excess trimethylamineoxide, eluting with dichloromethane, The solvent was then removed *in vacuo*. The crude reaction product(s) was run down a silica gel (100-200 mesh) column, eluting successively with 0, 1, 10, and 100 % solutions of methanol in dichloromethane, to give an orange, yellow, yellow and yellow band respectively. The fractions were taken to dryness *in vacuo*. The major band was the first orange band and this was further purified by TLC, eluting with dichloromethane. The product was crystallised from dichloromethane/n-hexane by vapour diffusion to give the product as red-orange crystals (0.0014 g, 1 %). Microanalytical data could not be obtained due to insufficient amount of sample. This compound is also observed in the ageing of **F.6.2-3** and in the synthesis of **F.6.2-4**.

Appendix - General Experimental Technique and Instrumentation

A.1 General Experimental Technique

Unless stated otherwise, all reactions were carried out under an inert atmosphere of dinitrogen or argon gas, however, no attempts were made to rigorously exclude air during subsequent isolation and purification of the products except in the case of the rhodium compounds, which were handled in a glove-box and/or using standard Schlenk techniques.

A.1.1 Purification of solvents

Solvents used as a reaction medium were purified by standard methods to remove water and oxygen.[1] Solvents used for recrystallisation, compound washing etc were of AR grade specification and used as commercially supplied, as were deuterated NMR solvents.

A.1.2 Chromatography

Preparative thin layer chromatography was performed on plates of dimensions 200 x 200 x 1 mm. These were prepared from Silica Gel 60 PF_{254}, from Merk, in a water slurry followed by drying at room temperature, then baking at 120 °C. Column chromatography was performed using aluminium oxide 90 (70-230 mesh) as supplied by Merck.

A.2 Instrumentation

NMR measurements in solution were performed on a JEOL GX270W spectrometer. Solid state CP/MAS ^{31}P NMR spectra were recorded as described elsewhere.[2] IR spectra were recorded on a Perkin Elmer FT-IR Paragon 1000 instrument. UV-vis spectra were performed using a Shimadzu UV-310PC UV-VIS-NIR scanning

---

[1] D. D. Perrin and W. L. F. Armarego, *Purification of Laboratory Chemicals*, 3rd Edition, 1988, Pergamon Press Ltd.

[2] G. A. Bowmaker, C. L. Brown, R. D. Hart, P. C. Healy, C. E. F. Rickard and A. H. White, *J. Chem. Soc., Dalton Trans.*, 1999, 881.

spectrometer. Mass spectra were obtained using a Varian VG70-250S double-focussing magnetic sector spectrometer by the method of liquid ion secondary mass spectroscopy using m-nitrobenzyl alcohol as the matrix. Isotope abundance simulations were performed to identify the parent ion. Microanalyses were performed by the Campbell Microanalytical Laboratory, University of Otago. Melting points were determined on a Bausch & Lomb hot plate melting point apparatus and are uncorrected with respect to calibration.